Newcastle University

The Role of SLC26 Transporters in Airway Epithelial Cell Function

James Peter Garnett

Thesis submitted in fulfilment of the requirements of the regulations for the degree of Doctor of Philosophy

Newcastle University
Faculty of Medical Sciences
Institute for Cell and Molecular Biosciences

August 2010

For my Big Bro

I'm sorry I didn't always have the time, but you were always on my mind

Acknowledgements

Thank you to everyone who has helped me during my PhD, in both the Epithelial Research Group at Newcastle and at Novartis. In particular my supervisors Mike and Emma, who showed faith in me to take me on as a student in their labs and have been a great source of knowledge and support during my PhD. Thanks to Steven and Burns for being excellent postdocs by showing me the ropes and for their friendship. Also a huge thank you to Helen, without whom the sheer volume of experiments I did during this project would not have been possible. To the members of the Jeff Pearson group, I thank you all for being a constant source of amusement and good will (and alcohol) during my four years in Newcastle. It turns out my imaginary exchanger was there after all! And a special thank you to Georgina, for being so unselfishly kind and always coming through for me.

I would not have got through my PhD had it not been for my family, who have all at some point taken me under their roofs, keeping me fed and watered. Also for being there for me every time I had a crisis. I feel very lucky to have such a supportive family, for which I am eternally grateful.

Abstract

HCO_3^- plays a vital role in the airways, as mucus viscosity and ciliary beat have both been shown to be dependent upon the pH of the airway surface liquid. In cystic fibrosis (CF), reduced HCO_3^- and fluid secretion produce dehydrated mucus, which impairs airway defence and predisposes the airways to bacterial infection. Calu-3 cells are used as a model of the serous cells of human tracheobronchial submucosal glands which are involved in CFTR (cystic fibrosis transmembrane conductance regulator)-dependent HCO_3^- secretion. CFTR is widely regarded as the sole mediator of apical Cl^- and HCO_3^- secretion in Calu-3 cells and human serous airway cells. However, the discovery of SLC26 Cl^-/HCO_3^- exchange activity linked to the expression of CFTR in tracheal epithelial cells, as well as a functional interaction between apically co-localised SLC26 exchangers and CFTR in mediating HCO_3^- secretion in many HCO_3^- secreting epithelia including the pancreas and gastrointestinal tract, has led to some doubt over this hypothesis. The aim of this work was to investigate the potential role of SLC26 anion exchange (AE) in HCO_3^- secretion from Calu-3 cells and its dependence on CFTR. AE activity was assessed by real time measurements of intracellular pH (pH_i) using the pH-sensitive dye BCECF-AM, from cells grown as monolayers on semi-permeable supports.

Calu-3 cells under non-stimulated conditions displayed Na^+-dependent basolateral Cl^-/HCO_3^- exchange, which was abolished by H_2-DIDS. No apical AE activity could be detected under resting conditions. Stimulation of cells with a cAMP agonist (forskolin, adenosine, VIP) produced a switch in AE activity, activating an apical AE and completely inhibiting the basolateral AE. The cAMP-activated apical AE activity was Na^+-independent, H_2-DIDS-insensitive and could transport a range of monovalent anions in exchange for HCO_3^- with the selectivity profile: Iodide=Br^->Cl^-=Formate =NO_3^-=SCN^-. The profile of this anion exchanger corresponds with Pendrin (SLC26A4), which quantitative RT-PCR analysis showed to be expressed in these Calu-3 cells. Consistent with this, Pendrin knockdown (KD) Calu-3 cells had a reduced rate of AE activity, compared to wild-type (WT) cells. Protein phosphatase 1 inhibition by okadaic acid activated an apical AE under non-stimulated conditions with a similar profile to Pendrin, which CFTR inhibitor studies demonstrated to be CFTR-independent. Interestingly, fluid secretion studies established that Calu-3 cells produced a more alkali fluid when treated with okadaic acid, consistent with enhanced HCO_3^- secretion. The role of CFTR in Cl^-/HCO_3^- AE activity was assessed using CFTR inhibitors and CFTR KD Calu-3 cells. Although apical AE activity in WT Calu-3 cells could be abolished by inhibiting CFTR (with either $CFTR_{inh}$-172 or GlyH-101), it could be restored by the addition of basolateral H_2-DIDS, suggesting that the CFTR inhibition reveals a H_2-DIDS-sensitive basolateral transport process which masks the effects of apical AE on pH_i, rather than abolishing apical AE activity itself. In CFTR KD Calu-3 cells the rate of apical AE activity was significantly decreased compared to WT cells. These results suggest a role for CFTR in regulating apical Cl^-/HCO_3^- exchange activity and/or contributing to Cl^--dependent HCO_3^- transport. Similarly cAMP inhibition of the basolateral AE was also found to be mediated via a CFTR-dependent mechanism, highlighting the importance of CFTR in the cAMP-dependent switch in Calu-3 AE activity. Such a switch in AE activity by cAMP, would favour bicarbonate secretion, consistent with the finding that cAMP enhances HCO_3^--dependent fluid secretion from Calu-3 cells. Apical AE activity was also observed in human bronchial epithelial cells (HBECs), which could not be blocked by GlyH-101, but was absent in CF HBECs.

Table of Contents

List of Figures

List of Tables

Abstract Publications

Garnett, J.P., Cuthbert, A.W., Hickman, E. & Gray, M.A. (2008). CFTR activation regulates both apical and basolateral Cl^-/HCO_3^- exchange activity in Calu-3 cells. *ECFS Conference - New Frontiers in Basic Science of Cystic Fibrosis, Douro, Portugal.* (Oral and poster communication).

Garnett, J.P., Hickman, E., Cuthbert, A.W., Yarham, J. & Gray, M.A. (2008). CFTR regulates apical chloride-bicarbonate exchange in Calu-3 cells. *Pediatr Pulmonol*, 43, (S31), pp. 234-235.

Garnett, J.P., Hickman, E., Burrows, R., Cuthbert, A.W. & Gray, M.A. (2009). Cystic fibrosis transmembrane conductance regulator regulates an apical chloride-bicarbonate exchanger in airway submucosal gland epithelial cells. *Proc Physiol Soc,* 16, C10.

Abbreviations

ACh – Acetylcholine

ADO - Adenosine

AE – Anion Exchanger

ALI – Air-Liquid Interface

ASL – Airway Surface Liquid

ATZ -Acetazolamide

BCECF – biscarboxyethylcarboxyfluorescein

BEBM - Bronchial Epithelial cell Basal Media

CF – Cystic Fibrosis

CFTR – Cystic Fibrosis Transmembrane Conductance Regulator

DIDS - diisothiocyanostilbene sulfonic acid

DMA - dimethylamiloride

DMEM - Dulbecco's Modified Eagles Medium

DNDS - 4,4'-dinitrostilbene-2,2'-disulfonate

DOG - 1,2-dioctanoyl-*sn*-glycerol

EIPA - 5-(N-Ethyl-N-isopropyl)-Amiloride

ENaC - Epithelial Sodium Channel

Epac - Exchange protein directly activated by cAMP

FSK – Forskolin

GAPDH - Glyceraldehyde 3-phosphate dehydrogenase

HBE cells – Human Bronchial Epithelial cells

H_2-DIDS - 4,4'-diisothiocyano-1,2-diphenylethane-2,2'-disulfonate

HEK cells – Human Embryonic Kidney cells

HEPES - (4-(2-Hydroxyethyl)piperazine-1-ethanesulfonic acid)

HNE - Human Nasal Epithelial

IDV - Integrated Density Value

IL - Interleukin

IONO – Ionomycin

KD – Knockdown

KO – Knockout

KRB solution – Krebs ringer HCO_3^--buffered solution

MEME – Minimum Essential Medium Eagle

MSD - Membrane-Spanning Domain

NBC - Na^+-HCO_3^- Cotransporter

NBD - Nucleotide-Binding Domain

NDCBE - Na^+-Driven Cl^-/HCO_3^- Exchanger

NHE - Na^+-H^+ Exchanger

NKCC - Na^+-K^+-Cl^- Cotransporter

OA – Okadaic Acid

ORCC - Outwardly Rectifying Chloride Channel

PAS assay - Periodic Acid-Shiff's assay

PBS – Phosphate Buffered Saline

PCL – Periciliary Liquid

pH_i - intracellular pH

PI3-kinase – phosphatidylinositol 3-kinase

PKA – Protein Kinase A

PKC – Protein Kinase C

PP1 - Protein Phosphatase 1

ShRNA - short hairpin RNA

SLC26 – Solute Carrier 26

SMG – Submucosal Glands

STAS domain - Sulfate Transporter and Anti-Sigma domain

SUB – Submerged

TBS - Tris-Buffered Saline

TEER - Transepithelial Electrical Resistance

VIP – Vasoactive Intestinal Peptide

WT – Wild-Type

ZO-1 – Zona Occludens 1

1. Introduction

1.1 Airway surface liquid: submucosal glands to airway lumen

The human airways are lined by mucus, a salt-rich fluid containing antioxidants, antiproteases, antimicrobials and mucins. Mucus traps and inactivates inhaled particles and pathogens. These infectious particles are then removed from the airways by mucociliary clearance, maintaining the sterility of the lungs. The primary source of airway mucus is the submucosal glands, which are estimated to produce approximately 95% of upper airway mucus in healthy individuals (Reid, 1960). Submucosal glands are comprised of ~61% serous and ~39% mucous cells by volume (Basbaum *et al*, 1990). Much of the contents of airway mucus, such as water, salts and antibacterial compounds, are produced by serous cells, whereas the mucous (and goblet) cells provide most of the mucins. Each gland contains a series of interconnecting tubules that feed into a collecting duct, which narrows into a ciliated duct that is continuous with the airway lumen (Meyrick & Reid, 1970). Fluid secretions from the submucosal glands travel through the series of tubules and ducts, along the way being supplemented with further mucosal secretions, finally reaching the bronchial lumen, where the fluid maintains the airway surface liquid (ASL).

The ASL is divided into a well-defined periciliary liquid (PCL) layer and a mucus layer. The underlying PCL is responsible for maintaining the mucus layer at an optimum distance from the airway surface epithelia, in order to sustain efficient mucus clearance via ciliary action (mucociliary clearance; Tarran, 2004). In normal airways, the PCL is approximately the length of the outstretched cilia (~7 μm), whereas the mucus layer varies considerably in height (7 to 70 μm *in vivo*; Jayaraman *et al*, 2001c). The volume and composition of the ASL is tightly regulated, to ensure

that the mucus layer is sufficiently hydrated. Airway surface epithelial ion transport is thought to play an important role in the regulation of the volume and composition of the PCL, through balanced Na^+ absorption (via epithelial sodium channels- ENaC) and Cl^- secretion (via the cystic fibrosis transmembrane conductance regulator-CFTR), thus providing the driving force for transepithelial fluid movement (see section 5.5 for further discussion). This can be seen in patients with Pseudohypoaldosteronism, who exhibit loss-of-function mutations in ENaC and have an excess of ASL due to reduced Na^+ absorption (Kerem *et al*, 1999). The osmotic gradient generated by the surface epithelium maintains the height of the PCL necessary for mucociliary clearance, as well as the salt concentration to provide optimum conditions for the activity of antimicrobial molecules (Smith *et al*, 1996; Travis *et al*, 2001).

The homeostasis of the ASL is of particular interest in cystic fibrosis (CF), as CF is associated with defective mucociliary clearance, due to the dehydrated viscous composition of the secreted mucus. In CF, defective submucosal gland (SMG) secretion, together with abnormal airway surface epithelial function, produces ASL dehydration (Matsui *et al*, 1998). This allows pathogens to remain in the airways, leading to infection, inflammation and tissue damage (see **Figure 1.01**).

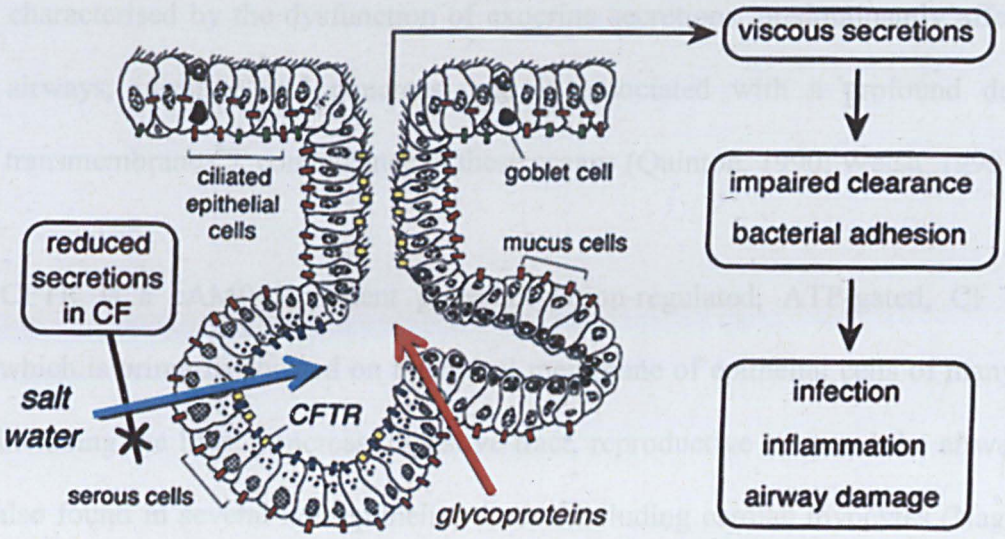

Figure 1.01 - Proposed mechanism of lung disease in CF. Schematic of airway submucosal gland showing watery fluid secreted by CFTR-expressing serous acini (indicated by blue arrow), addition of glycoproteins by mucous tubules (red arrow), and passage of fluid onto the airway surface through a collecting duct. Defective CFTR in serous glandular epithelial cells results in secretion of a reduced amount of a hyperviscous solution, which impairs bacterial clearance mechanisms leading to chronic airway infection, inflammation, and destruction. Yellow blocks represent sites of apical CFTR expression. Red blocks represent sites of basolateral Cl^-/HCO_3^- exchanger expression. Reproduced from Salinas *et al*, 2005.

1.2 CFTR

CF is caused by mutations in the gene encoding for the cystic fibrosis transmembrane conductance regulator (CFTR). At the time of writing, more than 1700 CFTR gene mutations have been discovered (according to the cystic fibrosis mutation database*). Deletion of phenylalanine at position 508 (deltaF508) is the most common CFTR mutation, affecting around 70% of CF sufferers (Davis, 2006). In cells containing the deltaF508 mutation, mature fully glycosylated CFTR proteins are not present in the membrane, as the protein does not fold normally, resulting in the retention of CFTR in the endoplasmic reticulum (ER), where it is ubiquitinated and retrotranslocated to the cytosol for proteasomal degradation (Cheng *et al*, 1990; Gelman *et al*, 2002). CF is

*http://www.genet.sickkids.on.ca/cftr

characterised by the dysfunction of exocrine secretions, predominantly affecting the airways, intestine and pancreas, and is associated with a profound decline in transmembrane Cl^- conductance in these organs (Quinton, 1990; Welsh, 1990).

CFTR is a cAMP-dependent phosphorylation-regulated, ATP-gated, Cl^- channel, which is primarily located on the apical membrane of epithelial cells of many organs including the liver, pancreas, digestive tract, reproductive tract and the airways. It is also found in several non-epithelial tissues including cardiac myocytes (Nagel *et al*, 1992), smooth muscle (Robert *et al*, 2005), skeletal muscle (Diavangahi *et al*, 2009), endothelia (Tousson *et al*, 1998) and erythrocytes (Sprague *et al*, 1998). This ATP-binding cassette (ABC) transporter-class protein conducts the movement of Cl^- and other monovalent anions, which together with the movement of Na^+, dominates the epithelial cell, resulting in the movement of water by osmosis towards the lumen. Initially, following the discovery of the gene encoding CFTR (Riordan *et al*, 1989), it was unclear whether CFTR regulated a Cl^- conductance or was itself a Cl^- channel. CF was associated with a low Cl^- permeability (Quinton, 1983) and cAMP was found to open apical Cl^- channels in normal but not CF airway epithelial cells (Schoumacher *et al*, 1987; Li *et al*, 1988). However, the disease also manifested in increased Na^+ absorption by CF airway epithelia (Boucher *et al*, 1986). It was subsequently discovered, following cloning of the CFTR gene, that CFTR was an ATP-regulated Cl^- channel, with a 9-11pS single-channel conductance and the permeability sequence: $Br^->Cl^->I^->F^-$ (Anderson *et al*, 1991 a&b; Bear *et al*, 1991). Patch clamp experiments in pancreatic duct cells showed that CFTR could also conduct HCO_3^-, although with a much lower permeability than Cl^- (HCO_3^-/Cl^- permeability ratio of 0.11-0.25; Gray *et al*, 1990). In addition, studies have since shown that CFTR not only functions as an

anion channel, but can interact with and regulate other ion channels, including Na^+ channels (Stutts *et al*, 1995) and outwardly rectifying chloride channels (ORCCs; Egan *et al*, 1992), as well as various other transport proteins including Cl^-/HCO_3^- exchangers (see section 1.5).

To date the structure of CFTR has not been fully determined, as the substantial hydrophobic regions present in the CFTR protein are difficult to crystallise, rendering X-ray crystallography of the protein extremely challenging. However, by comparing the CFTR amino acid sequence with that of other members of the ABC transporter family, a general model of the structure of CFTR was proposed by Riordan and colleagues (Riordan *et al*, 1989). CFTR consists of five domains: two membrane-spanning domains (MSD1 and MSD2) that together form the ion channel; two nucleotide-binding domains (NBD1 and NBD2) that bind and hydrolyze ATP; and a regulatory (R) domain that is unique to CFTR (not found in other ABC transporters or other proteins). Each MSD consists of six hydrophobic α helices, which are connected to the cytoplasmic NBD, with the two homologous halves of CFTR linked by the R domain to give the overall structural organisation: MSD1-NBD1-R-MSD2-NBD2. The exact function of the R domain was determined by studies of R domain deletion (CFTRΔR), which showed that CFTRΔR was constitutively active and no longer required cAMP/ATP to conduct chloride, suggesting that the unphosphorylated R domain inhibits CFTR channel activity and thus phosphorylation is required to overcome this inhibition (Rich *et al*, 1991). However, addition of an unphosphorylated R-domain to a CFTR variant in which the R-domain had been deleted (CFTR-ΔR/S660A) did not inhibit CFTR activity and addition of a phosphorylated R domain actually stimulated activity (Winter & Welsh, 1997).

Studies of CFTR channel gating, suggested that phosphorylation of the R domain increases the rate of channel opening due to enhanced sensitivity to ATP (Winter & Welsh, 1997). Thus, phosphorylation of the R domain by cAMP-dependent protein kinase (PKA), resulting from an elevation in cAMP levels, allows ATP to open and close the channel (Winter & Welsh, 1997; Ostedgaard *et al*, 2001). However, protein kinase C (PKC), cGMP-dependent kinase and tyrosine phosphorylation can also stimulate CFTR activity (Gadsby & Nairn, 1999; Sheppard & Welsh, 1999). In particular, CFTR phosphorylation by PKC, despite only producing weak channel activation, may potentiate or even be a prerequisite for CFTR activation by PKA (Chappe *et al*, 2003). Once phosphorylated, CFTR channels open via the dimerisation of the NBDs produced by ATP binding (and hydrolysis), which in turn causes a conformational change in the MSDs allowing passive anion flow through the pore (Hwang & Sheppard, 2009). The balance of a complex array of protein kinases and phosphatases, such as protein phosphatase 2A (see chapter 3 for further discussion), then controls CFTR opening and closing by phosphorylation/dephosphorylation (Berger *et al*, 1993).

Since lung disease is the greatest cause of mortality among CF sufferers, the observation of particular importance to CF is that CFTR within the airways is highly expressed in serous cells of the SMG (CFTR antibodies localise to the apical membrane of SMG serous cells *in situ*; Englehardt *et al*, 1992), which make up the majority of the surface area of the epithelium lining the glands as well as in the ciliated epithelium near gland orifices (Kreda *et al*, 2005).

1.3 Airway submucosal gland secretion

Since SMGs are small and most of their mass is embedded in the submucosal space, study of their secretions has proved problematic. One method pioneered by Quinton to measure SMG secretion, involves drying the airway surface using gas and then applying a layer of oil, so that when fluid emerges from SMG duct openings, it forms visible pools of liquid underneath the oil layer (Quinton, 1979). This liquid can then be collected using micropipettes for determination of volume and composition, or fluid volumes can be measured optically *in situ* from droplet dimensions (Joo *et al*, 2001). Another method used to isolate SMG secretions, was to abrasively remove the surface epithelium of isolated pig distal bronchi, leaving the submucosal glands intact (Ballard *et al*, 1999).

Airway SMG secretions are primarily controlled by nervous innervation from the parasympathetic nervous system (Wine, 2007). Airway intrinsic neurons release neurotransmitters including vasoactive intestinal peptide (VIP) and substance P, which induce liquid secretion in the SMG through stimulation of $VPAC_2$ and NK_1 tachykinin receptors, respectively (Groneberg *et al*, 2001; Phillips *et al*, 2003). Stimulation of the vagus nerve causes vigorous gland secretions in the feline trachea, which is mediated largely by the local release of acetylcholine (ACh; Ueki *et al*, 1980). This response can be mimicked by the direct application of ACh or other cholinergic agonists to the glands (Quinton, 1979), through the activation of M_3 muscarinic receptors, which increase $[Ca^{2+}]_i$ (Ishihara *et al*, 1992). Substance P is also thought to enhance SMG fluid secretion through increasing $[Ca^{2+}]_i$ (Nagaki *et al*, 1994), whereas VPAC receptors are coupled to adenylyl cyclase and thus VIP mediates gland secretion by elevating $[cAMP]_i$ (Groneberg *et al*, 2006).

The active secretion of both HCO_3^- and Cl^- drives fluid secretion by the SMG's (Ballard & Inglis, 2004). *In vitro* measurements in excised porcine bronchi, secreted ~15 $\mu l/cm^2/h$ when treated with ACh in the absence of surface epithelial secretion, which could not be further enhanced in bronchi with an intact surface epithelium, suggesting that the source of the liquid was the SMG (Ballard *et al*, 1999). Trout and colleagues investigated the role of Cl^- and HCO_3^- in gland fluid secretion by treating porcine bronchi with the Na^+-K^+-$2Cl^-$ cotransporter (NKCC) inhibitor bumetanide, or removal of Cl^- from the Krebs solution bathing the excised bronchi, and the Na^+-H^+ exchanger (NHE) inhibitor dimethylamiloride (DMA; Trout *et al*, 1998). The action of DMA is thought to result from the inhibition of H^+ extrusion across the basolateral membrane, which reduces the capacity of the epithelial cells to generate cytoplasmic HCO_3^- (Smith & Welsh, 1992). The Cl^- content of the secreted fluid in Trout and colleagues' study (Trout *et al*, 1998) was assessed by amperometric Cl^- titration, and the HCO_3^- content determined using electrometric titration (Maas, 1970). Trout *et al* (1998) demonstrated that ~70% of the ACh-stimulated SMG fluid secretion was driven by NKCC-dependent Cl^- secretion and the rest is supported by NHE-dependent HCO_3^- secretion. Similar results were obtained in porcine bronchi exposed to substance P (Trout *et al*, 2001). The magnitude of HCO_3^- secretion that occurs in ACh-stimulated bronchi is sufficient to induce a measurable alkalinisation in the luminal bathing fluid (Inglis *et al*, 2003). Under resting conditions, the distal bronchi cannulated in bath containing HCO_3^--buffered solution, secreted base equivalents, as pH electrode analysis showed an acidification of ~0.065 pH units. The addition of 10 μM ACh evoked an increase in luminal pH at a rate of ~0.003 pH units/min, which could be inhibited in HCO_3^--free (HEPES-buffered) solutions containing the carbonic anhydrase inhibitor acetazolamide, consistent with HCO_3^- secretion. The partial

HCO_3^--dependence of SMG fluid secretion was also observed in optical fluid secretion measurements in sheep SMGs, where carbachol-induced (cholinergic agonist) secretion was reduced ~67% by HCO_3^- replacement with HEPES (Joo *et al*, 2001a). Forskolin (directly activates adenylyl cyclase to produce cAMP) and VIP both induce porcine SMG fluid secretion (both at a rate ~40% lower than carbachol), which is also mediated by a combination of Cl^- and HCO_3^- secretion, with each contributing around 50% of the liquid secretion (Joo *et al*, 2002b). However, unlike ACh or substance P, forskolin induces SMG fluid secretion through both a DMA-sensitive pathway and a Na^+-dependent DIDS (diisothiocyanostilbene sulfonic acid)-sensitive pathway, believed to represent HCO_3^- uptake through a basolateral Na^+-HCO_3^- cotransporter (Ballard *et al*, 2004).

Most lines of evidence in studies of fluid secretion from human airway SMGs, suggest that secretion is dependent on apical CFTR. In addition to the expression of CFTR in SMG serous cells (which are believed to provide most of the liquid in gland secretions; Meyrick & Reid, 1970; Englehardt *et al*, 1992), the CFTR blocker, $CFTR_{inh}$-172 (Ma *et al*, 2002), inhibited pilocarpine- (cholinergic agonist) and forskolin- induced airway SMG secretion in pigs and humans without CF, but not in human bronchi with CF (Thiagarajah *et al*, 2004). Interestingly, pH measurements of the fluid droplets secreted from porcine SMGs, determined using the pH-sensitive fluorescent probe BCECF-dextran, showed that $CFTR_{Inh}$-172 had no effect on the pH of gland secretions under non-stimulated conditions (pH~6.9), but lowered the pH of pilocarpine-stimulated secretions from ~7.1 to ~6.7, consistent with the inhibition of CFTR-dependent HCO_3^- secretion (Thiagarajah *et al*, 2004).

Since other studies of human SMG secretion found that the VIP/forskolin-induced component of fluid secretion was absent in CF airways but the muscarinic component remained partially intact (Joo *et al*, 2002a), it was unclear whether CFTR is the sole apical transporter that mediates anion and liquid secretion in the airway submucosal glands.

1.4 Calu-3 cells

As serous cells are difficult to isolate and grow in culture, there was much excitement about Calu-3 cells, a cell line derived from a human lung adenocarcinoma, which have many properties of serous submucosal gland cells (Shen *et al*, 1994; Haws *et al*, 1994). Such properties included the production of antimicrobials (such as lysozyme and lactoferrin; Dubin *et al*, 2004), growth to confluence with high resistance (R_T >1000 $\Omega.cm^2$) and the expression of high levels of functional cAMP- and ATP-stimulated CFTR in their apical membranes (Haws *et al*, 1994; Illek *et al*, 1996). Unlike many immortalised cells, Calu-3 cells form sheets of cells that are joined by tight junctions (Wan *et al*, 2000). These sheets form a fully functional polarised epithelium that can transport large quantities of ions and fluid. Since Calu-3 cells have a high level of natural CFTR expression, they make an ideal model for studying the role of CFTR in serous cell secretions (Haws *et al*, 1994). However, caution must be employed when extrapolating the results of Calu-3 cell cultures to overall SMG function *in vivo*, since some important physiological aspects can be lost, (including nervous innervation) when cells are removed from their native environments and grown in media for prolonged periods.

Calu-3 cells are of special interest because they produce two kinds of anion secretion depending upon the mode of stimulation. When activated via agents that elevate intracellular cAMP (such as VIP or forskolin), Calu-3 cells secrete a HCO_3^- rich fluid (Irokawa *et al*, 2004). However, if activated by agents that elevate intracellular Ca^{2+} (such as acetylcholine stimulation of muscarinic receptors), Calu-3 cells secrete a Cl^--rich fluid (Devor *et al*, 1999), although it still contains a large component of HCO_3^- (Lee *et al*, 1998). More recently, it was shown that apically secreted HCO_3^- is partially neutralized by proton secretion under some conditions (Krouse *et al*, 2004). The source of the protons appears to be an H^+-K^+-ATPase, as it is ouabain-sensitive and requires apical K^+ (Krouse *et al*, 2004; it should be noted that the ouabain-sensitive apical H^+-K^+-ATPase present in Calu-3 cells is distinct from the H^+-K^+-ATPase found in the apical membrane of parietal cells, which can be inhibited by omeprazole, but is insensitive to ouabain). This may explain the unexpected similarity between the pH of CF and non-CF submucosal gland secretions, despite a lack of HCO_3^- secretion by CF serous cells (Jayarman *et al*, 2001a).

Calu-3 transport mechanisms have now been well studied and characterised, and are summarised in **Figure 1.02**. The dual nature of CFTR secretion as described above can be explained by a model proposed by Krouse and colleagues (Krouse *et al*, 2004). Increasing intracellular Ca^{2+} stimulates basolateral Ca^{2+}-activated K^+ channels (K_{Ca}), hyperpolarising the membrane. The proposed electrogenic Na^+-HCO_3^- cotransporter (NBC) can mediate entry or exit of HCO_3^- according to the membrane potential. Therefore hyperpolarising the basolateral membrane so that membrane potential is greater than the reversal potential of the NBC, causes HCO_3^- exit rather than entry. As the NBC is the primary source of HCO_3^- entry, $[HCO_3^-]_i$ decreases, producing a Cl^--

rich CFTR secretion. The Na^+-K^+-$2Cl^-$ cotransporter (NKCC) provides Cl^- entry into the cell, since the basal K^+ conductance is able to maintain the apical voltage above the Cl^- equilibrium potential. The basolateral Na^+-K^+-ATPase and apical H^+-K^+-ATPase provide the driving force for CFTR-mediated anion secretion, by the hydrolysis of ATP (Ito *et al*, 2000). The inwardly rectifying K^+ channel (K_{IR}), expressed on the apical membrane of Calu-3 cells, optimizes the rate of secretion and is involved in K^+ recycling for the apical H^+-K^+-ATPase (Wu *et al*, 2004). However, elevating intracellular cAMP (using forskolin), causes a predominantly HCO_3^- -rich secretion (to exit the cell) via CFTR, due to the presence of active basolateral Na^+-HCO_3^- cotransport.

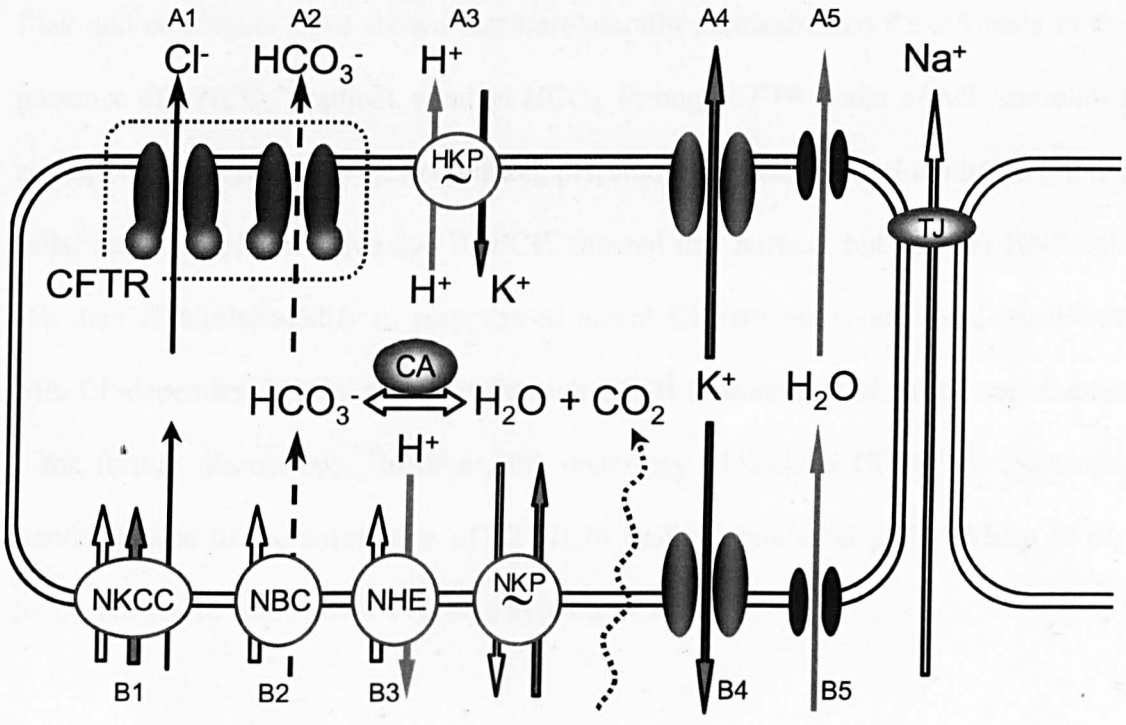

Figure 1.02 - Calu-3 transport mechanisms. On the apical membrane- CFTR (A1&A2; shown in duplicate due to evidence that its Cl^- and HCO_3^- conductances might be independently controlled), H^+-K^+-ATPase (A3), inwardly rectifying K^+ channel (K_{IR}; A4) and aquaporin (A5). On the basolateral membrane- Na^+-K^+-$2Cl^-$ cotransporter (NKCC; B1), Na^+-HCO_3^- cotransporter (NBC; B2), Na^+/H^+ exchanger (NHE; B3), K^+ channel (B4) and aquaporin (B5). All channels and exchangers shown are thought to be powered by basolateral Na^+-K^+-ATPase (indicated by NKP~). CO_2 and H_2O conversion by carbonic anhydrase (CA) is as an important source of cellular HCO_3^-. This Calu-3 transport model was reproduced from Krouse *et* al, 2004.

Basolateral exit of HCO_3^- may be mediated by Cl^-/HCO_3^- exchange. Previous RT-PCR and immunofluorescence studies have shown the presence of an AE2 (SLC4A2) exchanger in Calu-3 cells (Loffing *et al*, 2000). These findings are supported by intracellular pH (pH_i) measurements examining the recovery of pH_i following cell acidification with NH_4Cl, which revealed the presence of DNDS (4,4'-dinitrostilbene-2,2'-disulfonate)-sensitive, Cl^-/HCO_3^- exchange (Inglis *et al*, 2002; see chapter 4 for further discussion).

CFTR is widely regarded as the sole mediator of apical Cl^- and HCO_3^- secretion in Calu-3 cells and human airway epithelial cells (Lee *et al*, 1998; Krouse *et* al, 2004). Illek and colleagues have shown that basolaterally permeabilised Calu-3 cells in the presence of a HCO_3^- gradient, conduct HCO_3^- through CFTR under cAMP-stimulated conditions (Illek *et al*, 1997). In addition, pH_i studies in human nasal epithelial (HNE) cells, using the pH sensitive dye BCECF, showed that normal, but not CF, HNE cell pH_i may alkalinise/acidify in response to apical Cl^- removal/re-addition, consistent with Cl^--dependent HCO_3^- transport through CFTR (Paradiso *et al*, 2003; see chapter 3 for further discussion). However, the discovery of SLC26 Cl^-/HCO_3^- exchange activity linked to the expression of CFTR in tracheal epithelial cells (Wheat *et al*, 2000), has led to some doubt over this hypothesis.

1.5 SLC26 transporter family

An essential function for most secretory epithelia is transepithelial Cl^- and HCO_3^- transport. HCO_3^- is a vital biological buffer that maintains the pH of the protective mucosal layers that line epithelia and plays an important role in the solubilisation of mucins and digestive enzymes in secreted fluids (Flemstrom & Isenberg, 2001; Taylor

& Abswani, 2002). Transepithelial Cl^- transport, necessary for NaCl and fluid secretion, often involves Cl^- uptake via potassium-coupled chloride-transporters, such as the NKCC (Hass, 1994), and to a lesser extent by DIDS-sensitive Cl^-/HCO_3^- exchange activity mediated by anion exchangers of the SLC4 family (Alper, 2009). The SLC4 family also includes a number of Na^+-dependent HCO_3^- cotransporters (NBCs), which are critical to the uptake of HCO_3^-. Cl^- channels, such as CFTR, mediate Cl^- secretion across the luminal membrane. The transporters involved in luminal HCO_3^- exit remained unclear until the discovery of SLC26A3 (Melvin *et al*, 1999) and the SLC26 family of anion transporters (Mount & Romero, 2004). In most secretory epithelia, the coordinated function of CFTR and one or more SLC26 Cl^-/HCO_3^- exchangers mediate HCO_3^- secretion (Dorwart *et al*, 2008; Ohana *et al*, 2009).

The SLC26 genes encode a conserved family of anion transporter proteins. Ten SLC26 isoforms have been identified through cloning experiments (**Table 1.01**). SLC26A1 (SAT-1) encodes a SO_4^{2-} transporter, shown to exchange SO_4^{2-} for oxalate (Bissig *et al*, 1994). Positional cloning of disease genes identified other family members. Mutations in SLC26A2 (DTDST) lead to four different chondrodysplasias including diastrophic dysplasia, a cartilage disorder resulting in growth retardation (Hastbacka *et al*, 1992). SLC26A3 (DRA) is associated with congenital chloride diarrhoea (Hoglund *et al*, 1996). SLC26A4 (Pendrin) is associated with Pendred syndrome (a genetic disorder leading to hearing loss and hypothyroidism) and hereditary deafness (DFNB4; Everett *et al*, 1997). More recent studies have reported that SLC26A5 (Prestin) is defective in non-syndromic hearing impairment (Liu *et al*, 2003). SLC26A6 (PAT-1) is associated with calcium oxalate urolithiasis, as SLC26A6 knockout mice develop a high plasma oxalate concentration, consistent

with impaired intestinal oxalate secretion due to the absence of SLC26A6 mediated Cl^-/oxalate exchange (Jiang *et al*, 2006). These disease associations, as well as other characteristics of the SLC26 family, are summarised in **Table 1.01.**

Human Gene Name	Aliases	Reported substrates	Tissue Distribution	Disease association(s)
SLC26A1	SAT-1	SO_4^{2-}, oxalate	liver, kidney	
SLC26A2	DTDST	SO_4^{2-}, Cl^-	widespread	Chondrodysplasias
SLC26A3	DRA, CLD	SO_4^{2-}, Cl^-, HCO_3^-, OH^-, oxalate	intestine, sweat gland, pancreas, prostate	Congenital Chloride-losing Diarrhoea
SLC26A4	Pendrin	Cl^-, HCO_3^-, I^-, formate	inner ear, kidney, thyroid, airways	Pendred syndrome Deafness (DFNB4)
SLC26A5	Prestin	-	inner ear	Deafness
SLC26A6	CFEX, PAT-1	SO_4^{2-}, Cl^-, HCO_3^-, OH^-, oxalate, formate	widespread	Urolithiasis
SLC26A7	PAT-2	SO_4^{2-}, Cl^-, oxalate	kidney, stomach	
SLC26A8	TAT-1	SO_4^{2-}, Cl^-, oxalate	sperm, brain	
SLC26A9	PAT-4	SO_4^{2-}, Cl^-, oxalate	lung	
SLC26A10	none	pseudogene		
SLC26A11	PAT-5	SO_4^{2-}	widespread	

Table 1.01 - The characteristics of the SLC26 family of anion exchangers. Table adapted from Mount & Romero, 2004.

1.5.1 SLC26 Cl^-/HCO_3^- exchangers

Functional characterisation of the SLC26 proteins has revealed distinctive patterns of anion specificity and transport modes. All SLC26 proteins, except SLC26A5 (prestin; a motor protein of cochlear outer hair cells), can function as anion exchangers, transporting both monovalent and divalent anions. The modes of transport mediated by SLC26 members include the exchange of chloride for bicarbonate, hydroxyl, sulfate, formate, iodide, or oxalate with variable specificity. Functional studies in *Xenopus* oocytes revealed that mouse SLC26A6 transports most of these substrates (Xie *et al*, 2002), whereas human SLC26A4 transports only monovalent anions and not divalent anions (Scott *et al*, 1999).

Physiological interest in the characterisation of the SLC26 family members was stimulated in particular by the observation that SLC26A4 (Pendrin) can function as a Cl^-/formate exchanger in *Xenopus* oocytes, since Cl^-/formate exchange is thought to play an important role in the transepithelial transport of NaCl by the renal proximal tubule (Scott & Karniski, 2000). Cl^- and formate radioisotope (^{36}Cl and [^{14}C] formate) efflux measurements in *Xenopus* oocytes injected with human SLC26A4 demonstrated that addition of chloride to the external bathing solution stimulated the efflux of [^{14}C] formate and formate addition stimulated the efflux of ^{36}Cl in oocytes expressing Pendrin, consistent with Pendrin-mediated Cl^-/formate exchange (Scott & Karniski, 2000). However, subsequent immunolocalisation studies in the mammalian kidney (mouse, rat and human) failed to detect any evidence of Pendrin staining in the proximal tubules, but instead detected Pendrin on the apical surface of β-intercalated cells of the cortical collecting duct (Royaux *et al*, 2001). The same study discovered that Pendrin instead plays a pivotal role in renal HCO_3^- secretion, since perfused cortical collecting duct tubules isolated from alkali-loaded Wild-type (WT) mice secreted HCO_3^-, whereas tubules from alkali-loaded Pendrin knockout (KO) mice did not. More recent studies have shown that Pendrin KO mice display significantly acidic urine (pH 5.2 compared to 6.0 in WT mice) along with elevated serum HCO_3^- concentration *in vivo* (Amlal *et al*, 2010). Furthermore, pH_i experiments (determined using the pH-sensitive fluorophore, BCECF) in β-intercalated cells of the cortical collecting duct, showed a reduced alkalinisation in pH_i in response to bath Cl^- removal in Pendrin KO mice compared to WT mice, consistent with Pendrin mediating Cl^- /HCO_3^- exchange (Amlal *et al*, 2010).

Many of the SLC26 members mediate Cl^-/HCO_3^- exchange in a limited number of tissues including the gastrointestinal tract and kidney, with distinct subcellular (apical or basolateral) localization (Soleimani *et al*, 2006). These include: SLC26A3 in the pancreas (Ko *et al*, 2002) and intestine (Melvin *et al*, 1999); SLC26A4 in the thyroid and kidney (Soleimani *et al*, 2001); SLC26A6 in the pancreas (Ko *et al*, 2002) and intestine (Wang *et al*, 2006); SLC26A7 in the stomach (Petrovic *et al*, 2003) and kidney (Petrovic *et al*, 2004).

More recent functional measurements in *Xenopus* oocytes and HEK (human embryonic kidney) cells transfected with SLC26A7 showed that SLC26A7 functions as a Cl^- channel, since the extent of the Cl^- current was unaffected by HCO_3^- indicating that SLC26A7 is impermeable to HCO_3^- (Kim *et al*, 2005). Also, as the presence of HCO_3^- increased the selectivity of SLC26A7 for Cl^- due to the regulation of the channel by $[H^+]_i$, it was proposed that SLC26A7 may function as a pH_i sensor (Kim *et al*, 2005). SLC26A9 was also demonstrated to mediate Cl^-/HCO_3^- exchange activity when expressed in transfected *Xenopus* oocytes (Chang *et al*, 2009) and HEK cells (Xu *et al*, 2005). However, like SLC26A7, SLC26A9-mediated currents resemble a Cl^- channel with minimal permeability to HCO_3^- (Dorwart *et al*, 2007; see section 3.11.1 for further discussion). SLC26A3 appears to function both as a coupled anion exchanger and as a channel depending on the ions being transported (Shcheynikov *et al*, 2006). Evidence for SLC26A3 functioning as an anion channel was obtained when NO_3^- and SCN^- were used as substrates in oocytes and HEK cells expressing SLC26A3. Replacing Cl^- with NO_3^- (or SCN^-) in HEPES-buffered media produced a rapid increase in the outward current, measured at ~ +60 mV, due to influx of NO_3^-,

indicating that SLC26A3 has an anion channel capability that can conduct NO_3^- or SCN^- under these conditions.

Cl^-/HCO_3^- exchange mediated by SLC26A3 and SLC26A6, but not SLC26A4, can be inhibited by the anion transport inhibitor, DIDS, although the DIDS-sensitivity of SLC26A3 remains controversial. Intracellular Cl^- and pH measurements in SLC26A3 transfected HEK cells, using Cl^- and pH sensitive dyes (MQAE and BCECF, respectively), showed that SLC26A3 mediated Cl^-/HCO_3^- exchange could only be inhibited by ~22% in the presence of 1 mM DIDS and ~45% with 4 mM DIDS (Lamprecht *et al*, 2005). Similar experiments performed in SLC26A6 transfected *Xenopus* oocytes, demonstrated that SLC26A6 Cl^--dependent changes in oocyte pH_i could be abolished by 5 μM DIDS (Shcheynikov *et al*, 2006). Cl^- uptake measurements in the HEK-Phoenix cell line, showed that SLC26A4 overexpression (by SLC26A4 transfection) lead to an increase in Cl^- uptake, above the levels achieved in cells expressing endogenous levels of SLC26A4, which could not be significantly inhibited by 0.5 mM DIDS (Dossena *et al*, 2006). It is noteworthy that H_2-DIDS (a DIDS derivate that does not interfere with fluorescence) was shown to have no effect on anion transport through CFTR when applied externally (Haws *et al*, 1992), but DIDS can inhibit CFTR when added to the intracellular side of the membrane (Linsdell & Hanrahan, 1996).

The stoichiometry of Cl^-/HCO_3^- exchange appears to differ between SLC26 homologs, as determined by simultaneous measurements of HCO_3^- and Cl^- fluxes in transfected *Xenopus* oocytes, such that SLC26A3 transports Cl^- ≥2 ions per HCO_3^- ion, whereas SLC26A6 transports HCO_3^- ≥2 ions per Cl^- ion (Shcheynikov *et al*,

2006). The proposed 1:2 stoichiometry of the SLC26A6 Cl^-/HCO_3^- exchanger, was substantiated by the finding that luminal Cl^- removal, in guinea pig pancreatic duct cells expressing SLC26A6 (Stewart *et al*, 2009) or in SLC26A6 transfected *Xenopus* oocytes (Xie *et al*, 2002), caused membrane hyperpolarisation. However, functional studies using human SLC26A6 polypeptide variants, found SLC26A6 to exhibit electroneutral anion exchange (Chernova *et al*, 2005). The same study also discovered that mouse and human SLC26A6 proteins expressed in *Xenopus* oocytes, differ in their overall anion selectivity and transport mechanism. Therefore species differences must be taken into account when drawing comparisons between SLC26 protein function in human and animal tissue.

1.5.2 Regulation of SLC26 Cl^-/HCO_3^- exchangers by CFTR

Early patch-clamp studies investigating HCO_3^- transport across the luminal membrane of pancreatic duct cells, suggested that an apical Cl^- conductance (CFTR) working in parallel with a Cl^-/HCO_3^- exchanger, provided the mechanism for electrogenic HCO_3^- secretion by these cells (Gray *et al*, 1988; Novak *et al*, 1988). Analysis of tracheal epithelial cells isolated from CF patients (deltaF508 mutation) revealed that a SLC26A3 Cl^-/HCO_3^- exchanger was abundantly expressed in cells expressing functional CFTR, but not in cells that lacked CFTR or that expressed mutant CFTR (Wheat *et al*, 2000). Subsequent results have shown a direct interaction between apically co-localised SLC26 exchangers and CFTR in other tissues (Ko *et al*, 2002). For CFTR to regulate members of the SLC26 family, they need to exist in the same HCO_3^--transporting complex. Immunoprecipitation of pancreatic SLC26A3 caused CFTR to be co-immunoprecipitated from wild-type, but not in CF-deltaF508 mice, providing evidence for such a complex (Ko *et al*, 2002).

All ten of the mammalian SLC26 proteins, predict a hydrophobic core, for which the details of membrane topology are as yet unknown. However, since the amino- and carboxyl-terminal domains of SLC26A3 and A6 are intracellular, it is expected that these proteins span the plasma membrane 10 to 14 times (Mount & Romero, 2004; Dorwart *et al*, 2008). Some SLC26 proteins end with a class I PDZ interaction motif at their carboxyl terminus (Songyang *et al*, 1997), with the exception of SLC26A1, A2, A4, A5 and A11. PDZ (acronym representing the first three identified PDZ-containing proteins: PSD95, DLG, ZO-1) domains are protein-protein interaction domains that play an essential role in the assembly of multiprotein complexes involved in determining cell polarity, plasma membrane targeting and regulation of membrane proteins (Fanning & Anderson, 1999). PDZ domains mediate interactions between the carboxyl terminals of proteins that terminate in consensus PDZ binding sequences (Songyang *et al*, 1997). The CFTR PDZ interaction domain (TRL), has been shown to be required for binding to related PDZ domain proteins including Na^+/H^+ exchanger 3 (NHE3) regulatory factor (NHERF) and NHE3 kinase A regulatory protein (E3KARP) in Calu-3 cells (Sun *et al*, 2000). These interaction motifs may not be necessary for SLC26 transport function, as functional expression of SLC26A6 and three alternatively spliced variants of SLC26A6 with truncated carboxyl terminals in *Xenopus* oocytes, showed no difference between the Cl^- and SO_4^{2-} transport of the mutated and WT proteins (Lohi *et al*, 2003). However, interestingly the same study demonstrated by *in vitro* binding assays, that the carboxyl terminus of SLC26A6, which contains a PDZ interaction motif identical to that of CFTR, interacts with both NHERF and E3KARP, and that truncation of the carboxyl terminus abrogated these interactions.

The carboxyl-terminal cytoplasmic domain of all ten SLC26 proteins includes the STAS (Sulfate Transporter and Anti-Sigma) domain, uncovered due to the homology between the SLC26 gene family and bacterial anti-sigma factor antagonists (Aravind & Koonin, 2000). Structural analyses have indicated that CFTR and SLC26 transporters interact through their R and STAS domains, respectively (Ko *et al*, 2004). This interaction is enhanced by R domain phosphorylation by PKA, since co-immunoprecipitation of the STAS and R domains was higher from cells (HEK cells transfected with CFTR and SLC26A3) stimulated with forskolin (to activate PKA) than in cells treated with the PKA inhibitor H-89. The interaction between the SLC26 exchanger and CFTR is also modulated by PDZ-scaffold proteins, such as EBP50, that tether the two transporters into a multimeric complex with other regulatory proteins (Ko *et al*, 2004). These molecular interactions, in most cases, mutually stimulate the transport activity of both CFTR and the SLC26 exchanger, resulting in enhanced bicarbonate and fluid secretion from epithelial tissues. This structural coupling is summarised in **Figure 1.03**.

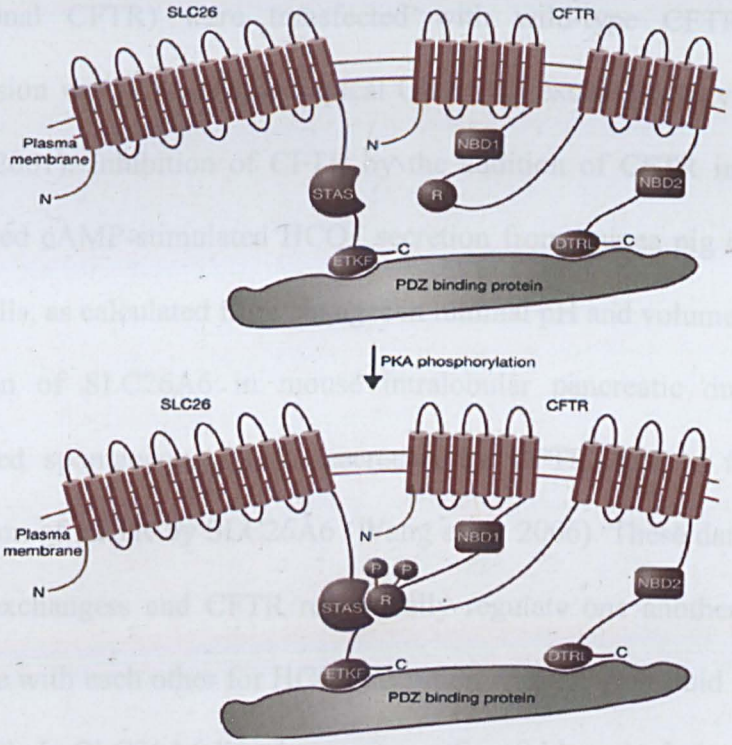

Figure 1.03 - Interactions between CFTR and SLC26 transporters. CFTR and SLC26 are envisaged to interact through binding of their respective R and STAS domains, a process that is enhanced by PKA-mediated phosphorylation of the CFTR R domain. PDZ-binding proteins, including EBP50 and E3KARP, help assemble all these proteins into a multi-component bicarbonate-transporting complex at the apical membrane of epithelial cells through interactions with the transporter's PDZ-binding motifs. Reproduced from Gray, 2004.

Pancreatic duct HCO_3^- secretion is proposed to be mediated by the co-ordinated transport of CFTR and apical SLC26 Cl^-/HCO_3^- exchange. Both SLC26A3 and SLC26A6 have been identified in pancreatic duct cells by Northern hybridisation and immunohistochemical studies (Greeley *et al*, 2001). SLC26A6 is likely to be the major Cl^-/HCO_3^- exchanger involved in HCO_3^- secretion across the apical membrane of ductal cells, since the apical AE activity present in guinea pig pancreatic duct cells can be inhibited by relatively low concentrations of DIDS (assessed by Cl^--dependent pH_i measurements; Stewart *et al*, 2009) and the co-localisation of CFTR and SLC26A6 in the apical membrane of rat pancreatic intralobular ducts (Shcheynikov *et al*, 2006). Also, when CFPAC-1 cells (human pancreatic cell line which lack

functional CFTR) were transfected with wild-type CFTR, SLC26A6 mRNA expression was enhanced and apical Cl^-/HCO_3^- exchange activity increased (Greeley *et al*, 2001). Inhibition of CFTR by the addition of CFTR inhibitor, $CFTR_{inh}$-172, enhanced cAMP-stimulated HCO_3^- secretion from guinea pig intralobular pancreatic duct cells, as calculated from changes in luminal pH and volume (Stewart *et al*, 2009). Deletion of SLC26A6 in mouse intralobular pancreatic duct cells revealed an enhanced spontaneous HCO_3^- secretion by CFTR, due to the removal of tonic inhibition of CFTR by SLC26A6 (Wang *et al*, 2006). These data suggest that SLC26 anion exchangers and CFTR reciprocally regulate one another, and compensate or compete with each other for HCO_3^- secretion with Cl^--rich fluid in the lumen (Song *et al*, 2009). In SLC26A6 knockout mice, a five-fold upregulation in the expression of SLC26A3 to compensate and potentially replace the function of SLC26A6 in pancreatic ducts was observed (Ishiguro *et al*, 2007). The proposed 2:1 stoichiometry of the SLC26A3 Cl^-/HCO_3^- exchanger is believed to help generate the 140 mM HCO_3^- -rich fluid produced by the pancreatic duct, as an electronetural 1:1 exchanger would be expected to reverse under such conditions.

In the villous epithelium of the duodenum, SLC26A6 mediated Cl^-/HCO_3^- exchange is facilitated by Cl^- 'leak' through CFTR under basal conditions, thus maintaining a favourable outside/inside Cl^- concentration gradient, as determined by the ~35% reduction in apical Cl^-/HCO_3^- exchange activity across the CF villous epithelium. A similar partial inhibition of apical Cl^-/HCO_3^- exchange was observed in WT duodenal epithelium following treatment with the CFTR-selective blocker glibenclamide (Simpson *et al*, 2005).

As well as regulating Cl^-/HCO_3^- exchange, CFTR has also been shown to markedly activate Cl^-/OH^- exchange mediated by SLC26A3, A4 and A6 (Ko *et al*, 2002). Such CFTR-regulated Cl^--OH^- / Cl^--HCO_3^- exchange in the airways, both in the submucosal and surface epithelial cells, may prove to be important in maintaining the pH of the ASL necessary for antimicrobial molecules and ultimately mucociliary clearance. The absence of such anion exchange could lead to a possible acidification of ASL, as has been reported in CF airways, which may further contribute to the characteristic weak lung defence (Coakley *et al*, 2003). Clearance of bacteria could be deficient in low pH due to the reduction in ciliary beat frequency in the bronchial epithelium following the acidification of external pH (Clary-Meinesz *et al*, 1998). In CF depleted PCL, a low pH could "tighten" adhesive interactions between reported membrane-bound mucins and mucins of the mucus layer of the ASL (Matsui *et al*, 1998), by altering the exposure of hydrophobic regions of the mucin molecules (Bhaskar *et al*, 1991), therefore reducing the effectiveness of the mucus against harmful inhaled particles. Also the fact that HCO_3^- secretion often accompanies mucus secretion suggests that HCO_3^- regulation is required for proper mucus production (see section 6.1; Holma & Hegg, 1989; Quinton, 2001; Garcia *et al*, 2009).

The roles of the SLC26 anion exchanger family are well documented in the kidney, intestine and pancreas. This, along with evidence for a reciprocal interaction between SLC26 Cl^-/HCO_3^- transporters and CFTR, suggests that CFTR may mediate HCO_3^- transport via apical SLC26 transporters and therefore SLC26-mediated HCO_3^- transport may play an important role in airway fluid homeostasis and have implications in CF research.

1.6 Aims

As described, most HCO_3^- secreting epithelia possess one or more SLC26 Cl^-/HCO_3^- exchangers, which together with CFTR, mediate HCO_3^- transport across the luminal membrane. In the airways, the apical transporters involved in HCO_3^- secretion remain unclear. Hence, the purpose of this study was to investigate the potential role of SLC26 Cl^-/HCO_3^- exchangers in airway epithelia; specifically in serous cells of the submucosal gland as well as at the airway surface by employing the Calu-3 cell line and primary human bronchial epithelial (HBE) cells, respectively.

The specific aims were:

1) To assess the expression of SLC26 transporters at the RNA level by quantitative real time-PCR in Calu-3 cells and HBE cells in order to identify the SLC26 Cl^-/HCO_3^- exchangers relevant for further study at the protein level.
2) To investigate SLC26 Cl^-/HCO_3^- exchange activity in Calu-3 cells and HBE cells by fluorimetry measurements of Cl^--dependent changes in intracellular pH_i (pH_i), using the fluorescent dye biscarboxyethylcarboxyfluorescein (BCECF).
3) To characterise Cl^-/HCO_3^- exchange activity in Calu-3 cells by anion selectivity and pharmacological studies.
4) To identify the contribution of individual SLC26 transporters using an RNA interference approach.
5) To examine the localisation of SLC26 protein expression in Calu-3 cells by immunocytochemical analysis.

6) To assess the role of CFTR in Calu-3 cell HCO_3^- transport, and its potential regulation of Cl^-/HCO_3^- exchange activity, using CFTR inhibitors and CFTR knockdown Calu-3 cells.

7) To establish the physiological role of Cl^-/HCO_3^- exchange in serous cell HCO_3^- and fluid secretion, by measuring the pH and volume of Calu-3 cell fluid secretion under differing buffer conditions and in the presence of pharmacological agents.

2. Methods

2.1 Cell culture

Routine tissue culture techniques were performed in a class II vertical laminar flow hood (Jouan Ltd, UK). All culture media, media supplements and consumables were obtained sterile or sterilised using a high pressure and temperature autoclave. Cell lines were routinely passaged once per week and frozen stocks were maintained in liquid nitrogen. In all cases culture media and solutions were pre-warmed in a water bath at 37 °C prior to use.

2.1.1 Calu-3 cells

The human adenocarcinoma-derived cell-line, Calu-3 (passage 20-50; Shen *et al*, 1994), were grown in T_{75} Costar cell culture flasks, at an initial seeding density of 3 million cells per flask. Cells were grown in a culture medium containing 30 mls of minimal essential medium eagle (MEME) supplemented with 10% foetal calf serum, 2 mM L-glutamine, 100 Uml^{-1} penicillin, 100 μgml^{-1} streptomycin and 5 mls 100x non-essential amino acids per 500 ml of medium (Sigma). The cells were incubated in humidified air containing 5% CO_2 at 37 °C.

CFTR knockdown (KD) Calu-3 cells, provided by Prof. Alan Cuthbert (Cambridge University), produced by small inhibitory RNA persistent down regulation of CFTR using a retroviral vector (MacVinish *et al*, 2007), were cultured in Calu-3 media (as above) supplemented with geneticin (400 µg/ml; G418; Sigma). SLC26A4, SLC26A9 and cyclophilin B knockdown Calu-3 cells were grown in media supplemented with puromycin (10 µg/ml; Sigma; see section 2.2).

Generally cells reached confluency after 7 days, as determined by light microscopy. To subculture, media was removed and cells were washed 3 times with sterile phosphate buffered saline (PBS; Sigma). Cell flasks were then incubated in 5 ml of trypsin solution (0.05% trypsin and 0.02% ethylenediaminetetraacetic acid, EDTA, in Earle's balanced salt solution; Sigma) for 5-15 minutes in a humidified incubator at 37 °C. Following incubation 15 ml of pre-warmed culture medium was added to the flask and the suspension was agitated gently. The resulting cell suspension was centrifuged at 800g for 5 min. The supernatant was discarded and the cell pellet was re-suspended in 10 ml of media.

Cells were then seeded at 250,000 cells cm^{-2} onto clear Costar Transwell® or Snapwell® inserts (0.45 μm pore size, 1.12 cm^2 surface area), for microfluorimetery and Ussing chamber studies, respectively. Transwells and Snapwells were supplied with 0.5 ml of media to the apical surface and 1.5 ml basolaterally. Cells grown under air-liquid interface (ALI) conditions, spent 5 days submerged before the media from the apical surface was removed from the Transwell/Snapwell insert. Calu-3 cells generally formed a confluent monolayer after 5 days growth on Transwell inserts, with an organised cytoskeleton (**Figure 2.01**). Experiments were carried out 7-14 days post-seeding.

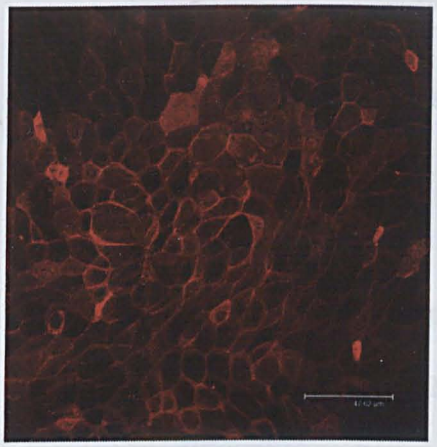

Figure 2.01- Confluent Calu-3 cell monolayer cytoskeleton staining by phalloidin. Phalloidin TRITC staining of the actin cytoskeleton of a confluent Calu-3 cell monolayer grown on a Transwell insert under submerged conditions for 7 days post-seeding. Scale bar represents 47.62 μM.

The integrity (confluence) of the cell monolayer and hence the viability of the cells was routinely assessed by measuring transepithelial resistance (R_T) using an epithelial voltohmmeter (EVOM; World Precision Instruments, UK) attached to 'chopstick' electrodes. Calu-3 cells grown on Transwell inserts normally reached a stable resistance of ~800 $\Omega.cm^2$ after 5-7 days and resistance remained stable for up to a further 7 days (**Figure 2.02**).

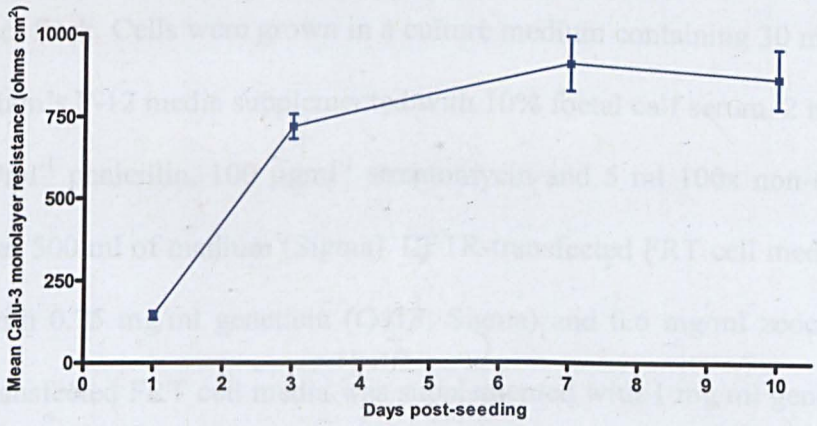

Figure 2.02 - WT Calu-3 cell monolayer resistances. Mean wild-type Calu-3 cell monolayer resistances ($\Omega.cm^2$) after 1, 3, 7 and 10 days post-seeding on Transwell inserts, grown under submerged conditions. The resistance of a blank Transwell insert (without cells) was subtracted from R_T measurements. mean ± S.E.M. n=24.

For $[Ca^{2+}]_i$ measurements, Calu-3 cells were seeded onto 22 mm x 40 mm glass coverslips and grown for 5-7 days submerged in 1 ml of media until confluent.

2.1.2 FRT cells

Fischer rat thyroid (FRT) cells stably transfected with Pendrin or CFTR (Pedemonte *et al*, 2007; Pedemonte *et al*, 2010), were a gift from Dr Luis Galietta (Istituto Giannina Gaslini, Genova, Italy). In brief, human Pendrin was cloned by extracting RNA from human bronchial epithelial cells, which was retrotranscribed into cDNA, from which the full-length Pendrin-coding sequence could be amplified. FRT cells, already expressing the yellow fluorescent protein (YFP)-H148Q/I152L, were transfected with a plasmid vector carrying the Pendrin-coding sequence and neomycin-resistance gene, using lipofectamine. FRT cells were also transfected with a plasmid vector containing wild-type CFTR.

Non-transfected (control), Pendrin-transfected and CFTR-transfected FRT cells were grown in T_{75} Costar cell culture flasks, at an initial seeding density of 2 million cells per flask. Cells were grown in a culture medium containing 30 ml of Coon's modified Ham's F-12 media supplemented with 10% foetal calf serum, 2 mM L-glutamine, 100 Uml^{-1} penicillin, 100 μgml^{-1} streptomycin and 5 ml 100x non-essential amino acids per 500 ml of medium (Sigma). CFTR-transfected FRT cell media was supplemented with 0.75 mg/ml geneticin (G418; Sigma) and 0.6 mg/ml zeocin (Sigma). Pendrin-transfected FRT cell media was supplemented with 1 mg/ml geneticin (G418; Sigma) and 0.5 mg/ml hygromycin (Sigma). The cells were incubated in humidified air containing 5% CO_2 at 37 °C and cultured using the same methods as Calu-3 cells.

2.1.3 Primary human bronchial epithelial cells

Human bronchial epithelial cells (HBE cells; Clonetics) were isolated by an enzymatic method, cultured and harvested for cryopreservation. These cryopreserved cells were then defrosted and grown in 50 ml of bronchial epithelial cell basal media (BEBM) containing BEGM singlequots (Clonetics) in a T-162 flask (Fisher) until confluent. P_1 (passage 1) cells were trypsinised with 10 ml trypsin EDTA at 37 °C for 5 min. Cells were reseeded at 5 x 10^5 cells to T-162 flasks in 50 ml differentiation media containing 50% BEBM: 50% dulbecco's modified eagles medium (DMEM; 4.5g ml^{-1} glucose), BEGM singlequots (without triiodothreonine, retinoic acid and GA1000), gentamicin (1:1000) and *all trans* retinoic acid ($5x10^{-8}$ M; all Clonetics). HBE cells were seeded at $8.25x10^4$ cells/well on Costar Transwell inserts (0.45 μm pore size, 1.12 cm^2 surface area) and fed with differentiation media (as above), 0.5 ml apically and 1.5 ml basolaterally, every 2 days. For SLC26 expression studies, HBE cells were grown on transwells under 3 different protocols: 7 days submerged (submerged protocol); 7 days submerged and 7 days at ALI (D7 protocol); 7 days submerged and 14 days at ALI (D14 protocol). For pH_i experiments, HBE cells were grown using the D14 protocol.

2.2 shRNA knockdown of SLC26A4 and SLC26A9 in Calu-3 cells

SLC26A4, SLC26A9 and cyclophilin B (control) knockdown Calu-3 cells were provided by Dr Emma Hickman (Novartis, Horsham, UK). Short hairpin RNA (shRNA) knockdown of the relevant gene expression was achieved by applying Sigma MISSION lentiviral transduction particles to Calu-3 cells according to the manufacturers instructions, using a multiplicity of infection ratio of 1 and knockdown cells were selected using 10 μg/ml puromycin (Sigma; **Table 2.01**).

Product No.	shRNA Target Sequence	Target Gene
TRCN0000044283	CCGGGCGATTGTGATGATCGCCATTCTCGAGAATGGCGA TCATCACAATCGCTTTTTG	SLC26A4
TRCN0000044284	CCGGCCAGCAGCAATGGAACTGTATCTCGAGATACAGTT CCATTGCTGCTGGTTTTTG	
TRCN0000044285	CCGGCCAACCTGAAAGGGATGTTTACTCGAGTAAACATCC CTTTCAGGTTGGTTTTTG	
TRCN0000044287	CCGGCCCTATCCTGACATACTTTATCTCGAGATAAAGTAT GTCAGGATAGGGTTTTTG	
TRCN0000044049	CCGGCCAGAAAGTATTACTAGCCAACTCGAGTTGGCTAGT AATACTTTCTGGTTTTTG	SLC26A9
TRCN0000044050	CCGGCCCAGGTGTACAATGACATTACTCGAGTAATGTCAT TGTACACCTGGGTTTTTG	
TRCN0000044051	CCGGGTGGGAGAGAAACTTCGCAATCTCGAGATTGCGAA GTTTCTCTCCCACTTTTTG	
TRCN0000044052	CCGGGATCCTGATTTCGGTGCTCAACTCGAGTTGAGCAC CGAAATCAGGATCTTTTTG	
TRCN0000049248	CCGGCCATCGTGTAATCAAGGACTTCTCGAGAAGTCCTTG ATTACACGATGGTTTTTG	cyclophilin B
TRCN0000049249	CCGGCTTCGGAAAGACTGTTCCAAACTCGAGTTTGGAACA GTCTTTCCGAAGTTTTTG	
TRCN0000049250	CCGGCCGGGTGATCTTTGGTCTCTTCTCGAGAAGAGACC AAAGATCACCCGGTTTTTG	
TRCN0000049251	CCGGGTTCTTCATCACGACAGTCAACTCGAGTTGACTGTC GTGATGAAGAACTTTTTG	
TRCN0000049252	CCGGGCCTTAGCTACAGGAGAGAAACTCGAGTTTCTCTC CTGTAGCTAAGGCTTTTTG	

Table 2.01 – SLC26A4, SLC26A9 and cyclophilin B gene shRNA product information.

2.3 Measurement of pH_i

Cells were loaded with 10 μM of the pH-sensitive fluorescent dye, 2',7'-bis-(2-carboxyethyl)-5(6)-carboxyfluorescein acetoxymethyl ester (BCECF-AM), in Hepes-buffered salt solution (composition given below) for 45-60 minutes at 37 °C (Hegyi *et al*, 2004). This time period was chosen as it resulted in little pH_i buffering by BCECF-AM, but achieved sufficient loading to adequately measure changes in pH_i for up to 90 minutes, as monitored by the signal to noise ratio of the fluorescence traces.

Transwells were placed in a perfusion chamber and mounted onto an inverted microscope (Nikon) stage. Cells were brought into focus using a x60 magnification fluorescence lens (Nikon) and perfused with a HCO_3^--buffered Krebs solution, gassed with a 95% O_2, 5% CO_2 mixture at 37 °C, to maintain solution pH at 7.4. The

temperature of the solution was heated to 37 °C by running the perfusion inlet tubes through tubing circulating hot water connected to a water bath. HEPES-buffered solutions were not gassed. Transwell apical and basolateral bath volumes were 0.5 and 1 ml and were perfused at a rate of 3 and 6 ml min^{-1}, respectively. pH_i was measured using a Life Sciences Microfluorimeter System (Life Sciences Resources, UK). To measure pH_i, patches of 15-20 cells were excited alternately at 490 nm and 440 nm wavelengths with a xenon-quartz lamp at a frequency of 2 Hz using a Rainbow filter wheel (Life Sciences Resources, UK) and the fluorescent light emitted by the cells was detected at 535 nm every 512 milliseconds using a photomultiplier tube. The filter wheel was synchronised with the computer data collection software such that photomultiplier tube counts were recorded using photon counters at specified times when light excitation was maximal.

The ratio (R) between the counts at 490 nm (proton-bound BCECF; pH_i-dependent count) and 440 nm (proton-free BCECF; pH_i-independent count) was recorded using PhoCal software and used to calculate pH_i. R values were calibrated to pH_i using the K^+-H^+ exchanger ionophore, nigericin (10μM), in high K^+ solutions of various pH values from 5.6-8.6 (see section 2.10). Nigericin equilibrates pH_i with pH_e, so that pH_i is determined by the high K^+ solution's pH and therefore the R value that results will be equal to the pH of the solution (Marilyn, 1992). An example of a nigericin calibration is shown in **Figure 2.03**.

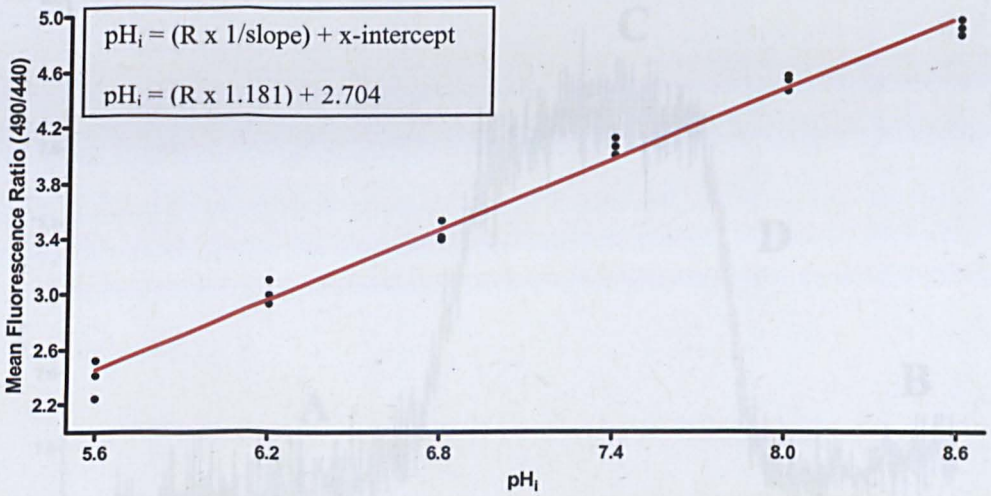

Figure 2.03 - Mean fluorescence ratio-pH_i calibration standard curve for WT Calu-3 cells. Fluorescence ratio (490/440) was measured using high K^+ nigericin solutions of known pH_i values (5.6-8.6) in WT Calu-3 cells. Red line indicates line of best-fit, correlating mean fluorescence data (indicated by black circles; all data points from 3 experiments) with pH_i values. n=3.

2.3.1 Analysis of pH_i data

Mean changes in pH_i were estimated by calculating the average pH_i over 60 second periods (120 data points). Mean pH_i values were calculated immediately before (labelled **A** in **Figure 2.04**) and after (labelled **B**) a new solution was applied, to establish a basal pH_i. This value was then subtracted from the mean pH_i obtained once a new steady state had been established (labelled **C**), to determine the mean change in pH_i. The initial rate of pH_i change ($\Delta pH_i/\Delta t$) was calculated by linear regression fitted to a minimum of 40 data points, upon re-acidification (labelled **D**). Linear regression data were only used with an r^2 (regression coefficient) value >0.5.

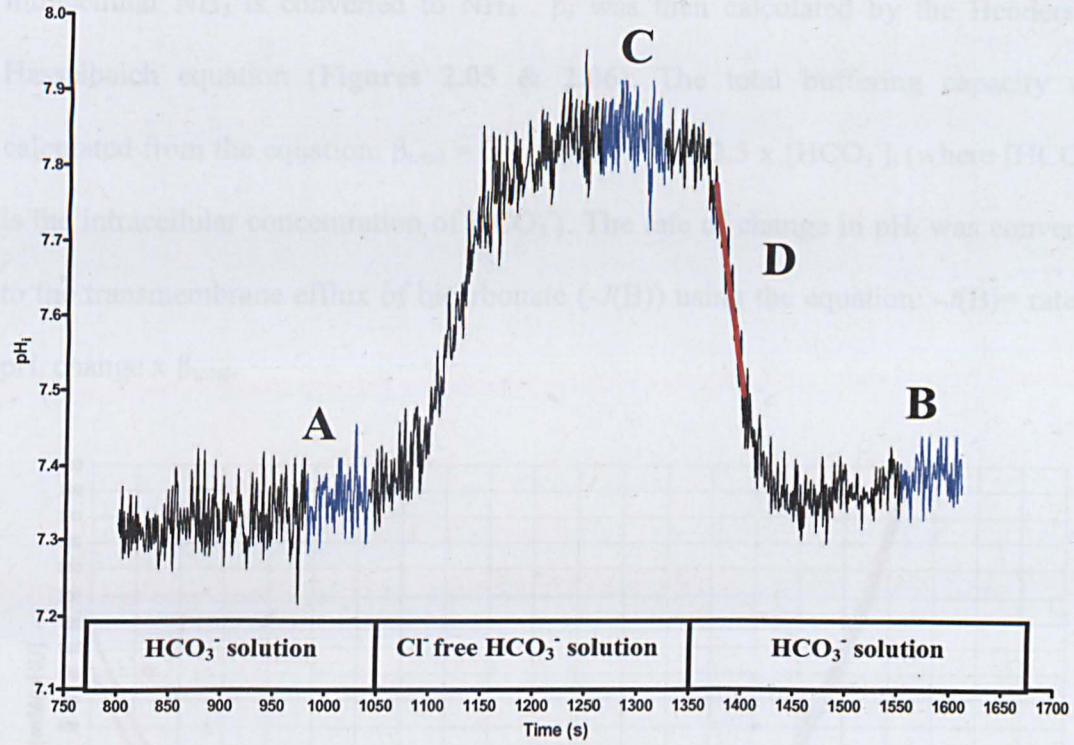

Figure 2.04 - Analysis of pH_i data. Standard zero-Cl^- response, illustrating the effects of standard and Cl^-free HCO_3^--buffered solutions on pH_i in Calu-3 cells. Blue areas indicate data used to calculate mean pH_i change and the red line indicates the plot of linear regression used to determine the rate of pH_i change (re-acidification).

2.3.2 Determination of Calu-3 cell buffering capacity

In order to convert changes in pH_i into rates of base equivalent flux, cellular buffering capacity had to be taken into account. The total intracellular acid/base buffering capacity (β_{total}) is the sum of the CO_2-HCO_3^--dependent buffering capacity ($\beta_{HCO_3^-}$) and the intrinsic CO_2-independent buffering capacity (β_i). Wild-type and CFTR KD Calu-3 cell β_i was estimated using the ammonium pulse technique (Roos & Boron, 1981). Cells were exposed to varying concentrations of NH_4Cl (0, 2.5, 5, 10, 20, 30 mM/L) in the absence of Na^+ and HCO_3^- from the bath solution to block Na^+- and HCO_3^--dependent pH regulatory mechanisms (see solutions section 2.10). Exposure of cells to a solution of NH_3-NH_4^+ leads to the rapid entry of membrane-permanent NH_3 into the cell, causing an alkalinisation in pH_i due to the consumption of H^+ as

intracellular NH_3 is converted to NH_4^+. β_i was then calculated by the Henderson-Hasselbalch equation (**Figures 2.05 & 2.06**). The total buffering capacity was calculated from the equation: $\beta_{total} = \beta_i + \beta_{HCO_3^-} = \beta_i + 2.3 \times [HCO_3^-]_i$ (where $[HCO_3^-]_i$ is the intracellular concentration of HCO_3^-). The rate of change in pH_i was converted to the transmembrane efflux of bicarbonate ($-J(B)$) using the equation: $-J(B)$= rate of pH_i change x β_{total}.

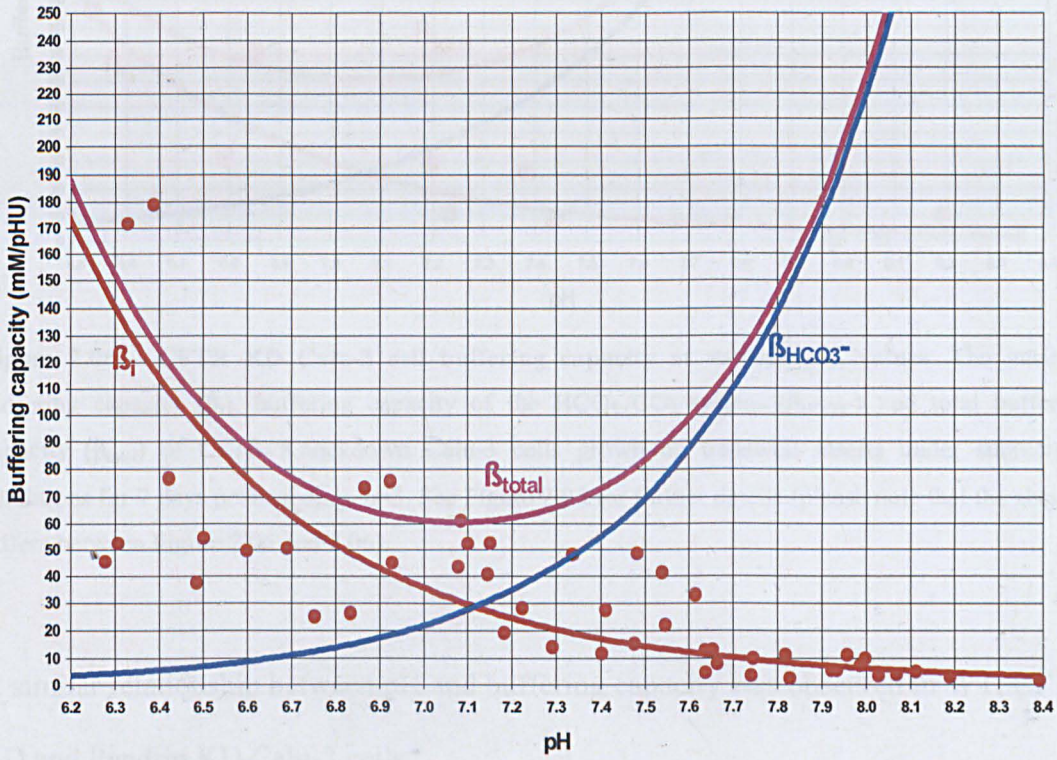

Figure 2.05 – Wild-type Calu-3 cell buffering capacity at various pH_i values. The intrinsic buffering capacity (β_i), buffering capacity of the HCO_3^-/CO_2 system ($\beta_{HCO_3^-}$) and total buffering capacity (β_{total}) of WT Calu-3 cells grown on transwell inserts under submerged conditions for 7 days post-seeding. n=4. Lines indicate line of best-fit, correlating mean fluorescence data (all data points from 4 experiments).

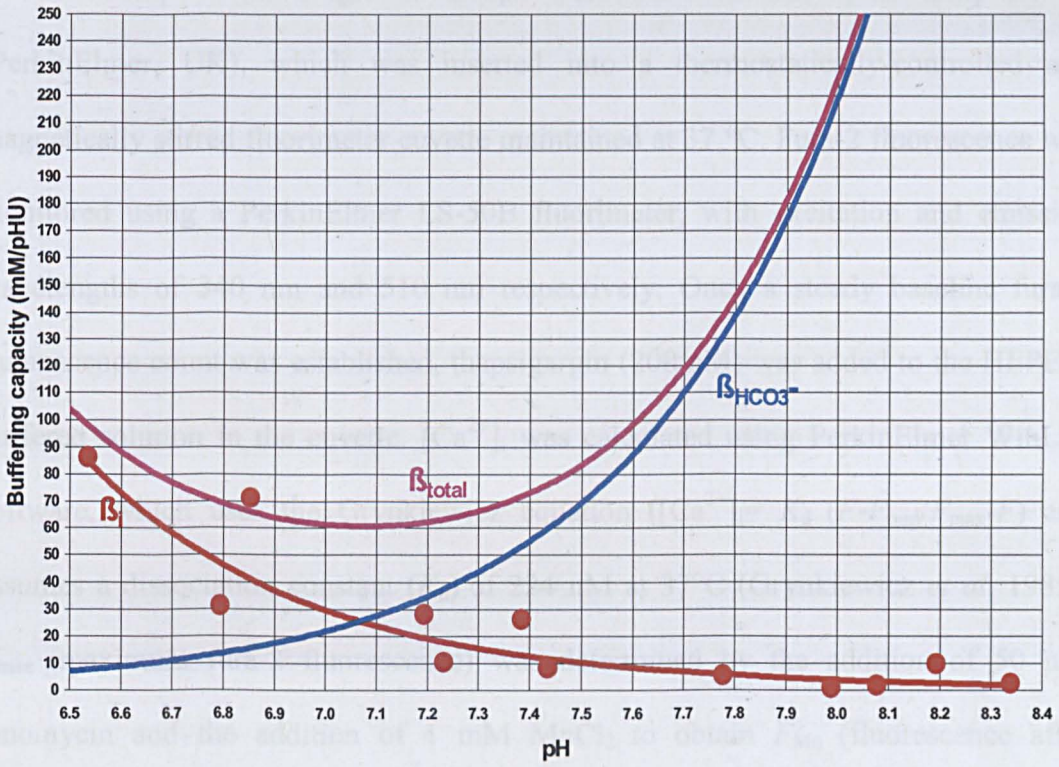

Figure 2.06 – CFTR KD Calu-3 cell buffering capacity at various pH_i values. The intrinsic buffering capacity (β_i), buffering capacity of the HCO_3^-/CO_2 system (β_{HCO3-}) and total buffering capacity (β_{total}) of CFTR Knockdown Calu-3 cells grown on transwell inserts under submerged conditions for 7 days post-seeding. n=3. See Figure 2.05 for further details (please note that the absicca differs between Figure 2.05 and 2.06).

A similar relationship between pH and buffering capacity was observed in WT, CFTR KD and Pendrin KD Calu-3 cells.

2.4 Measurement of $[Ca^{2+}]_i$

$[Ca^{2+}]_i$ was measured in confluent Calu-3 cell monolayers grown on coverslips, using the Ca^{2+}-sensitive dye, fura-2, in a methodology similar to that previously described in neuroblastoma cells (Brown *et al*, 2005). Cells were washed in HEPES-buffered solution, and loaded with fura-2 by incubating coverslips in a solution of 3 μM Fura-2 acetoxymethyl ester (AM; Molecular Probes) in HEPES buffered solution for 45 min

at room temperature. Single coverslips were mounted into a coverslip holder (PerkinElmer, UK), which was inserted into a thermostatically-controlled and magnetically stirred fluorimeter cuvette maintained at 37 °C. Fura-2 fluorescence was monitored using a PerkinElmer LS-50B fluorimeter, with excitation and emission wavelengths of 340 nm and 510 nm respectively. Once a steady baseline fura-2 fluorescence count was established, thapsigargin (200 nM) was added to the HEPES-buffered solution in the cuvette. $[Ca^{2+}]_i$ was calculated using PerkinElmer WinLab software, which uses the Grynkiewicz equation ($[Ca^{2+}]_i = K_d\ (F-F_{min}/F_{max}-F)$ and assumes a dissociation constant (K_d) of 224 nM at 37°C (Grynkiewicz *et al*, 1985). F_{max} (maximum fura-2 fluorescence) was determined by the addition of 50 μM ionomycin and the addition of 1 mM $MnCl_2$ to obtain F_{Mn} (fluorescence after quenching of fura-2), was used to calculate F_{min} (minimum fura-2 fluorescence) using the equation: $F_{min} = {}^1/_3(F_{max} - F_{Mn}) + F_{Mn}$. *In situ* calibrations were performed at the end of each experiment to account for variations in Calu-3 cell confluence and Fura-2 loading.

2.5 Short-circuit current measurements

Short-circuit current (I_{SC}) measurements were performed on Calu-3 cells cultured on Snapwell inserts, mounted in Ussing-type chambers on a gas and heating manifold (Costar). Cells were submerged in HCO_3^--buffered Krebs solution, perfused with a 95% O_2, 5% CO_2 gas mixture and heated at 37 °C, to maintain solution pH at 7.4. Chambers were connected to an automatic voltage-clamp apparatus (World Precision Instruments) via KCl/agar salt-bridges and reversible electrodes (Ag/AgCl for current passage, calomel for voltage sensing). Two chambers were used simultaneously to allow direct comparison between submerged and ALI grown Calu-3 cells. After 5

minutes of equilibrium in Krebs solution, the offset potential was corrected for using the offset circuit setting on the voltage clamp. In open-circuit mode, the transepithelial voltage was checked (usually around –10 mV for Calu-3 cells), to ensure that electrodes were properly connected and to test for air-bubbles. Then the voltage clamp was switched to short-circuit mode and I_{SC} values were recorded. Agonists and inhibitors were added to the static Krebs solution of the chambers by pipette.

2.6 Fluid and mucin secretion assays

2.6.1 Fluid secretion volume measurements

Confluent Calu-3 cell monolayers, grown for 7-10 days on Costar transwell supports under submerged conditions, were washed three times with PBS (1ml to apical and basolateral compartments) to remove any mucus secretions from the apical surface of the monolayer. PBS was carefully aspirated from the apical and basolateral compartments to ensure no residual fluid remained on either side of the transwell. The rate of fluid secretion was determined by applying 200 µl and 1 ml of Krebs solution to the apical and basolateral surfaces of the cells, respectively, as well as the desired agonist or inhibitor. Cells were placed in a humidified CO_2 incubator at 37 °C and the volume of the apical fluid was measured using an appropriate Gilson pipette, after 24/48/72 hours. For HCO_3^--free experiments, Calu-3 transwells bathed in HEPES-buffered solution were placed in a humidified incubator maintained at 37 °C without CO_2 gassing. Krebs solutions were used instead of media for fluid secretion studies, as this allowed alterations to be made to the composition of the external fluid bathing the cells (such as Cl^- removal), in the same way as the pH_i experiments. After the required incubation time the total fluid volume was measured by removing the first 180 µl of apical fluid, with the reminder removed 1 µl at a time, to ensure accuracy.

Evaporation was taken into account by measuring the reduction in the apical volume of fluid on transwells coated with silicone gel to stop fluid leakage across the membrane, which equated to 2.0 ± 0.4 µl/cm^2/24 h (n=12). All fluid secretion values have been corrected for evaporation.

2.6.2 pH measurements of secreted fluid

For pH measurements, the first 180 µl of apical fluid was removed and the pH of this solution measured using a micro pH electrode (Hamilton, Switzerland) attached to a pH meter (pH meter 240, Corning). pH was measured immediately upon removal of the transwell from the incubator, one transwell at a time, to minimise changes in pH when the HCO_3^--buffered solutions were exposed to air. Measurement of the rate of change in pH of the HCO_3^--buffered solutions following removal from the CO_2 gassed incubator, determined that solution pH alkalinised by 0.04 pH units min^{-1}, which should be taken into consideration when approximating the margin of error of these measurements. The remaining fluid volume was then measured and later analysed for mucin content.

2.6.3 PAS assay

The mucin content of the apical fluid was measured using a periodic acid-Shiff's (PAS) assay (Mantle & Allen, 1978). PAS is a non-specific staining method used to detect glycoproteins, such as mucins, through the oxidisation of glucose by periodic acid. This creates aldehydes that react with the Schiff reagent to form a purple stain that can be detected by spectrophotometry. Aliquots of Calu-3 cell fluid secretions were thoroughly mixed and 100 µl sample used for each PAS analysis. The 100 µl secretion sample was made up to 1 ml with deionised water. For the standard curve,

purified digested porcine mucin was used (1mg/ml in deionised water; mucin obtained from Prof. Jeff Pearson, Newcastle University) and diluted into 50, 20, 10, 5, 2 and 1 μg/ml samples using deionised water. As a negative control, a 1:10 dilution of HCO_3^--buffered Krebs solution was used. The fluid secretion, mucin standard curve and negative control samples were individually combined with 100 μl of periodic acid mixture (made from 10 ml of 7% acetic acid plus 20μl of 50% periodic acid) in 5 ml glass test tubes and placed in a water bath for 1 hour at 37 °C, covered with foil to avoid evaporation. Schiffs solution was made by combining 6 ml of Schiffs reagent with 0.1 g sodium metabisulfite in a 10ml test tube, which was also placed in the 37 °C water bath for 1 hour. 100 μl of Schiffs solution was then applied to each sample (including mucin standard curve and negative control samples) and left to develop for 30 minutes at room temperature. The relative PAS staining in each sample was read using a spectrophotometer (UNICAM 8625) at an absorbance wavelength of 555 nm. The negative control Krebs solution was used to set the spectrophotometer reading to zero. The absorbance readings of the Calu-3 fluid secretion samples were then converted to glycoprotein (mucin) concentrations using the standard curve (**Figure 2.07**).

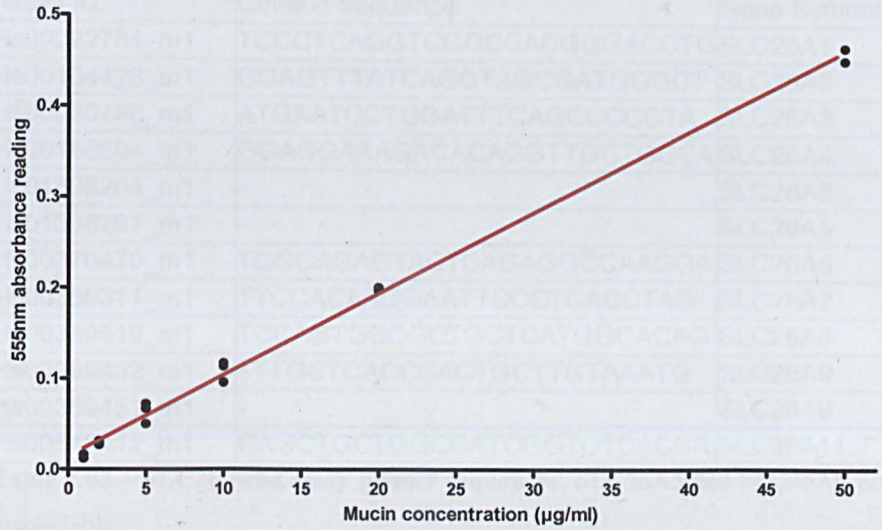

Figure 2.07 – Mucin concentration standard curve. Spectrophotometer 555 nm absorbance readings for known concentrations of digested porcine mucin samples (50, 20, 10, 5, 2 and 1 µg/ml). Red line indicates line of best-fit, correlating mean absorbance readings (indicated by black circles) with mucin concentration.

2.7 Quantitative RT-PCR analysis of SLC26 gene expression

Total RNA was isolated and cDNA prepared as described below. Quantitative RT-PCR (Taqman) analysis was used to ascertain levels of test gene and endogenous control mRNA present in the Calu-3 and HBE cell samples at various time points. Glyceraldehyde 3-phosphate dehydrogenase (GAPDH) was used as a housekeeping gene control and was quantified using pre-optimised Taqman primer probe mixes (Applied Biosystems). SLC26 gene expression was assayed using previously optimized primer probe sets (Applied Biosystems, Assays-on-Demand) described in **Table 2.02** below. Amplicons were designed to span intron-exon boundaries to preclude possible amplification of genomic DNA sequences.

Assay ID	Context Sequence	Gene Symbol	Target Exons
Hs00222784_m1	TCCCTCAGGTCGGCCACGGGACCTG	SLC26A1	1
Hs00164423_m1	GGAGTTTATCAGGTAGCGATGGGCT	SLC26A2	1
Hs00230798_m1	ATGAATCCTGGATTTCAGCCCCCTA	SLC26A3	8
Hs00166504_m1	GGAGGAAAGACACAGGTTGCTGGCA	SLC26A4	10
Hs01398264_m1	-	SLC26A5	4
Hs01398267_m1	-	SLC26A5	7
Hs00370470_m1	TGGCAGAGTACTCAGAGGCCAAGGA	SLC26A6	14
Hs00369311_m1	TTCCACAAGGAATTCCCTCACCTAG	SLC26A7	7
Hs00369519_m1	TCCAGTGCCGCTGCTCATGGCACAG	SLC26A8	2
Hs00369432_m1	TTTGCTCACCCACTGCTTGTAAATG	SLC26A9	1
Hs00369451_m1	-	SLC26A9	20
Hs00543412_m1	GAGCTGCTGGCCATCGGTCTCACCA	SLC26A11	3

Table 2.02 – SLC26 gene assay primer sequences. SLC26A5 and SLC26A9 primer sequences were unavailable.

Total RNA was isolated from HBE cells using the Qiagen RNeasy mini-prep kit according to the manufacturer's instructions. RNA was quantified and checked for purity and integrity using the Bioanalyser 2100 (Agilent Technologies) and RNA total nano chips and reagent kits (Agilent Technologies). cDNA synthesis performed with the GeneAmp RT-PCR kit (Applied Biosystems cat no.N808-0143) as advised by the manufacturer and at a concentration of 20 ng/ml total RNA. A standard was generated from pooled cDNA generated in the same way from commercially manufactured total RNA derived from a variety of human tissues (liver, spleen, kidney, lung, testis, pancreas, brain, and foetal brain – Total RNAs purchased individually from Clontech).

Reactions were performed in 25 µl reaction volumes. 'Assay-on-demand' (FAM-labelled) and Endogenous control (VIC-labelled) Primer/MGB Probe mixes (both from Applied Biosystems) were used at a 1:20 dilution as recommended. Reactions also contained 12.5 µl of 2x Taqman Universal PCR mastermix (Applied Biosystems) and a final volume of 5 µl cDNA at the appropriate dilution. Sterile water was added

to 25 µl and also used as a negative control for cDNA. The standard curve was prepared from serial dilutions of mixed human cDNA to generate total starting RNA curve of 100 ng down to 6.25 ng. The unknown samples were loaded at 50 ng starting RNA per well and all standards and samples were tested in triplicate. Reactions were performed in 96-well optical plates and were analysed on an ABI PRISM 7700 sequence detector (Applied Biosystems) with the following programme: 50 °C for 2 min and 95 °C for 10 min followed by 45 cycles of 95 °C for 15 s and 60 °C 1 min. Data were quantified by the relative method from the standard curve (ABI PRISM 7700 Sequence Detection System. User Bulletin No.2, PE Applied Biosystems, 1997) and RNA expressed as percentage compared to standard curve with normalisation against the individual endogenous controls.

2.8 Immunocytochemistry

Calu-3 cells grown for 7-14 days post-seeding on transwell inserts, were fixed and permeabilised using methanol. This involved washing the transwells with PBS prior to, and following, incubation with cold 100% methanol (-20 °C) for 15 minutes on ice. Following fixation the membrane of the transwell inserts were removed using a scalpel and placed in a 24-well plate.

Non-specific binding sites were blocked by incubating with 3 % horse serum (diluted in PBS) for 1 hour at room temperature on an orbital shaker. The primary antibody, mouse anti-Pendrin polyclonal antibody (Abnova) at 1:200 or mouse anti-CFTR antibody (R & D systems) at 1:200, diluted in 3 % horse serum, was then added and incubated overnight at 4 °C following 1 hour incubation at room temperature on an orbital shaker. Cells were then washed with PBS followed by further blocking with 3

% goat serum in PBS for 1 hour at room temperature on an orbital shaker. Finally, a 1 hour incubation at room temperature on an orbital shaker with goat anti-mouse Alexa Fluor 488 (green; Molecular Probes, Invitrogen) at 1:100 in 3 % goat serum was carried out for secondary detection. Cells were then rinsed in PBS. Control experiments omitted the primary antibody.

In some cases cells were co-stained for the tight junctional protein zona occludens 1 (ZO-1), by applying a rabbit anti-ZO-1 antibody at 1:500, and the secondary antibody, goat anti-rabbit Alexa Fluor 568 (red; Molecular Probes, Invitrogen) in parallel with other primary and secondary antibodies.

The actin cytoskeleton of cells was stained using Alexa Fluor 633 Phalloidin (Molecular Probes, Invitrogen) at a concentration of 1:500.

Following incubation with relevant secondary antibodies, membranes were washed three times in PBS and mounted on a glass microscope slide, sandwiched between a minimal quantity of Vector shield (Molecular Probes, Invitrogen) and overlaid with a coverslip. Cells were imaged using confocal laser scanning microscopy (CLSM) using a Leica TCS-NT system (Leica UK Ltd.) with appropriate excitation and emission filter sets for dual fluorophore detection and *Z* or *XY*-series images collected, using x100 oil immersion lens. *Z*-section images were captured at ~1 μm intervals. For each experiment, positive signals were verified by comparison with no-primary antibody controls. Leica software, under identical conditions of imaging, illumination intensity and photo-multiplier settings for each cell type, was used to capture images.

2.9 Western blot analysis

The relative level of CFTR protein expression in CFTR KD, Cyclophilin B KD (control KD) and Pendrin KD Calu-3 cells, compared to WT Calu-3 cells, was determined by Western blot analysis.

Calu-3 cells on transwell inserts were washed once with ice cold PBS followed by 5 min incubation on ice with modified radio immunoprecipitation assay (RIPA) buffer containing: 50 mM Tris buffer pH 7.5, 1% Nonidet P-40 (Sigma), 0.25% sodium deoxycholate (Sigma), 150 mM sodium chloride (Fisher), 1 mM sodium fluoride (Sigma), 5 mM B-glycerolphosphate (Sigma), 1 complete protease inhibitor cocktail tablet + EDTA (Roche), 0.5 mM phenylmethylsulphonylfluoride (PMSF) (Sigma), 1mM sodium orthovanadate (Sigma), and made up to 50 ml with water. PMSF and sodium orthovanadate were added to aliquots of modified RIPA buffer just prior to use. After incubation with modified RIPA buffer, cells were scraped off transwell inserts using a cell scraper. The cell lysate was then centrifuged at 21,000 g and 4 °C for 10 min to remove cell debris and DNA.

Total cell protein concentration was quantified using using a bicinchoninic acid (BCA) assay. A BCA Protein Assay Kit (Pierce/Uptima) was used according to the manufacturer's instructions. Measurement of the absorbance of a range of bovine serum albumin (BSA) standards (0.025-2 µg; Sigma) at 562 nm and the subsequent construction of a standard curve allowed the protein concentration of unknown samples to be estimated. Samples were analysed using a SpectraMax 250 microplate reader and SOFTmax Pro analysis software (Molecular Devices).

Polyacrylamide gels for electrophoresis were prepared from liquid polyacrylamide before being poured between glass plates that were clamped together with a 1 mm divide. Separating gel consisted of: 375 mM Tris pH 8.8, 10% Acrylamide/Bis 19:1 solution, 0.1% SDS. Stacking gel consisted of: 125 mM Tris pH 6.8, 4% Acrylamide/Bis 19:1 solution, 0.1% SDS. Stacking gel was laid on top of the separating gel and had a comb inlaid to form wells. Protein samples were prepared to contain equal amounts of total protein and SDS sample buffer (50 mM Tris HCl pH 6.8, 2% SDS, 6% glycerol, 0.02% bromophenol blue, and 1% β-mercaptoethanol) before being loaded into the gel wells with a lane reserved for a coloured protein standard (used to estimate the molecular weight of the resulting protein bands).

Gels were immersed in SDS-PAGE running buffer (25 mM Tris Base, 192 mM glycine, 3.5 mM SDS in water) and electrophoresis ran over 1-2 hours at 100 V increasing to 180 V when the loading dye had entered the separating gel. When the protein samples had run far enough through the gel (assessed using the prestained protein standards) the protein was transferred to a nitrocellulose membrane. The gel was placed in a sandwich between blotting paper against the nitrocellulose membrane and immersed in transfer buffer (25 mM Tris Base, 192 mM glycine, 0.35 mM SDS, and 20% methanol in water). Transfer occurred over 1 hour at 100 V incubated at 4 °C. The protein-bound membrane was then removed from the sandwich and blocked by incubation in Tris-buffered saline (TBS; Tris 12.6 mM, NaCl 137 mM adjusted to pH 7.6 with HCl) containing non-fat milk powder (4%) and Tween-20 (0.1%), with mild agitation overnight at 4 °C. This reduces the incidence of non-specific binding directly to the membrane and thus high background signal. The membrane was then incubated with mouse anti-CFTR antibody prepared in the TBS-milk-Tween solution

at a 1:500 dilution, for 2 hours at room temperature, inside a tube with constant rolling. After primary antibody incubation the membrane was washed three times with TBS-0.1% Tween solution before incubation with anti-mouse polyclonal IgG conjugated to horse radish peroxidase (HRP; Abcam) at a 1:1000 dilution (in TBS-milk-Tween solution), for 2 hours at room temperature inside a tube with constant rolling, after which time, the membrane was washed again in TBS-0.1% Tween.

To visualise immunostained proteins, membranes were stained for 5 min with a chemiluminescence solution (ECL Plus Western Blotting Detection Reagent, 6E Healthcare) prepared just before use according to the manufacturer's instructions. The membranes were then imaged using a Fujifilm FLA-3000 fluorescent image analyser.

The antibodies were stripped from the nitrocellulose in order to re-stain the membrane with a GAPDH antibody to double-check the relative concentration of protein in the samples. Nitrocellulose was immersed in stripping buffer (200 mM glycine (Fisher), 3.5 SDS (Fisher), 1% Tween 20 in H_2O with pH adjusted to 2.2) for two 10 min incubations, before two 5 min washes in TBS-0.1% Tween solution, with mild agitation, at room temperature. Membranes were then re-blocked ready for addition of the anti-GAPDH monoclonal antibody (used at dilution of 1:10000; Cell Signaling Technology, UK).

Western blot images were scanned into a computer and analysed using AlphaEaseFC 5.0 Software (Alpha Innotech). The integrated density value (IDV) of each band was measured. The IDV is the sum of the values of the average pixel intensity in the

selection, which is equivalent to the product of the area and mean background pixel intensities. The IDV was corrected for intensity of the background. The selection area remained constant for each set of bands analysed. Graphs and statistical analyses of band IDVs normalised to GAPDH were done using GraphPad Prism software.

2.10 Solutions and reagents

The standard Krebs ringer HCO_3^--buffered (KRB) bath solution contained (in mM): 115 NaCl, 5 KCl, 25 $NaHCO_3$, 1 $MgCl_2$, 1 $CaCl_2$ and 10 D-glucose. In the high K^+ KRB solution, the KCl concentration was increased to 115 mM and NaCl reduced to 5 mM to maintain osmolarity. In the Cl^--free KRB solution, Cl^- was substituted for gluconate, with 6 mM Ca-gluconate replacing 1 mM $CaCl_2$ to compensate for the Ca^{2+} buffering capacity of gluconate and 5 mM KCl was replaced with 2.5 mM K_2SO_4. The Na^+-free KRB solution consisted of (in mM): 115 NMDG-Cl (from a 1M stock solution- pH to 7.0 at 37 °C using HCl), 5 KCl, 1 $MgCl_2$, 1 $CaCl_2$, 25 choline HCO_3^- and 10 D-glucose, with 10 μM atropine added just before use to prevent possible activation of muscarinic receptors by choline.

The HCO_3^--free, HEPES (4-(2-Hydroxyethyl)piperazine-1-ethanesulfonic acid) - buffered solution consisted of (in mM): 130 NaCl, 5 KCl, 1 $MgCl_2$, 1 $CaCl_2$, 10 Na-HEPES and 10 D-glucose. The Cl^--free HEPES-buffered solution contained (in mM): 130 Na-gluconate, 2.5 K_2SO_4, 1 Mg-gluconate, 6 Ca-gluconate, 10 HEPES (free acid) and 10 D-glucose. All HEPES-buffered solutions were set to pH 7.4 by the addition of either HCl or NaOH and HCO_3^- solutions adjusted to pH 7.4 by bubbling with 5% CO_2- 95% O_2 at 37 °C.

High K^+ calibration solutions contained (in mM): 5 NaCl, 130 KCl, 1 $MgCl_2$, 1 $CaCl_2$, 10 Na-HEPES, 10 D-glucose and 10 μM nigericin. High K^+ solutions were made to a range of pH values (5.6-8.6) using HCl. For pH 8.6, a TRIS-buffer was used in place of HEPES. For pH 6.2 and 5.6, MES-buffer was used.

The ammonium pulse solutions (used to calculate buffering capacity) consisted of (in mM): 115 NMDG-Cl, 4.5 KCl, 1 $MgCl_2$, 2 $CaCl_2$, 10 HEPES (free acid), 30 NH_4Cl, 5 $BaCl_2$ and 10 D-glucose (pH to 7.4 at 37 °C using CsOH). The concentration of NH_4Cl was lowered to 20, 10, 5, 2.5 and 0 mM, by replacement with equimolar NMDG-Cl (125, 135, 140, 142.5 and 145 mM respectively).

All stock solutions of agonists and inhibitors used for pH_i and fluid secretion experiments were made in dimethyl sulfoxide (DMSO), except nigericin, fostriecin (both made in 100% ethanol), 8CPT-2Me-cAMP, VIP, carbachol and adenosine (all dissolved in deionised water).

All general chemicals were purchased from Sigma-Aldrich (Sigma-Aldrich Company Ltd., UK), except forskolin (Tocris), BAPTA-AM (Fulka), 8CPT-2Me-cAMP (Tocris) and okadaic acid (Calbiochem).

2.11 Statistical analysis

Statistical analysis was performed using either paired Student's *t* test or one-way ANOVA with Bonferroni's *post hoc* test, depending on the number of groups being analysed. P values of <0.05 were considered statistically significant. Results are presented as mean ± S.E.M, where *n* indicates the number of experiments. All

statistical analysis was undertaken using GraphPad Prism software (GraphPad Software, U.S.A.).

3. Apical Cl^-/HCO_3^- exchange activity in Calu-3 cells

3.1 Introduction

In most HCO_3^- secreting epithelia, apical HCO_3^- transport is mediated via CFTR and Cl^-/HCO_3^- exchange. In airway serous submucosal gland cells, from which the Calu-3 cell line is derived, CFTR is widely regarded as the sole mediator of apical Cl^- and HCO_3^- secretion (Illek *et al*, 1997; Lee *et al*, 1998; Krouse *et* al, 2004). However, the discovery of SLC26 Cl^-/HCO_3^- exchange activity linked to the expression of CFTR in tracheal epithelial cells, has led to some doubt over this hypothesis (Wheat *et al*, 2000).

The presence of Cl^-/HCO_3^- anion exchange (AE) was assessed in Calu-3 cells by the removal and re-addition of Cl^- independently from the apical and basolateral perfusates. Cl^- removal should reverse an active Cl^-/HCO_3^- exchanger, with Cl^- exiting the cell down its concentration gradient, driving HCO_3^- influx and thus raising intracellular pH (pH_i), as has been previously shown in pancreatic duct cells (Zhao *et al*, 1994; Lee *et al*, 1999; Rakonczay *et al*, 2008). Following the subsequent re-addition of Cl^-, a Cl^-/HCO_3^- exchanger would be expected to transport in the forward mode (Cl^-_{IN}: $HCO_3^-_{OUT}$) and thus re-acidify pH_i.

3.2 cAMP-dependent stimulation

Initial experiments focussed upon the potential presence of apical and basolateral Cl^-/HCO_3^- exchange activity under non-stimulated and cAMP-stimulated conditions, by directly activating adenylyl cyclase using forskolin (**Figure 3.01**). Forskolin has been previously shown to stimulate an almost pure HCO_3^- secretion from voltage-clamped Calu-3 cells grown on permeable supports (Devor *et al*, 1999). Under non-stimulated

conditions apical Cl^- removal had no effect on pH_i. However removal of basolateral Cl^- produced an alkalinisation in pH_i of 0.43 ± 0.01 pH units (mean ± s.e.m.; P<0.001 paired t-test; n=35; **Figure 3.02**), which subsequently re-acidified back to baseline pH_i following Cl^- re-addition to the basolateral perfusate at a rate of 0.52 ± 0.03 pH units min^{-1} ($-J(B)$= 49.08 ± 6.96 mM B min^{-1}; n=35).

The addition of forskolin (5 μM added to apical solution) in the presence of bilateral Cl^- (**Figure 3.01**), produced an acidification of 0.13 ± 0.01 pH units (n=35) at a rate of 0.08 ± 0.01 pH units min^{-1} ($-J(B)$= 2.26 ± 0.32 mM B min^{-1}). Forskolin-stimulation produced a 'switch' in AE activity, activating an apical anion exchanger and inhibiting basolateral AE. Apical Cl^- removal caused an alkalinisation of 0.64 ± 0.03 pH units (P<0.001, n=35) after forskolin stimulation (**Figure 3.02**). In contrast to the alkalinisation seen on removal of basolateral Cl^-, this alkalinisation was somewhat biphasic, with an initial fast rate of change, followed by a much slower gradual increase in pH_i until a plateau in pH_i was reached. The rate of this apical AE activity was 0.77 ± 0.08 pH units min^{-1} (P<0.001, n=35) measured following apical Cl^- re-addition ($-J(B)$= 67.26 ± 13.34 mM B min^{-1}). No change in pH_i was observed following the removal of basolateral Cl^- under forskolin-stimulated conditions.

Neither activation of the apical AE nor basolateral AE inhibition was seen upon application of dideoxyforskolin, an inactive analogue of forskolin, confirming that changes in $[cAMP]_i$ are responsible for the forskolin-induced 'switch' in AE activity (P>0.05 compared to non-stimulated apical & basolateral Cl^- dependent changes in pH_i; n=3). The addition of dideoxyforskolin had no significant effect on pH_i.

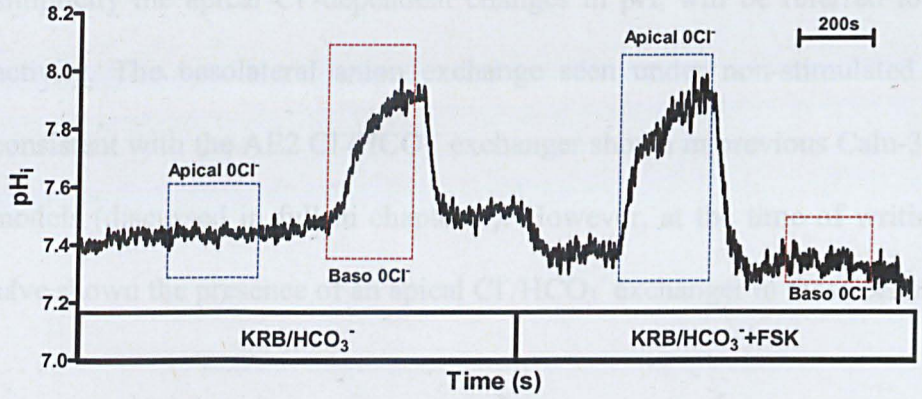

Figure 3.01- pH_i experimental trace of forskolin-induced 'switch' in AE activity in Calu-3 cells. The effects of forskolin (5μM) on changes in pH_i following the independent removal of apical or basolateral chloride in Calu-3 cells. *Apical 0Cl⁻* denotes the removal of apical chloride and *Baso 0Cl⁻* the removal of chloride basolaterally.

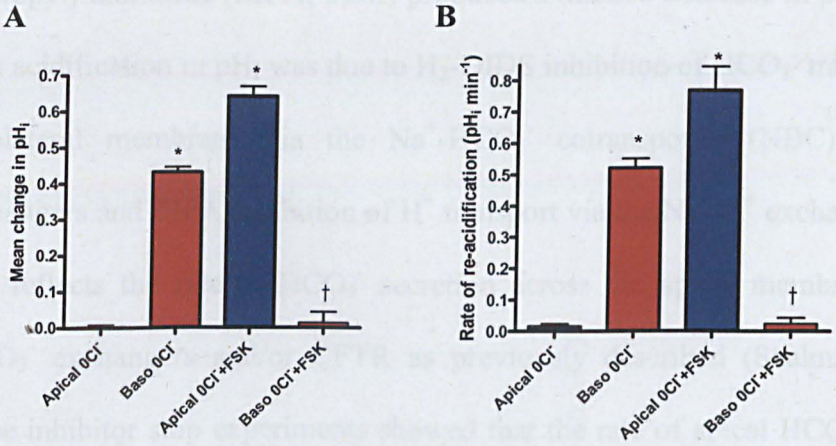

Figure 3.02- Forskolin-induced 'switch' in AE activity in Calu-3 cells. Mean alkalinisation (pH_i) produced by chloride removal (**A**) and the rate of re-acidification upon chloride re-addition in Calu-3 cells (**B**), under non-stimulated and forskolin-stimulated (FSK; 5 μM) conditions. n=35. Paired observations. A: *P<0.001 compared to apical $0Cl^-$. †P<0.001 compared to baso $0Cl^-$. B: *P<0.001 compared to apical $0Cl^-$. †P<0.001 compared to baso $0Cl^-$.

Both the alkalinisation in pH_i produced upon basolateral Cl^- removal in non-stimulated Calu-3 cells and the alkalinisation in pH_i following the removal of apical Cl^- under forskolin-stimulated conditions, are consistent with Cl^-/HCO_3^- exchange activities. However, the apical zero Cl^- induced alkalinisation may also represent Cl^--dependent HCO_3^- influx through CFTR, which will be discussed later, but for

simplicity the apical Cl^--dependent changes in pH_i will be referred to as apical AE activity. The basolateral anion exchange seen under non-stimulated conditions is consistent with the AE2 Cl^-/HCO_3^- exchanger shown in previous Calu-3 cell transport models (discussed in full in chapter 4). However, at the time of writing, no studies have shown the presence of an apical Cl^-/HCO_3^- exchanger in these cells.

HCO_3^- secretion across the apical membrane was investigated using the inhibitor stop method (Hegyi *et al*, 2003). Exposing Calu-3 cells to basolateral 4,4'-diisothiocyano-1,2-diphenylethane-2,2'-disulfonate (H_2-DIDS; 500μM) and 5-(N-Ethyl-N-isopropyl)-amiloride (EIPA; 3μM) produced a marked decrease in pH_i (**Figure 3.03**). This acidification in pH_i was due to H_2-DIDS inhibition of HCO_3^- transport across the basolateral membrane via the Na^+-HCO_3^- cotransporter (NBC) and Cl^-/HCO_3^- exchangers and EIPA inhibition of H^+ transport via the Na^+/H^+ exchanger (NHE), and thus reflects the rate of HCO_3^- secretion across the apical membrane through Cl^-/HCO_3^- exchangers and/or CFTR as previously described (Szalmay *et al*, 2001). These inhibitor stop experiments showed that the rate of apical HCO_3^- secretion was enhanced by forskolin-stimulation ($P<0.05$; n=4; **Figure 3.04**), which complements the stimulation of apical AE by forskolin. This forskolin-mediated increase in the rate of acidification in pH_i could be abolished ($P<0.01$; n=4) by the addition of CFTR pore blocker GlyH-101 (Muanprasat *et al*, 2004; for a general review of the mechanisms of CFTR inhibition see Li & Sheppard, 2009). Interestingly, EIPA addition alone had no significant effect on pH_i in either non-stimulated or forskolin-stimulated Calu-3 cells, suggesting the basolateral NHE does not contribute to pH_i changes under these conditions ($P>0.05$; n=4). The base efflux under non-stimulated and forskolin-stimulated conditions in Calu-3 cells, was approximately a quarter of the base efflux

previously observed in non-stimulated and secretin-stimulated (also elevates cAMP) pancreatic duct cells respectively, which are known to secrete a HCO_3^--rich fluid of ~140 mM [HCO_3^-] (Hegyi et al, 2003).

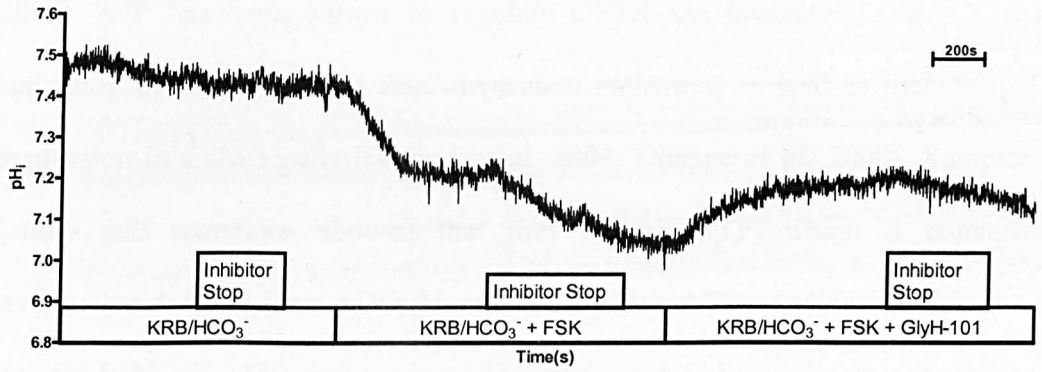

Figure 3.03- pH_i experimental trace of forskolin-stimulated HCO_3^- secretion in Calu-3 cells. Intracellular acidification after basolateral application of H_2-DIDS (500 μM) and amiloride (3 μM) under non-stimulated conditions and forskolin-stimulated (5 μM) conditions in the presence and absence of CFTR inhibitor GlyH-101.

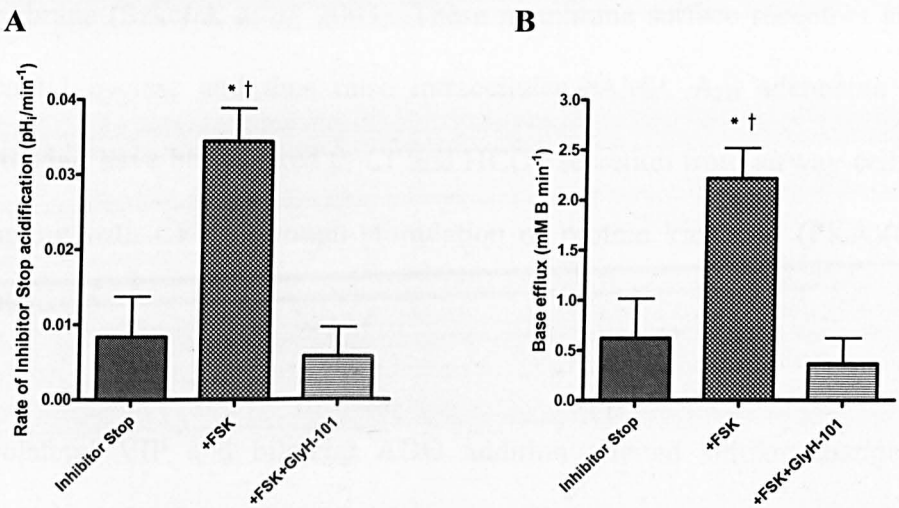

Figure 3.04- Forskolin-stimulated HCO_3^- secretion in Calu-3 cells. The rate of intracellular acidification (pH_i min^{-1}; **A**) and base efflux (mM B min^{-1}; **B**), following the basolateral application of H_2-DIDS and amiloride (inhibitor stop method) under non-stimulated conditions and forskolin-stimulated conditions (+FSK), in the presence and absence of CFTR inhibitor GlyH-101. n=4. Paired observations. A: *P<0.01 compared to control inhibitor stop †P<0.01 compared to inhibitor stop+FSK+GlyH-101. B: *P<0.05 compared to control inhibitor stop †P<0.01 compared to inhibitor stop+FSK+GlyH-101.

The cAMP dependence of the apical AE was further investigated using physiological cAMP agonists vasoactive intestinal peptide (VIP) and adenosine (ADO). VIP released by non-cholinergic neurons innervating airway submucosal glands stimulates a HCO_3^- rich fluid secretion by elevating cAMP and activating CFTR (Wine & Joo, 2004). VIP has been shown to regulate CFTR via basolateral VPAC1 receptor activation of both PKA and PKC-dependent pathways, as well as increasing CFTR expression in Calu-3 cells (Derand *et al*, 2004; Chappe *et al*, 2008). Samples from Calu-3 cell secretions showed that they release ATP, which is converted by ectonucleotidases to form ADO (Huang *et al*, 2001). ATP signalling in Calu-3 cells is thought to be via ADO, rather than ATP itself, since Calu-3 cells do not express P2Y receptors (Communi *et al*, 1999). A_{2A} and A_{2B} adenosine receptor mRNA have been shown to be expressed in Calu-3 cells, with short-circuit measurements indicating the presence of A_{2B} receptors on both membranes and A_{2A} receptors on the basolateral membrane (Szkotak *et al*, 2003). These membrane surface receptors are coupled to adenylyl cyclase and thus raise intracellular cAMP. A_{2B} adenosine receptors, in particular, have been linked to Cl^- and HCO_3^- secretion from airway cells due to their coupling with CFTR through stimulation of protein kinase A (PKA)(Clancy *et al*, 1999).

Basolateral VIP and bilateral ADO addition elicited similar changes in pH_i in response to the removal of apical chloride, compared to forskolin ($P>0.05$; $n=4$; **Figure 3.05**).

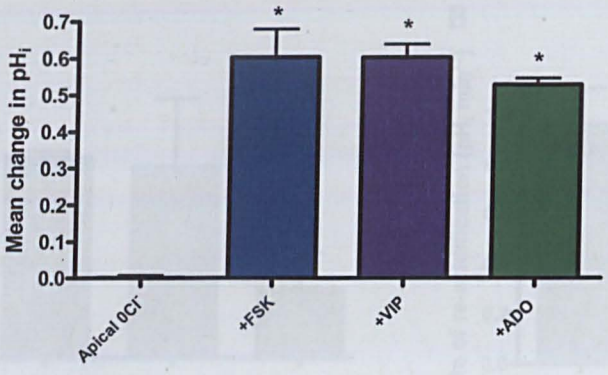

Figure 3.05- cAMP agonists VIP & adenosine stimulate apical AE activity in Calu-3 cells. The effect of apical forskolin (FSK; 5μM), basolateral vasoactive intestinal peptide (VIP; 150nM) and bilateral adenosine (ADO; 10μM) on the mean alkalinisation in pH_i following the removal of apical Cl^- in Calu-3 cells. n=4. Agonists ran in parallel in separate experiments. *P<0.001 compared to apical $0Cl^-$.

Interestingly, the extent of apical AE activation was dependent on which membrane ADO was applied to (**Figure 3.06**). The mean change in pH_i produced in response to apical Cl^- removal after exposure to basolateral ADO was significantly smaller (P<0.05; n=3) compared to bilateral ADO addition. In contrast, apical ADO addition produced a similar stimulation of the apical AE compared to bilateral ADO, highlighting the importance of local changes in cAMP on apical AE activity. This is consistent with the finding that the addition of apical ADO stimulates Cl^- secretion in Calu-3 cells, with little change in intracellular cAMP levels, suggesting localised activation of CFTR by apical adenosine receptors (Huang et al, 2001).

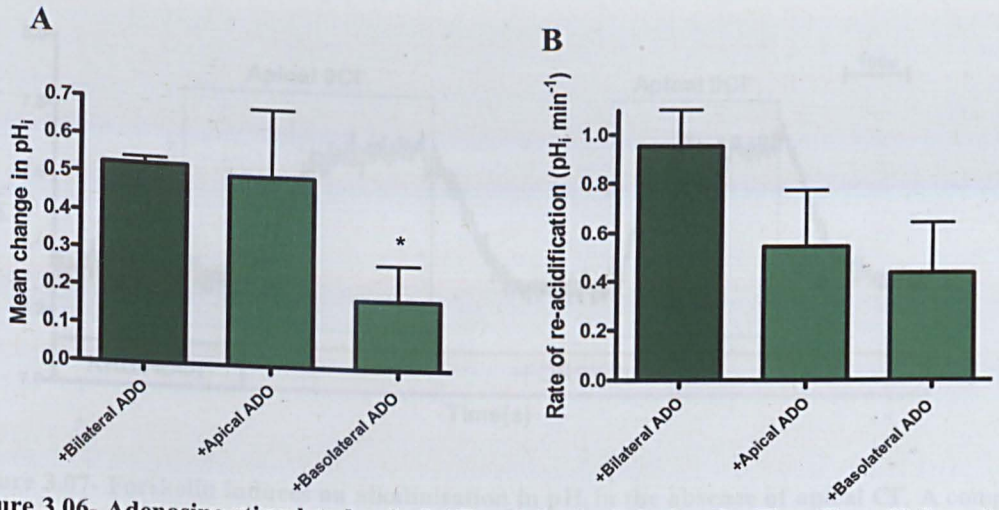

Figure 3.06- Adenosine-stimulated apical AE activity in Calu-3 cells. The effect of bilateral, apical only and basolateral only adenosine (ADO; 10 μM) addition on the mean alkalinisation (pH_i) produced by apical chloride removal (**A**) and the rate of re-acidification upon apical chloride re-addition in Calu-3 cells (**B**). n=3. Each condition ran in parallel in separate experiments. A: *P<0.05 compared to bilateral ADO.

An alternative way of looking at forskolin stimulation of the apical AE was to apply forskolin after the removal of apical Cl^- (**Figure 3.07**). Under these conditions forskolin (5 μM) addition did not produce a gradual alkalinisation in pH_i (response **1**). In the absence of apical Cl^-, forskolin addition produced a rapid alkalinisation in pH_i after 37.5 ± 4.0 s (n=4), at a rate and magnitude (ΔpH_i change) similar to that produced upon removal of apical Cl^- with prior incubation with forskolin (5 μM; response **2**; P>0.05; n=4).

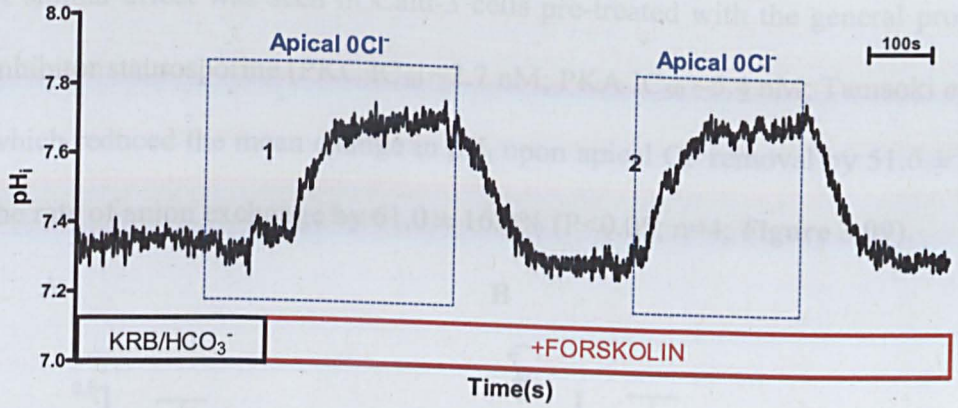

Figure 3.07- Forskolin induces an alkalinisation in pH_i in the absence of apical Cl^-. A comparison between the effects of the addition of forskolin (5 μM) during apical zero Cl^- and the removal of apical Cl^- following prior incubation with forskolin on pH_i in Calu-3 cells.

To further investigate the mechanisms involved in the stimulation of apical AE activity by cAMP, the effects of the protein kinase A (PKA) inhibitor H-89 (50 μM) on AE activity was examined in Calu-3 cells (PKA IC_{50} ~48 nM; Chijiwa *et al*, 1990). **Figure 3.08** shows that the forskolin-stimulated apical AE was inhibited by 64.9 ± 8.9% (mean change in pH_i; $P<0.001$; n=8) in Calu-3 cells treated with H-89, compared to untreated 'control' cells.

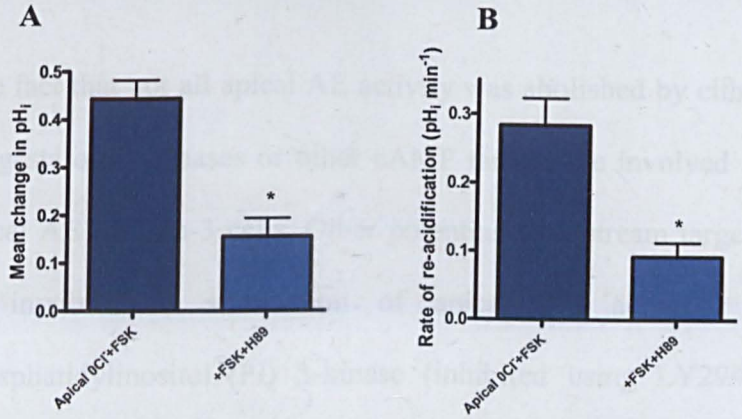

Figure 3.08- Inhibition of apical AE by PKA inhibitor H-89. The effect of PKA inhibitor H-89 (50μM) on the mean alkalinisation (pH_i) produced by apical chloride removal (**A**) and the rate of re-acidification upon apical chloride re-addition in forskolin-stimulated Calu-3 cells (**B**). n=8. Calu-3 cells pre-treated with 50 μM H-89 for 60mins and H-89 present in bilateral solutions throughout the experiments. H-89 treated and untreated Calu-3 cell experiments ran in parallel. A: *$P<0.001$ compared to apical $0Cl^-$+FSK. B: *$P<0.001$ compared to apical $0Cl^-$+FSK.

A similar affect was seen in Calu-3 cells pre-treated with the general protein kinase inhibitor staurosporine (PKC IC_{50} ~2.7 nM; PKA IC_{50} ~5.4 nM; Tamaoki *et al*, 1990), which reduced the mean change in pH_i upon apical Cl^- removal by 51.6 ± 10.9% and the rate of anion exchange by 61.0 ± 16.0% ($P<0.05$; n=4; **Figure 3.09**).

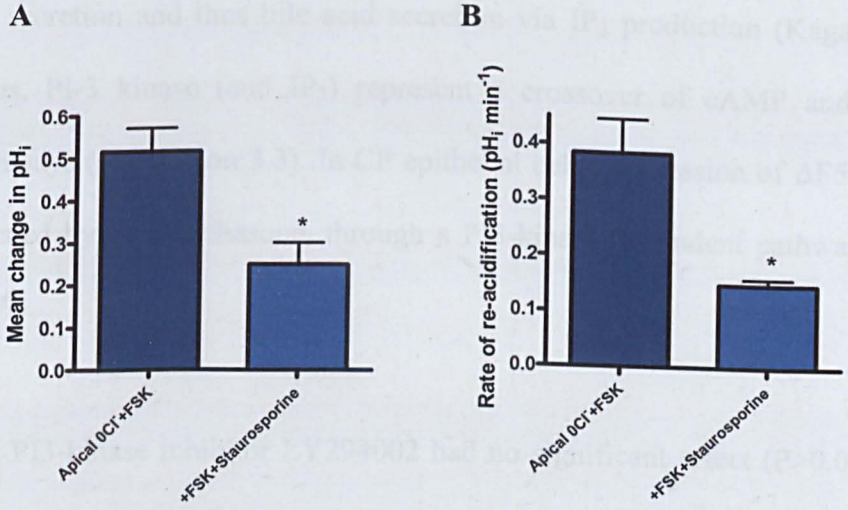

Figure 3.09- Inhibition of apical AE by protein kinase inhibitor staurosporine. The effect of protein kinase inhibitor staurosporine (cells pre-treated with 1 μM staurosporine for 60 mins) on the mean alkalinisation (pH_i) produced by apical chloride removal (**A**) and the rate of re-acidification upon apical chloride re-addition in forskolin-stimulated Calu-3 cells (**B**). n=4. Staurosporine treated and untreated Calu-3 cell experiments were run in parallel. A: *P<0.05 compared to apical $0Cl^-$+FSK. B: *P<0.05 compared to apical $0Cl^-$+FSK.

The fact that not all apical AE activity was abolished by either H-89 or staurosporine suggests other kinases or other cAMP targets are involved in the stimulation of the apical AE in Calu-3 cells. Other potential downstream targets of cAMP, which may be involved in stimulation of apical AE activity, were tested including phosphatidylinositol (PI) 3-kinase (inhibited using LY294002) and the guanine-nucleotide exchange protein directly activated by cAMP (Epac; stimulated using agonist 8CPT-2Me-cAMP). PI-3 kinases are members of the PI kinase family of enzymes that convert PI to PI phosphates, which in turn can be cleaved to form inositol 1,4,5-trisphosphate (IP_3). IP_3 is an important secondary messenger as it

elevates $[Ca^{2+}]_i$ by promoting Ca^{2+} release from intracellular stores such as the endoplasmic reticulum. Studies of Cl^- currents using the path-clamp technique demonstrate that PI3-kinase is involved in bile secretion from biliary epithelial cells (Feranchak *et al*, 1999). cAMP activates PI3-kinase activity, which in turn stimulates Cl^- secretion and thus bile acid secretion via IP_3 production (Kagawa *et al*, 2002). Thus, PI-3 kinase (and IP_3) represent a crossover of cAMP and Ca^{2+} signalling pathways (see section 3.3). In CF epithelial cells, expression of ΔF508-CFTR can be rescued by dexamethasone, through a PI3-kinase dependent pathway (Caohuy et al, 2009).

The PI3-kinase inhibitor LY294002 had no significant effect (P>0.05) on apical AE activity under either basal or forskolin stimulated conditions (**Figure 3.10**).

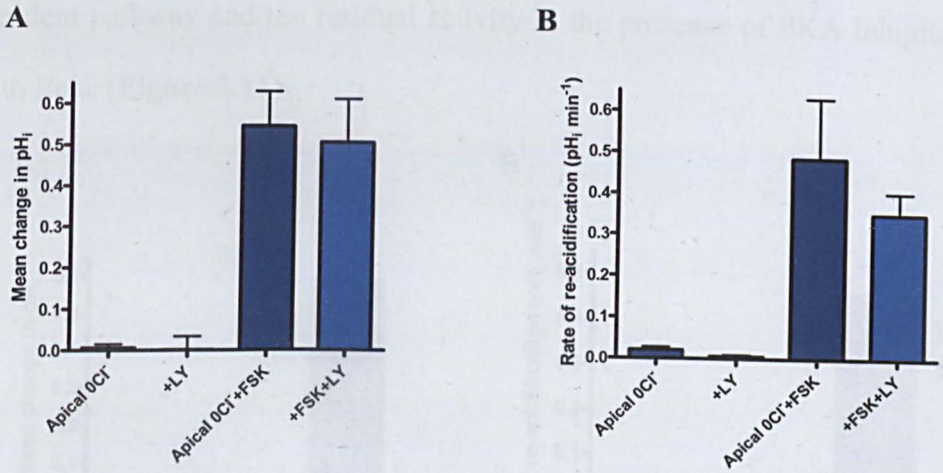

Figure 3.10- PI3-kinase inhibitor LY294402 does not affect Calu-3 apical AE activity. The effects of PI3-kinase inhibitor (LY294402; cells pre-treated with 20 μM LY for 60 mins and LY present in perfusate throughout the experiments) on the mean alkalinisation (pH_i) produced by apical chloride removal (**A**) and the rate of re-acidification upon apical chloride re-addition in unstimulated and forskolin-stimulated Calu-3 cells (**B**). n=4. LY treated and untreated Calu-3 cell experiments ran in parallel.

Epac (1&2) are guanine-nucleotide-exchange factors for the Ras-like small GTPase Rap1 and are directly activated by cAMP (de Rooij *et al*, 1998). Short-circuit current studies demonstrated that Epac1 mediates the PKA-independent stimulation of intestinal Cl^- secretion by forskolin (Hoque *et al*, 2010). The effects of the Epac agonist 8CPT-2Me-cAMP could be abolished by the Ca^{2+} chelator BAPTA-AM, suggesting that, like PI3-kinase in biliary epithelial cells, Epac activates Cl^- secretion by elevating $[Ca^{2+}]_i$. 8CPT-2Me-cAMP has also been shown to stimulate Ca^{2+} release from intracellular Ca^{2+}stores in pancreatic β-cells (Kang *et al*, 2003).

The addition of the membrane permeable Epac agonist 8CPT-2Me-cAMP to the apical perfusate was also unable to stimulate apical AE activity. Furthermore, apical AE in Epac-stimulated cells was still responsive to forskolin. These results suggest that cAMP stimulation of the apical exchanger is predominately through a PKA-dependent pathway and the residual activity in the presence of PKA inhibitors is not due to Epac (**Figure 3.11**).

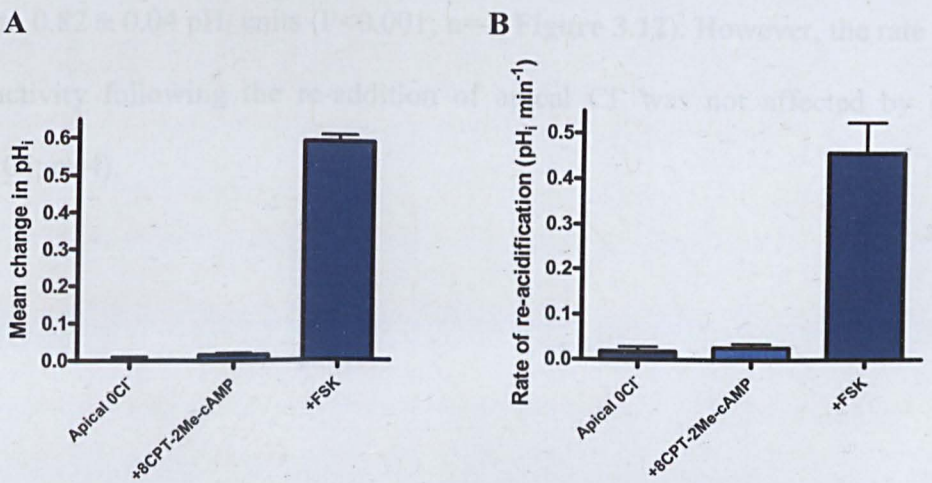

Figure 3.11- Epac activation does not stimulate apical AE activity in Calu-3 cells. The effect of Epac agonist 8CPT-2Me-cAMP (50 μM) on the mean alkalinisation (pH_i) produced by apical chloride removal (**A**) and the rate of re-acidification upon apical chloride re-addition in Calu-3 cells (**B**). n=3. Paired observations from same experiments.

Genistein (4,5,7-trihydroxyisoflavone), is a tyrosine kinase inhibitor (Akiyama *et al*, 1987), but it has been shown to potentiate cAMP-stimulated CFTR activity (Illek *et al*, 1996; Hwang *et al*, 1999). The actions of genistein are thought to involve enhanced phosphorylation of CFTR, via the inhibition of protein phosphatases (Reenstra *et al*, 1996) or by direct binding of genistein to CFTR to alter channel gating (French *et al*, 1997; Hwang *et al*, 1999) and even inducing increased CFTR expression (Schmidt *et al*, 2008). However, elevated concentrations of genistein (100 μM) can inhibit CFTR, by altering channel gating or blocking the channel pore (Lansdell *et al*, 2000). In Calu-3 cells genistein addition alone stimulated chloride efflux and enhanced cAMP-stimulated HCO_3^- and Cl^- currents across the apical membrane (Illek *et al*, 1997). In light of these results I investigated whether genistein might be involved in activating or potentiating apical AE activity.

Genistein did not stimulate apical AE alone, but enhanced the mean change in pH_i upon apical Cl^- removal in the presence of the cAMP agonist forskolin, from 0.62 ± 0.02 to 0.82 ± 0.04 pH_i units ($P<0.001$; n=4; **Figure 3.12**). However, the rate of apical AE activity following the re-addition of apical Cl^- was not affected by genistein ($P>0.05$; n=4).

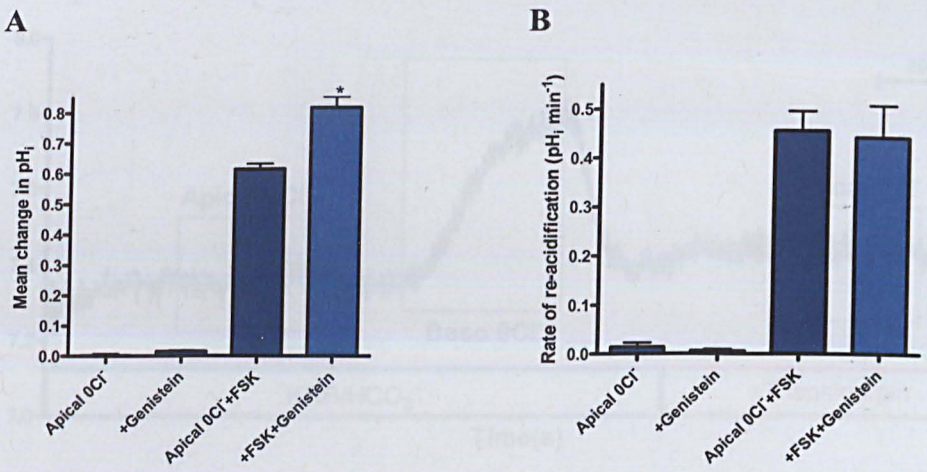

Figure 3.12- Potentiation of apical AE activity by genistein in forskolin-stimulated Calu-3 cells. The effects of genistein (30 μM) on the mean alkalinisation (pH_i) produced by apical chloride removal (**A**) and the rate of re-acidification upon apical chloride re-addition in unstimulated and forskolin-stimulated (5 μM) Calu-3 cells (**B**). n=4. Paired observations. A: *P<0.001 compared to apical $0Cl^-$ +FSK.

3.3 Effects of Ca^{2+} on apical Cl^-/HCO_3^- exchange activity

Calu-3 cells are known to secrete HCO_3^- upon stimulation by both cAMP and Ca^{2+} agonists (Krouse *et al*, 2004). Ca^{2+} is a known to regulate a variety of transporters including anion exchangers (Green et al, 1990). Elevation of $[Ca^{2+}]_i$ is known to stimulate CFTR-dependent Cl^-/HCO_3^- exchange in pancreatic duct cells, as revealed by $[Ca^{2+}]_i$ and pH_i measurements in ATP treated CAPAN-1 cells (Namkung *et al*, 2003). Also since there was potential for cross-talk between cAMP and Ca^{2+} signalling pathways (such as via IP_3), it was important to test the effects of increases in intracellular Ca^{2+} on apical AE activity in Calu-3 cells. Thapsigargin, which raises $[Ca^{2+}]_i$ by inhibiting Ca^{2+} uptake into the endoplasmic reticulum through the Ca^{2+} ATPase (Thastrup *et al*, 1990), did not stimulate apical AE activity (**Figure 3.13**). Similarly no apical Cl^-/HCO_3^- exchange could be seen following carbachol addition (**Figure 3.14**).

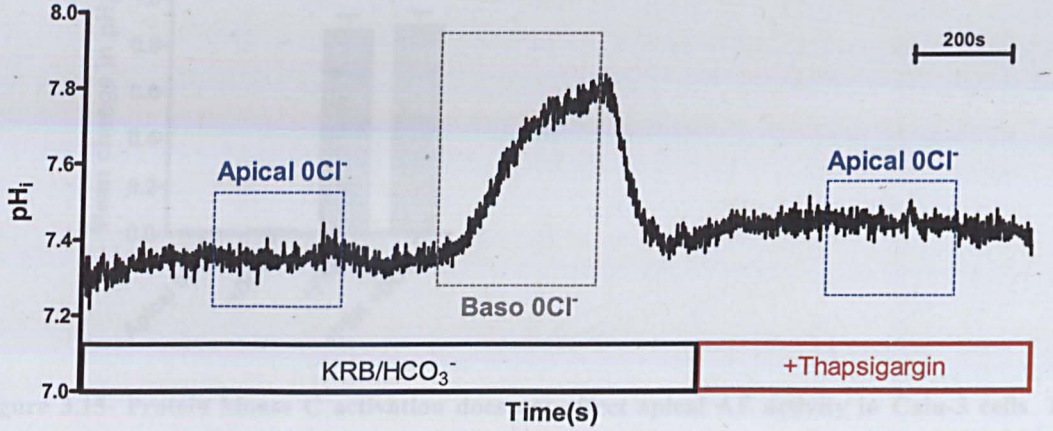

Figure 3.13- Elevation of $[Ca^{2+}]_i$ by thapsigargin fails to stimulate apical AE activity. The effect of thapsigargin (200 nM) on changes in pH_i following the removal of apical or basolateral Cl^- in Calu-3 cells. *Apical 0Cl⁻* denotes the removal of Cl^- from the apical solution and *Baso 0Cl⁻* the removal of Cl^- from the basolateral solution.

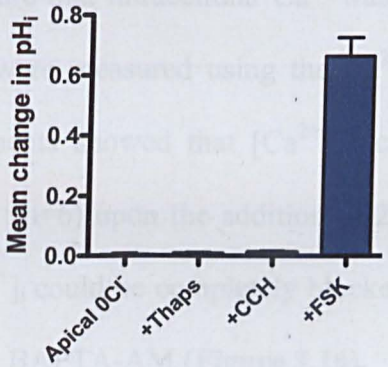

Figure 3.14- Elevation of $[Ca^{2+}]_i$ fails to stimulate apical AE activity. The effects of Ca^{2+} agonists thapsigargin (200 nM) and carbachol (10 μM) on the mean alkalinisation in pH_i following the removal of apical Cl^- in Calu-3 cells. n=4. Each agonist was applied in separate experiments, that were run in parallel.

Ca^{2+} signalling via protein kinase C (PKC) also appears to have little involvement with apical AE activity, since the PKC agonist, 1,2-dioctanoyl-*sn*-glycerol (DOG), failed to either stimulate apical AE under basal conditions or alter apical activity under forskolin-stimulated conditions (**Figure 3.15**).

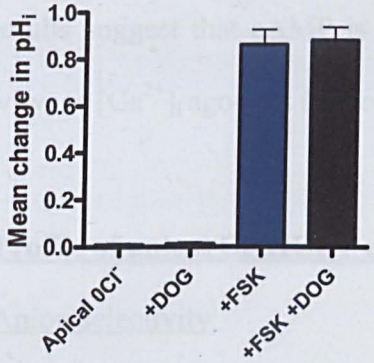

Figure 3.15- Protein kinase C activation does not affect apical AE activity in Calu-3 cells. The effects of PKC agonist DOG (cells pre-treated with 5 μM DOG for 60 mins) on the mean alkalinisation in pH_i following the removal of apical Cl^- in Calu-3 cells. n=4. DOG pre-treated and untreated Calu-3 cell experiments ran in parallel.

To ensure that intracellular Ca^{2+} was being increased under these conditions, $[Ca^{2+}]_i$ levels were measured using the Ca^{2+} sensitive dye FURA-2 (see methods). These experiments showed that $[Ca^{2+}]_i$ increased from 166 ± 35 nM to 581 ± 108 nM ($P<0.01$; n=6) upon the addition of 200 nM thapsigargin. The effect of thapsigargin on $[Ca^{2+}]_i$ could be completely blocked by pre-loading the Calu-3 cells with the Ca^{2+} chelator BAPTA-AM (**Figure 3.16**).

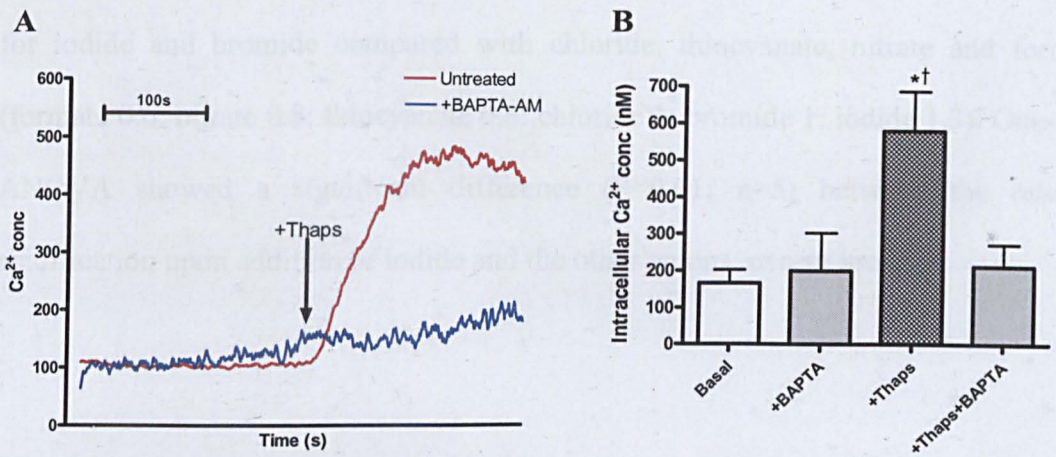

Figure 3.16- Thapsigargin elevates $[Ca^{2+}]_i$ in Calu-3 cells. Raw trace of fura-2 Ca^{2+} experiment (**A**) and the effect of thapsigargin (200 nM) on changes in $[Ca^{2+}]_i$ in untreated and BAPTA-AM (50 μM)

pre-loaded Calu-3 cells (**B**). n=6. BAPTA pre-treated and untreated cell experiments ran in parallel. *P<0.01 compared to basal. †P<0.05 compared to +BAPTA and +Thaps+BAPTA.

These results suggest that cAMP is the primary mediator of the activation of apical AE activity, as $[Ca^{2+}]_i$ agonists fail to stimulate apical AE.

3.4 Profile of apical Cl^-/HCO_3^- exchanger

3.4.1 Anion selectivity

All SLC26 proteins, except SLC26A5, can function as anion exchangers, transporting both monovalent and divalent anions. The modes of transport mediated by SLC26 members include the exchange of chloride for bicarbonate, hydroxyl, sulfate, formate, iodide, thiocyanate or oxalate with variable specificity.

The anion selectivity of the apical AE was then examined by measuring the rate of re-acidification after Cl^- withdrawal from the apical solution, using a range of monovalent (iodide, bromide, nitrate, formate and thiocyanate) and divalent (sulphate and oxalate) anions (**Figure 3.17**). The recovery of pH_i following the re-addition of apical Cl^- could only be mimicked by the equimolar addition of monovalent anions, but with variable rates of recovery (**Figure 3.18**). The exchanger has a greater affinity for iodide and bromide compared with chloride, thiocyanate, nitrate and formate (formate 0.6: nitrate 0.8: thiocyanate 0.8: chloride 1: bromide 1: iodide 1.3). One-way ANOVA showed a significant difference ($P<0.01$; n=5) between the rate of acidification upon addition of iodide and the other anions, except bromide.

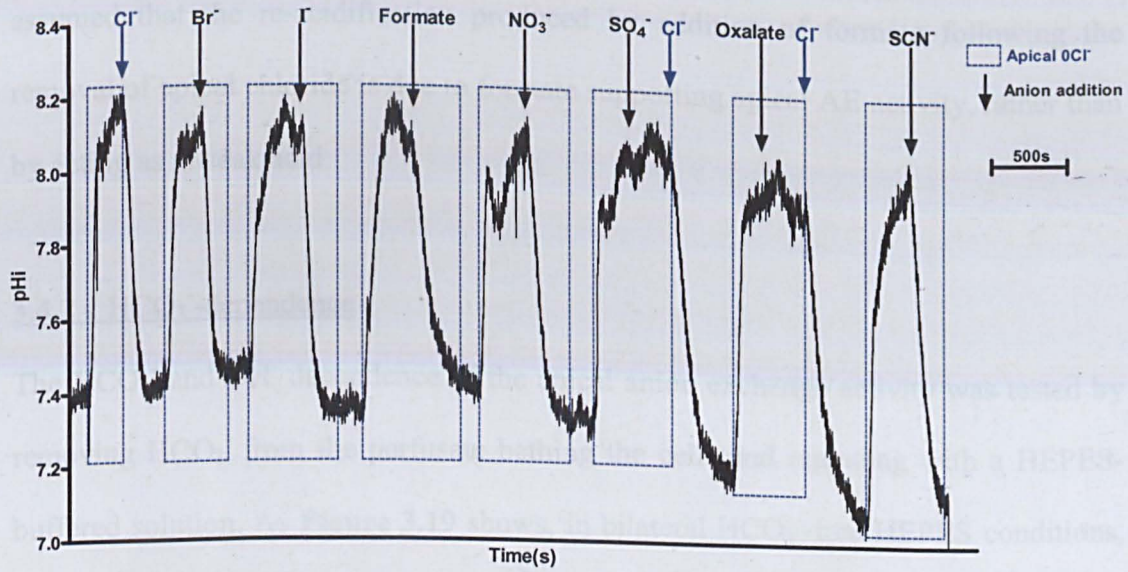

Figure 3.17- pH_i experimental trace of the anion selectivity of apical AE in Calu-3 cells. The recovery of pH_i by the introduction of monovalent (iodide, bromide, nitrate, formate and thiocyanate) and divalent (sulphate and oxalate) anions in zero Cl^- conditions. Equimolar substitution of anions for Cl^- (124mM).

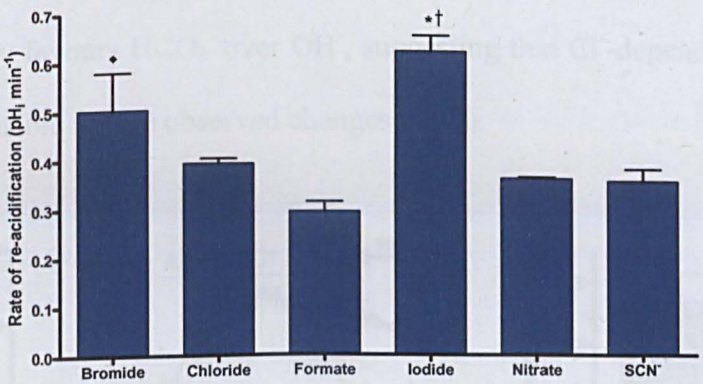

Figure 3.18- Anion selectivity of apical Cl^-/HCO_3^- exchange activity in Calu-3 cells. The rate of recovery of pH_i by the introduction of monovalent anions (iodide, bromide, nitrate, formate and thiocyanate) in apical zero Cl^- conditions. n=5. Paired observations. *P<0.01 compared to chloride. †P<0.001 compared to formate, nitrate and SCN^-. ♦P<0.01 compared to formate.

Because formate is a weak acid, this anion could affect pH_i directly. Exposing the cells to a solution containing 115mM NaFormate did not cause a significant change in pH_i under either non-stimulated (0.004 ± 0.007 pH units; P>0.05; n=3) or forskolin-stimulated conditions (-0.001 ± 0.10 pH units; P>0.05; n=3). Therefore, it can be

assumed that the re-acidification produced by addition of formate following the removal of apical chloride is due to formate supporting apical AE activity, rather than by acting as a weak acid.

3.4.2 HCO_3^--dependence

The HCO_3^- and OH^- dependence of the apical anion exchange activity was tested by removing HCO_3^- from the perfusate bathing the cells and replacing with a HEPES-buffered solution. As **Figure 3.19** shows, in bilateral HCO_3^--free HEPES conditions, Cl^- removal produced a slow alkalinisation in pH_i of 0.27 ± 0.05 pH units, suggesting that there maybe some OH^- transport by the exchanger. However re-addition of external Cl^- only produced a small re-acidification of 0.04 ± 0.03 pH units, which was consistently seen in all HEPES experiments. These data demonstrated that apical AE activity favours HCO_3^- over OH^-, suggesting that Cl^--dependent HCO_3^- transport was responsible for the observed changes in pH_i.

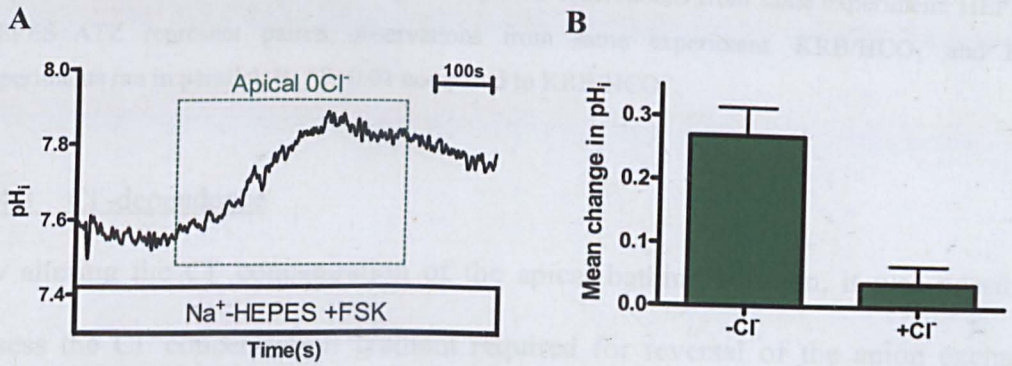

Figure 3.19- Apical AE activity under HCO_3^--free conditions. Raw trace of HEPES experiment (**A**) and the effects of apical chloride removal ($-Cl^-$) and subsequent chloride re-addition ($+Cl^-$) on pH_i under bilateral HCO_3^- free conditions, in forskolin-stimulated (5 μM) Calu-3 cells (**B**). n=4. Paired observations.

To investigate a potential interaction between carbonic anhydrase (CA) and the apical AE, Calu-3 cells were exposed to the potent CA inhibitor acetazolamide (100 μM;

Figure 3.20). Acetazolamide addition had no significant effect on pH_i in cells perfused with HEPES-buffered solutions ($P>0.05$; n=4). Although in the presence of external HCO_3^-, acetazolamide decreased the rate of apical AE activity by 33.7 ± 5.7% ($P<0.01$; n=4).

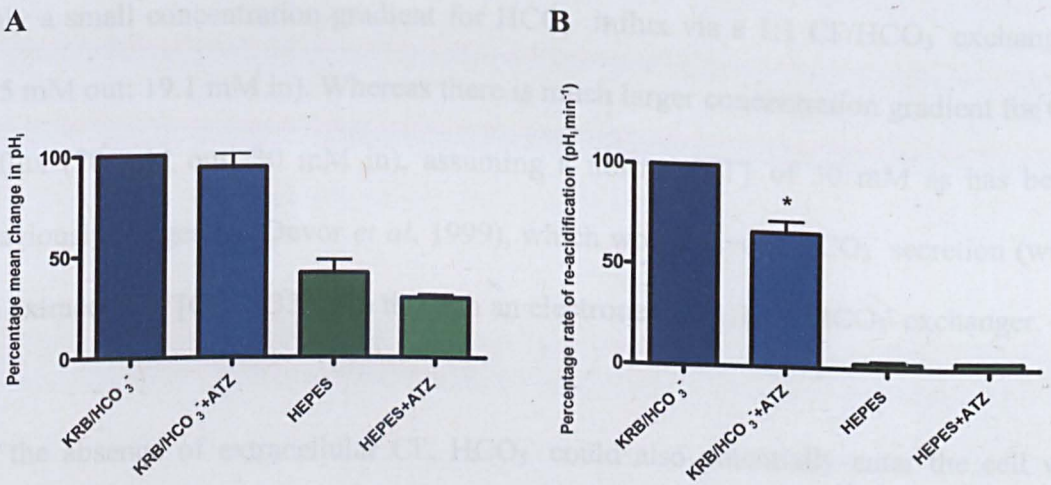

Figure 3.20- Carbonic anhydrase inhibition reduces the rate of apical AE activity. The effect of carbonic anhydase inhibitor acetazolamide (ATZ; 100 μM), in the presence and absence of external HCO_3^-, on the mean alkalinisation (pH_i) produced by apical chloride removal (**A**) and the rate of re-acidification upon apical chloride re-addition in forskolin-stimulated Calu-3 cells (**B**). n=4. KRB/HCO_3^- and KRB/HCO_3^-+ATZ represent paired observations from same experiment. HEPES and HEPES+ATZ represent paired observations from same experiment. KRB/HCO_3^- and HEPES experiments ran in parallel. B: *$P<0.01$ compared to KRB/HCO_3^-.

3.4.3 Cl^--dependence

By altering the Cl^- concentration of the apical bathing solution, it was possible to assess the Cl^- concentration gradient required for reversal of the anion exchanger. Normal [Cl^-] was 124 mM in the standard KRB/HCO_3^- solution and [Cl^-] was isoosmotically replaced with NaGluconate (**Figure 3.21**). Apical AE activity was supported in a concentration-dependent manner from complete Cl^- removal to 70 mM Cl^-. The removal of 24 mM Cl^- (100 mM Cl^- solution) did not produce a significant change in pH_i ($P>0.05$; n=4). If we assume a normal intracellular Cl^- concentration of 30 mM, then with an extracellular [Cl^-] of 0 or 10 mM an apical Cl^-/HCO_3^- exchanger

would be expected to reverse and absorb HCO_3^-. However, in the presence of 70 mM $[Cl^-]$ in the external bathing solution a 1:1 Cl^-/HCO_3^- exchanger would be unlikely to reverse. In forskolin-stimulated Calu-3 cells pH_i is 7.30 ± 0.04, which equates to an $[HCO_3^-]_i$ of 19 mM (using the Henderson-Hasselbach equation). Therefore there is only a small concentration gradient for HCO_3^- influx via a 1:1 Cl^-/HCO_3^- exchanger (25 mM out: 19.1 mM in). Whereas there is much larger concentration gradient for Cl^- influx (70 mM out: 30 mM in), assuming a normal $[Cl^-]_i$ of 30 mM as has been previously suggested (Devor *et al*, 1999), which would favour HCO_3^- secretion (with an extracellular $[Cl^-] > 33$ mM) through an electroneutral 1:1 Cl^-/HCO_3^- exchanger.

In the absence of extracellular Cl^-, HCO_3^- could also potentially enter the cell via CFTR, as Cl^- efflux through CFTR would be expected to depolarise the apical membrane potential, causing HCO_3^- influx driven by the electrical gradient (see section 3.9). Again assuming a $[Cl^-]_i$ of 30 mM, HCO_3^- could potentially be driven through CFTR by a Cl^- gradient, with an extracellular $[Cl^-] < 39$ mM, as determined by the Nernst equation.

Therefore the alkalinisation in pH_i following a decrease in extracellular $[Cl^-]$ from 124 mM to 0/10/30 mM may represent Cl^--dependent HCO_3^- transport by both an apical Cl^-/HCO_3^- exchanger and CFTR. However, neither reversal of a 1:1 Cl^-/HCO_3^- exchanger, nor HCO_3^- influx through CFTR can explain the increase in pH_i observed in the presence of 70 mM extracellular $[Cl^-]$. However, as HCO_3^- transport via a Cl^-/HCO_3^- exchanger is dependent on the Cl^- gradient in both forward and reverse modes, a decrease in extracellular $[Cl^-]$ from 124 mM to 70 mM would decrease the driving force for HCO_3^- secretion and therefore may produce an alkalinisation in pH_i.

Also, lowering external [Cl^-] would depolarise the apical membrane potential and this would reduce HCO_3^- efflux via CFTR, so this could also possibly explain the increase in pH_i at 70 mM extracellular [Cl^-]. Another explanation is that $[Cl^-]_i$ is greater than expected, which in the case of HCO_3^- influx through CFTR would require a $[Cl^-]_i > 53$ mM to counter an extracellular [Cl^-] of 70 mM. Or that HCO_3^- transport under these conditions is mediated by a Cl^-/HCO_3^- exchanger with a stoichiometry of 1:2 or 1:3.

Also, by calculating $[HCO_3^-]_i$ at each of the pH_i values achieved from lowering extracellular [Cl^-], it is possible to determine the equilibrium potential (using the Nernst equation) for both HCO_3^- and Cl^- under each condition (V_{HCO3-} and V_{Cl-}; assuming a $[Cl^-]_i$ of 30 mM). Under each extracellular [Cl^-] tested, V_{HCO3-} and V_{Cl-} varied greatly from one another (e.g. at 70 mM extracellular [Cl^-], $[HCO_3^-]_i$ reaches 31 mM, which equates to V_{HCO3-} of +6 mV; compared to V_{Cl-} of –23 mV, assuming a $[Cl^-]_i$ of 30 mM), suggesting that these changes in pH_i cannot be simply explained by the relative concentration gradients of these two anions alone and that membrane potential is likely to be an important factor in these responses.

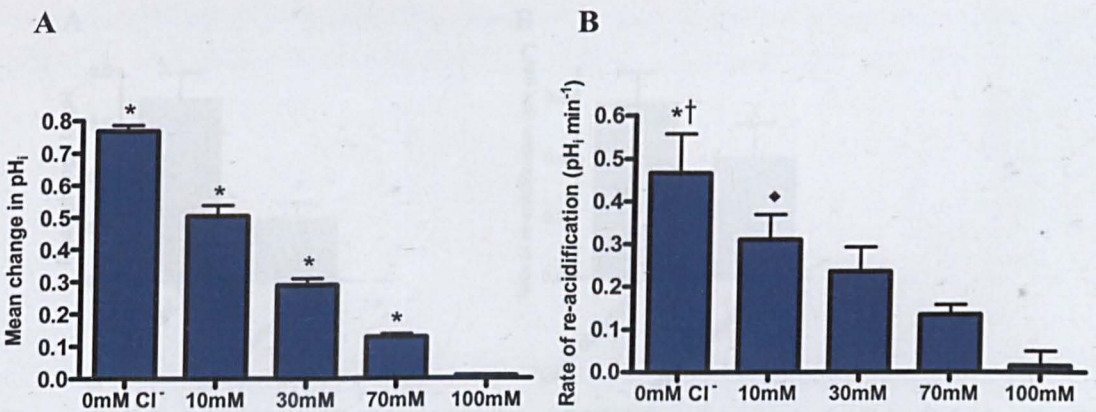

Figure 3.21- Cl^- gradient required for apical AE reversal. The mean changes in pH_i after altering extracellular apical chloride concentration from 0 mM to 100 mM (**A**) and the subsequent rate of re-acidification upon restoration of 124 mM external chloride (**B**) in forskolin stimulated Calu-3 cells. n=4. Paired observations. A: *P<0.001 compared to all concentrations. B: *P<0.05 compared to 70 mM. †P<0.001 compared to 100 mM. ◆P<0.05 compared to 100 mM.

The Na^+-K^+-$2Cl^-$ co-transporter (NKCC) present on the basolateral membrane of Calu-3 cells is involved in providing Cl^- for secretion via CFTR (Krouse *et al*, 2004). By inhibiting the NKCC, $[Cl^-]_i$ would be expected to fall, reducing the Cl^- gradient necessary for apical AE reversal in the absence of external Cl^- and therefore may reduce HCO_3^- intake through an apical Cl^-/HCO_3^- exchanger in the reverse mode.

Inhibiting Cl^- uptake through the basolateral NKCC, by using the NKCC inhibitor bumetanide (20 μM), the alkalinisation in pH_i upon apical Cl^- removal was diminished by 66.6 ± 15.5% ($P<0.01$; n=4), highlighting the importance of intracellular Cl^- to support AE activity (**Figure 3.22**). However, no difference was observed in the rate of apical AE activity following Cl^- re-addition, despite a probable increase in the external-to-internal Cl^- gradient ($P>0.05$; n=4). It should be noted that bumetanide has also been shown to partially inhibit CFTR Cl^- conductance in human sweat ducts (Reddy & Quinton, 1999), therefore the inhibition of apical AE by bumetanide may not be solely due to the inhibition of the basolateral NKCC.

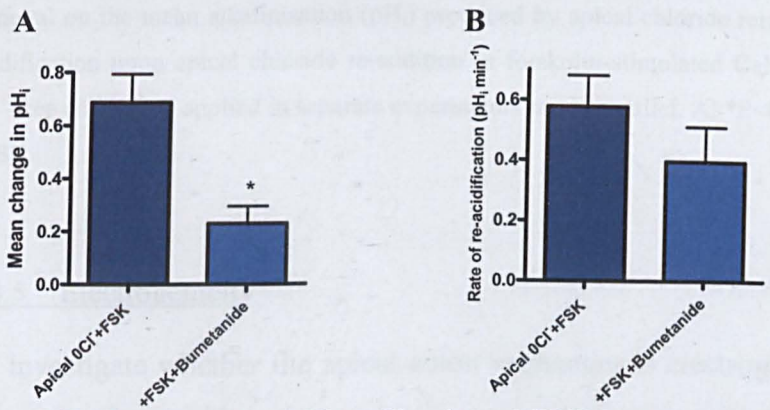

Figure 3.22- Bumetanide inhibition of basolateral NKCC reduces apical AE in Calu-3 cells. The effect of basolateral bumetanide (20 μM) on the mean alkalinisation (pH_i) produced by apical chloride removal (**A**) and the rate of re-acidification upon apical chloride re-addition in forskolin-stimulated Calu-3 cells (**B**). n=4. Paired observations. A: *$P<0.01$ compared to apical $0Cl^-$+FSK.

3.4.4 Na^+-dependence

To examine the Na^+ dependence of the apical AE, extracellular NaCl was replaced with NMDGCl in the apical solution. Removal of external Na^+ enhanced the alkalinisation in pH_i caused by the removal of apical chloride under forskolin-stimulated conditions from 0.49 ± 0.07 to 0.63 ± 0.03 pH units ($P<0.05$; n=4), suggesting that while apical AE can still be supported without extracellular Na^+, its activity maybe modulated indirectly by transporters that are Na^+-dependent (**Figure 3.23**).

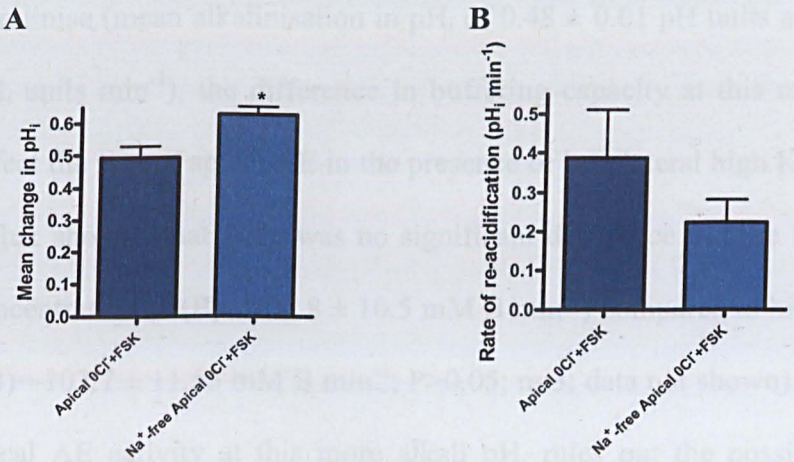

Figure 3.23- Na^+-dependence of apical AE activity in Calu-3 cells. The effect of bilateral Na^+ removal on the mean alkalinisation (pH_i) produced by apical chloride removal (**A**) and the rate of re-acidification upon apical chloride re-addition in forskolin-stimulated Calu-3 cells (**B**). n=4. Na^+ and Na^+-free conditions applied in separate experiments ran in parallel. A: *$P<0.05$ compared to apical $0Cl^-$ +FSK.

3.4.5 Electrogenicity

To investigate whether the apical anion exchanger is electrogenic, Calu-3 cells were exposed to a bilateral high external K^+ concentration (115 mM) and the K^+ channel agonist, 1-ethyl-2-benzimidazolinone (1-EBIO; 1 mM), in order to clamp the resting membrane potential to 0mV. In Calu-3 cells, 1-EBIO activates Ca^{2+}-activated K^+ channels, which in turn hyperpolarise the cells (Tamada *et al*, 2001). A high $[K^+]$

solution was applied to prevent changes in membrane potential during the experiment by K^+ channels. Bilateral high K^+ and EBIO, did not significantly affect apical AE activity when applied individually, but together reduced the mean alkalinisation induced by chloride removal as well as the rate of re-acidification upon chloride re-addition by 26.7 ± 9.7% and 23.7 ± 2.3%, respectively ($P<0.05$; n=4; **Figure 3.24A**). Interestingly, when high K^+ was applied only to the basolateral membrane, the mean alkalinisation was enhanced by 39.9 ± 2.3% ($P<0.001$), but the rate of re-acidification was decreased by 48.1 ± 7.4% compared to normal [K^+] ($P<0.05$; **Figure 3.24B**). However, since the addition of the high K^+ solution basolaterally itself caused pH_i to alkalinise (mean alkalinisation in pH_i of 0.48 ± 0.01 pH units at a rate of 0.15 ± 0.02 pH_i units min^{-1}), the difference in buffering capacity at this more alkali pH_i would affect the rate of apical AE in the presence of basolateral high K^+. Conversion to base efflux showed that there was no significant difference in base flux under normal K^+ concentration ($-J(B)$= 108.8 ± 10.5 mM B min^{-1}) compared to high K^+ basolaterally ($-J(B)$= 103.7 ± 11.55 mM B min^{-1}; $P>0.05$; n=3; data not shown). Also the presence of apical AE activity at this more alkali pH_i rules out the possibility that the AE is stimulated by the acidification produced following the addition of forskolin, rather than by the rise in cAMP.

From these experiments the electrogenicity of the apical AE activity is uncertain.

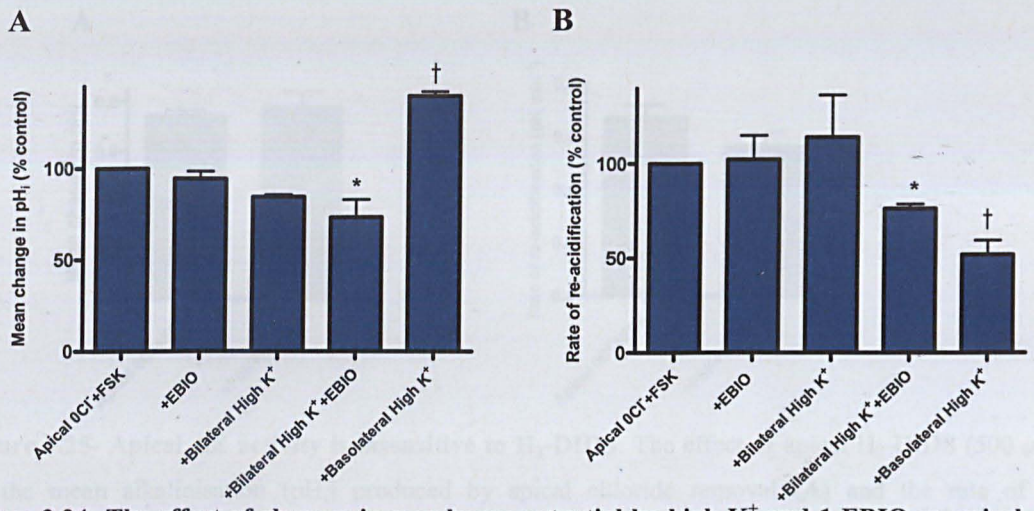

Figure 3.24- The effect of changes in membrane potential by high K^+ and 1-EBIO on apical AE activity. The effect of bilateral high K^+ (115 mM), basolateral only high K^+ and K^+ channel opener EBIO (1 mM) on the mean alkalinisation (pH_i) produced by apical chloride removal (**A**) and the rate of re-acidification upon apical chloride re-addition in forskolin-stimulated (5 μM) Calu-3 cells (**B**). pH_i responses in the presence of high K^+ and 1-EBIO compared to control apical $0Cl^-$+FSK responses. n=4. Each condition in separate experiments ran in parallel. A: *P<0.05 compared to apical $0Cl^-$+FSK. †P<0.001 compared to all conditions. B: *P<0.05 compared to apical $0Cl^-$+FSK. †P<0.05 compared to apical $0Cl^-$+FSK and +bilateral high K^+.

3.4.6 H_2-DIDS sensitivity

H_2-DIDS is known to inhibit a wide variety of anion transporters including many of the SLC26 members (Mount & Romero, 2004). Apical H_2-DIDS (500 μM) addition did not significantly affect either the mean alkalinisation of pH_i upon chloride removal or the rate of acidification following Cl^- re-addition (P>0.05; **Figure 3.25**).

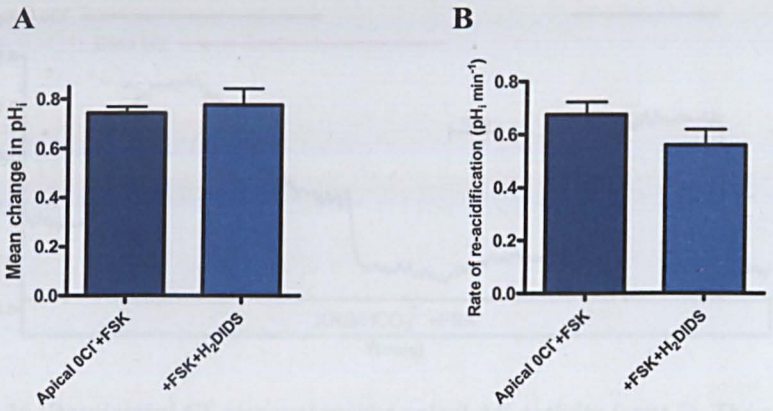

Figure 3.25- Apical AE activity is insensitive to H_2-DIDS. The effect of apical H_2-DIDS (500 μM) on the mean alkalinisation (pH_i) produced by apical chloride removal (**A**) and the rate of re-acidification upon apical chloride re-addition in forskolin-stimulated Calu-3 cells (**B**). n=4. Paired observations.

3.4.7 Bilateral Cl^- removal

So far the properties of the apical AE had only been studied by removing Cl^- from the apical (luminal) membrane. In order to investigate whether the removal of basolateral Cl^- might impact on the measurement of pH_i caused by apical Cl^- removal, Cl^- was removed bilaterally. **Figure 3.26** shows that the alkalinisation produced by removal of apical Cl^- was reversed by an equal acidification upon basolateral Cl^- removal. However, the re-addition of apical Cl^- then produced a further acidification, suggesting that the removal of basolateral Cl^- did not inhibit apical AE, but produced an acidification under these conditions through another pathway (**Figure 3.26**). At this new acidic pH_i, apical AE activity was still present (active) and was not significantly different in either rate or amplitude to the control ($P>0.05$; n=4; data not shown).

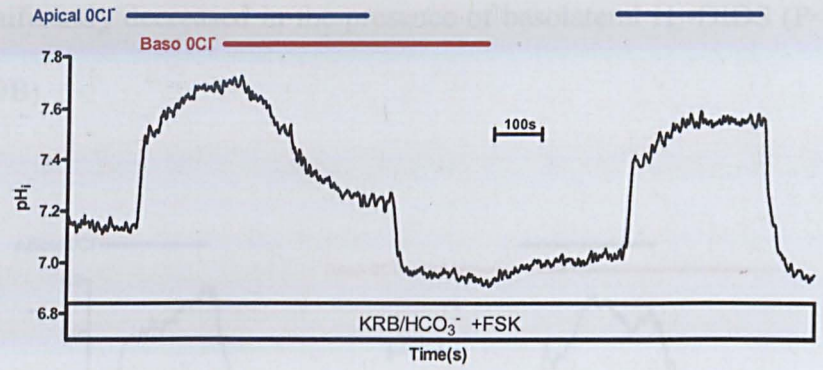

Figure 3.26- Basolateral Cl^- removal masks apical AE activity (expt.1). The effect of basolateral Cl^- removal on apical Cl^-/HCO_3^- exchange activity in forskolin-stimulated (5 μM) Calu-3 cells.

Prior exposure to basolateral zero Cl^- also abolished the substantial alkalinisation induced by apical Cl^- removal, although an initial transient response to apical Cl^- removal was seen (**Figure 3.27**). Upon re-addition of basolateral Cl^-, the apical Cl^- gradient caused an alkalinisation of pH_i, suggesting that the apical AE was still active.

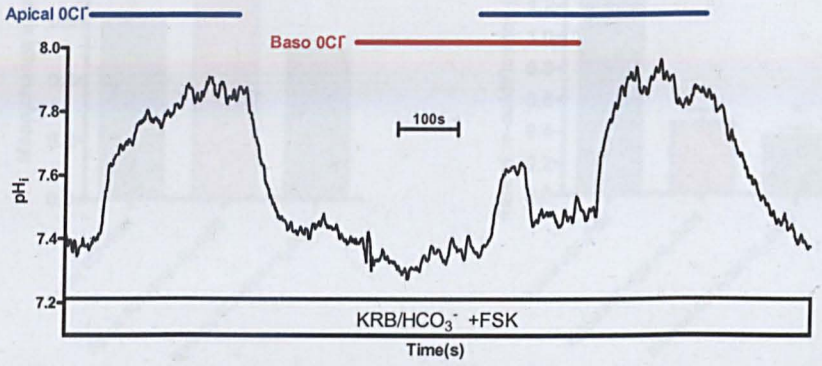

Figure 3.27- Basolateral Cl^- removal masks apical AE activity (expt.2). The effect of basolateral Cl^- removal on apical Cl^-/HCO_3^- exchange activity in forskolin-stimulated (5 μM) Calu-3 cells.

In order to attempt to block the effects of basolateral Cl^- removal on pH_i, H_2-DIDS (500 μM) was applied to the basolateral membrane (**Figure 3.28**). In the presence of H_2-DIDS the apparent inhibition of the apical AE by basolateral Cl^- removal was eliminated (**Figure 3.29A**). However, the rate of apical AE activity was still

significantly decreased in the presence of basolateral H_2-DIDS ($P<0.01$; n=3; **Figure 3.29B**).

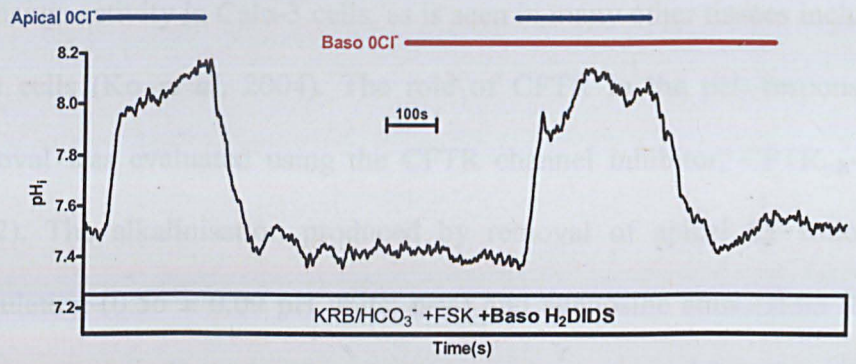

Figure 3.28- pH_i experimental trace of basolateral Cl^- removal masking apical AE activity through a H_2-DIDS sensitive mechanism. The effect of basolateral H_2-DIDS on changes in pH_i induced by bilateral Cl^- removal in forskolin-stimulated Calu-3 cells.

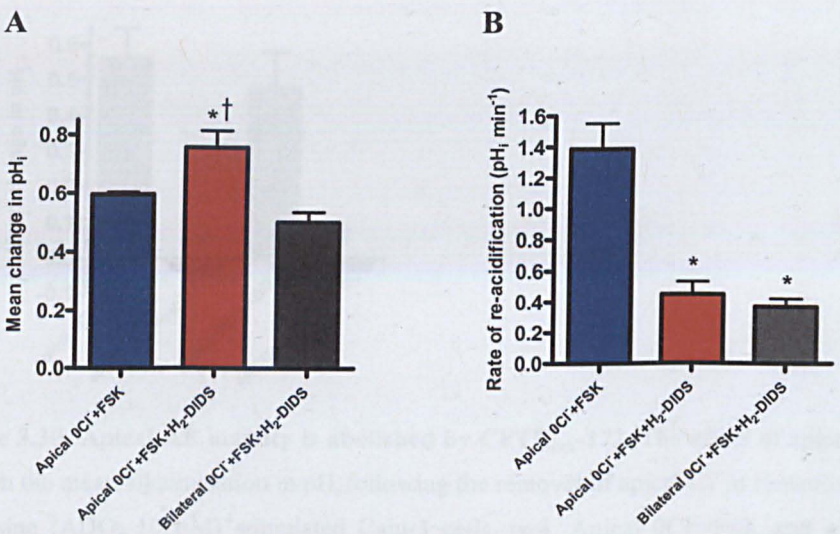

Figure 3.29- Basolateral Cl^- removal masks apical AE activity through a H_2-DIDS sensitive mechanism. The effects of basolateral H_2-DIDS on mean changes in pH_i following the removal of apical or bilateral Cl^- (**A**) and on the rate of re-acidification upon re-addition of apical Cl^- in Calu-3 cells (**B**). n=3. Paired observations. A: *$P<0.05$ compared to apical $0Cl^-$+FSK. †$P<0.01$ compared to bilateral $0Cl^-$+FSK+H_2DIDS. B: *$P<0.01$ compared to apical $0Cl^-$+FSK.

3.5 Regulation of apical Cl^-/HCO_3^- exchange by CFTR

A key part of the project was to investigate if CFTR expression and/or CFTR activation by cAMP agonists is involved in the regulation of apical Cl^-/HCO_3^- exchange activity in Calu-3 cells, as is seen in many other tissues including pancreatic duct cells (Ko *et al*, 2004). The role of CFTR in the pH_i response to apical Cl^- removal was evaluated using the CFTR channel inhibitor, $CFTR_{inh}$-172 (Ma *et al*, 2002). The alkalinisation produced by removal of apical Cl^- following forskolin stimulation (0.56 ± 0.09 pH units; n=4) and adenosine stimulation (0.48 ± 0.10 pH units; n=4), were both significantly inhibited (P<0.001 and P<0.01 respectively) by 10 μM $CFTR_{inh}$-172 (**Figure 3.30**).

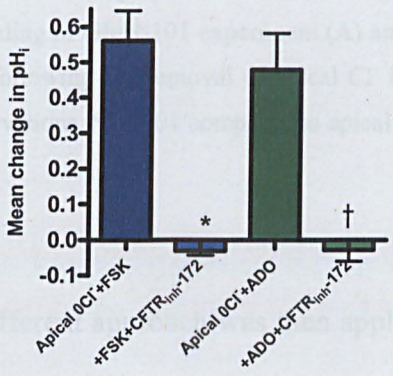

Figure 3.30- Apical AE activity is abolished by $CFTR_{inh}$-172. The effect of apical $CFTR_{inh}$-172 (10 μM) on the mean alkalinisation in pH_i following the removal of apical Cl^- in forskolin (FSK; 5 μM) and adenosine (ADO; 10 μM) stimulated Calu-3 cells. n=4. Apical $0Cl^-$+FSK and +FSK+$CFTR_{inh}$-172 represent paired observations from same experiment. Apical $0Cl^-$+ADO and +ADO+$CFTR_{inh}$-172 also represent paired observations from same experiment. FSK and ADO experiments ran in parallel. *P<0.001 compared to apical $0Cl^-$+FSK. †P<0.01 compared to apical $0Cl^-$+ADO.

Another CFTR inhibitor, the pore blocker GlyH-101, was also tested (Muanprasat *et al*, 2004). The addition of GlyH-101 (10 μM) produced an alkalinisation of 0.23 ± 0.02 pH units (n=4), opposing the equivalent acidification produced by the prior

addition of forskolin. Interestingly, prior addition of either CFTR inhibitor abolished the acidification in pH_i normally produced by forskolin addition. In the presence of GlyH-101, apical AE was abolished, suggesting that apical AE activity was dependent on the anion transport by CFTR (**Figure 3.31**).

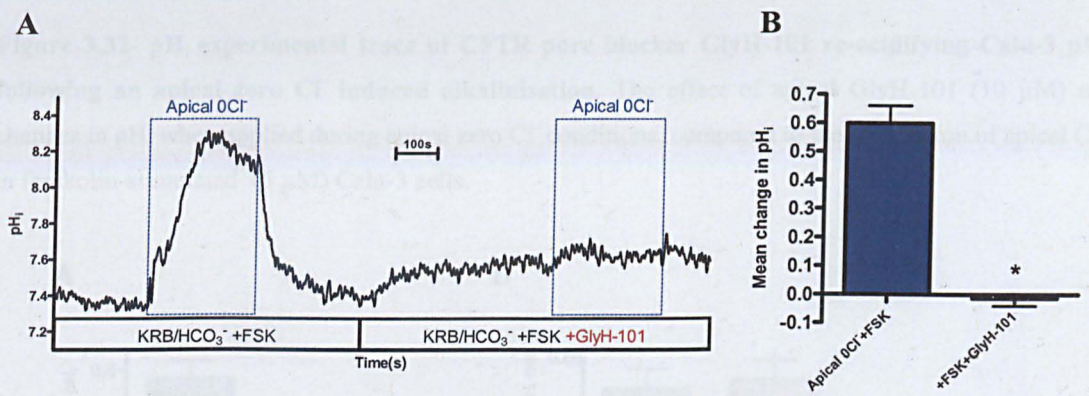

Figure 3.31- Apical AE activity is abolished by CFTR pore blocker GlyH-101. Representative recording of GlyH-101 experiment (**A**) and the effect of apical GlyH-101 (10 μM) on mean changes in pH_i following the removal of apical Cl^- in forskolin-stimulated (5 μM) Calu-3 cells (**B**). n=4. Paired observations. *P<0.01 compared to apical $0Cl^-$+FSK.

A different approach was then applied to inhibit CFTR, by adding apical GlyH-101 in zero Cl^- conditions to determine if it was still possible to re-acidify the cells by the re-addition of Cl^- (**Figure 3.32**). Unexpectedly, application of GlyH-101 during an apical zero Cl^- induced alkalinisation produced a rapid re-acidification in pH_i, at a rate similar to that of the re-addition of Cl^- (**Figure 3.33**). However pH_i did not return to pre GlyH-101 values.

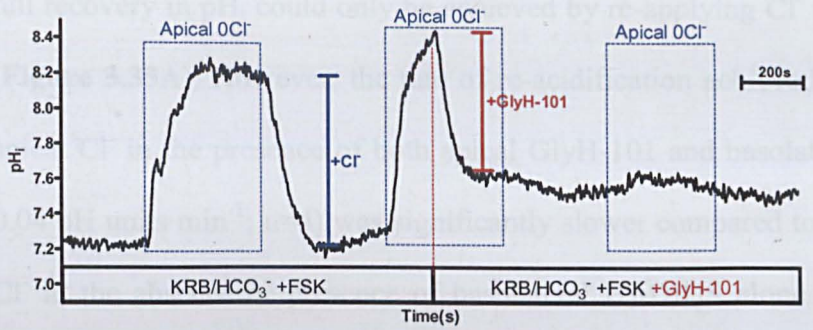

Figure 3.32- pH_i experimental trace of CFTR pore blocker GlyH-101 re-acidifying Calu-3 pH_i following an apical zero Cl^- induced alkalinisation. The effect of apical GlyH-101 (10 μM) on changes in pH_i when applied during apical zero Cl^- conditions, compared to the re-addition of apical Cl^- in forskolin-stimulated (5 μM) Calu-3 cells.

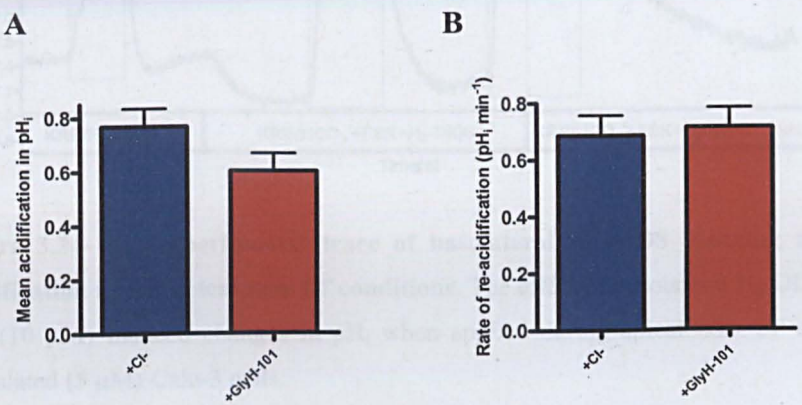

Figure 3.33- CFTR pore blocker GlyH-101 re-acidifies Calu-3 pH_i following an apical zero Cl^- induced alkalinisation. Comparison of the mean acidification (**A**) and rate of acidification in pH_i (**B**), produced by the re-addition of Cl^- or by the addition of GlyH-101 (10 μM), following the removal of apical Cl^- in forskolin-stimulated (5 μM) Calu-3 cells. n=4. Paired observations.

These experiments were then repeated using basolateral H_2-DIDS to investigate if a basolateral transporter could be involved in the rapid re-acidification caused by GlyH-101. In the presence of basolateral H_2-DIDS, the mean acidification upon apical Cl^- removal was enhanced ($P<0.001$; n=4), while the rate of AE activity decreased ($P<0.001$), as was also seen in the bilateral $0Cl^-$ experiments (**Figures 3.29 & 3.34**). The addition of H_2-DIDS basolaterally was sufficient to inhibit 77.4 ± 11.3% (n=4) of the re-acidification produced by applying GlyH-101 under zero Cl^- conditions and a

full recovery in pH_i could only be achieved by re-applying Cl^- to the apical perfusate (**Figure 3.35A**). However, the rate of re-acidification achieved by the re-addition of apical Cl^- in the presence of both apical GlyH-101 and basolateral H_2-DIDS (0.28 ± 0.04 pH units min^{-1}; n=4) was significantly slower compared to the addition of apical Cl^- in the absence or presence of basolateral H_2-DIDS alone ($P<0.001$ and $P<0.05$ respectively; n=4; **Figure 3.35B**).

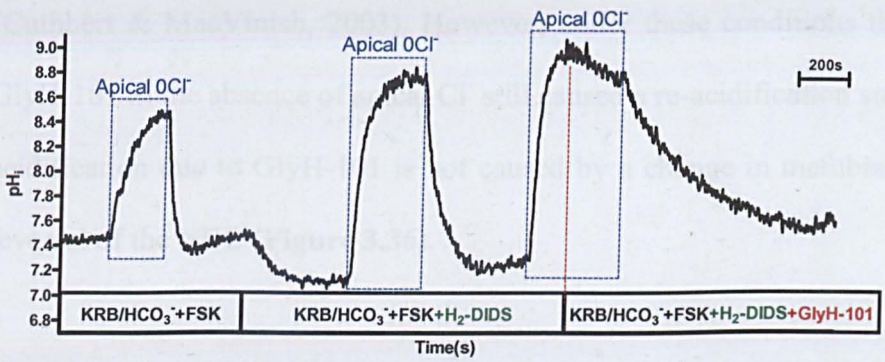

Figure 3.34- pH_i experimental trace of basolateral H_2-DIDS blocking the GlyH-101-induced acidification under apical zero Cl^- conditions. The effect of basolateral H_2-DIDS (500 μM) on GlyH-101 (10 μM) induced changes in pH_i when applied during apical zero Cl^- conditions in forskolin-stimulated (5 μM) Calu-3 cells.

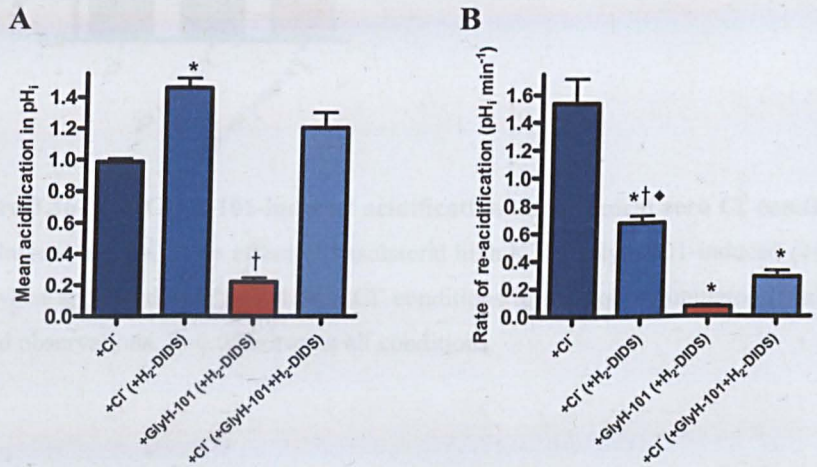

Figure 3.35- Basolateral H_2-DIDS blocks the GlyH-101-induced acidification under apical zero Cl^- conditions. The effect of basolateral H_2-DIDS (500 μM) on the mean acidification (**A**) and rate of re-acidification in pH_i (**B**) induced by either the re-addition of apical chloride ($+Cl^-$) or addition of apical GlyH-101 (10 μM), during apical zero Cl^- conditions in forskolin-stimulated (5 μM) Calu-3 cells. n=4. Paired observations. A: *$P<0.001$ compared to $+Cl^-$. †$P<0.001$ compared to all conditions. B: *$P<0.001$ compared to $+Cl^-$. †$P<0.01$ compared to +GlyH-101($+H_2$-DIDS). ◆$P<0.05$ compared to $+Cl^-$(+GlyH-101+H_2-DIDS).

A possible explanation for the effect of GlyH-101 is that inhibition of anion permeation through CFTR may cause a repolarisation of membrane potential. The repolarisation caused by GlyH-101 maybe large enough to cause the reversal of the basolateral NBC, producing an efflux of HCO_3^-. To test this hypothesis the $[K^+]$ of the basolateral solution was increased in order to depolarise the basolateral membrane and thus counter any change in membrane potential caused by the blockage of CFTR (Cuthbert & MacVinish, 2003). However, under these conditions the application of GlyH-101 in the absence of apical Cl^- still caused a re-acidification suggesting that the acidification due to GlyH-101 is not caused by a change in membrane potential and reversal of the NBC (**Figure 3.36**).

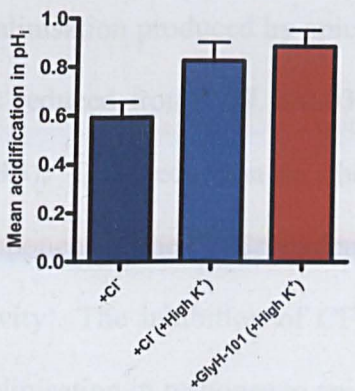

Figure 3.36- The GlyH-101-induced acidification under apical zero Cl^- conditions is insensitive to basolateral high K^+. The effect of basolateral high K^+ on GlyH-101-induced (10 μM) acidification in pH_i when applied during apical zero Cl^- conditions in forskolin-stimulated (5 μM) Calu-3 cells. n=3. Paired observations. P>0.05 between all conditions.

In addition to basolateral H_2DIDS blocking the GlyH-101-induced acidification under apical zero Cl^- conditions, prior application of basolateral H_2DIDS also overcame the inhibition of the apical AE by GlyH-101 (**Figure 3.37**).

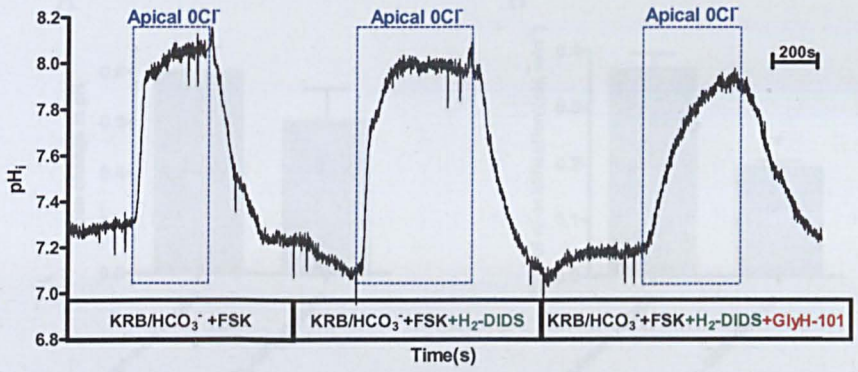

Figure 3.37- pH_i experimental trace of CFTR inhibitor GlyH-101 abolishing apical AE activity through a basolateral H_2-DIDS-sensitive mechanism. The effect of basolateral H_2-DIDS (500 μM) on changes in pH_i following the removal of apical Cl^- in the presence of apical CFTR inhibitor GlyH-101 (10 μM), in forskolin-stimulated (5 μM) Calu-3 cells.

In the presence of basolateral H_2-DIDS, GlyH-101 had no significant effect on the alkalinisation produced by apical Cl^- removal (**Figure 3.38A**), however the rate of AE was reduced from 0.37 ± 0.03 to 0.19 ± 0.01 pH_i units min^{-1} ($P<0.01$; n=4; **Figure 3.38B**). This reduction in the rate of re-acidification may represent the CFTR component of the Cl^--dependent HCO_3^- transport, which is required for maximal 'AE activity'. The inhibition of CFTR may also be reflected by the slower monophasic alkalinisation in response to apical Cl^- removal in the presence of basolateral H_2-DIDS and apical GlyH-101, compared to the biphasic alkalinisation in the absence of GlyH-101 (see **Figure 3.37**).

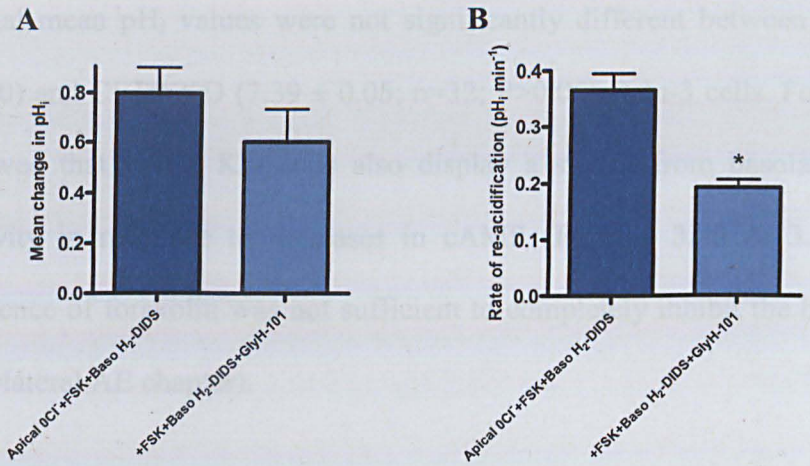

Figure 3.38- CFTR inhibitor GlyH-101 abolishes apical AE activity through a basolateral H_2-DIDS-sensitive mechanism. The effect of basolateral H_2-DIDS (100 μM), in the absence and presence of CFTR inhibitor GlyH-101 (10 μM), on the mean alkalinisation (pH_i) produced by apical chloride removal (**A**) and the rate of re-acidification upon apical chloride re-addition (**B**), in forskolin-stimulated (5 μM) Calu-3 cells. n=4. Paired observations. B: *P<0.01 compared to apical $0Cl^-$+FSK+baso H_2DIDS.

3.5.1 CFTR Knockdown cells

To further investigate the role of CFTR in regulating Cl^-/HCO_3^- AE activity, experiments were conducted on CFTR Knockdown (KD) Calu-3 cells, which have a CFTR content of <5% and show 25% of the cAMP-dependent Cl^- secretion of that of wild-type (WT) Calu-3 cells (MacVinish *et al*, 2007). The reduced expression of CFTR in Calu-3 KD cells was confirmed by immunocytochemical analysis (**Figure 3.39**).

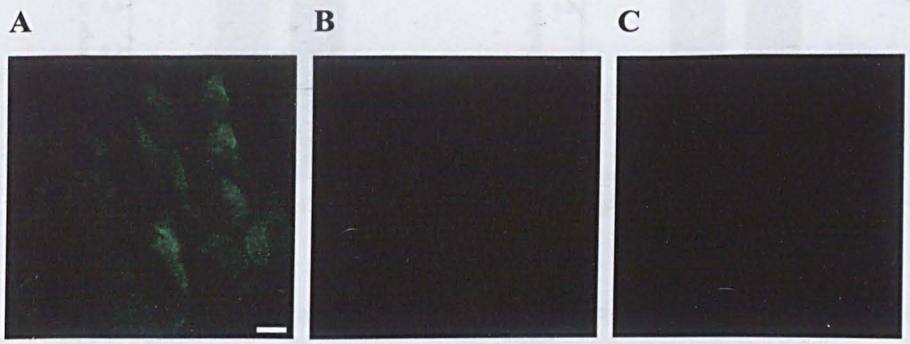

Figure 3.39- Reduced CFTR expression in CFTR KD Calu-3 cells. Immunofluorescent staining of CFTR using a mouse anti-CFTR antibody (green) in WT Calu-3 cells (**A**), no primary negative control (**B**), and in CFTR KD Calu-3 cells (**C**). All images are *XY* sections. Scale bar represents 10 μm. n=3.

Initial mean pH_i values were not significantly different between WT (7.43 ± 0.03; n=50) and CFTR KD (7.39 ± 0.05; n=32; P>0.05) Calu-3 cells. Forskolin stimulation showed that CFTR KD cells also display a switch from basolateral to apical AE activity in response to increases in cAMP (**Figures 3.40 & 3.41**). Although the presence of forskolin was not sufficient to completely inhibit the basolateral AE (see basolateral AE chapter).

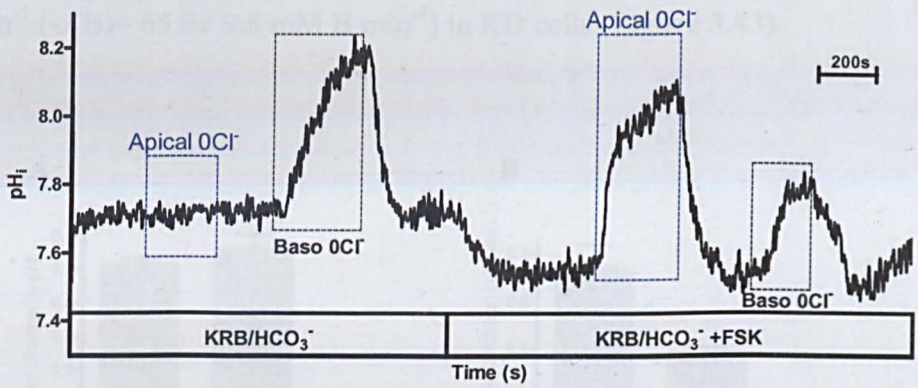

Figure 3.40- pH_i experimental trace of the forskolin-induced changes in AE activity in CFTR KD Calu-3 cells. The effect of forskolin (FSK; 5 μM) on changes in pH_i following the removal of apical and basolateral chloride in CFTR Knockdown (KD) Calu-3 cells.

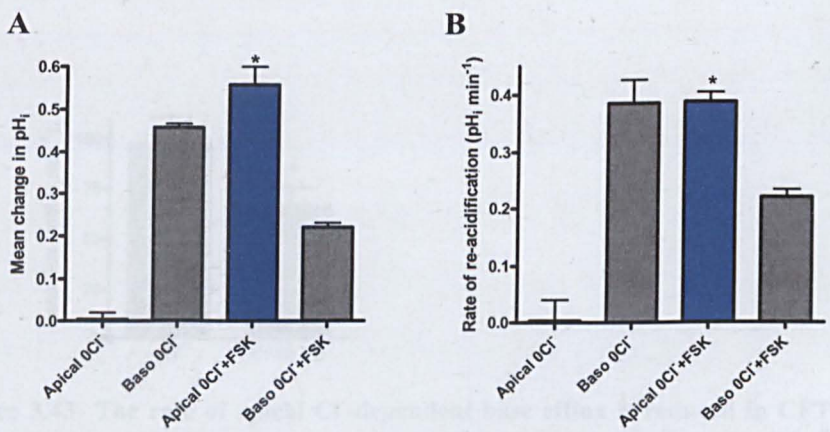

Figure 3.41- Forskolin-induced changes in AE activity in CFTR KD Calu-3 cells. Mean alkalinisation (pH_i) produced by chloride removal (**A**) and the rate of re-acidification upon chloride re-addition in CFTR KD Calu-3 cells (**B**), under non-stimulated and forskolin-stimulated (FSK; 5 μM) conditions. n=4. Paired observations. A: *P<0.001 compared to apical $0Cl^-$. B: *P<0.001 compared to apical $0Cl^-$.

CFTR KD Calu-3 cells produced a similar alkalinisation (0.56 ± 0.04 pH units) in response to apical Cl^- removal in the presence of forskolin, as WT Calu-3 cells (0.51 ± 0.01 pH units; P>0.05; n=4; **Figure 3.42A**). However the reduced expression of CFTR in the KD Calu-3 cells appears to be reflected in the significantly reduced rates of re-acidification compared to WT cells (**Figure 3.42B**). The rate of the apical Cl^-/HCO_3^- exchange was reduced in CFTR KD cells by ~48% (P<0.01) from 0.75 ± 0.09 pH units min^{-1} ($-J(B)$= 97.6 ± 13.3 mM B min^{-1}) in WT cells to 0.39 ± 0.02 pH units min^{-1} ($-J(B)$= 65.9± 9.8 mM B min^{-1}) in KD cells (**Figure 3.43**).

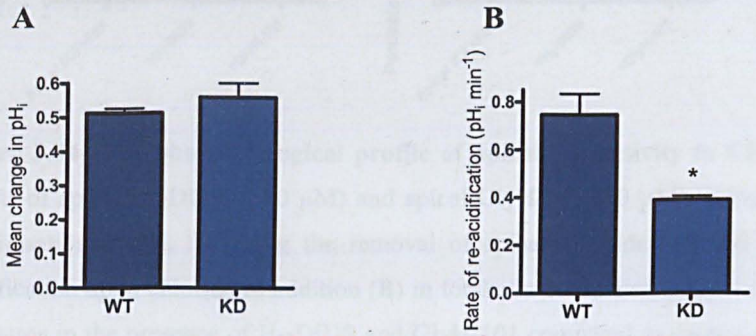

Figure 3.42- The rate of apical AE activity is reduced in CFTR KD Calu-3 cells. Comparison of the mean changes in pH_i following removal of apical chloride (**A**) and the rate of re-acidification upon chloride re-addition (**B**), between Wild-type (WT) and CFTR Knockdown (KD) Calu-3 cells. n=4. WT and CFTR KD cell experiments carried out in parallel. B: *P<0.01 compared to WT.

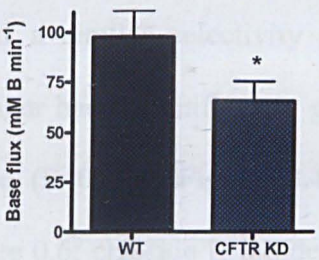

Figure 3.43- The rate of apical Cl^--dependent base efflux is reduced in CFTR KD Calu-3 cells. Comparison of the rate of base efflux (mM B min^{-1}) produced by the re-addition of Cl^-, following the removal of apical Cl^- in forskolin stimulated WT and CFTR KD Calu-3 cells. n=4. WT and CFTR KD cell experiments carried out in parallel. *P<0.05 compared to WT.

Similar to WT cells, the alkalinisation in pH_i following apical Cl^- removal in CFTR KD Calu-3 cells was insensitive to the anion exchange inhibitor H_2-DIDS (0.46 ± 0.07 pH units; P>0.05; n=4) and was almost abolished (inhibited by 91.3 ± 1.8%) by pre-exposure to CFTR inhibitor GlyH-101 (P<0.05; n=4; **Figure 3.44**).

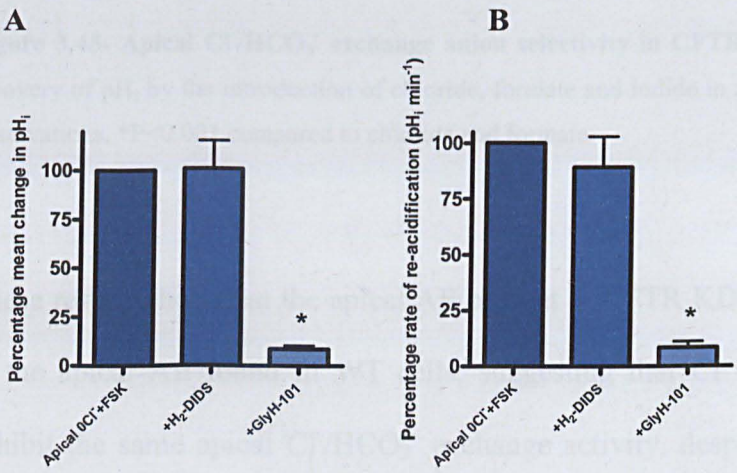

Figure 3.44- The pharmacological profile of apical AE activity in CFTR KD Calu-3 cells. The effects of apical H_2-DIDS (500 μM) and apical GlyH-101 (10 μM) addition on the percentage mean alkalinisation in pH_i following the removal of apical chloride (**A**) and the percentage rate of re-acidification upon chloride re-addition (**B**) in forskolin-stimulated (5 μM) CFTR KD Calu-3 cells. pH_i responses in the presence of H_2-DIDS and GlyH-101 compared to control apical $0Cl^-$+FSK responses. n=4. H_2-DIDS and GlyH-101 experiments carried out in parallel. A: *P<0.001 compared to apical $0Cl^-$ +FSK and +H_2-DIDS. B: *P<0.001 compared to apical $0Cl^-$+FSK and +H_2-DIDS.

Apical AE activity was only supported by monovalent anions in CFTR KD cells and showed a similar selectivity profile to WT Calu-3 cells (see Figure 3.18); the exchanger had a significantly greater affinity for iodide compared with chloride and formate (P<0.001; **Figure 3.45**). Comparing the Cl^-/X selectivity ratios of WT (formate 0.6: chloride 1: iodide 1.3) and CFTR KD Calu-3 cells (chloride 1: formate 1.2: iodide 2.1), suggests that iodide is transported with greater affinity in CFTR KD cells in relation to chloride.

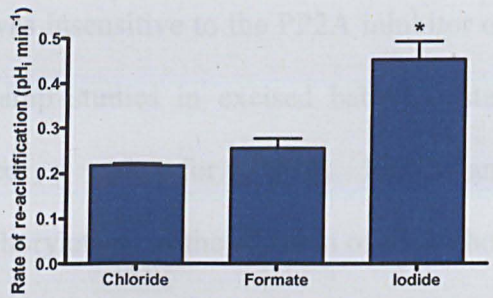

Figure 3.45- Apical Cl^-/HCO_3^- exchange anion selectivity in CFTR KD Calu-3 cells. The rate of recovery of pH_i by the introduction of chloride, formate and iodide in zero Cl^- conditions. n=4. Paired observations. *P<0.001 compared to chloride and formate.

These results show that the apical AE present in CFTR KD cells has a similar profile to the apical AE found in WT cells, suggesting that CFTR KD Calu-3 cells may exhibit the same apical Cl^-/HCO_3^- exchange activity, despite reduced expression of CFTR.

3.6 Regulation of apical Cl^-/HCO_3^- exchange by protein phosphatase activity

Several epithelial transporters are regulated by protein phosphatase (PP) activity, including the basolateral NKCC and apical CFTR present in Calu-3 cells (Liedtke *et al*, 2005; Thelin *et al*, 2005). Bumetanide-sensitive ^{86}Rb uptake studies showed a four-fold increase in NKCC activity following addition of the PP1/PP2A inhibitor okadaic acid and immunoblot analysis detected both PP2A and PP1 in Calu-3 cells lysates (Liedtke *et al*, 2005). Patch-clamp experiments on NIH 3T3 fibroblasts stably expressing CFTR revealed that PKA-activated Cl^- currents were decreased by PP2A addition (the effects of which could be blocked by PP2A inhibitor calyculin A), but not PP1 or PP2B, suggesting PP2A-mediated dephosphorylation of CFTR is involved in channel rundown (Berger *et al*, 1993). However, studies in excised patches of Chinese hamster ovary and human airway epithelial cells showed that rundown of

CFTR was insensitive to the PP2A inhibitor okadaic acid (Becq *et al*, 1994). Further patch-clamp studies in excised baby hamster kidney cells over-expressing CFTR suggested a role for PP2A, PP2C and alkaline phosphatase in CFTR dephosphorylation, as the addition of each phosphatase could reduced CFTR channel activity by >90% (Luo et al, 1998). Thus, CFTR regulation by phosphatases appears to be cell-type specific (Gadsby *et al*, 1999). In intestinal and airway epithelia, PP2A and PP2C have been shown to inactivate CFTR (Travis *et al*, 1997; Thelin *et al*, 2005). In Calu-3 cells, mass spectrometry revealed that PP2A regulatory subunits can physically associate with the carboxyl terminus of CFTR (Thelin *et al*, 2005). As protein phosphatases can be activated by increases in cAMP, through a PKA-independent pathway (Feschenko *et al*, 2002), they represent a potential mechanism for regulating HCO_3^- transport processes on both the apical and basolateral membranes.

To investigate whether protein phosphatases can regulate AE activity, wild-type Calu-3 cells were pre-treated with the PP1/PP2A inhibitor okadaic acid (100 nM) for 60 minutes during BCECF-AM loading. Calu-3 cells pre-treated with okadaic acid had a more acidic initial pH_i compared to untreated cells (7.03 ± 0.06; $P<0.01$; n=15). Surprisingly, okadaic acid exposure produced a switch in AE activity, completely inhibiting the basolateral AE and activating an apical AE activity under basal conditions (**Figure 3.46**). The alkalinisation in pH_i following apical Cl^- removal in okadaic acid treated cells was further enhanced by forskolin (5 μM) addition (from 0.22 ± 0.01 to 0.45 ± 0.02 pH units; $P<0.001$; n=5; **Figure 3.47A**). While the rate of apical AE activity in forskolin-stimulated cells was comparable between untreated and okadaic acid-treated cells (**Figure 3.47B**), the mean alkalinisation in pH_i upon

apical Cl^- removal in okadaic acid-treated Calu-3 cells was not as large ($P<0.05$; n=5). Forskolin addition produced a similar acidification in pH_i, in both magnitude and rate, in okadaic acid treated cells compared to untreated Calu-3 cells ($P>0.05$; n=5).

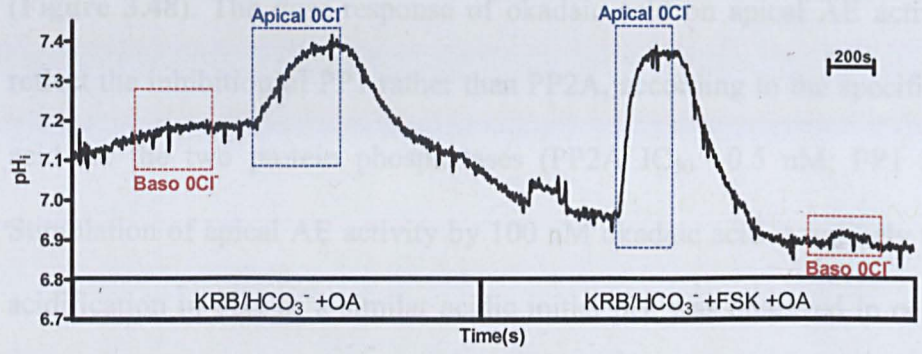

Figure 3.46- pH_i experimental trace of protein phosphatase inhibitor okadaic acid activating apical AE activity in Calu-3 cells. The effects of protein phosphatase inhibitor okadaic acid (OA; 100 nM) on changes in pH_i following the removal of chloride in unstimulated and forskolin-stimulated (5 μM) WT Calu-3 cells.

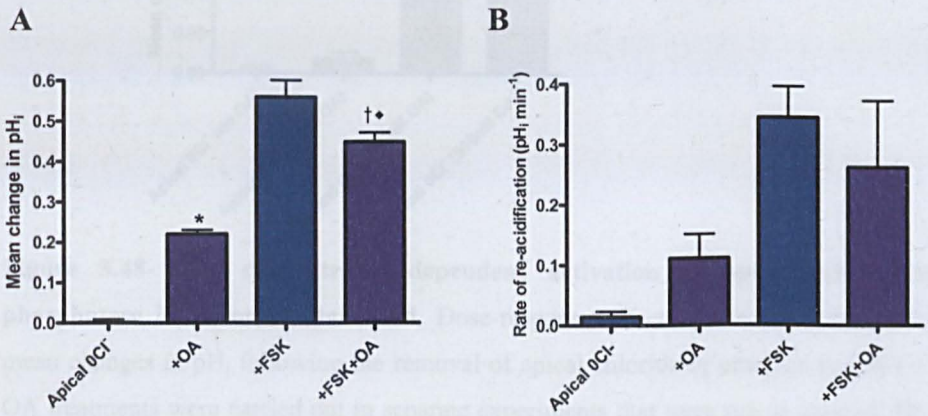

Figure 3.47- Protein phosphatase inhibitor okadaic acid activates apical AE activity in Calu-3 cells. The effects of okadaic acid (OA; 100 nM) on the mean change in pH_i following the removal of chloride (**A**) and the mean rate of re-acidification in pH_i upon the re-addition of chloride (**B**) in unstimulated and forskolin-stimulated (5 μM) WT Calu-3 cells. n=5. OA treated and untreated Calu-3 cell experiments were run in parallel. A: *$P<0.001$ compared to apical $0Cl^-$. †$P<0.05$ compared to +FSK. ♦$P<0.001$ compared to +OA. B: no significant difference between OA treated and untreated cells.

Increasing the concentration of okadaic acid from 100 nM to 500 nM did not further enhance okadaic acid stimulation of apical AE activity under basal conditions, but lowering the okadaic acid concentration to 10 nM abolished apical AE stimulation (**Figure 3.48**). The dose-response of okadaic acid on apical AE activity appears to reflect the inhibition of PP1 rather than PP2A, according to the specificity of okadaic acid for the two protein phosphatases (PP2A IC_{50} ~0.5 nM; PP1 IC_{50} ~50 nM). Stimulation of apical AE activity by 100 nM okadaic acid is unlikely to be due to an acidification in pH_i, as a similar acidic initial pH_i was observed in cells treated with 10 nM okadaic acid (7.09 ± 0.25; P>0.05; n=3).

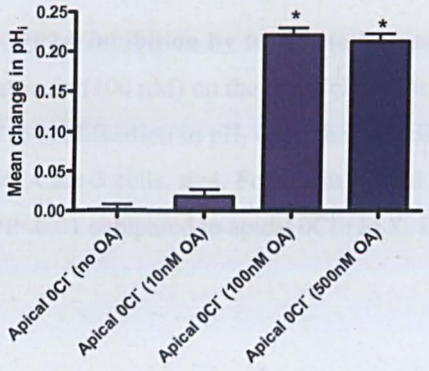

Figure 3.48- The concentration-dependent activation of apical AE activity by protein phosphatase inhibitor okadaic acid. Dose-response effect of okadaic acid (0,10,100,500 nM) on mean changes in pH_i following the removal of apical chloride in unstimulated WT Calu-3 cells. n=4. OA treatments were carried out in separate experiments that were run in parallel. *P<0.001 compared to no OA and 10 nM OA.

To test whether PP2A was involved in the stimulation of the apical AE by okadaic acid, the effect of another PP inhibitor, fostriecin, was examined. Fostriecin is a potent inhibitor of PP2A (IC_{50} ~1.5 nM) and only inhibits PP1 at high concentrations (IC_{50} ~130 μM). At 100 nM, a concentration that should only inhibit PP2A, fostriecin was unable to stimulate apical AE activity, in marked contrast to 100 nM okadaic

acid. However, fostriecin pre-treatment did decrease the activity of the forskolin-stimulated apical AE (both mean alkalinisation and rate of re-acidification; **Figure 3.49**).

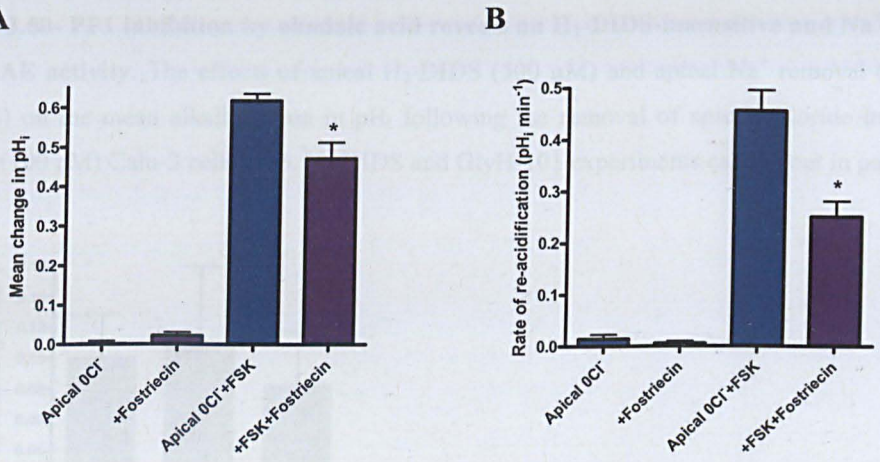

Figure 3.49- PP2A inhibition by fostriecin fails to activate apical AE activity in Calu-3 cells. The effects of fostriecin (100 nM) on the mean change in pH_i following the removal of chloride (**A**) and the mean rate of re-acidification in pH_i upon the re-addition of chloride (**B**) in unstimulated and forskolin-stimulated WT Calu-3 cells. n=4. Fostriecin treated and untreated Calu-3 cell experiments were run in parallel. A: *P<0.01 compared to apical $0Cl^-$+FSK. B: *P<0.001 compared to apical $0Cl^-$+FSK.

These results therefore suggest that PP1 inhibition by okadaic acid is responsible for the stimulation of apical AE activity under basal conditions. However, PP2A appears to be involved in regulating apical AE in the presence of forskolin.

The profile of the basal apical AE exchange activity in okadaic acid treated WT Calu-3 cells was similar to the forskolin-stimulated AE activity seen in untreated cells: H_2-DIDS insensitive, Na^+-independent (**Figure 3.50**) and only transports monovalent anions (**Figure 3.51**).

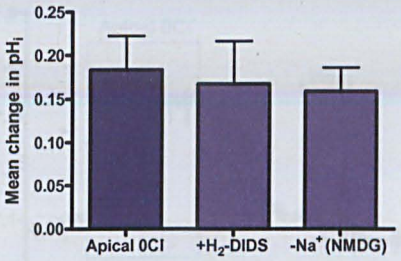

Figure 3.50- PP1 inhibition by okadaic acid reveals an H_2-DIDS-insensitive and Na^+-independent apical AE activity. The effects of apical H_2-DIDS (500 μM) and apical Na^+ removal (replaced with NMDG) on the mean alkalinisation in pH_i following the removal of apical chloride in okadaic acid treated (100 nM) Calu-3 cells. n=3. H_2-DIDS and GlyH-101 experiments carried out in parallel.

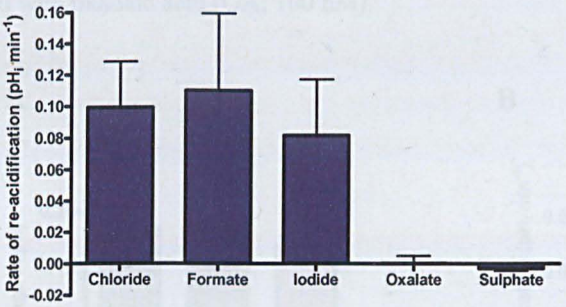

Figure 3.51- Anion selectivity of apical Cl^-/HCO_3^- exchange in okadaic acid treated Calu-3 cells. The rate of recovery of pH_i by the introduction of monovalent (iodide, formate and chloride) and divalent (oxalate and sulphate) anions in zero Cl^- conditions, in okadaic acid (100 nM) treated WT Calu-3 cells. n=4. Paired observations.

Interestingly GlyH-101 (10 μM) studies showed that the basal apical AE activity observed in the presence of okadaic acid was not blocked by GlyH-101 suggesting that it is independent of CFTR. In contrast, the enhancement of apical AE activity by forskolin was prevented by GlyH-101, showing that this was likely due to CFTR activation (**Figures 3.52 & 3.53**).

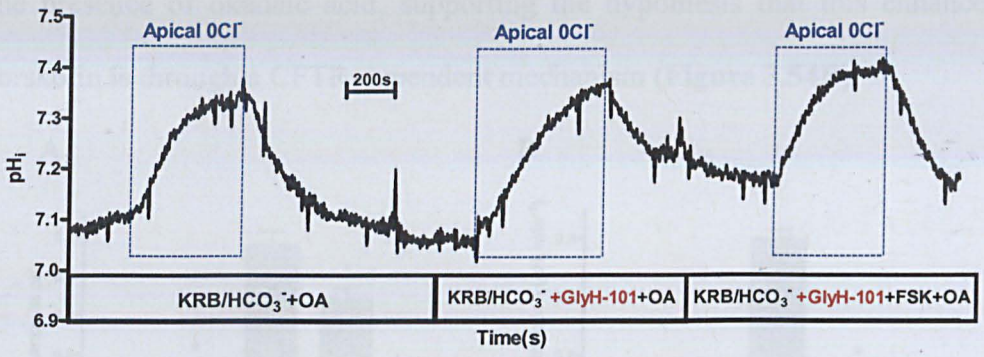

Figure 3.52- pH$_i$ experimental trace of CFTR-independent apical AE activity in okadaic acid treated Calu-3 cells. The effects of apical CFTR inhibitor GlyH-101 (10 μM) on changes in pH$_i$ following the removal of chloride in unstimulated and forskolin-stimulated (5 μM) WT Calu-3 cells treated with okadaic acid (OA; 100 nM).

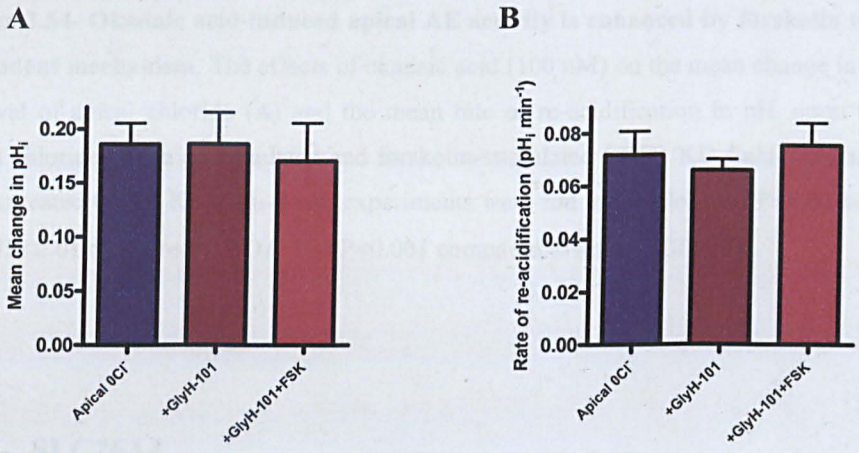

Figure 3.53- CFTR-independent apical AE activity in okadaic acid-treated Calu-3 cells. The effects of apical CFTR inhibitor GlyH-101 on the mean alkalinisation in pH$_i$ following the removal of apical chloride (**A**) and the mean rate of re-acidification in pH$_i$ upon re-addition of apical chloride (**B**), in unstimulated and forskolin-stimulated WT Calu-3 cells treated with okadaic acid (100 nM). n=4. Paired observations.

The CFTR-dependence of the okadaic acid stimulated apical AE activity was also investigated in CFTR KD Calu-3 cells. Okadaic acid-treated CFTR KD cells also exhibited apical AE under basal conditions, which could be enhanced by forskolin addition (**Figure 3.54A**). However, unlike WT Calu-3 cells (see Figure 3.47), the rate of AE activity in forskolin-stimulated CFTR KD cells was significantly decreased in

the presence of okadaic acid, supporting the hypothesis that this enhancement by forskolin is through a CFTR-dependent mechanism (**Figure 3.54B**).

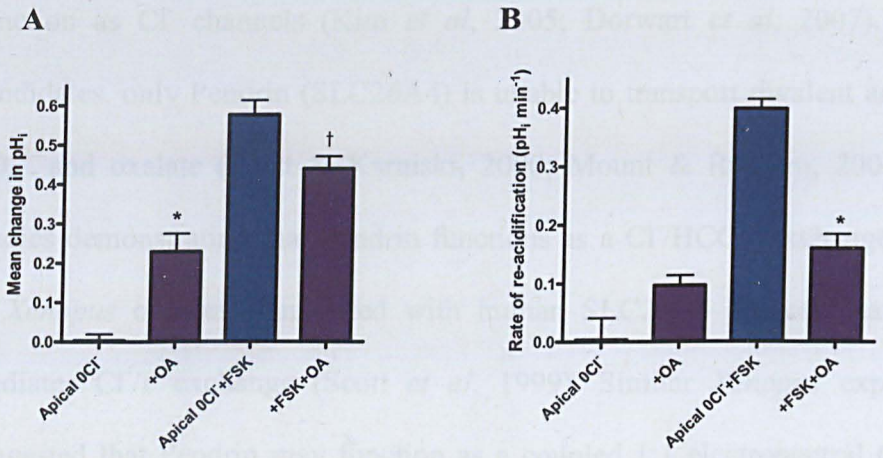

Figure 3.54- Okadaic acid-induced apical AE activity is enhanced by forskolin through a CFTR-dependent mechanism. The effects of okadaic acid (100 nM) on the mean change in pH_i following the removal of apical chloride (**A**) and the mean rate of re-acidification in pH_i upon the re-addition of apical chloride (**B**) in unstimulated and forskolin-stimulated CFTR KD Calu-3 cells. n=5. OA treated and untreated CFTR KD Calu-3 cell experiments were run in parallel. A: *P<0.01 compared to apical $0Cl^-$. †P<0.01 compared to +OA. B: *P<0.001 compared to apical $0Cl^-$+FSK.

3.7 SLC26A4

Results so far, show that Calu-3 cells exhibit cAMP-dependent apical Cl^-/HCO_3^- exchange activity. This apical AE is insensitive to H_2-DIDS, Na^+-independent and exchanges HCO_3^- with a range of monovalent anions (I^-=Br^->Cl^-=Formate=NO_3^- =SCN^-), but is not supported by divalent anions.

The apical AE found in Calu-3 cells is believed to be a member of the SLC26 family. Several SLC26 proteins can function as Cl^-/HCO_3^- exchangers in a variety of tissues and cell types including: A3 in the pancreas (Ko *et al*, 2002) and intestine (Melvin *et al*, 1999); A4 in the thyroid and kidney (Soleimani *et al*, 2001); A6 in the pancreas (Ko *et al*, 2002) and intestine (Wang *et al*, 2002); A7 in the stomach (Petrovic *et al*,

2003) and kidney (Petrovic *et al*, 2004); A9 in transfected *Xenopus* oocytes (Chang *et al*, 2009) and HEK cells (Xu *et al*, 2005). However, SLC26A7 and SLC26A9 can also function as Cl^- channels (Kim *et al*, 2005; Dorwart *et al*, 2007). Of these five candidates, only Pendrin (SLC26A4) is unable to transport divalent anions including SO_4^{2-} and oxalate (Scott & Karniski, 2000; Mount & Romero, 2004). As well as studies demonstrating that Pendrin functions as a Cl^-/HCO_3^- exchanger, experiments in *Xenopus* oocytes transfected with human SLC26A4 showed that Pendrin also mediates Cl^-/I^- exchange (Scott *et al*, 1999). Similar *Xenopus* experiments even suggested that Pendrin may function as a coupled 1:1 electroneutral Cl^-/I^-, I^-/HCO_3^- and Cl^-/ HCO_3^- exchanger, which preferentially transports I^- (Shcheynikov et al, 2008). The same study found that apically expressed Pendrin mediates I^- secretion from mouse parotid duct cells, which could be enhanced by forskolin and was absent in SLC26A4 knockout mice. Therefore the profile of the apical anion exchanger is most consistent with Pendrin (SLC26A4), due to its selectivity for monovalent anions, affinity for iodide and insensitivity to H_2-DIDS.

To investigate which of the 10 known SLC26 isoforms may be acting as an apical Cl^-/HCO_3^- exchanger, quantitative Real-Time PCR (RT-PCR) experiments were carried out to identify which SLC26 isoforms are present in Calu-3 cells and to quantify the relative expression of each isoform compared to one another. Cells were grown to confluence on transwell supports to be consistent with the conditions used for pH_i experiments.

Quantitative RT-PCR (Taqman) analysis showed that many SLC26 transporters are expressed in Calu-3 cells, several of which have been shown to act as Cl^-/HCO_3^-

exchangers (SLC26A4, A6, A7 and A9). SLC26A2 and A6 were highly expressed, relative to the lower expression of A4, A5, A7, A9 and A11. SLC26A1 and A3 were very weakly expressed and A8 was not present in Calu-3 cells (**Figure 3.55**).

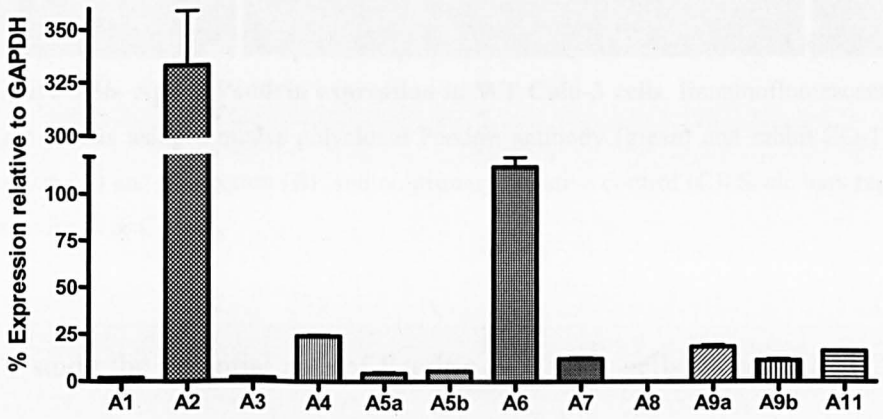

Figure 3.55- SLC26 mRNA expression in WT Calu-3 cells. Quantative RT-PCR (Taqman) analysis of SLC26 expression in WT Calu-3 cells grown on transwell supports, relative to standard curve and normalised to GAPDH (%). n=3.

Pendrin expression in WT Calu-3 cells was confirmed by immunofluorescent staining, using a mouse polyclonal anti-Pendrin antibody (ABNOVA) and showed a punctuate pattern of staining across the monolayer (**Figure 3.56**). Co-staining with an antibody for the tight junction protein zona occludins 1 (ZO-1), revealed that Pendrin appeared to be localised to the apical membrane of Calu-3 cells. Western blot analysis of Pendrin expression was unsuccessful with the ABNOVA antibody.

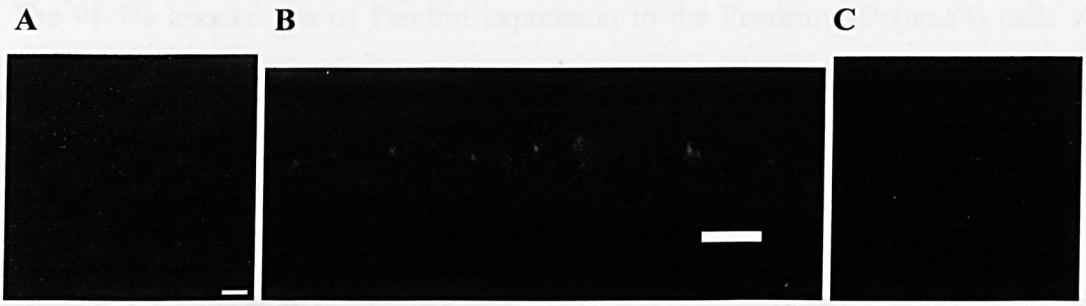

Figure 3.56- Apical Pendrin expression in WT Calu-3 cells. Immunofluorescent co-staining of WT Calu-3 cells using a mouse polyclonal Pendrin antibody (green) and rabbit ZO-1 antibody (red), *XY* section (**A**) and *XZ* section (**B**), and no primary negative control (**C**). Scale bars represent 10μm. Scale same for **A** & **C**. n=3.

To study the potential role of Pendrin in Calu-3 cells, Pendrin KD Calu-3 cells were developed using an shRNA approach (see Methods section 2.2). Several knockdown cell lines were produced, with Pendrin (mRNA) expression varying from 32.1 ± 4.4% (No.83 KD) to 8.5 ± 0.7% (No.84) of that in control Calu-3 cells (**Figure 3.57**). The no.84 KD cell line was selected for pH_i experiments due to similar transepithelial resistance and growth patterns to that of the WT cells. Cyclophilin B KD Calu-3 cells were also produced alongside the Pendrin KD cells, using the same shRNA method, to act as a control.

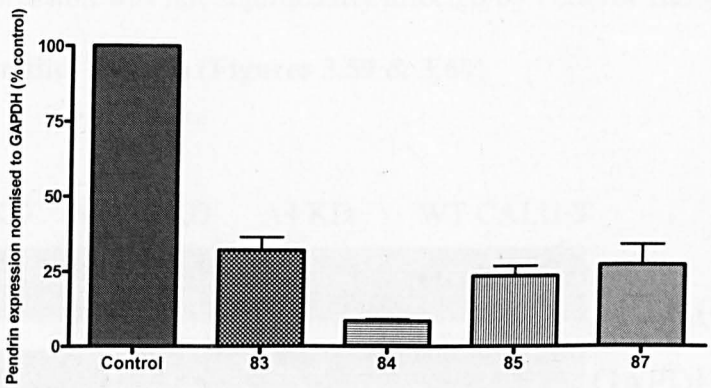

Figure 3.57- Pendrin mRNA expression in knockdown Calu-3 cells. Quantative RT-PCR (Taqman) analysis of the percentage Pendrin expression in Pendrin KD Calu-3 cells (83,84,85,87) normalised to GAPDH, compared to that of control cyclophilin B KD Calu-3 cells. n=3.

The 91.5% knockdown of Pendrin expression in the Pendrin KD (no.84) cells was apparent from the lack of Pendrin staining, compared to WT and control KD Calu-3 cells (**Figure 3.58**).

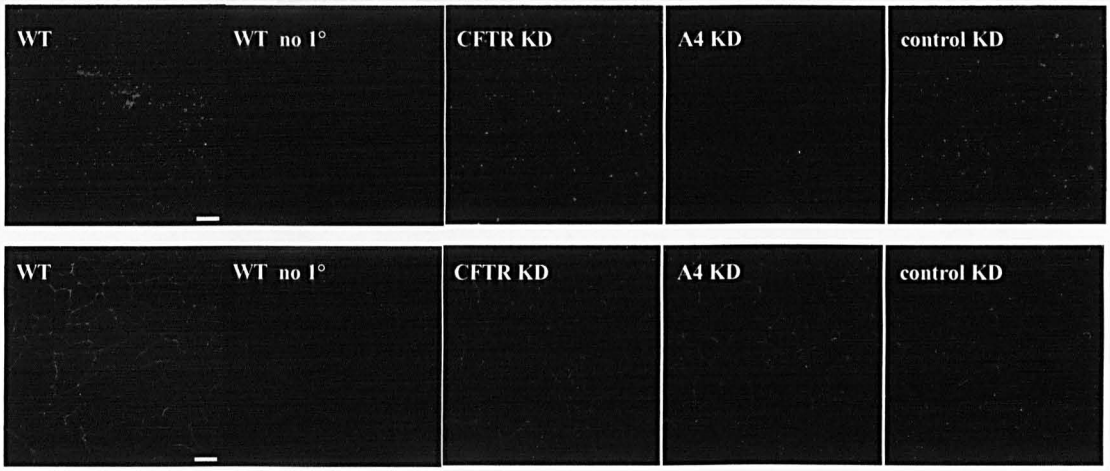

Figure 3.58- Reduced Pendrin expression in Pendrin KD Calu-3 cells. Immunofluorescent staining of Wild-type (WT), CFTR knockdown (CFTR KD), Pendrin knockdown no.84 (A4 KD) and cyclophilin B knockdown (control KD) Calu-3 cells using a mouse polyclonal Pendrin antibody (green, above) and rabbit ZO-1 antibody (red, below). WT no 1° represents immunofluorescence from WT Calu-3 cells with only the secondary antibodies applied. Note: cells stained with either antibody are separate *XY* sections taken from the same confluent monolayer of each cell type. Scale bars represent 10μm. n=3.

CFTR expression was not significantly affected by Pendrin knockdown, as confirmed by Western Blot analysis (**Figures 3.59 & 3.60**).

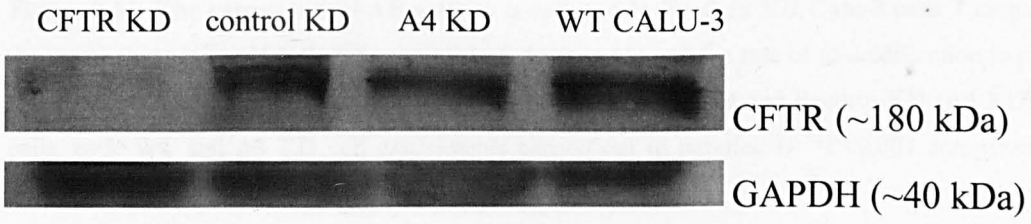

Figure 3.59- Western blot CFTR expression in wild-type and knockdown Calu-3 cells. CFTR and GAPDH Western Blot staining of CFTR KD, Cyclophilin B KD (CON KD), Pendrin KD no.84 (A4 KD) and WT Calu-3 cells. CFTR/GAPDH band intensity ratios: CFTR KD= 0.45; control KD= 2.98; A4 KD= 2.34; WT CALU-3= 2.18. n=3.

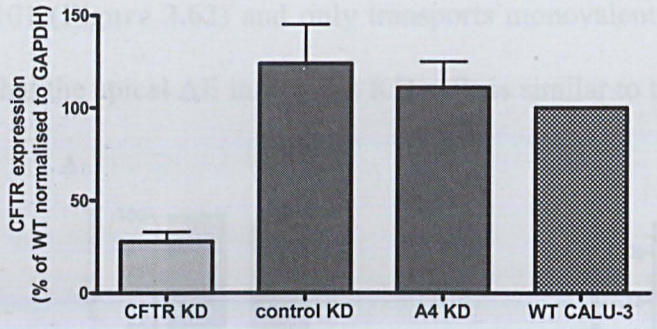

Figure 3.60- Western blot analysis of CFTR expression in wild-type and knockdown Calu-3 cells. Percentage CFTR expression of CFTR KD, cyclophilin B KD (control KD) and Pendrin KD (A4 KD) Calu-3 cells compared to WT Calu-3 cells, derived from CFTR/GAPDH band intensity ratios. n=3.

Pendrin (A4) KD Calu-3 cells still showed a forskolin-stimulated apical AE, but the rate of activity was reduced by 47.6 ± 2.4% in the A4 KD cells compared to control cyclophilin B KD cells ($P<0.001$; n=5; **Figure 3.61**), results which are similar to apical AE present in CFTR KD Calu-3 cells (see Figure 3.41).

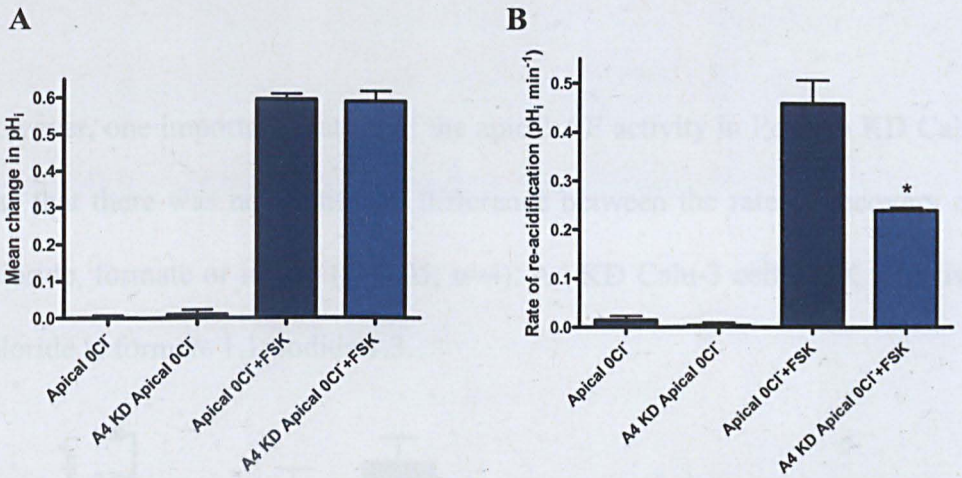

Figure 3.61- The rate of apical AE activity is reduced in Pendrin KD Calu-3 cells. Comparison of the mean changes in pH_i following removal of chloride (**A**) and the rate of re-acidification in pH_i upon the re-addition of chloride (**B**), between control cyclophilin B KD and Pendrin KD (A4 KD) Calu-3 cells. n=5. WT and A4 KD cell experiments carried out in parallel. B: *P<0.001 compared to WT apical $0Cl^-$+FSK.

The profile of the apical AE activity in Pendrin KD Calu-3 cells was also studied. The apical AE was H_2-DIDS insensitive, completely inhibited by CFTR inhibitor GlyH-

101 (**Figure 3.62**) and only transports monovalent anions (**Figure 3.63**), suggesting that the apical AE in Pendrin KD cells is similar to that in WT Calu-3 cells.

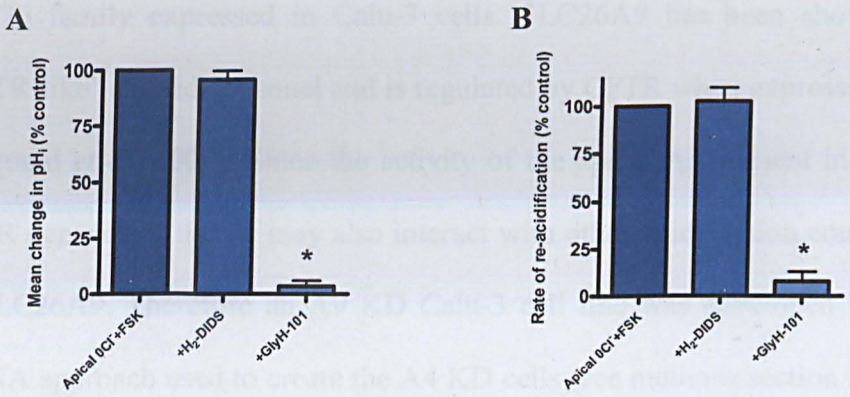

Figure 3.62- The pharmacological profile of apical AE activity in Pendrin KD Calu-3 cells. The effects of apical H_2-DIDS (500 μM) and apical GlyH-101 (10 μM) addition on the percentage mean alkalinisation in pH_i following the removal of apical chloride (**A**) and the percentage rate of re-acidification upon chloride re-addition (**B**) in forskolin-stimulated (10 μM) Pendrin KD Calu-3 cells. pH_i responses in the presence of H_2-DIDS and GlyH-101 compared to control apical $0Cl^-$+FSK responses. n=4. H_2-DIDS and GlyH-101 experiments carried out in parallel. A: *P<0.001 compared to apical $0Cl^-$+FSK and +H_2DIDS. B: *P<0.001 compared to apical $0Cl^-$+FSK and +H_2DIDS.

However, one important feature of the apical AE activity in Pendrin KD Calu-3 cells, was that there was no significant difference between the rate of recovery of pH_i by chloride, formate or iodide (P>0.05; n=4). A4 KD Calu-3 cell Cl^-/X selectivity ratio: chloride 1: formate 1.1: iodide 1.3.

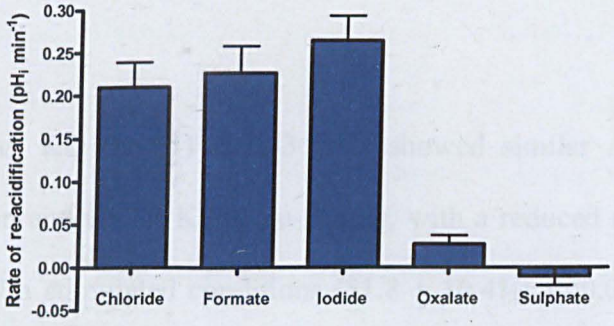

Figure 3.63- Anion selectivity of apical Cl^-/HCO_3^- exchange in forskolin-stimulated Pendrin KD Calu-3 cells. The rate of recovery of pH_i by the introduction of monovalent (iodide, formate and chloride) and divalent (oxalate and sulphate) anions in zero Cl^- conditions. n=4. Paired observations.

3.8 SLC26A9

As previously shown in Figure 3.55, SLC26A9 is one of several members of the SLC26 family expressed in Calu-3 cells. SLC26A9 has been shown to act as a 'CFTR-like' chloride channel and is regulated by CFTR when expressed in HEK cells (Bertrand *et al*, 2009). Since the activity of the apical AE present in Calu-3 cells is CFTR dependent, then it may also interact with other apical anion conductances such as SLC26A9. Therefore an A9 KD Calu-3 cell line was developed using a similar shRNA approach used to create the A4 KD cells (see methods section 2.2). The no.51 KD cell line was selected for pH_i experiments due to its ~48% reduced expression of SLC26A9 compared to control cyclophilin B KD Calu-3 cells (**Figure 3.64**).

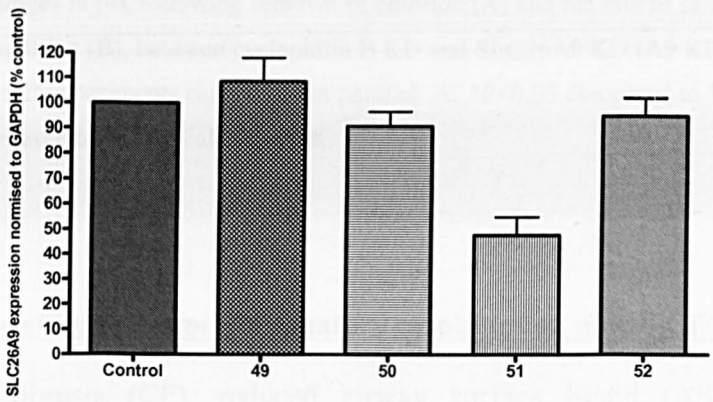

Figure 3.64- SLC26A9 mRNA expression in knockdown Calu-3 cells. Quantative RT-PCR (Taqman) analysis of the percentage SLC26A9 expression in SLC26A9 KD Calu-3 cells (49,50,51,52) normalised to GAPDH, compared to that of control cyclophilin B KD Calu-3 cells. n=6.

The A9 KD (no.51) Calu-3 cells showed similar AE activity profile to both the Pendrin and CFTR KD Calu-3 cells, with a reduced rate of apical AE activity under forskolin stimulated conditions (51.8 ± 10.4%; $P<0.01$; n=6; **Figure 3.65B**). Unlike the other KD cells, A9 KD Calu-3 cells also exhibited a 17.4 ± 6.6% reduction in the

overall mean alkalinisation induced by apical zero Cl^- exposure ($P<0.05$; n=6; **Figure 3.65A**).

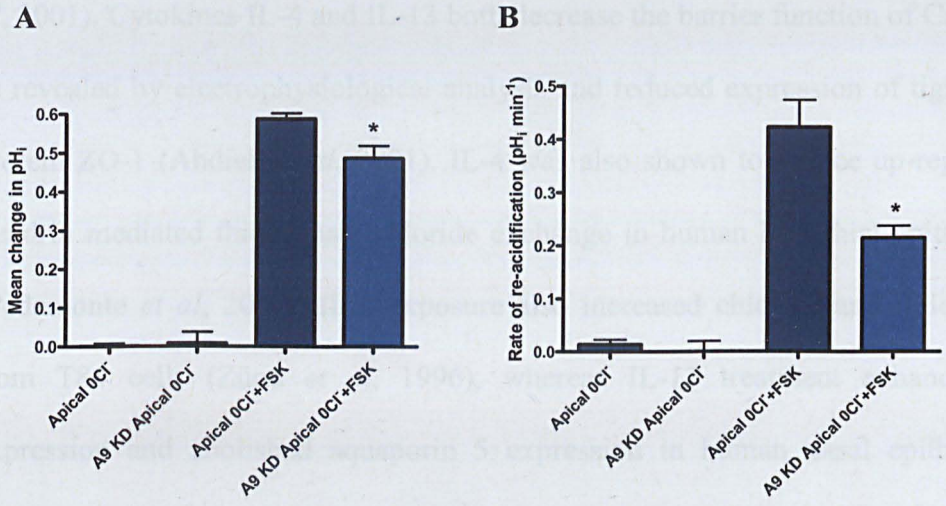

Figure 3.65- The rate of apical AE activity is reduced in SLC26A9 KD Calu-3 cells. Comparison of the mean changes in pH_i following removal of chloride (**A**) and the rate of re-acidification in pH_i upon chloride re-addition (**B**), between cyclophilin B KD and SLC26A9 KD (A9 KD) Calu-3 cells. n=6. WT and A9 KD cell experiments carried out in parallel. A: *$P<0.05$ compared to WT apical $0Cl^-$+FSK. B: *$P<0.01$ compared to WT apical $0Cl^-$+FSK.

3.9 The effects of proinflammatory cytokines on apical Cl^-/HCO_3^- exchange

In cystic fibrosis (CF), reduced airway surface liquid (ASL) production and thickening of the mucus within the ASL prevents mucociliary clearance, providing favourable conditions for bacterial formation. Airway disease in CF is characterised by chronic infection resulting in an inflammatory response dominated by the mass recruitment of neutrophils in the airways, which produce inflammatory cytokines in aid of eradicating the infectious pathogens (Courtney *et al*, 2004). Excessive amounts of proinflammatory cytokines have been observed in the airways of CF sufferers (Khan *et al*, 1995).

Interleukin (IL)-1β treatment has been demonstrated to increase CFTR mRNA expression in Calu-3 cells and could therefore alter apical AE activity (Brouillard *et al*, 2001). Cytokines IL-4 and IL-13 both decrease the barrier function of Calu-3 cells, as revealed by electrophysiological analysis and reduced expression of tight junction protein ZO-1 (Ahdieh *et al*, 2001). IL-4 was also shown to induce up-regulation of Pendrin mediated thiocyanate-chloride exchange in human bronchial epithelial cells (Pedemonte *et al*, 2007). IL-4 exposure also increased chloride and fluid secretion from T84 cells (Zünd *et al*, 1996), whereas IL-13 treatment enhanced CFTR expression and abolished aquaporin 5 expression in human nasal epithelial cells during differentiation (Skowron-zwarg *et al*, 2007). But of particular importance and relevance to apical AE activity was the finding that IL-17A induced CFTR-dependent HCO_3^- secretion in human bronchial epithelial cells (Kreindler *et al*, 2009). Ussing chamber studies showed that IL-17A treatment enhanced forskolin-stimulated HCO_3^- dependent I_{sc}, which alkalinised the pH of the mucosal fluid bathing the bronchial epithelial cells.

Proinflammatory cytokines IL-1β, IL-4, IL-13 and IL-17A were applied to the media of Calu-3 cells for 48 hours prior to qRT-PCR mRNA analysis and pH_i experiments. qRT-PCR analysis of potential SLC26 Cl^-/HCO_3^- exchangers expressed in Calu-3 cells showed SLC26A4 (Pendrin) mRNA expression was not significantly altered by any interleukin treatment ($P>0.05$; n=3; **Figure 3.66**), whereas IL-4 and IL-13 enhanced both SLC26A6 ($P<0.01$; n=3; **Figure 3.67**) and A9 ($P<0.001$; n=3; **Figure 3.68**) mRNA expression.

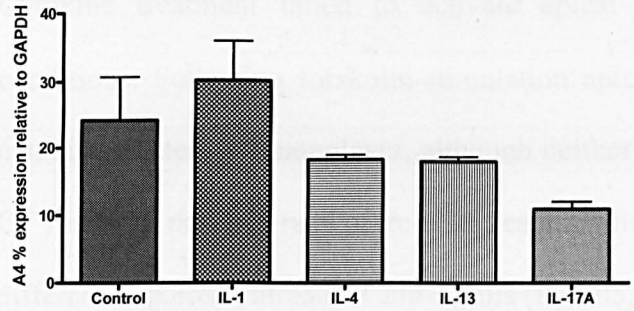

Figure 3.66- SLC26A4 mRNA expression in cytokine treated Calu-3 cells. Quantative RT-PCR (Taqman) analysis of SLC26A4 expression in cytokine-treated Calu-3 cells relative to standard curve and normalised to GAPDH (%). Calu-3 cells pre-treated with cytokine IL-1β (20ng/ml), IL-4 (10ng/ml), IL-13 (10ng/ml) and IL-17A (50ng/ml). n=3.

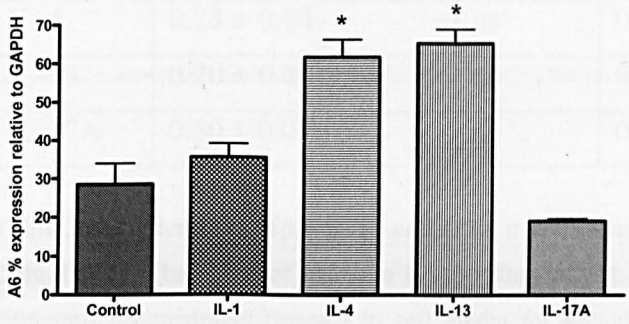

Figure 3.67- SLC26A6 mRNA expression in cytokine treated Calu-3 cells. Quantative RT-PCR (Taqman) analysis of SLC26A6 expression in cytokine-treated Calu-3 cells relative to standard curve and normalised to GAPDH (%). Calu-3 cells pre-treated with cytokine IL-1β (20ng/ml), IL-4 (10ng/ml), IL-13 (10ng/ml) and IL-17A (50ng/ml). n=3. *P<0.01 compared to untreated control Calu-3 cells.

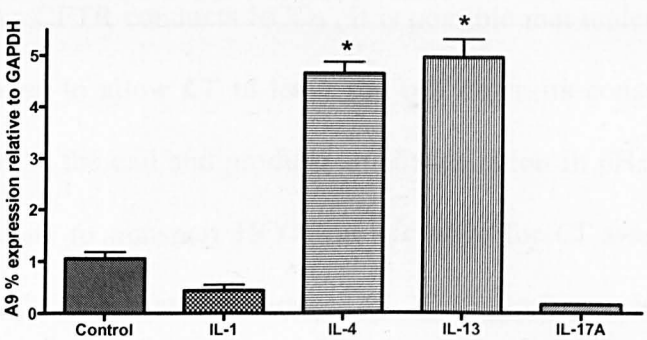

Figure 3.68- SLC26A9 mRNA expression in cytokine treated Calu-3 cells. Quantative RT-PCR (Taqman) analysis of SLC26A9 expression in cytokine-treated Calu-3 cells relative to standard curve and normalised to GAPDH (%). Calu-3 cells pre-treated with cytokine IL-1β (20ng/ml), IL-4 (10ng/ml), IL-13 (10ng/ml) and IL-17A (50ng/ml). n=3. *P<0.001 compared to untreated control Calu-3 cells.

Cytokine treatment failed to activate apical AE activity under non-stimulated conditions. Following forskolin-stimulation apical AE activity was present in each cytokine treated cell monolayer, although neither the mean change in pH_i upon apical Cl^- removal nor the rate of re-acidification after Cl^- re-addition was significantly different to paired untreated Calu-3 cells ($P>0.05$; **Table 3.01**).

Cytokine	Mean change in pH_i (pH units)	P value vs WT	Rate of re-acidification (pH_i min^{-1})	P value vs WT	n
IL-1β	0.47 ± 0.11	ns	0.35 ± 0.05	ns	6
IL-4	0.28 ± 0.04	ns	0.31 ± 0.05	ns	6
IL-13	0.20 ± 0.05	ns	0.14 ± 0.03	ns	5
IL-17A	0.50 ± 0.07	ns	0.34 ± 0.05	ns	7

Table 3.01- Interleukin-1β, -4, -13 and -17A pre-treatment has no effect on apical AE activity in Calu-3 cells. The effect of cytokine IL-1β (20ng/ml), IL-4 (10ng/ml), IL-13 (10ng/ml) and IL-17A (50ng/ml) pre-treatment (present in cell media for 48hours) on the mean changes in pH_i following removal of chloride and the rate of re-acidification in pH_i upon the re-addition of chloride in Calu-3 cells. ns: P value >0.05 compared to untreated Calu-3 cells.

3.10 Cl^--dependent pH_i changes in FRT cells: Pendrin vs CFTR

As CFTR conducts HCO_3^-, it is possible that under zero Cl^- conditions, CFTR would open to allow Cl^- to leave the cell down its concentration gradient and HCO_3^- may enter the cell and produce an alkalinisation in pH_i. The ability of Pendrin and CFTR alone to transport HCO_3^- in exchange for Cl^- was tested in stably transfected FRT cells (see Methods section 2.1.2). Control, non-transfected FRT cells produced an alkalinisation of 0.24 ± 0.01 pH units in response to basolateral Cl^- removal, which was not enhanced by forskolin stimulation (0.32 ± 0.05 pH units; $P>0.05$). This constitutively active basolateral AE activity was not significantly altered by either

Pendrin or CFTR transfection. Importantly, the control FRT cells showed no significant response to apical Cl^- removal, under basal or forskolin stimulated conditions.

Pendrin (A4) transfected FRT cells produced an alkalinisation in pH_i of 0.16 ± 0.06 pH units following apical Cl^- removal under non-stimulated conditions (**Figures 3.69 & 3.71**). Re-addition of apical Cl^- produced a re-acidification at a rate of 0.10 ± 0.02 pH units min^{-1}. Forskolin addition did not produce a significant change in pH_i ($P>0.05$; n=6) and neither the mean alkalinisation nor the rate of re-acidification, due to Cl^- removal and Cl^- re-addition respectively, were significantly increased in A4 FRT cells ($P>0.05$; n=6).

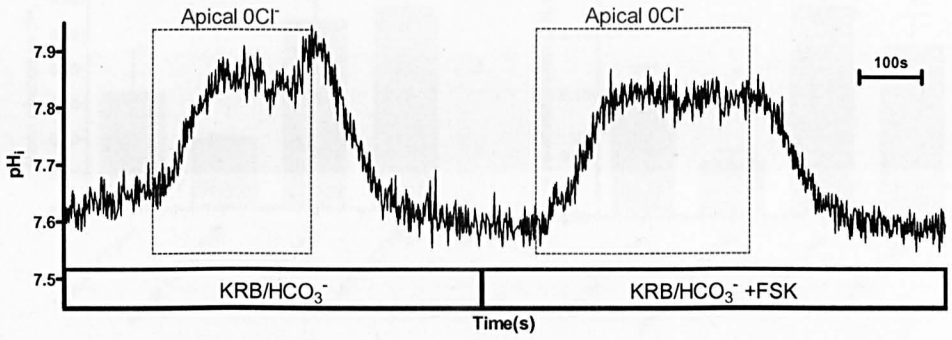

Figure 3.69- Apical AE activity in Pendrin transfected FRT cells. The effects of forskolin (5 μM) on changes in pH_i following the removal of apical chloride in Pendrin transfected FRT cells.

CFTR transfected FRT cells had a more neutral initial pH_i (7.26 ± 0.05) compared to A4 FRT cells (7.64 ± 0.08; n=13; $P<0.001$). CFTR transfected cells also produced an alkalinisation in response to apical Cl^- removal under basal conditions, however this change in pH_i was enhanced following forskolin addition (0.10 ± 0.01 to 0.28 ± 0.03 pH units; $P<0.05$; n=6; **Figures 3.70 & 3.71**). Likewise the rate of re-acidification

increased from 0.05 ± 0.01 to 0.14 ± 0.03 pH units min^{-1} upon forskolin stimulation ($P<0.05$; n=6).

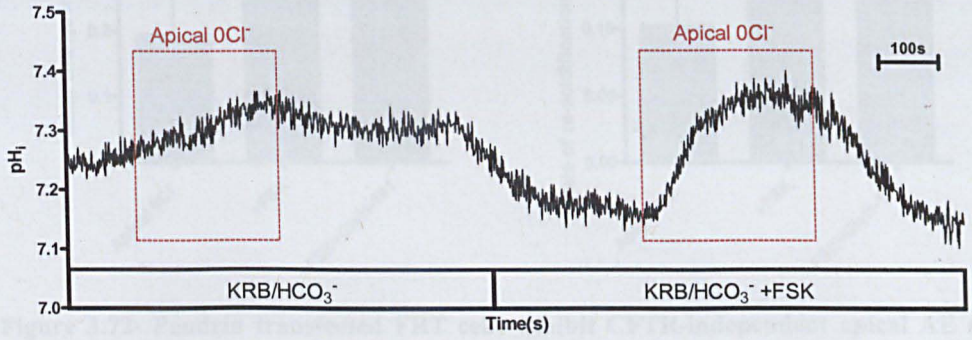

Figure 3.70- Forskolin enhances apical Cl^- removal induced pH_i changes in CFTR transfected FRT cells. The effects of forskolin (5 μM) on changes in pH_i following the removal of apical chloride in CFTR transfected FRT cells.

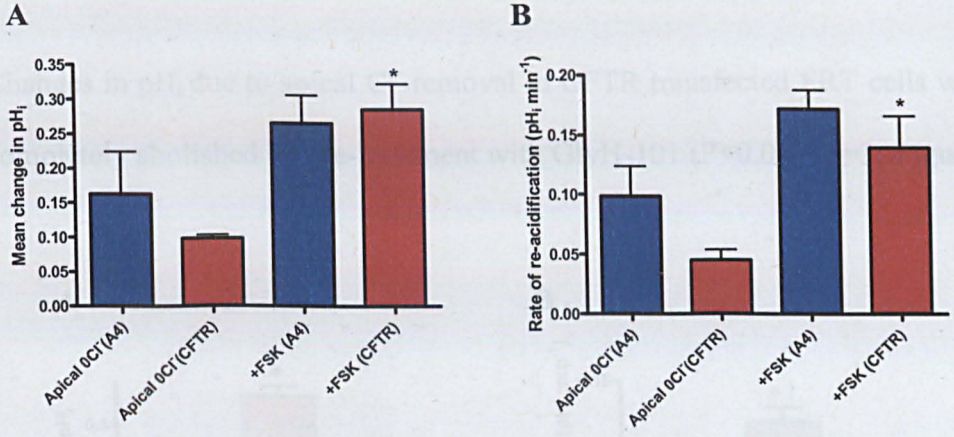

Figure 3.71- Apical Cl^- removal and re-addition induced changes in pH_i in Pendrin and CFTR transfected FRT cells. Comparison of the mean changes in pH_i following removal of chloride (**A**) and the rate of re-acidification in pH_i following the re-addition of chloride (**B**), in control, Pendrin transfected (A4) and CFTR transfected (CFTR) FRT cells, in the presence and absence of forskolin. n=6. A4 and CFTR transfected FRT cell experiments ran in parallel. A: *$P<0.05$ compared to apical $0Cl^-$ (CFTR). B: *$P<0.05$ compared to apical $0Cl^-$ (CFTR).

Apical AE activity in Pendrin transfected FRT cells was unaffected by the CFTR inhibitor GlyH-101 (**Figure 3.72**).

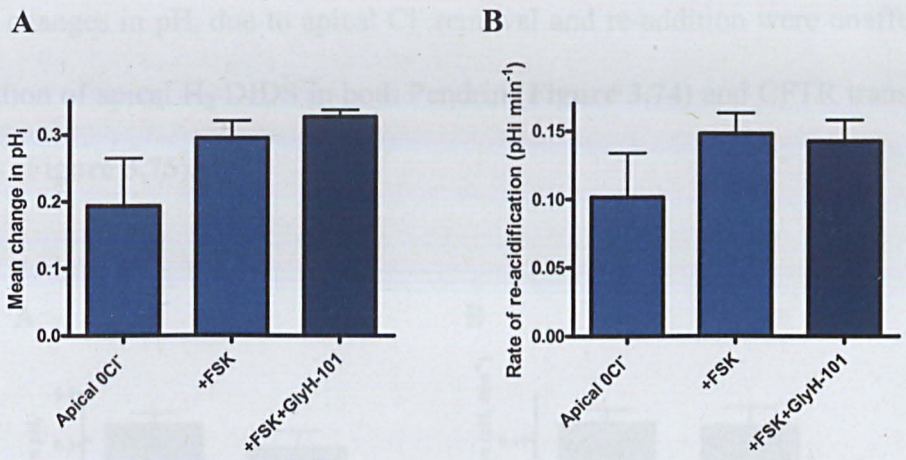

Figure 3.72- Pendrin transfected FRT cells exhibit CFTR-independent apical AE activity. The effects of apical CFTR inhibitor GlyH-101 (10 μM) on the mean alkalinisation (pH_i) produced by apical chloride removal (**A**) and the rate of re-acidification upon apical chloride re-addition (**B**), in unstimulated and forskolin-stimulated (5 μM) Pendrin transfected FRT cells. n=3. Paired observations.

Changes in pH_i due to apical Cl^- removal in CFTR transfected FRT cells were almost completely abolished by pre-treatment with GlyH-101 ($P<0.001$; n=3; **Figure 3.73**).

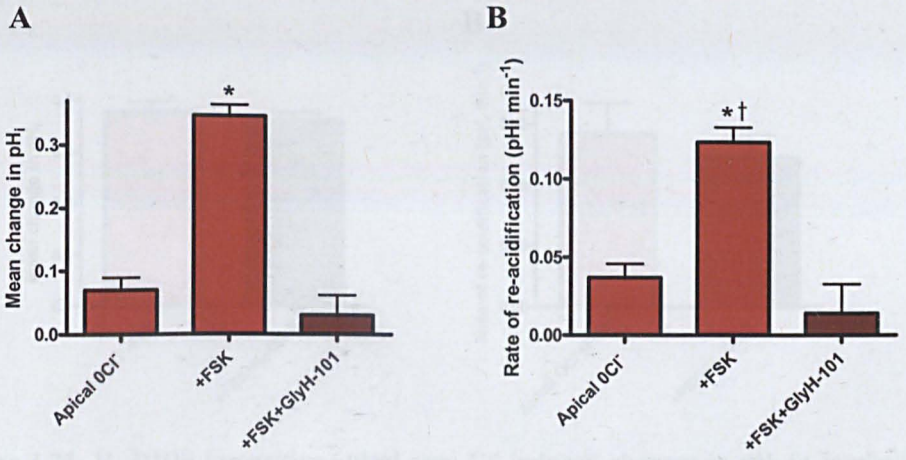

Figure 3.73- Apical zero Cl^- induced changes in pH_i in forskolin-stimulated CFTR transfected FRT cells is inhibited by GlyH-101. The effects of apical CFTR inhibitor GlyH-101 (10 μM) on the mean alkalinisation (pH_i) produced by apical chloride removal (**A**) and the rate of re-acidification upon apical chloride re-addition (**B**), in unstimulated and forskolin-stimulated (5 μM) CFTR transfected FRT cells. n=3. Paired observations. A: *$P<0.001$ compared to apical $0Cl^-$ and +FSK+GlyH-101. B: *$P<0.05$ compared to apical $0Cl^-$. †$P<0.01$ compared to +FSK+GlyH-101.

The changes in pH_i due to apical Cl^- removal and re-addition were unaffected by the addition of apical H_2-DIDS in both Pendrin (**Figure 3.74**) and CFTR transfected FRT cells (**Figure 3.75**).

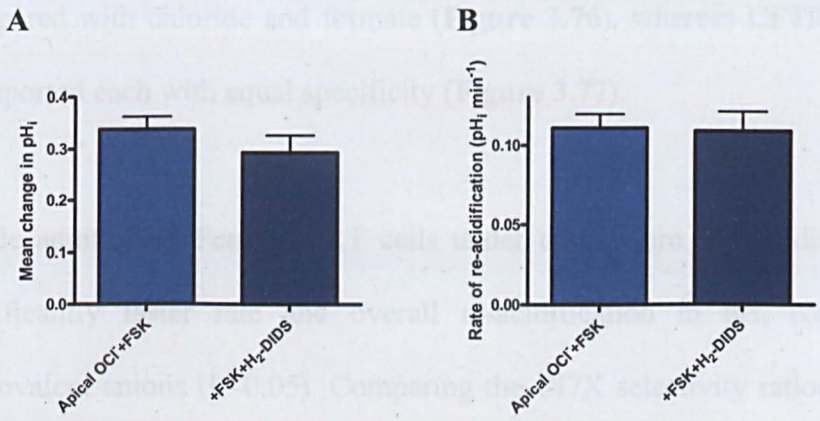

Figure 3.74- H_2-DIDS insensitive apical AE activity in forskolin-stimulated Pendrin transfected FRT cells. The effect of apical H_2-DIDS (500 μM) on the mean alkalinisation (pH_i) produced by apical chloride removal (**A**) and the rate of re-acidification upon apical chloride re-addition (**B**), in forskolin-stimulated (5 μM) Pendrin transfected FRT cells. n=3. Paired observations.

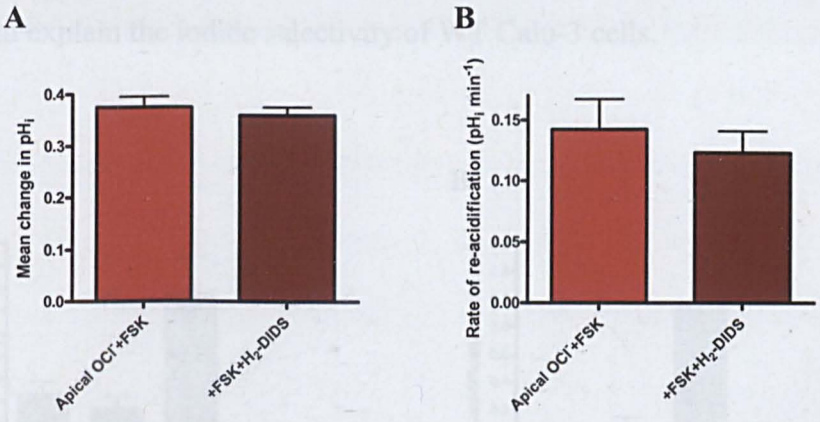

Figure 3.75- H_2-DIDS insensitive apical zero Cl^- induced changes in pH_i in forskolin-stimulated CFTR transfected FRT cells. The effect of apical H_2-DIDS (500 μM) on the mean alkalinisation (pH_i) produced by apical chloride removal (**A**) and the rate of re-acidification upon apical chloride re-addition (**B**), in forskolin-stimulated (5 μM) CFTR transfected FRT cells. n=3. Paired observations.

An important difference between apical Cl^--dependent changes in pH_i in Pendrin and CFTR transfected FRT cells was their anion selectivity profiles. Both cell types were only able to transport monovalent anions (AE activity was not supported by divalent anions oxalate or sulphate), but A4 transfected cells had a greater affinity for iodide compared with chloride and formate (**Figure 3.76**), whereas CFTR transfected cells transported each with equal specificity (**Figure 3.77**).

Iodide addition in Pendrin FRT cells under apical zero Cl^- conditions, produced a significantly faster rate and overall re-acidification in pH_i compared to other monovalent anions ($P<0.05$). Comparing the Cl^-/X selectivity ratios of Pendrin FRT (chloride 1: formate 1.1: iodide 3.2) and CFTR FRT cells (chloride 1: iodide 1.1: formate 1.3) with that of WT Calu-3 cells (formate 0.6: chloride 1: iodide 1.3), would suggest that neither CFTR nor Pendrin are solely responsible for the apical anion selectivity seen in Calu-3 cells. However, the greater affinity of Pendrin for iodide would explain the iodide selectivity of WT Calu-3 cells.

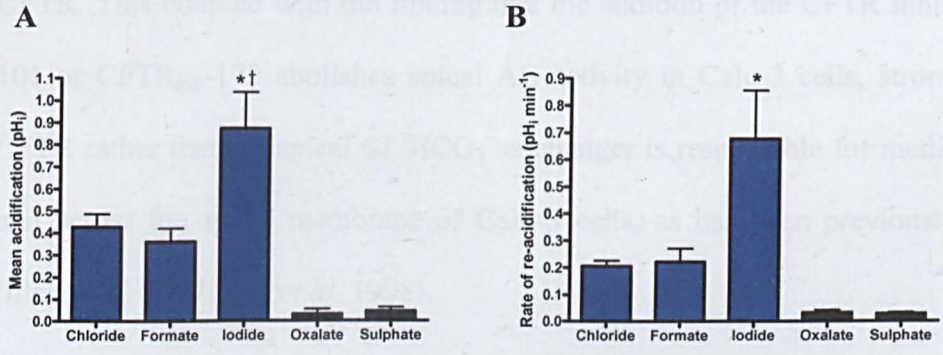

Figure 3.76- Anion selectivity of re-acidification in pH_i following apical Cl^- removal in Pendrin transfected FRT cells. The mean acidification (**A**) and rate of recovery (**B**) of pH_i by the introduction of monovalent (iodide, formate and chloride) and divalent (oxalate and sulphate) anions in zero Cl^- conditions. n=4. Paired observations. A: *$P<0.05$ compared to chloride. †$P<0.01$ compared to formate. B: *$P<0.05$ compared to chloride and formate.

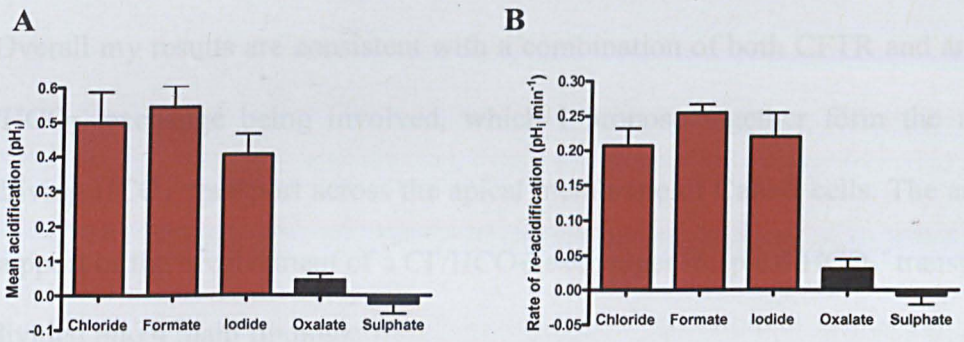

Figure 3.77- Anion selectivity of re-acidification in pH_i following apical Cl^- removal in CFTR transfected FRT cells. The mean acidification (**A**) and rate of recovery (**B**) of pH_i by the introduction of monovalent (iodide, formate and chloride) and divalent (oxalate and sulphate) anions in zero Cl^- conditions. n=4. Paired observations.

3.11 Discussion

The cAMP-activated apical AE activity present in Calu-3 cells is Na^+-independent, H_2-DIDS-insensitive and can transport a range of monovalent anions in exchange for HCO_3^- with the selectivity profile Iodide=Br^->Cl^-=Formate =NO_3^-=SCN^-. The profile of this exchanger is most consistent with Pendrin. However, as seen in CFTR transfected FRT cells, apical Cl^- removal could also induce HCO_3^- influx through CFTR. This coupled with the finding that the addition of the CFTR inhibitors GlyH-101 or $CFTR_{inh}$-172 abolishes apical AE activity in Calu-3 cells, strongly suggests CFTR rather than an apical Cl^-/HCO_3^- exchanger is responsible for mediating HCO_3^- exit across the apical membrane of Calu-3 cells, as has been previously postulated (Illek *et al*, 1997; Lee *et al*, 1998).

3.11.1 Apical AE activity in Calu-3 cells: SLC26 Cl^-/HCO_3^- exchanger or CFTR?

The alkalinisation seen in cAMP-stimulated Calu-3 cells following apical Cl^- removal and the subsequent re-acidification in pH_i upon Cl^- re-addition can be interpreted as

being due to HCO_3^- flux through CFTR and/or due to Cl^-/HCO_3^- exchange activity. Overall my results are consistent with a combination of both CFTR and an apical Cl^-/HCO_3^- exchange being involved, which I propose together form the mechanism driving HCO_3^- transport across the apical membrane of Calu-3 cells. The argument in support of the involvement of a Cl^-/HCO_3^- exchanger in apical HCO_3^- transport can be divided into 4 main findings:

1. Affinity of apical AE activity for iodide is inconsistent with CFTR anion selectivity.

The iodide selectivity of the apical AE present in Calu-3 cells is consistent with the high affinity of Pendrin for iodide as seen in the Pendrin transfected FRT cells. My results in WT Calu-3 cells suggest that the apical AE has the selectivity profile: Iodide=Br^->Cl^-=Formate=NO_3^-=SCN^-. Apical AE activity in Pendrin transfected FRT cells had an anion selectivity of Iodide>Cl^-=Formate, whereas CFTR transfected cells transported each of these monovalent anions at equal rates. Previous CFTR I_{SC} anion substitution measurements performed in α-toxin permeabilised Calu-3 cells determined the cAMP-stimulated CFTR anion selectivity to be: Br^->Cl^->NO_3^->SCN^- >Iodide>Formate>HCO_3^- (Illek *et al*, 1997). The same study found that CFTR did not conduct divalent anions such as SO_4^{2-} and was blocked by both formate and iodide. Also in studies using excised inside-out membrane patches from CFTR transfected CHO cells, iodide (150 mM) blocked CFTR (Tabcharani *et al*, 1992). The permeability of iodide compared to chloride through CFTR has led to conflicting results, although this maybe due to differences in iodide permeability according to whether measurements were made from the cytoplasmic or luminal side of the CFTR channel (Linsdell *et al*, 1997). Although iodide block of CFTR would suggest that the

anion selectivity of the apical AE activity in Calu-3 cells and its high affinity for iodide are not consistent with the selectivity profile of CFTR, by blocking CFTR, iodide addition during an apical Cl^- removal induced alkalinisation may result in a re-acidification similar to that seen upon the addition CFTR pore blocker GlyH-101. Therefore potential future work into the profile and selectivity of the Calu-3 apical AE activity should include the addition of basolateral H_2-DIDS during anion substitution studies in order to determine whether the exchanger transports iodide, or the re-acidification in pH_i is due to iodide blocking CFTR resulting in activation of a H_2-DIDS-sensitive basolateral HCO_3^- transporter. However, my experiments in CFTR transfected FRT cells would suggest that CFTR has a similar permeability for iodide compared to chloride under these experimental conditions and is therefore unlikely to be blocked by iodide.

SLC26A9, a Cl^- channel preferentially expressed in lung tissue (Lohi *et al*, 2002) and which my mRNA studies have shown to be expressed in Calu-3 cells, is known to be highly selective for iodide when expressed in *Xenopus* oocytes (selectivity sequence- Iodide> Br^-> NO_3^->Cl^-; Dorwart *et al*, 2007; Loriol *et al*, 2008). Like CFTR, iodide is known to block Cl^- conductance through SLC26A9 (Dorwart *et al*, 2007). However, simultaneous measurement of membrane potential, pH_i and $[Cl^-]_i$ have revealed that OH^- and HCO_3^- flux through SLC26A9 in transfected oocytes is very small (A9-mediated HCO_3^- flux ~0.33 mM min^{-1}; Dorwart *et al*, 2007), with little or no change in pH_i observed following Cl^- removal (Dorwart *et al*, 2007; Loriol *et al*, 2008). Cl^- current measurements in HEK cells showed that SLC26A9 is constitutively active and its activity is not enhanced by forskolin (Bertrand *et al*, 2009). Also, SLC26A9 Cl^- currents can be partially inhibited by 0.1 mM DIDS (by ~36%; Dorwart *et al*, 2007).

These results would suggest that SLC26A9 is unlikely to be responsible for the changes in pH_i observed in Calu-3 cells. A recent study in the bronchial cell line, CFBE41o, expressing CFTR and transduced with SLC26A9, found that SLC26A9 expression resulted in an increase in CFTR-dependent, forskolin-stimulated currents (Avella *et al*, 2010). SLC26A9 expression enhanced CFTR expression and co-immunoprecipitation experiments showed that SLC26A9 physically interacts with CFTR in the apical membrane of these cells. Therefore, as SLC26A9 expression maybe required for maximal CFTR activity and/or expression, the reduced rate of apical AE activity seen in forskolin-stimulated SLC26A9 knockdown Calu-3 cells could perhaps be due to a decrease in Cl^- conductance through CFTR, rather than SLC26A9.

The iodide selectivity of the apical AE activity may also suggest the presence of an outwardly rectifying chloride channel (ORCC) in Calu-3 cells, as has been previously reported in patch-clamp experiments (Haws et al, 1994). ORCCs have a greater permeability for iodide relative to chloride and can be regulated by CFTR (Gabriel *et al*, 1993). However, ORCCs are unlikely to be responsible for the apical 'AE' activity seen in Calu-3 cells as ORCCs can be inhibited by H_2-DIDS (Schwiebert *et al*, 1995) and are more likely to be found on the basolateral membrane, as more recent patch clamp studies of Calu-3 cells demonstrated that ORCCs are only occasionally seen in the apical membrane of confluent monolayers, but are found with more abundance in non-polarised individual cells (Xia *et al*, 1997).

As neither CFTR, SLC26A9 nor ORCCs can explain the high affinity of the apical AE for iodide, I believe that Pendrin is the most likely candidate to mediate Cl^--dependent HCO_3^- transport.

2. Apparent inhibition of apical AE activity by CFTR pore blocker GlyH-101 due to the masking effect of a H_2-DIDS sensitive basolateral transporter.

pH_i experiments showed that while forskolin-stimulated apical AE activity was abolished by inhibiting CFTR (with either $CFTR_{inh}$-172 or GlyH-101), it was restored by the addition of basolateral H_2-DIDS. This result would suggest that the inhibition of apical CFTR actually reveals a H_2-DIDS-sensitive basolateral transport process which masks the effects of apical AE reversal on pH_i. The identity of this basolateral transporter and the mechanism by which CFTR inhibition leads to its activation are currently unknown, but its sensitivity to H_2-DIDS would suggest that the transporter responsible maybe the NBC (in reverse mode), a basolateral Cl^-/HCO_3^- exchanger or even a basolateral anion channel. Both pNBC1 and NBC4 mRNA expression have been detected in Calu-3 cells, both of which are electrogenic and have different stoichiometries (either 1:2 or 1:3) according to the cell type in which they are expressed (Kreindler *et al*, 2006). My data certainly suggests that the basolateral NBC is active under forskolin-stimulated conditions, as the addition of basolateral H_2-DIDS reduces the rate of apical AE activity, presumably due to blocking HCO_3^- uptake through the NBC. Intracellular pH studies carried out in normal and CF pancreatic duct cells (CAPAN-1, CFPAC-1) highlighted the role of CFTR Cl^- transport in the cAMP-dependent potentiation of NBC activity, which was not present in CF cells (Schumaker *et al*, 1999). Therefore inhibiting CFTR in Calu-3 cells may result in an

alteration of NBC activity. However, reversal of the NBC seems unlikely as Calu-3 Ussing chamber studies demonstrated that in the presence of 1-EBIO, which would be predicted to cause cellular hyperpolarisation by stimulating K^+ channels, the NBC was not reversed as HCO_3^- secretion continued (Krouse *et al*, 2004). The same study also predicted that for an NBC with a 1:2 (Na^+:HCO_3^-) stoichiometry, as postulated by their data, the reversal potential would be greater than –100 mV. Such a large hyperpolarisation in membrane potential is unlikely to be achieved by either CFTR inhibition or bilateral Cl^- removal under forskolin-stimulated conditions. However, the basolateral NBC present in Calu-3 cells may have a stoichiometry of 1:3, as has been previously suggested by microelectrode analysis (Tamada *et al*, 2001), which could potentially enable NBC reversal under these conditions.

The potential for a basolateral Cl^-/HCO_3^- exchanger being involved in the H_2-DIDS-sensitive re-acidification upon GlyH-101 inhibition of CFTR also seems unlikely under these conditions, as forskolin inhibits basolateral AE activity (see chapter 4 for further discussion). pH_i experiments carried out in the absence of bilateral Cl^- under forskolin-stimulated conditions, suggested that the effects of apical AE activity on pH_i could be masked by an acidification produced by a H_2-DIDS-sensitive basolateral Cl^--dependent transporter. Since external Cl^- removal would be likely to favour HCO_3^- entry via a Cl^-/HCO_3^- exchanger, a basolateral AE fulfilling this role appears doubtful. These results bear some similarities to the anion exchange profile of human nasal epithelial (HNE) cells (Paradiso, *et al* 2003). Fluorimetry studies in HNE cells showed the presence of both apical and basolateral 'AE activities', using a Cl^- removal and addition technique. Apical Cl^- removal produced only a transient alkalinisation in pH_i. The hypothesis behind this transient response was that Cl^-

removal at the apical membrane could potentially reach the basolateral membrane and thus affects the H_2-DIDS-sensitive basolateral AE present in these cells. The addition of basolateral H_2-DIDS enhanced this alkalinisation and blocked the re-acidification back to baseline, which could then only be achieved by the re-addition of apical Cl^-. The constitutively active apical AE activity present in HNE cells was attributed to Cl^- dependent HCO_3^- transport by CFTR, due to its insensitivity to H_2-DIDS and inhibition by the CFTR inhibitor DPC. Unfortunately DPC was not tested in the presence of basolateral H_2-DIDS, so the involvement of a basolateral AE in the DPC inhibition of the apical alkalinisation cannot be ruled out.

Another possible explanation for the effects of basolateral Cl^- removal on apical AE activity is that $[Cl^-]_i$ could be depleted under these conditions, which would abolish the Cl^- gradient necessary for apical AE reversal. Basolateral Cl^- removal could trigger Cl^- efflux across the basolateral membrane, via a basolateral H_2-DIDS-sensitive anion channel, such as an ORCC. Patch-clamp experiments using forskolin and the PKA inhibitor H-89, identified a cAMP/PKA-dependent basolateral ORCC in Calu-3 cells (Szkotak *et al*, 2003). siRNA studies on $^{36}Cl^-$ flux have proposed that this basolateral Cl^- conductance is mediated by a member of the bestrophin family of putative Cl^- channels (Duta *et al*, 2004). Therefore basolateral Cl^- channels are likely to be active under forskolin-stimulated conditions and could influence apical AE activity.

Since in the presence of basolateral H_2-DIDS and apical GlyH-101, apical Cl^- removal can still evoke a large alkalinisation in pH_i and a further re-acidification following apical Cl^- re-addition, then it would appear that apical Cl^--dependent HCO_3^- transport can be mediated independently of CFTR.

3. PP1 inhibition reveals a CFTR-independent apical AE activity.

Okadiac acid (OA) inhibition of PP1 (as confirmed by okadaic acid dose-response and the lack of inhibition by PP2A inhibitor fostriecin) revealed an apical AE activity under non-stimulated conditions. This apical AE activity had a similar profile to that seen under forskolin-stimulated conditions; it was insensitive to H_2-DIDS and was only able transport monovalent anions in exchange for HCO_3^-. Although no difference was seen in the rate of AE activity driven by chloride, formate or iodide, the small magnitude and rate of re-acidification under these conditions made it difficult to detect any subtle differences. Importantly, in OA treated Calu-3 cells, the CFTR pore blocker GlyH-101 could not inhibit apical AE activity under non-stimulated conditions. Apical AE activity was also present in non-stimulated CFTR KD Calu-3 cells. As Pendrin is constitutively active in FRT cells, the okadaic acid experiments may suggest that the apical AE present in forskolin-stimulated Calu-3 cells is inhibited under non-stimulated conditions by dephosphorylation involving PP1.

Forskolin enhanced the apical AE activity in OA treated cells, through a CFTR-dependent mechanism, although the level of AE activity was still lower than in untreated Calu-3 cells. As the forskolin-stimulated AE activity in fostriecin treated cells was also reduced compared to untreated cells and 100 nM okadaic acid can also inhibit PP2A, this reduction maybe due to PP2A inhibition. One possible explanation is that by enhancing the activity of the basolateral NKCC, PP2A inhibition by fostriecin would potentially increase $[Cl^-]_i$, thus reducing the rate of the Cl^-/HCO_3^- exchanger in the forward direction (Cl^- uptake in exchange for HCO_3^- exit) by

decreasing the Cl^- gradient. Although how PP2A inhibition would reduce the overall magnitude of the alkalinisation caused by AE reversal is more difficult to determine.

4. Pendrin KD Calu-3 cells exhibit a reduce rate of apical AE activity.

The hypothesis that Pendrin Cl^-/HCO_3^- exchange contributes to HCO_3^- transport across the apical membrane of Calu-3 cells was supported by the finding that the rate of apical AE activity was reduced in Pendrin KD Calu-3 cells. Western blot analysis of CFTR protein expression showed no difference between WT and A4 KD cells, which suggests that this decrease in HCO_3^- transport across the apical membrane of A4 KD Calu-3 cells was due to a decrease in Pendrin expression rather than CFTR.

However, despite a 90% knockdown of Pendrin mRNA expression in A4 KD cells, the mean alkalinisation induced by apical Cl removal was not significantly different to WT Calu-3 cells, although the rate of apical AE activity was reduced. If the apical AE is SLC26A4, then another mechanism is likely to be contributing to the transport of HCO_3^- in these cells, such as a second Cl^-/HCO_3^- exchanger (as seen in pancreatic duct cells) or CFTR itself.

3.11.2 Role of CFTR in Calu-3 cell HCO_3^- transport

My experiments in CFTR transfected FRT cells highlighted the potential of CFTR to transport HCO_3^- in response to apical Cl^- removal. Therefore under the conditions tested CFTR is likely to be involved in transporting HCO_3^- across the apical membrane of Calu-3 cells. Certainly from the Cl^--dependence experiments, with changes in apical $[Cl^-]$ of bathing solutions still producing an alkalinisation in pH_i at

concentrations that would not favour Cl^-/HCO_3^- exchanger reversal (<30 mM), there is evidence to suggest that another transport pathway contributes to Cl^--dependent HCO_3^- transport.

While it is difficult to distinguish between CFTR HCO_3^- transport and CFTR regulating Cl^-/HCO_3^- exchange activity, it is clear that CFTR has an important role to play in mediating apical HCO_3^- transport in Calu-3 cells. Three independent lines of evidence support this hypothesis:

1. Although basolateral H_2-DIDS addition overcame the apparent inhibition of apical AE by GlyH-101 in WT Calu-3 cells, the rate of apical AE activity in the presence of both apical GlyH-101 and basolateral H_2-DIDS was significantly slower compared to activity in the absence or presence of basolateral H_2-DIDS alone. However, this result may also reflect differences in $[Cl^-]$ gradients under the two conditions, rather than simply HCO_3^- transport by CFTR.
2. In okadaic acid treated cells, apical AE activity was enhanced by forskolin-stimulation, through a GlyH-101-sensitive mechanism.
3. Apical AE activity was significantly reduced in CFTR KD Calu-3 cells, compared to WT cells.

Therefore I propose that CFTR has a role in regulating apical Cl^-/HCO_3^- exchange activity and/or contributing to Cl^--dependent HCO_3^- transport in Calu-3 cells. CFTR inhibitor studies also suggest that CFTR maybe important in regulating basolateral

HCO_3^- transport. For these reasons the role of CFTR in regulating basolateral Cl^- /HCO_3^- exchange was investigated in Calu-3 cells.

4. Basolateral Cl^-/HCO_3^- exchange activity in Calu-3 cells

4.1 Introduction

There are two families of genes encoding for Cl^-/HCO_3^- exchangers: SLC26 and SLC4. As already demonstrated in chapter 3, several members of the SLC26 family are expressed in Calu-3 cells, including SLC26A4 (Pendrin), which is localised to the apical membrane. Previous transport models of Calu-3 cells included the basolateral SLC4A2 Cl^-/HCO_3^- exchanger (AE2; Loffing *et al*, 2000). Together with the electrogenic Na^+-HCO_3^- cotransporter NBC1, AE2 is involved in basolateral HCO_3^- transport which regulates pH_i in Calu-3 cells and, in addition to the NKCC, also mediates basolateral Cl^- uptake (Loffing *et al*, 2000; Inglis *et al*, 2002).

The SLC4 family of 10 genes encode for HCO_3^- transport proteins that play a vital role in mediating Na^+ and/or Cl^--dependent HCO_3^- across many tissues and cell types (Pushkin and Kurtz, 2006). The SLC4 transporter family includes three types of HCO_3^- transporters: Na^+-independent Cl^-/HCO_3^- exchangers (AE), Na^+-HCO_3^- cotransporters (NBC) and Na^+-driven Cl^-/HCO_3^- exchangers (NDCBE). SLC4A1 (AE1), -A2 (AE2), -A3 (AE3) and -A9 (AE4), were reported as electroneutral Cl^-/HCO_3^- exchangers (Romero, 2005). AE1 is expressed in red blood cells (Hunter, 1977) and renal collecting duct α-intercalated cells of the collecting duct (Verlander *et al*, 1988). AE2 is expressed broadly in epithelia including the gastric mucosa (Stuart-Tilley *et al*, 1994), colon (Gawenis *et al*, 2010), kidney (Alper *et al*, 1997) and respiratory tracts (Dudeja *et al*, 1999). AE3 is expressed in the brain and heart (Kopito *et al*, 1989). AE4 expression is less well characterised, but appears to be mainly in the kidney (Parker *et al*, 2001).

RT-PCR analysis of cells from various segments of the tracheobronchial tree detected the expression of AE2 and brain-AE3 isoforms, but not AE1 or cardiac-AE3 isoforms (Al-Bazzaz *et al*, 2001). The levels of AE2 mRNA expression were shown to be similar from the trachea all the way down to the small bronchi, with immunohistochemical analysis indicating that AE2 is specific to airway epithelial cells.

The activity of AE2 expressed in *Xenopus* oocytes, as measured by $^{36}Cl^-$ influx and efflux studies, was activated by exposure to alkaline media and inhibited by exposure to acidic media (Humphreys *et al*, 1994). Subsequent studies in *Xenopus* oocytes revealed that AE2 is regulated by both external and internal pH, which is sensed by (His) residues within the AE2 COOH-terminal transmembrane domain and regions of its NH_2-terminal cytoplasmic domain (Zhang *et al*, 1996; Stewart *et al*, 2001; Stewart *et al*, 2007). The extracellular pH (pH_o) at which AE2 activity is half-maximal [$pH_{o(50)}$] was measured at ~6.9 by AE2-mediated $^{36}Cl^-$ efflux studies, with truncation of the NH_2-terminal cytoplasmic domain shifting $pH_{o(50)}$ by ~0.7 pH units and abolishing the pH_i sensitivity of AE2 (Stewart *et al*, 2001).

4.2 Profile of basolateral Cl^-/HCO_3^- exchanger

4.2.1 H_2-DIDS sensitivity

As described in chapter 3, Calu-3 cells appear to exhibit a basolateral Cl^-/HCO_3^- exchange activity under non-stimulated conditions, which is abolished upon increases in $[cAMP]_i$. As shown in **Figure 4.01**, removal of basolateral Cl^- (substituted with gluconate) produced an alkalinisation in pH_i of 0.45 ± 0.02 pH units (n=4). This response to Cl^- removal was abolished by the generic anion exchange inhibitor H_2-

DIDS ($P<0.05$, paired t-test; n=4; **Figure 4.02**), consistent with the presence of a basolateral DIDS-sensitive AE (SLC4A2), as previously reported in Calu-3 cells (Loffing *et al,* 2000). However, the inhibition of the basolateral AE by H_2-DIDS, may be due to the acidification of pH_i induced by the addition of H_2-DIDS (0.12 ± 0.03 pH units, at a rate of 0.05 ± 0.01 pH units min^{-1}; n=4). As basolateral H_2-DIDS addition will also inhibit the basolateral Na^+-HCO_3^- cotransporter (NBC), this acidification is consistent with the inhibition of HCO_3^- uptake via the NBC. However, since the subsequent removal of H_2-DIDS from the perfusate resulted in the restoration of basolateral AE activity without a significant recovery in pH_i, it is unlikely that the H_2-DIDS-sensitivity of the basolateral AE is indirectly due to intracellular acidification.

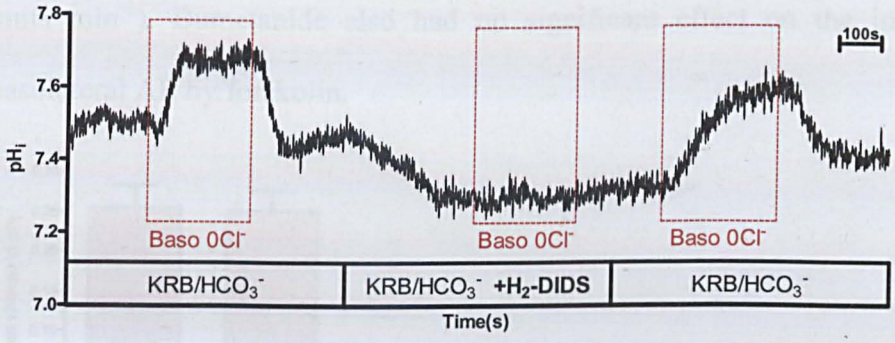

Figure 4.01- Inhibition of basolateral AE by H_2-DIDS. The effect of basolateral H_2-DIDS (500μM) on changes in pH_i following the removal of basolateral Cl^- in Calu-3 cells.

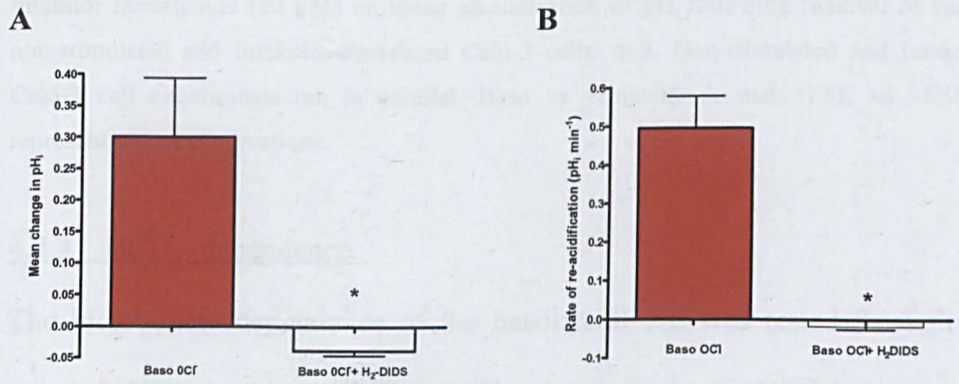

Figure 4.02- H_2-DIDS sensitivity of basolateral AE activity. The effect of basolateral H_2-DIDS (500 μM) on mean alkalinisation of pH_i following removal of basolateral Cl^- (**A**) and the mean rate of re-acidification upon re-addition of Cl^- in Calu-3 cells (**B**). n=4. Paired observations. A: *$P<0.05$ compared to Baso $0Cl^-$. B: *$P<0.05$ compared to Baso $0Cl^-$.

4.2.2 Bumetanide sensitivity

As the removal of extracellular Cl^- may affect other basolateral Cl^- transporters, such as the $Na^+/K^+/2Cl^-$ co-transporter (NKCC1), which may result in changes in $[Cl^-]_i$ and/or pH_i, the effects of basolateral Cl^- removal in the presence of the NKCC inhibitor bumetanide was also tested. Basolateral AE activity was unaffected by inhibiting Cl^- uptake through the basolateral NKCC, following the addition of bumetanide (20 μM) to the basolateral bathing solution ($P>0.05$; n=3; **Figure 4.03**). Calu-3 cells exposed to basolateral zero Cl^- in the presence of bumetanide showed a similar alkalinisation in pH_i and rate of re-acidification upon Cl^- re-addition, to untreated cells (+Bumetanide= 0.42 ± 0.01 pH units min^{-1}; untreated= 0.38 ± 0.04 pH units min^{-1}). Bumetanide also had no significant effect on the inhibition of the basolateral AE by forskolin.

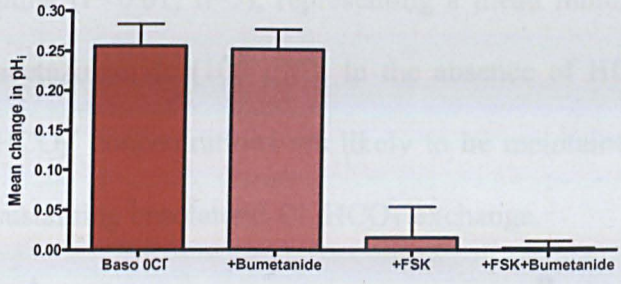

Figure 4.03- The effect of NKCC inhibition on basolateral AE activity. The effects of NKCC inhibitor bumetanide (20 μM) on mean alkalinisation of pH_i following removal of basolateral Cl^- in non-stimulated and forskolin-stimulated Calu-3 cells. n=3. Non-stimulated and forskolin-stimulated Calu-3 cell experiments ran in parallel. Baso vs +Bumetanide and +FSK vs +FSK+Bumetanide represent paired observations.

4.2.3 HCO_3^--dependence

The bicarbonate dependence of the basolateral AE was tested through removal of external HCO_3^-, using HEPES buffered solutions. In HCO_3^--free conditions the removal of basolateral Cl^- did not produce an alkalinisation, but instead caused a small acidification in pH_i of 0.07 ± 0.04 pH units ($P<0.05$; n=4; data not shown). Addition

of forskolin abolished any significant effect on pH_i following basolateral Cl^- removal in HCO_3^--free conditions. These results suggest that there is little or no OH^- transport by the basolateral exchanger.

Studies have shown that the basolateral AE2 is sensitive to acetazolamide because of its association with the cytoplasmic form of carbonic anhydrase (CA) II (Vince & Reinhart, 2000), therefore it was important to test the effects of CA on basolateral Cl^-/HCO_3^- exchange activity. The complete inhibition of basolateral AE by HCO_3^-/CO_2 removal from the bathing medium could not be mimicked by the CA inhibitor acetazolamide in the presence of HCO_3^-. However, acetazolamide did produce a slight inhibition of the basolateral AE (**Figure 4.04**). The mean change in pH_i upon basolateral Cl^- removal was reduced from 0.28 ± 0.01 pH units to 0.17 ± 0.02 pH units ($P<0.01$; n=5), representing a mean inhibition of 38 ± 9% in the presence of acetazolamide (100 μM). In the absence of HCO_3^- production by CA, intracellular HCO_3^- concentrations are likely to be maintained by uptake through the NBC, thus sustaining basolateral Cl^-/HCO_3^- exchange.

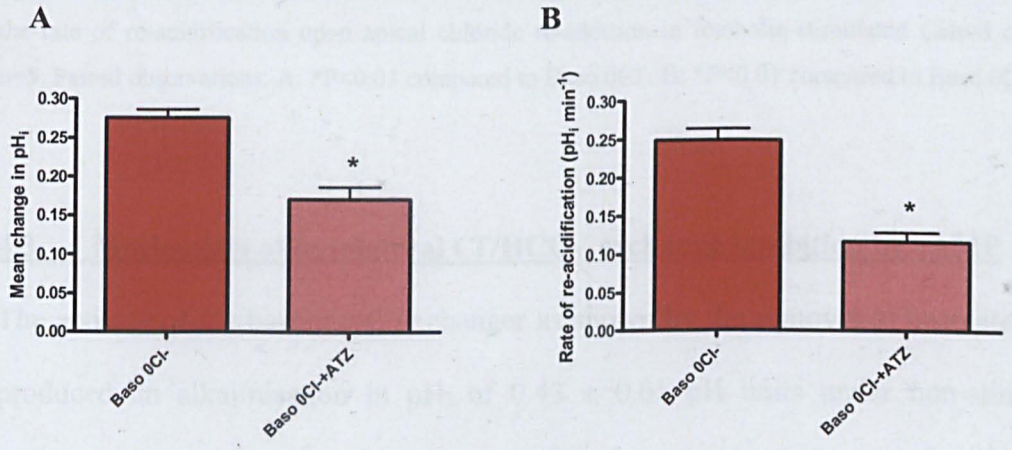

Figure 4.04- The effect of carbonic anhydrase inhibition on basolateral AE activity. The effects of carbonic anhydrase inhibitor acetazolamide (ATZ; 100 μM) on mean alkalinisation of pH_i following removal of basolateral Cl^- (**A**) and the mean rate of re-acidification upon re-addition of Cl^- in Calu-3 cells (**B**). n=5. A: *$P<0.01$ compared to Baso $0Cl^-$. B: *$P<0.001$ compared to Baso $0Cl^-$.

4.2.4 Na^+-dependence

To examine the Na^+ dependence of the basolateral AE, extracellular Na^+ was replaced with NMDG. Na^+ removal initially produced an acidification in pH_i of 0.37 ± 0.01 pH units. Like H_2-DIDS, extracellular Na^+ removal is likely to inhibit the basolateral NBC, thus depleting the intracellular HCO_3^- concentration and acidifying pH_i. Basolateral AE activity was completely abolished following the removal of external Na^+ ($P<0.01$; n=5; **Figure 4.05**). This result may represent a direct Na^+-dependence of the basolateral Cl^-/HCO_3^- exchanger or it may reflect an indirect effect of the acidification produced by inhibition of the NBC.

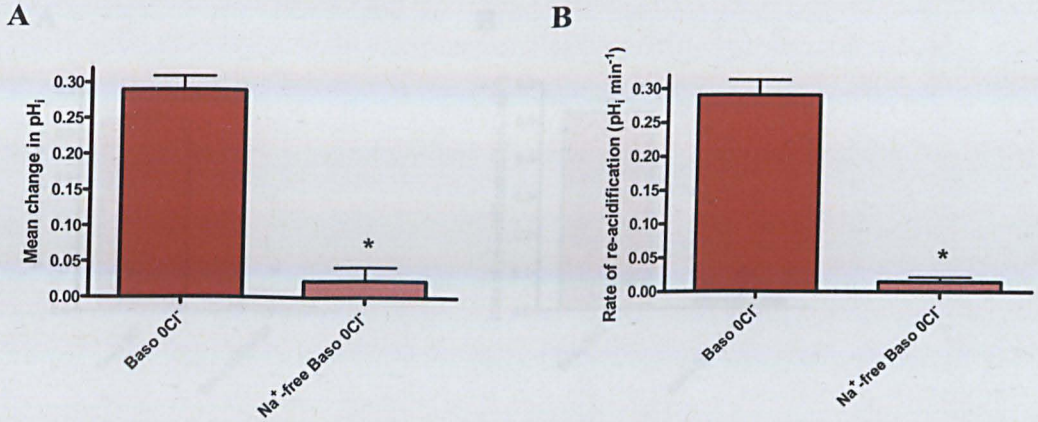

Figure 4.05- Na^+-dependence of basolateral AE activity. The effect of bilateral Na^+ removal (NaCl replaced by NMDGCl) on the mean alkalinisation (pH_i) produced by apical chloride removal (**A**) and the rate of re-acidification upon apical chloride re-addition in forskolin-stimulated Calu-3 cells (**B**). n=5. Paired observations. A: *$P<0.01$ compared to Baso $0Cl^-$. B: *$P<0.01$ compared to Baso $0Cl^-$.

4.3 Mechanism of basolateral Cl^-/HCO_3^- exchange inhibition by cAMP

The activity of the basolateral exchanger as shown by the removal of basolateral Cl^-, produced an alkalinisation in pH_i of 0.43 ± 0.01 pH units under non-stimulated conditions (n=35; **Figures 4.06 & 4.07A**). The rate of basolateral AE activity was measured at 0.52 ± 0.03 pH units min^{-1} upon re-addition of basolateral Cl^- (**Figure 4.07B**). Basolateral AE activity was completely abolished following the addition of

cAMP agonist forskolin (P<0.01; n=35), but dideoxyforskolin had no effect (P>0.05; n=3).

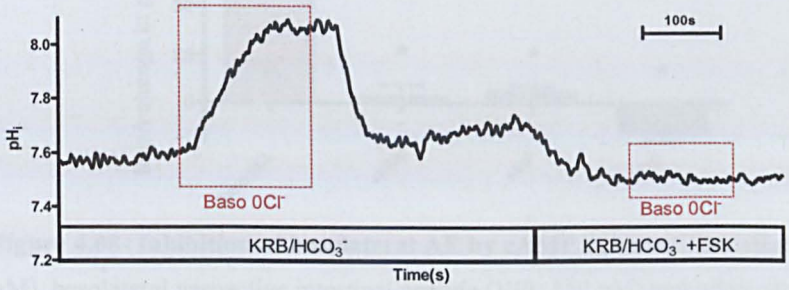

Figure 4.06- Forskolin-induced inhibition of basolateral AE activity. The effects of forskolin (FSK; 5 μM) on changes in pH_i following the removal of basolateral chloride in Calu-3 cells. *Baso 0Cl* denotes the removal of Cl^- (replaced with gluconate) from the basolateral solution.

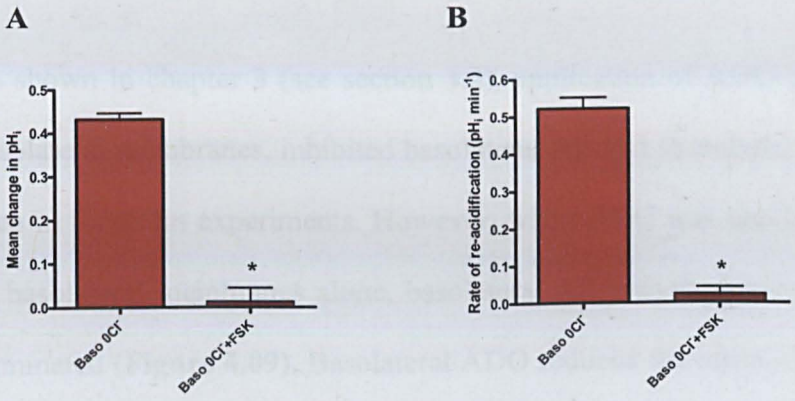

Figure 4.07- Inhibition of basolateral AE by forskolin. Mean alkalinisation (pH_i) produced by basolateral chloride removal (**A**) and the rate of re-acidification upon basolateral chloride re-addition (**B**), in non-stimulated and forskolin-stimulated (FSK) Calu-3 cells. n=35. Paired observations. A: *P<0.01 compared to Baso $0Cl^-$. B: *P<0.001 compared to Baso $0Cl^-$.

The inhibition of the basolateral AE activity was also seen in cells stimulated by basolateral VIP and bilateral ADO, confirming that increases in $[cAMP]_i$ were responsible for the forskolin-induced basolateral AE inhibition (**Figure 4.08**).

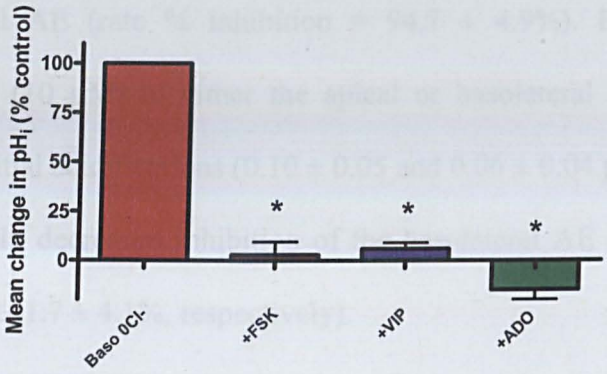

Figure 4.08- Inhibition of basolateral AE by cAMP agonists. The effect of apical forskolin (FSK; 5 μM), basolateral vasoactive intestinal peptide (VIP; 150 nM) and bilateral adenosine (ADO; 10 μM) on the percentage mean alkalinisation in pH_i following the removal of basolateral Cl^- in Calu-3 cells. pH_i responses in the presence of FSK, VIP and ADO compared to control baso $0Cl^-$ responses. n=4. Agonists ran in parallel in separate experiments. *P<0.001 compared to Baso $0Cl^-$.

As shown in chapter 3 (see section 3.2), application of ADO to both the apical and basolateral membranes, inhibited basolateral AE and stimulated apical AE activity, as seen in forskolin experiments. However, when ADO was applied to either the apical or basolateral membranes alone, basolateral AE activity was reduced, but no longer eliminated (**Figure 4.09**). Basolateral ADO reduced the mean alkalinisation produced by basolateral Cl^- removal by 40.5 ± 9.2% (P<0.01; n=3). Apical ADO addition did not significantly inhibit the basolateral AE (P>0.05; n=3), despite the apical AE being fully activated. These results suggest that activation of apical AE alone is not sufficient to inhibit basolateral AE activity and that local changes in cAMP concentration at both membranes are required to produce a 'switch' in AE activity.

From the adenosine experiments there appeared to be a correlation between the extent of the acidification in pH_i produced by the agonist and the amount of inhibition of the basolateral AE. The addition of bilateral adenosine (10 μM) produced the greatest mean acidification of 0.23 ± 0.01 pH_i units and also the greatest inhibition of the

basolateral AE (rate % inhibition = 94.7 ± 4.9%). By contrast the addition of adenosine (10 μM) to either the apical or basolateral membranes alone produced smaller initial acidifications (0.10 ± 0.05 and 0.06 ± 0.04 pH_i units, respectively) and a significantly decreased inhibition of the basolateral AE (rate % inhibition = 24.6 ± 14.5% and 41.7 ± 4.1%, respectively).

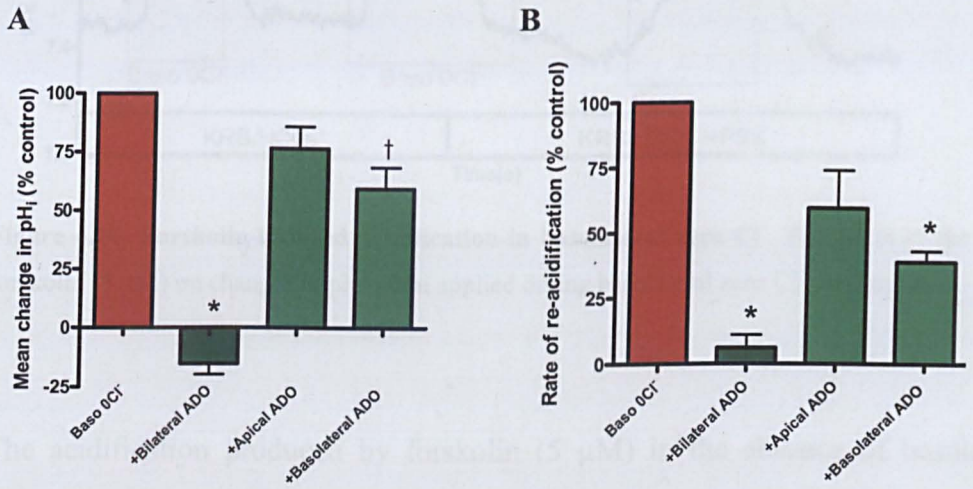

Figure 4.09- Membrane dependent adenosine inhibition of basolateral AE. The effect of bilateral, apical only and basolateral only adenosine (ADO; 10 μM) addition on the percentage mean change in pH_i produced by basolateral chloride removal (**A**) and the percentage rate of re-acidification upon basolateral chloride re-addition in Calu-3 cells (**B**). pH_i responses in the presence of bilateral ADO, apical ADO and basolateral ADO compared to control baso $0Cl^-$ responses. n=3. Each condition ran in parallel in separate experiments. A: *P<0.001 compared to Baso $0Cl^-$. †P<0.01 compared to Baso $0Cl^-$. B: *P<0.001 compared to Baso $0Cl^-$.

An alternative way of examining forskolin inhibition of the basolateral AE was to apply forskolin under basolateral zero Cl^- conditions (**Figure 4.10**). Like stimulation of the apical AE, forskolin addition in the absence of basolateral Cl^- did not produce a gradual change in pH_i. Under basolateral zero Cl^- conditions, forskolin produced a rapid acidification in pH_i of a similar magnitude to the acidification produced by Cl^- re-addition (+FSK = 0.47 ± 0.01 pH units; $+Cl^-$ = 0.48 ± 0.02 pH units; P>0.05; n=4). The rate of re-acidifcaition was also similar to that produced upon re-addition of

basolateral Cl^- (+FSK = 0.62 ± 0.10 pH units min^{-1}; +Cl^- = 0.74 ± 0.25 pH units min^{-1}; P>0.05; n=4).

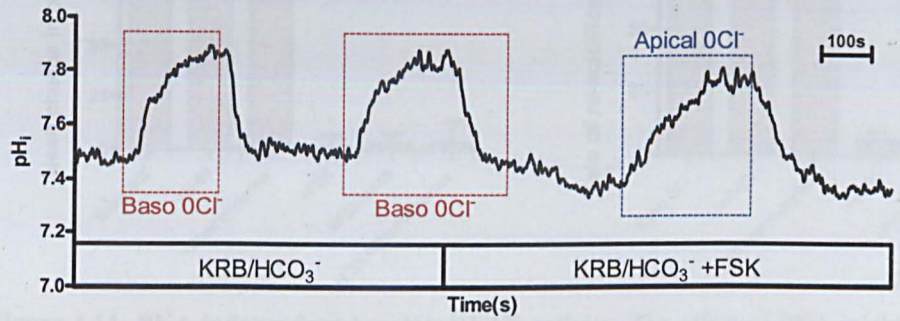

Figure 4.10- Forskolin-induced acidification in basolateral zero Cl^-. The effect of the addition of forskolin (5 μM) on changes in pH_i when applied during basolateral zero Cl^- conditions.

The acidification produced by forskolin (5 μM) in the absence of basolateral Cl^- occurred after 17 ± 2 s (n=4; **Figure 4.10**). When compared to the time delay between forskolin addition in the absence of apical Cl^- and the resulting alkalinisation in pH_i (38 ± 4 s; P<0.01; n=4; Figure 3.07), it would appear that forskolin inhibits the basolateral AE prior to stimulating apical AE activity.

Potential downstream targets of cAMP were tested to investigate the mechanisms involved in the inhibition of the basolateral AE in Calu-3 cells. Despite PKA being involved in apical AE stimulation (see Figure 3.08), neither the PKA inhibitor H-89 nor the general protein kinase inhibitor staurosporine showed any significant effect on basolateral AE activity under non-stimulated conditions, or forskolin-induced inhibition of the basolateral AE (P>0.05; **Figure 4.11**).

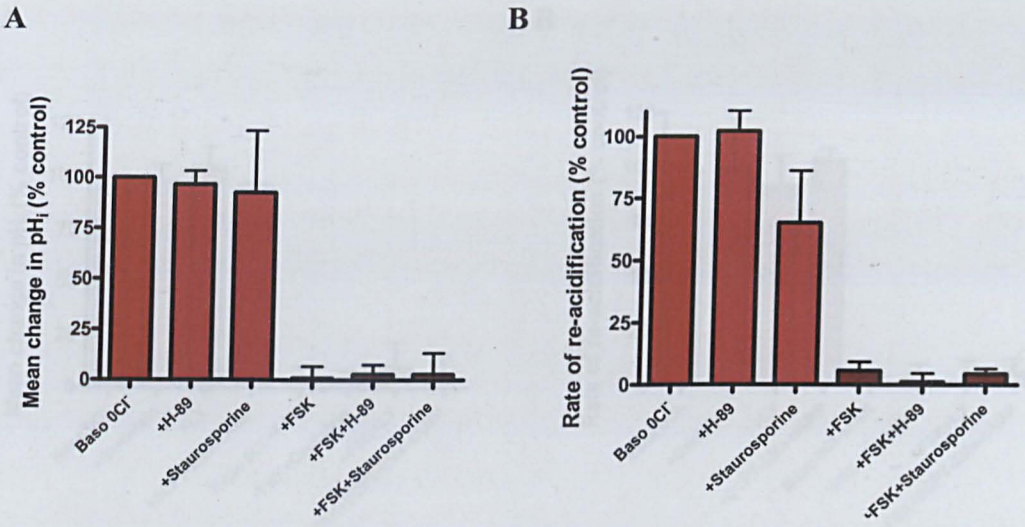

Figure 4.11- PKA-independent basolateral AE activity. The effect of PKA inhibitor H-89 (50 μM; n=8) and of protein kinase inhibitor staurosporine (1 μM; n=4) on the percentage mean change in pH_i produced by apical chloride removal (**A**) and the percentage rate of re-acidification upon apical chloride re-addition in non-stimulated and forskolin-stimulated Calu-3 cells (**B**). pH_i responses in the presence of H-89 and staurosporine compared to control baso $0Cl^-$ responses (±FSK). n=4. H-89 and staurosporine experiments ran in parallel.

Similarly, protein tryrosine kinases (inhibited using genistein), PI3-kinase (inhibited using LY294002) and Epac (stimulated using agonist 8CPT-2Me-cAMP) did not show any involvement in the inhibition of the basolateral AE by forskolin ($P>0.05$; **Figure 4.12**).

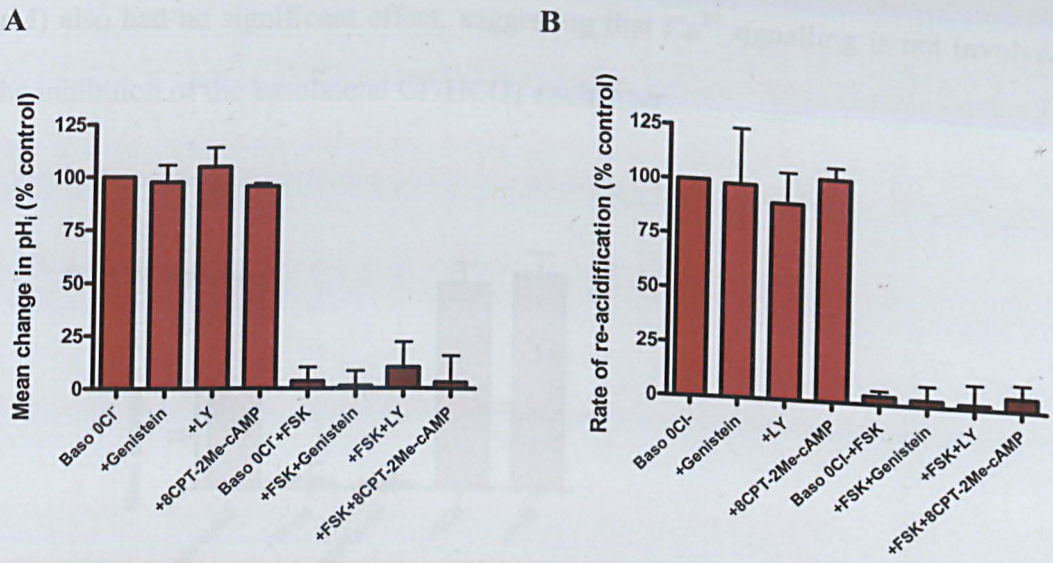

Figure 4.12- Inhibition of the basolateral AE by forskolin is not affected by genistein, PI3 kinase or Epac. The effects of genistein (30 μM), PI3 kinase inhibitor (LY294002; 20 μM) and Epac agonist 8CPT-2Me-cAMP (50 μM) on the mean change in pH_i produced by apical chloride removal (**A**) and the rate of re-acidification upon apical chloride re-addition in non-stimulated and forskolin-stimulated Calu-3 cells (**B**). pH_i responses in the presence of genistein, LY and 8CPT-2Me-cAMP (±FSK) compared to control baso $0Cl^-$ (±FSK) responses. n=4. Genistein, LY and 8CPT-2Me-cAMP ran in parallel.

4.4 Effects of Ca^{2+} on basolateral Cl^-/HCO_3^- exchange activity

Raising intracellular Ca^{2+} using thapsigargin (200 nM) appeared to inhibit the basolateral AE, however subsequent experiments with cells pre-loaded with the Ca^{2+} chelator BAPTA-AM (50 μM) revealed that the effects of thapsigargin were independent of changes in $[Ca^{2+}]_i$ (**Figure 4.13**). Ca^{2+} measurements in Calu-3 cells confirmed that BAPTA-AM blocks thapsigargin induced rises in $[Ca^{2+}]_i$ (see Figure 3.16). The Ca^{2+}-independent inhibition of the basolateral AE by thapsigargin may be due to the acidification of pH_i upon thapsigargin addition (highly variable), which was seen in both untreated and BAPTA-AM loaded Calu-3 cells, although the mechanisms involved in this acidification are unknown. Another Ca^{2+} agonist, carbachol (10 μM), had no effect on basolateral AE activity ($P>0.05$; n=4). The PKC agonist DOG (5

μM) also had no significant effect, suggesting that Ca^{2+} signalling is not involved in the inhibition of the basolateral Cl^-/HCO_3^- exchanger.

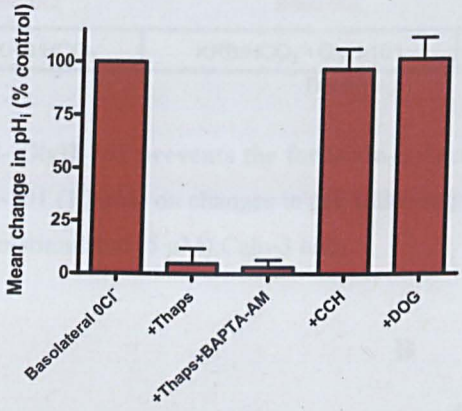

Figure 4.13- The effects of intracellular Ca^{2+} on basolateral AE activity. The effects of Ca^{2+} agonists thapsigargin (Thaps; 200 nM) ±Ca^{2+} chelator BAPTA-AM (50 μM), carbachol (CCH; 10 μM) and PKC agonist DOG (5 μM), on the mean change in pH_i following the removal of basolateral Cl^- in Calu-3 cells. pH_i responses in the presence of Thaps, Thaps+BAPTA-AM, CCH and DOG compared to control baso $0Cl^-$ responses. n=4. Thaps, Thaps+BAPTA-AM, CCH and DOG experiments ran in parallel.

4.5 Regulation of basolateral Cl^-/HCO_3^- exchange by CFTR

To test whether CFTR is involved in the inhibition of the basolateral AE, the apical membrane of Calu-3 cells were exposed to the CFTR pore blocker GlyH-101 (**Figure 4.14**). Under non-stimulated conditions GlyH-101 had no affect on the mean alkalinisation produced by the removal of basolateral Cl^- ($P>0.05$; n=4; **Figure 4.15A**), but the rate of re-acidification decreased from 0.46 ± 0.07 to 0.26 ± 0.04 pH units min^{-1} ($P<0.05$; n=4; **Figure 4.15B**). Interestingly following forskolin stimulation in the presence of GlyH-101, the basolateral AE was no longer abolished by forskolin, with 56.1 ± 19.9% of the AE induced pH_i change still present ($P<0.05$; n=4). This would suggest that cAMP inhibition of basolateral Cl^-/HCO_3^- exchange is mediated, in part, through an apical CFTR-dependent mechanism.

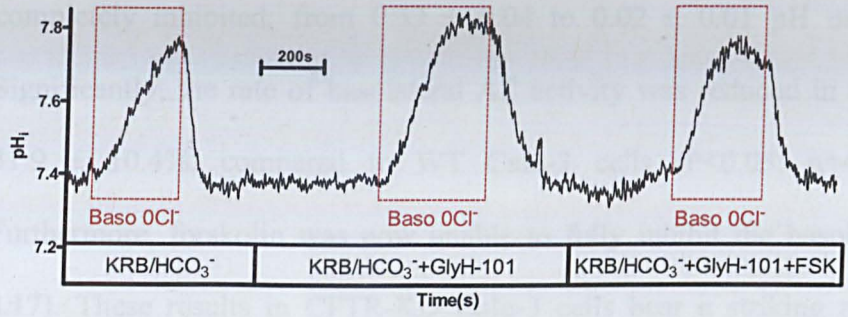

Figure 4.14- GlyH-101 prevents the forskolin-induced inhibition of basolateral AE. The effects of apical GlyH-101 (10 μM) on changes in pH_i following the removal of basolateral Cl^- in non-stimulated and forskolin-stimulated (5 μM) Calu-3 cells.

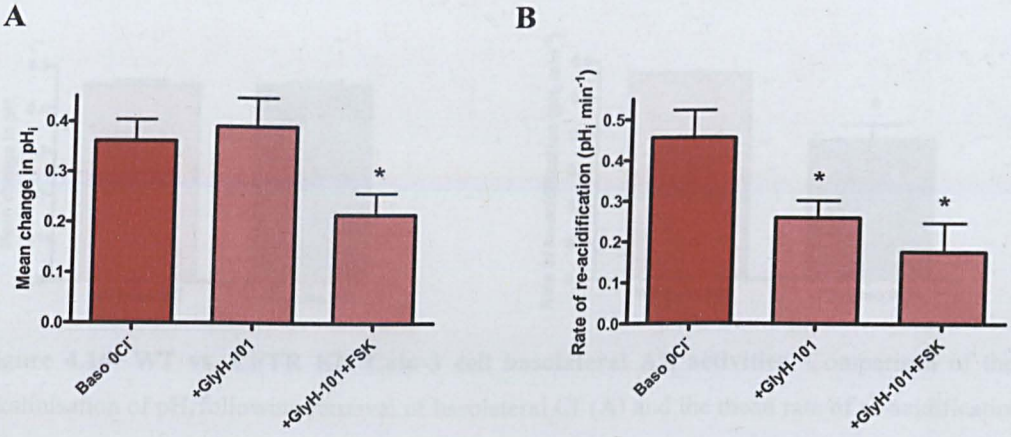

Figure 4.15- The effect of CFTR inhibition on basolateral AE activity. The effects of CFTR inhibitor GlyH-101 (10 μM) on mean alkalinisation of pH_i following removal of basolateral Cl^- (**A**) and the mean rate of re-acidification upon re-addition of Cl^- (**B**), in non-stimulated and forskolin-stimulated Calu-3 cells. n=4. Paired observations. A: *P<0.05 compared to Baso $0Cl^-$. B: *P<0.05 compared to Baso $0Cl^-$.

4.5.1 CFTR KD cells

To further investigate the role of CFTR in regulating basolateral Cl^-/HCO_3^- exchange activity, experiments were conducted on CFTR-KD Calu-3 cells. The removal of basolateral Cl^- under non-stimulated condition produced an alkalinisation of 0.46 ± 0.01 pH units (P>0.05 compared to WT Calu-3 cells; n=4; **Figure 4.16A**). The basolateral AE present in these cells showed a similar sensitivity to H_2-DIDS as WT Calu-3 cells (mean alkalinisation in response to basolateral $0Cl^-$ was almost

completely inhibited; from 0.33 ± 0.04 to 0.02 ± 0.01 pH units; $P<0.05$; n=3). Significantly, the rate of basolateral AE activity was reduced in CFTR-KD cells by 31.9 ± 10.4%, compared to WT Calu-3 cells ($P<0.05$; n=4; **Figure 4.16B**). Furthermore, forskolin was now unable to fully inhibit the basolateral AE (**Figure 4.17**). These results in CFTR-KD Calu-3 cells bear a striking resemblance to the effects of CFTR inhibition by GlyH-101 in WT Calu-3 cells (**Figure 4.15**).

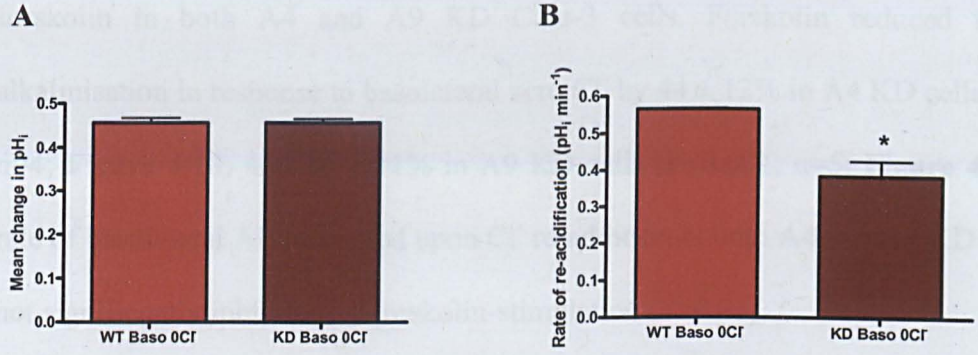

Figure 4.16- WT vs. CFTR KD Calu-3 cell basolateral AE activities. Comparison of the mean alkalinisation of pH_i following removal of basolateral Cl^- (**A**) and the mean rate of re-acidification upon re-addition of Cl^- (**B**), between non-stimulated WT and CFTR KD Calu-3 cells. n=4. WT and CFTR KD Calu-3 cell experiments ran in parallel. B: *$P<0.05$ compared to Baso $0Cl^-$.

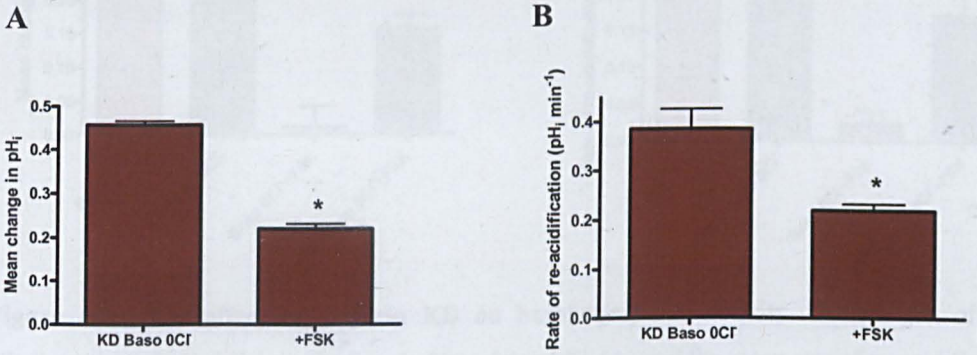

Figure 4.17 - Forskolin does not fully inhibit basolateral AE in CFTR KD cells. The effects of forskolin (FSK; 5 μM) on the mean alkalinisation of pH_i following removal of basolateral Cl^- (**A**) and the mean rate of re-acidification upon re-addition of Cl^- (**B**), in CFTR KD Calu-3 cells. n=4. Paired observations. A: *$P<0.05$ compared to Baso $0Cl^-$. B: *$P<0.05$ compared to Baso $0Cl^-$.

4.6 Basolateral AE in SLC26A4 & SLC26A9 knockdown Calu-3 cells

To investigate if either SLC26A4 or SLC26A9 expression could also influence the basolateral AE (like CFTR), AE activity was measured in A4 and A9 knockdown Calu-3 cells. Both A4 and A9 KD cells produced an alkalinisation in pH_i following basolateral Cl^- removal and subsequent re-acidification upon Cl^- re-addition of a similar magnitude and rate compared to control cyclophilin B KD cells. However, like CFTR KD cells, basolateral AE activity was no longer completely inhibited by forskolin in both A4 and A9 KD Calu-3 cells. Forskolin reduced the mean alkalinisation in response to basolateral zero Cl^- by 44 ± 12% in A4 KD cells ($P<0.01$; n=4; **Figure 4.18**) and 50 ± 11% in A9 KD cells ($P<0.001$; n=5; **Figure 4.19**). The rate of basolateral AE measured upon Cl^- re-addition in both A4 and A9 KD cells was not significantly inhibited by forskolin-stimulation ($P>0.05$).

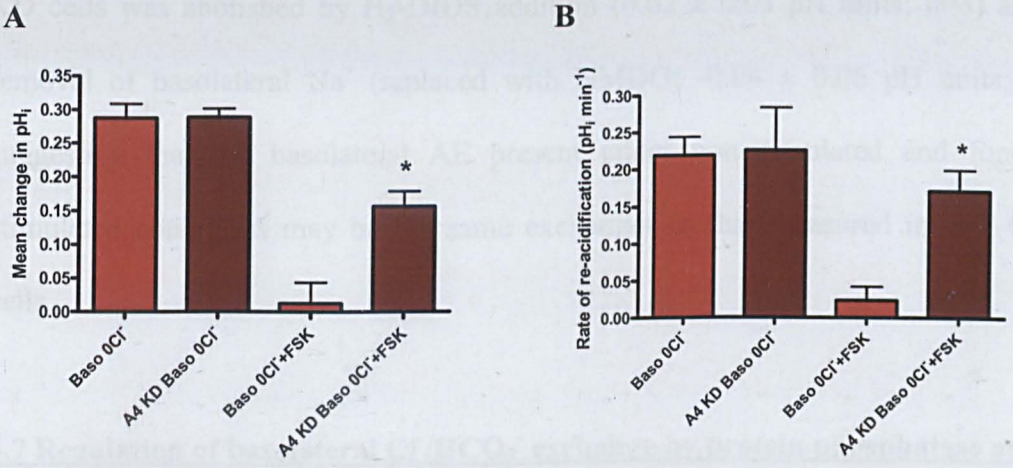

Figure 4.18- The effect of Pendrin KD on basolateral AE activity. Comparison of the mean alkalinisation of pH_i following removal of basolateral Cl^- (**A**) and the mean rate of re-acidification upon re-addition of Cl^- (**B**), between control cyclophilin B KD and Pendrin Knockdown (A4 KD) Calu-3 cells, under non-stimulated and forskolin-stimulated (5 μM) conditions. n=4. WT and A4 KD cell experiments carried out in parallel. A: *$P<0.01$ compared to Baso $0Cl^-$+FSK. B: *$P<0.05$ compared to Baso $0Cl^-$+FSK.

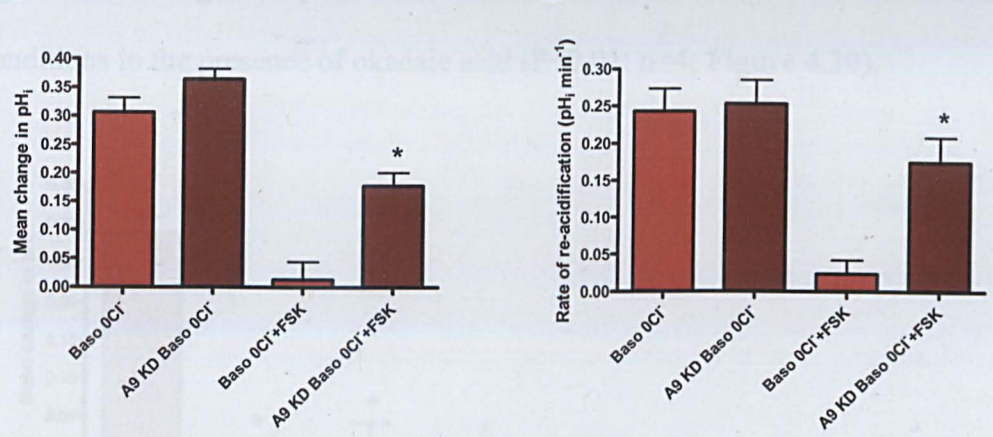

Figure 4.19- The effect of SLC26A9 KD on basolateral AE activity. Comparison of the mean alkalinisation of pH_i following removal of basolateral Cl^- (**A**) and the mean rate of re-acidification upon re-addition of Cl^- (**B**), between control cyclophilin B KD and SLC26A9 Knockdown (A9 KD) Calu-3 cells, under non-stimulated and forskolin-stimulated (5 μM) conditions. n=5. WT and A9 KD cell experiments carried out in parallel. A: *P<0.01 compared to Baso 0Cl$^-$+FSK. B: *P<0.05 compared to Baso 0Cl$^-$+FSK.

The alkalinisation in pH_i following basolateral Cl^- removal in forskolin-stimulated A9 KD cells was abolished by H_2-DIDS addition (0.02 ± 0.03 pH units; n=3) and the removal of basolateral Na^+ (replaced with NMDG; -0.04 ± 0.06 pH units; n=3), suggesting that the basolateral AE present under non-stimulated and forskolin-stimulated conditions may be the same exchanger as that measured in WT Calu-3 cells.

4.7 Regulation of basolateral Cl^-/HCO_3^- exchange by protein phosphatase activity

As shown previously in chapter 3 (see **Figure 3.46**), Calu-3 cells pre-treated for 60 minutes with the protein phosphatase inhibitor okadaic acid, produced a 'switch' in AE activity, completely inhibiting basolateral AE and activating an apical AE activity under non-stimulated conditions. Basolateral Cl^- removal failed to produce a

significant change in pH_i under either non-stimulated or forskolin-stimulated conditions in the presence of okadaic acid ($P<0.01$; n=4; **Figure 4.20**).

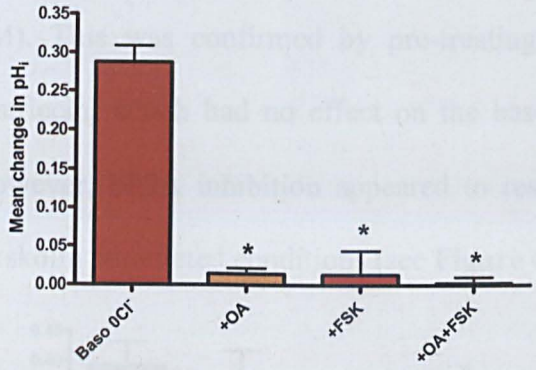

Figure 4.20- Inhibition of basolateral AE by okadaic acid. The effects of okadaic acid (100 nM) on the mean changes in pH_i following the removal of basolateral Cl^- in non-stimulated and forskolin-stimulated WT Calu-3 cells. n=4. OA treated and untreated Calu-3 cell experiments ran in parallel. *$P<0.01$ compared to Baso $0Cl^-$.

The inhibition of basolateral zero Cl^--induced pH_i changes by okadaic acid was only seen when using higher concentrations of the inhibitor (100 nM and 500 nM). Pre-treatment with 10 nM okadaic acid failed to inhibit the basolateral AE ($P>0.05$; n=3; **Figure 4.21**).

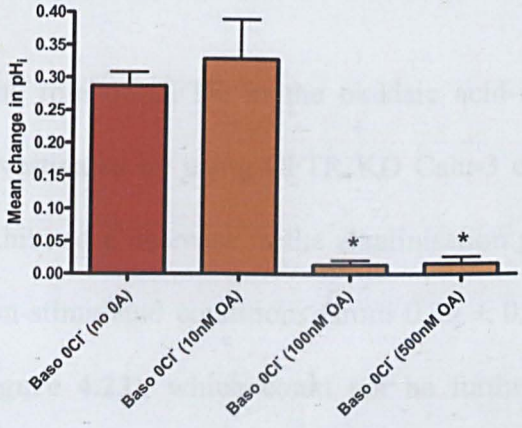

Figure 4.21- Dose-response of okadaic acid induced inhibition of basolateral AE. Dose-response effect of okadaic acid (0, 10, 100 nM) on mean changes in pH_i following the removal of basolateral Cl^- in non-stimulated WT Calu-3 cells. n=3. OA treatments were carried out in separate experiments that were run in parallel. *$P<0.01$ compared to Baso $0Cl^-$.

The dose-response of okadaic acid inhibition of basolateral AE activity appeared to reflect the inhibition of PP1 rather than PP2A, according to the specificity of okadaic acid for the two protein phosphatases (okadaic acid PP2A IC_{50} ~0.5 nM; PP1 IC_{50} ~50 nM). This was confirmed by pre-treating cells with the PP2A specific inhibitor fostriecin, which had no effect on the basolateral AE ($P>0.05$; n=4; **Figure 4.22**). However, PP2A inhibition appeared to restore some basolateral AE activity under forskolin stimulated conditions (see **Figure 4.22**).

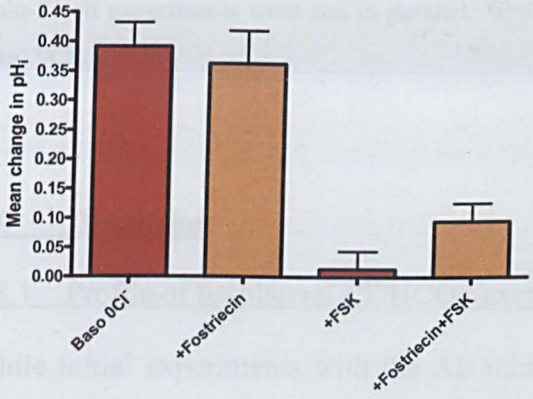

Figure 4.22- The effects of PP2A inhibition on basolateral AE activity. The effects of fostriecin (100 nM) on the mean changes in pH_i following the removal of basolateral Cl^- in non-stimulated and forskolin-stimulated WT Calu-3 cells. n=4. Fostriecin treated and untreated Calu-3 cell experiments were run in parallel.

The role of CFTR in the okadaic acid-induced inhibition of basolateral AE was investigated by using CFTR KD Calu-3 cells. Okadaic acid-treated CFTR KD cells exhibited a decrease in the alkalinisation produced by basolateral Cl^- removal under non-stimulated conditions (from 0.39 ± 0.06 to 0.13 ± 0.03 pH units; $P<0.01$; n=4; **Figure 4.23**), which could not be further inhibited by forskolin. The incomplete inhibition of basolateral AE by okadaic acid in CFTR KD cells reflects the importance of CFTR in the regulation of the 'switch' in AE activity and in particular its role in the inhibition of the basolateral exchanger.

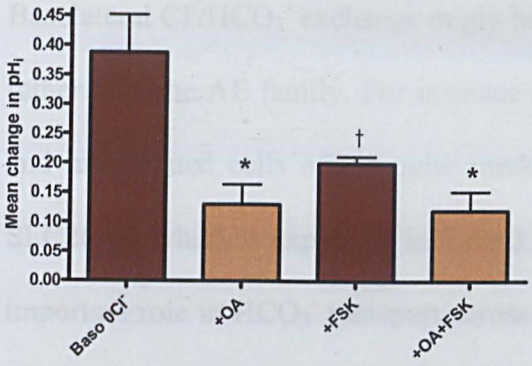

Figure 4.23- Inhibition of basolateral AE by okadaic acid in CFTR KD Calu-3 cells. The effects of okadaic acid (100 nM) on the mean changes in pH_i following the removal of basolateral Cl^- in non-stimulated and forskolin-stimulated CFTR KD Calu-3 cells. n=4. OA treated and untreated CFTR KD Calu-3 cell experiments were run in parallel. *P<0.01 compared to Baso $0Cl^-$. †P<0.05 compared to Baso $0Cl^-$.

4.8 Discussion

4.8.1 Profile of basolateral Cl^-/HCO_3^- exchange in Calu-3 cells

While initial experiments with the AE inhibitor H_2-DIDS supported the presence of AE2 on the basolateral membrane of Calu-3 cells, its inhibition following the removal of Na^+ from the bathing solution does not, as AE2 is known to be Na^+-independent. The inhibition of the basolateral AE in Na^+-free conditions may indirectly be due to the acidification of pH_i upon Na^+ removal (due to inhibition of the basolateral NBC). This would correlate with AE2, which has been shown to be inhibited by acidic intracellular conditions (Stewart *et al*, 2001). However, experiments with H_2-DIDS and KD (CFTR, A4 &A9) Calu-3 cells suggest otherwise. H_2-DIDS addition produced an acidification of pH_i and inhibited the basolateral AE. Basolateral Cl^-/HCO_3^- exchange was restored following removal of H_2-DIDS, without a recovery in pH_i. In CFTR KD, A4 KD and A9 KD Calu-3 cells, basolateral AE could not be fully inhibited under forskolin-stimulated conditions, despite a forskolin-induced acidification of a similar magnitude (ΔpH_i change) to WT Calu-3 cells.

Basolateral Cl^-/HCO_3^- exchange might be mediated by a member of the SLC26 family rather than the AE family. For instance in gastric parietal cells (Petrovic *et al*, 2003) and intercalated cells of the outer medullary collecting duct (Petrovic *et al*, 2004), SLC26A7, which is expressed in Calu-3 cells (see **Figure 3.55**), is thought to play an important role in HCO_3^- transport across the basolateral membrane of parietal cells, a role presumed to be filled by AE2 (on the basis of previous functional studies demonstrating mediation of Cl^-/HCO_3^- exchange and its basolateral localization; Rossman *et al*, 2001). SLC26A7 knockout mice show reduced gastric acid secretion, proposed to be due to either impaired HCO_3^- secretion across the basolateral membrane or reduced Cl^- entry into the parietal cell (Xu *et al*, 2009). SLC26A7 displays many of the same transport characteristics as AE2 and sensitivity to DIDS, which can cause SLC26A7 to be misidentified as AE2. Importantly, SLC26A7 has been shown to mediate Cl^-/HCO_3^- exchange when expressed in *Xenopus* oocytes at both acidic and alkiali pH_i (Petrovic *et al*, 2003). This was determined by pH_i (as measured by BCECF fluorescence) experiments in oocytes injected with SLC26A7 cRNA, which produced an alkalinisation in pH_i in response to Cl^- removal from the HCO_3^--buffered bathing solution, consistent with the reversal of a Cl^-/HCO_3^- exchanger. Switching back to a Cl^--containing solution produced a re-acidification of pH_i, suggesting that SLC26A7 is active at alkali pH_i. These responses could be completely inhibited by the addition of 500 μM H_2-DIDS. Removal of HCO_3^- from the perfusate, resulted in an intracellular acidification in both control and SLC26A7-injected oocytes, with HCO_3^- re-addition only producing a recovery of pH_i in SLC26A7-injected oocytes. Therefore, SLC26A7-mediated Cl^-/HCO_3^- exchange might explain the presence of basolateral AE in Calu-3 cells under acidic pH_i. However, the same study failed to detect SLC26A7 mRNA expression in mouse lung

tissue by Northern blot analysis, and like AE2, it mediates Na^+-independent Cl^-/HCO_3^- exchange. Current measurements in *Xenopus* oocytes and HEK cells transfected with SLC26A7 suggested that SLC26A7 functions as a Cl^- channel, since the magnitude of the Cl^- current was unaffected by HCO_3^-, indicating that SLC26A7 is impermeable to HCO_3^- (Kim *et al*, 2005). Therefore it is still unclear whether SLC26A7 functions as an anion channel or exchanger, or both. SLC26A7 might potentially be involved in the basolateral Cl^-/HCO_3^- exchange activity present in Calu-3 cells either alone or together with co-expressed AE2, provided that the apparent Na^+-dependence of the basolateral AE is indirectly due to inhibition/reversal of the basolateral NBC. Since AE2 can be inhibited by a much lower concentration of DIDS than SLC26A7 (IC_{50} = 126 μM; Petrovic *et al*, 2003), a dose-response of the H_2-DIDS inhibition of basolateral AE activity in Calu-3 cells might be useful to distinguish between the two exchangers.

However, the apparent Na^+-dependence of the basolateral AE may favour the presence of a Na^+-driven Cl^-/HCO_3^- exchanger (NDCBE). NDCBE'S are not well characterised. The first NDCBE was cloned from *Drosophila*, the Na^+-driven anion exchanger 1 (NDAE1) and was shown to mediate DIDS-sensitive transport of Cl^-, Na^+, H^+, and HCO_3^- (Romero *et al*, 2000). RT-PCR studies failed to detect mRNA for NDAE1 in Calu-3 cells, but also failed to detect NDAE1 in rat kidney, in which Na^+-dependent Cl^-/HCO_3^- exchange activity had previously been detected (Inglis *et al*, 2002). Northern blot analysis showed SLC4A8 (NDCBE1) mRNA expression in regions of the human brain, testis, kidney and ovary (Grichtchenko *et al*, 2001). Cloning of NDCBE1 from the human brain and expression in *Xenopus* oocytes, led to NDCBE1 being characterised as a DIDS-sensitive electroneutral Na^+-driven Cl^-

/HCO_3^- exchanger. Unlike *Drosophila* NDAE1, NDCBE1 is HCO_3^--dependent. Subsequent RT-PCR studies have detected SLC4A8 expression (identified in this study as NBC3) in Calu-3 cells while investigating the presence of electrogenic NBC's (Kriendler *et al*, 2006). Therefore the possible involvement of a basolateral NDCBE in regulating Calu-3 cell pH_i and mediating basolateral Cl^- uptake cannot be ruled out. As it would difficult to distinguish between AE2 and NDCBE using inhibitors (both are H_2-DIDS-sensitive), knockdown of the basolateral NBC1 would allow the Na^+-dependence of the basolateral AE to be assessed independently of NBC in pH_i experiments.

4.8.2 Regulation of basolateral Cl^-/HCO_3^- exchange

From the CFTR inhibitor and knockdown cell studies I would conclude that the cAMP inhibition of the basolateral AE is mediated via a CFTR-dependent mechanism. However, as SLC26A4 and SLC26A9 KD Calu-3 cells exhibited a similar dysregulation of basolateral AE to CFTR KD cells, this would suggest that basolateral AE regulation is linked to more than just CFTR activity. A common factor such as Cl^- transport via these apical transporters could alter $[Cl^-]_i$ and thus inhibit the basolateral AE.

SLC4 Cl^-/HCO_3^- exchangers have been previously shown to be active under cAMP-stimulated conditions in several tissues, such as AE2 in the murine proximal colon (Gawenis *et al*, 2010). However, basolateral Cl^-/HCO_3^- exchange was demonstrated to be inhibited by elevation of intracellular cAMP in guinea pig pancreatic duct cells, where basolateral H_2-DIDS-sensitive chloride transport (as assessed by intracellular Cl^- measurements using a Cl^- sensitive fluoroprobe) was abolished following

stimulation with forskolin (Ishiguro *et al*, 2002). As H-89 and 8CPT-2Me-cAMP, failed to either cause basolateral AE inhibition or overcome its inhibition by forskolin, it appears that the cAMP-dependent inhibition of the basolateral AE in Calu-3 cells is through a PKA and Epac-independent mechanism. Interestingly, PP1 inhibition in okadaic acid-treated cells abolished basolateral Cl^-/HCO_3^- exchange, suggesting that a cAMP-dependent process may inhibit AE by phosphorylation and that PP1 is involved in regulation of the basolateral AE under non-stimulated conditions.

Inhibition of the basolateral Cl^-/HCO_3^- exchanger is important for HCO_3^- secretion under stimulated conditions as active basolateral AE would deplete $[HCO_3^-]_i$ and thus greatly impair basolateral-to-apical HCO_3^- secretion. CFTR KD cells exhibit residual basolateral AE activity following forskolin-stimulation, highlighting the potential for impaired basolateral AE inhibition in CF serous cells, as dysregulation of Cl^-/HCO_3^- exchange would be predicted to reduce HCO_3^- and fluid secretion and contribute to the pathological changes observed in CF submucosal glands.

5. Air-liquid interface vs submerged Calu-3 and HBE cell cultures

5.1 Introduction

The majority of previous experiments on Calu-3 cells grown on permeable supports have been carried on cell monolayers exposed to air, whereby cultures are initially grown in the presence of media on both membranes until confluent, at which point media is removed from the apical surface (Shen *et al*, 1994; Lee *et al*, 1998; Devor *et al*, 1999). This culturing method is known as air-interface or air-liquid interface (ALI). ALI is known to markedly improve the differentiation of primary human bronchial epithelial (HBE) cell cultures (Yamaya *et al*, 1992) and increase CFTR expression at the cell surface (in Madin-Darby canine kidney cells; Bebök *et al*, 2001), and has therefore been applied to other airway derived cell lines, including Calu-3 cells. This is surprising, given that Calu-3 cells are a cell line of airway serous submucosal gland (adenocarcinoma) origin, a location that would suggest liquid covered conditions *in vivo*.

Several studies have compared submerged and ALI cultured Calu-3 cells, with many focussing on the permeability characteristics of the two culture types with regard to drug delivery (Forbes & Ehrhardt, 2005). A number of these studies incorrectly associated Calu-3 cells with surface bronchial epithelial cells (Grainger *et al*, 2006). However, Calu-3 cells do not represent a good model for most airway surface epithelial cells, which have much lower expression of CFTR compared to Calu-3 cells but also highly express the epithelial Na^+ channel (ENaC) and exhibit cilia on their apical surface. Surface cells of the upper airways are primarily involved in absorption

of Na^+ and fluid (Smith & Welsh, 1992), whereas submucosal gland serous cells are involved in HCO_3^-, Cl^- and fluid secretion.

The overall morphology of submerged and ALI grown Calu-3 monolayers were reported to be similar as detected by light microscopy, scanning electron microscopy (SEM) and immunocytochemical analysis (Fiegel *et al*, 2003). Calu-3 cells grown under both conditions form tight monolayers consisting of closely apposed cuboidal cells in a 'cobblestone' like morphology. Tight junctional proteins ZO-1 and occludin showed regular expression along the intercellular junctions of both monolayers. Several investigators have reported the presence of cilia on Calu-3 cell monolayers grown under ALI, consistent with an airway surface-like morphology (Florea *et al*, 2003; Grainger *et al*, 2006). Cilia have also been observed under submerged conditions, although cilia were much shorter and thicker compared to those present in ALI cultures and have been seen in relatively few studies (Patal *et al*, 2002). In general, cilia are not widely reported to be present in submerged grown Calu-3 cells, nor were cilia present in primary cell cultures derived from the acini of human tracheobronchial submucosal glands (Yamaya *et al*, 1992), and thus submerged Calu-3 cells better represent the morphology of serous submucosal gland cells *in vivo*.

As the Calu-3 cell line is a heterogeneous population of both serous and mucus secreting cells, mucus production, as determined by staining of glycoproteins typically found in mucus, has been observed in both submerged (Pezron *et al*, 2002) and ALI Calu-3 cultures (Fiegel *et al*, 2003). Comparison of mucus secretion using this method showed greater staining on the surface of ALI grown monolayers, with relatively little staining in submerged cell layers (Grainger *et al*, 2006). These results

would suggest that a thick layer of mucus forms on the surface of ALI grown cells, whereas mucus secreted under submerged conditions disperses into the apical media and is removed by changing the media.

Transepithelial electrical resistance (TEER) is routinely used to determine the integrity of confluent epithelial monolayers cultured on permeable supports, due to the presence of functional intercellular tight junctions. Most commonly TEER is measured using chopstick electrodes attached to an epithelial voltohmmeter (EVOM), but TEER can also be determined by Ussing chamber studies. TEER values varied greatly between different studies and were as low as ~350 $\Omega.cm^2$ (peak TEER, 8 days post-seeding; Wan *et al*, 2000) to >2000 $\Omega.cm^2$ in submerged Calu-3 monolayers (7 days post-seeding; Fiegel *et al*, 2003) and from ~300 $\Omega.cm^2$ (peak TEER, 9 days post-seeding; Grainger *et al*, 2006) to ~1100 $\Omega.cm^2$ in ALI grown Calu-3 monolayers (peak TEER, 8 days post-seeding; Mathias *et al*, 2002). While many studies comparing TEER in submerged and ALI grown Calu-3 monolayers reported much higher TEER in submerged cultures (Fiegel *et al*, 2003; Grainger *et al*, 2006), some have also observed the opposite (Florea *et al*, 2003). One difficulty with determining the TEER of ALI grown monolayers is that the apical membrane must be rehydrated in culture medium in order to measure TEER with chopstick electrodes. As re-addition of apical media would likely affect TEER itself, the time given to allow TEER values to stabilise will undoubtedly affect measurements and thus may explain some of the variability in TEER values from different studies (rehydration time= 30 mins, peak TEER ~550 $\Omega.cm^2$, 9 days post-seeding, Foster *et al*, 2000; rehydration time not mentioned, peak TEER ~1100 $\Omega.cm^2$, 8 days post-seeding, Mathias *et al*, 2002; both measured by EVOM). Other cell culture factors such as seeding densities,

transwell coatings and serum supplements also complicate comparisons between different studies (Forbes & Ehrhardt, 2005). Although a recent study looking at the effects of cell passage number in Calu-3 cells grown under ALI, found that TEER was not significantly affected by passage number (compared passage no. 30, 36 & 40 in Calu-3 monolayers 2-21 days post-seeding; Haghi *et al*, 2010). Therefore, while it has been suggested ALI grown Calu-3 cells best represents *in vivo* submucosal gland cells due to similarities in TEER (primary acini cells of human tracheobronchial submucosal glands TEER ~580 $\Omega.cm^2$; Yamaya *et al*, 1992), vast differences in culture methods and large TEER variability between different studies, makes evaluations based on TEER measurements very difficult.

Ussing chamber studies revealed a six-fold increase in Calu-3 cell basal I_{SC} in cells grown at ALI compared to submerged cultures (Singh *et al*, 1997). This is perhaps due to differences in CFTR expression between the two culture conditions (Bebök *et al*, 2001), as RT-PCR analysis showed a large decrease in CFTR mRNA expression in submerged Calu-3 monolayers, compared to those at ALI (Guimbellot *et al*, 2008). The same study concluded that CFTR expression was diminished in submerged cultures due to hypoxia, as several hypoxia-inducible genes were upregulated under these conditions.

Due to apparent differences in ciliogenesis, mucus secretion, TEER and short-circuit current between submerged and ALI grown Calu-3 cell cultures, the effects of cell culture methods on Calu-3 AE activity was investigated. AE expression and activity was also examined in ALI grown primary HBE cells, primarily as HBE cells are known to secrete HCO_3^-, but also as a comparison to ALI grown Calu-3 cells.

5.2 Quantitative real-time PCR

Calu-3 cells were seeded at ~$2.5x10^5$ cm^{-2} on semi-permeable supports and grown for 5-14 days until confluent and resistant monolayers were formed. Calu-3 monolayers were fed bilaterally with media for the first 5 days post-seeding, after which cells were taken to ALI by removing apical media or continued under submerged conditions. Calu-3 cells cultured on transwell inserts under submerged conditions typically reached a stable resistance of between 800-1000 $\Omega.cm^2$ after 5-7 days post-seeding (see methods, **Figure 2.02**). ALI cultured Calu-3 monolayers reached a stable resistance of between 400-600 $\Omega.cm^2$ after 2 days in the absence of apical media (7 days post-seeding). ALI grown monolayers produced a thick layer of mucus across the apical surface, which was removed by washing the cells with PBS when replacing media and prior to experiments. A mucus layer did not form in submerged cultures, however, consistent with previous reports (Grainger *et al*, 2006).

The relative mRNA expression of potential SLC26 Cl^-/HCO_3^- exchangers was investigated in submerged and ALI grown cells (**Figure 5.01**). Both A6 and A9 mRNA expression was elevated in ALI grown Calu-3 cells, compared to submerged cells. However, Pendrin (A4) mRNA expression in ALI cultures declined relative to submerged Calu-3 cells. Although mRNA expression may not be comparable to actual protein expression, these results suggested that SLC26 expression in Calu-3 cells was affected by growth conditions.

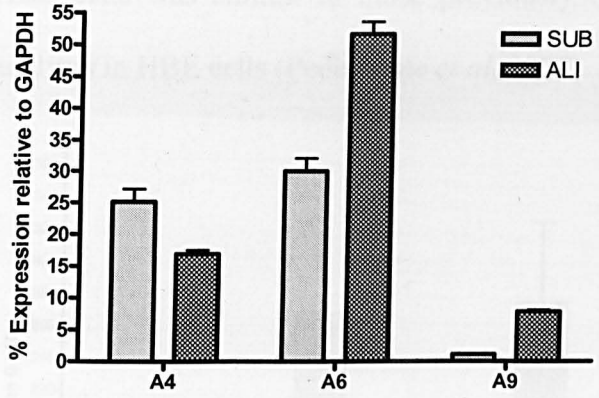

Figure 5.01- SLC26 mRNA expression in submerged and ALI grown Calu-3 cells. Quantative RT-PCR (Taqman) analysis of SLC26-A4, -A6 and -A9 expression in WT Calu-3 cells grown on transwell supports, under submerged (SUB) and air-liquid interface (ALI) conditions, relative to standard curve and normalised to GAPDH expression (%). n=3.

The expression of SLC26 transporters in primary cultures of HBE cells was also examined, to compare with their expression in Calu-3 cells (**Figures 5.02, 5.03 & 5.04**). HBE cell monolayers were grown on transwell inserts for 7 days under submerged conditions until confluent (termed Day 0) and then under ALI for a further 7-14 days. The findings were considerably different to the expression profiles found in Calu-3 cells (see **Figure 3.55**). Although SLC26A2 and A6 were still highly expressed, there was a marked increase in the expression of SLC26A4. Also differences in expression could be seen between growth conditions, with SLC26A9 being more highly expressed under submerged conditions (**Figures 5.02**) in comparison with ALI (**Figures 5.03 & 5.04**). Like Calu-3 cells, no SLC26A3 expression could be detected in HBE cells under any growth condition. Interestingly, in light of the apparent role of Pendrin as an apical Cl^-/HCO_3^- exchanger in Calu-3 cells, SLC26A4 mRNA expression increased in a time-dependent manner in HBE cells grown under ALI. A similar SLC26 mRNA profile was obtained in HBE cells from another donor. The expression of SLC26A2, A4, A6 and A11 in ALI grown

HBE cells was similar to those previously reported from global gene microarray analysis in HBE cells (Pedemonte *et al*, 2007).

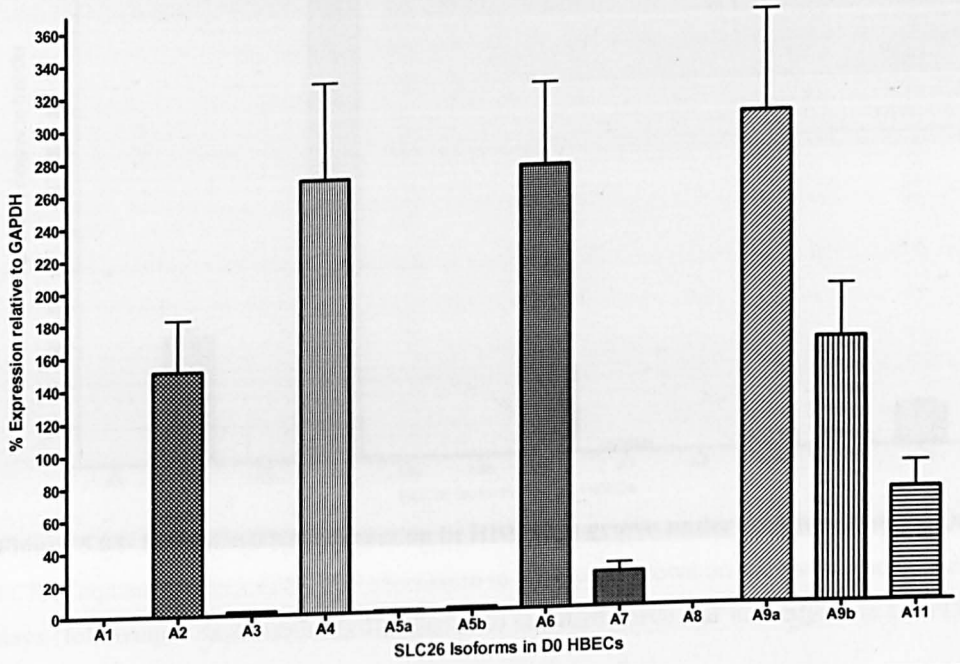

Figure 5.02- SLC26 mRNA expression in submerged HBE cells. Quantative RT-PCR (Taqman) analysis of SLC26 expression in HBE cells grown on transwell inserts under submerged conditions for 7 days, relative to standard curve and normalised to GAPDH expression (%). n=3.

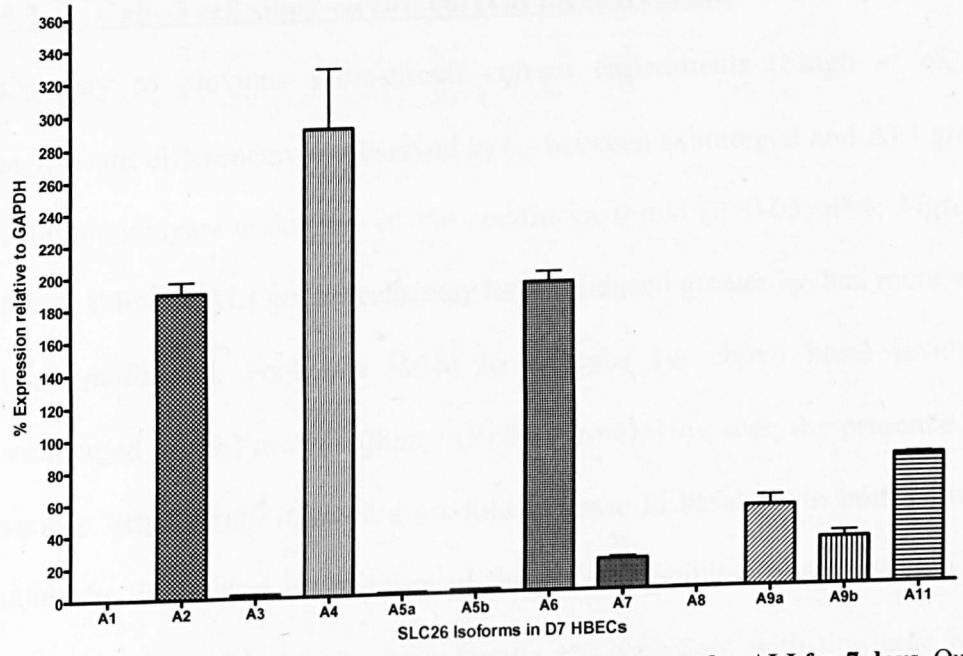

Figure 5.03- SLC26 mRNA expression in HBE cells grown under ALI for 7 days. Quantative RT-PCR (Taqman) analysis of SLC26 expression in HBE cells grown on transwell inserts under ALI for 7 days (following 7 days submerged), relative to standard curve and normalised to GAPDH expression (%). n=3.

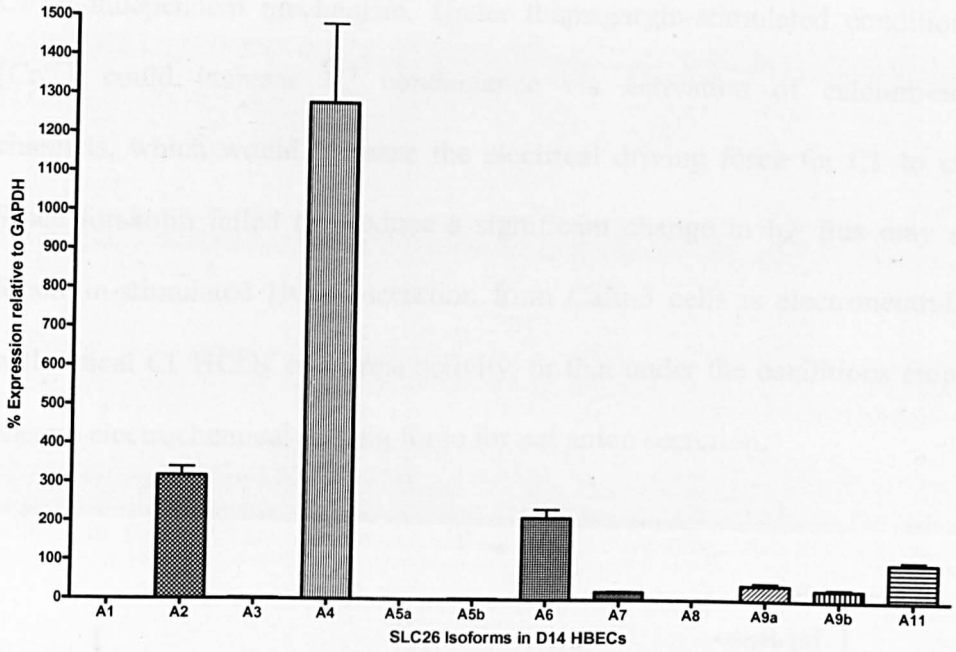

Figure 5.04- SLC26 mRNA expression in HBE cells grown under ALI for 14 days. Quantative RT-PCR (Taqman) analysis of SLC26 expression in HBE cells grown on transwell inserts under ALI for 14 days (following 7 days submerged), relative to standard curve and normalised to GAPDH expression (%). n=3.

5.3 Calu-3 cell short-circuit current measurements

Contrary to previous short-circuit current experiments (Singh *et al*, 1997), no significant difference was observed in I_{SC} between submerged and ALI grown Calu-3 cells monolayers under any of the conditions tested ($P>0.05$; n=4; **Figures 5.05 & 5.06**), although ALI grown cells may have produced greater I_{SC} had more experiments been performed. Forskolin failed to enhance I_{SC} above basal levels in either submerged or ALI grown cultures ($P>0.05$; n=4). However, the presence of the Ca^{2+} agonist thapsigargin induced a six-fold increase in basal I_{SC} in both cultures, which could be diminished by addition of the NKCC inhibitor piretanide, but not by the CFTR inhibitor GlyH-101. These results are consistent with the large bumetanide-sensitive elevation in I_{SC} produced by thapsigargin and the more variable effects of forskolin on I_{SC}, seen previously in Calu-3 cells (Moon *et al*, 1997), albeit through a

CFTR-independent mechanism. Under thapsigargin-stimulated conditions, elevated $[Ca^{2+}]_i$ could increase K^+ conductance via activation of calcium-activated K^+ channels, which would increase the electrical driving force for Cl^- to exit the cell. Since forskolin failed to produce a significant change in I_{SC}, this may suggest that forskolin-stimulated HCO_3^- secretion from Calu-3 cells is electroneutral, consistent with apical Cl^-/HCO_3^- exchange activity, or that under the conditions employed there was no electrochemical driving force for net anion secretion.

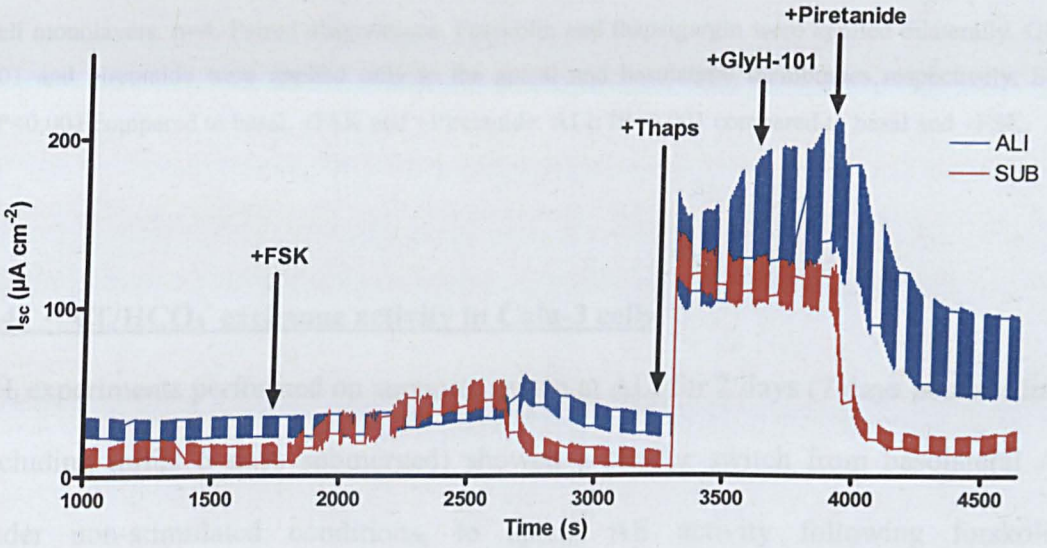

Figure 5.05- I_{SC} measurements in submerged and ALI grown Calu-3 cell monolayers. The effects of forskolin (FSK; 10 μM), thapsigargin (Thaps; 200 nM), GlyH-101 (10 μM) and piretanide (10 μM) on short-circuit current (I_{SC}) in submerged (SUB) and air-liquid interface (ALI) grown Calu-3 cell monolayers.

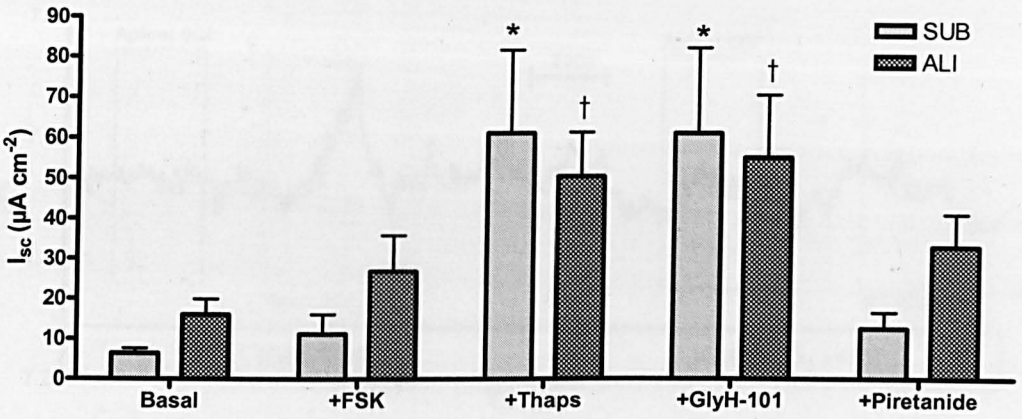

Figure 5.06- I_{SC} measurements in submerged and ALI grown Calu-3 cell monolayers. The effects of forskolin (FSK; 10μM), thapsigargin (Thaps; 200 nM), GlyH-101 (10 μM) and piretanide (10 μM) on mean short-circuit current (I_{SC}) in submerged (SUB) and air-liquid interface (ALI) grown Calu-3 cell monolayers. n=4. Paired observations. Forskolin and thapsigargin were applied bilaterally. GlyH-101 and piretanide were applied only to the apical and basolateral membranes respectively. SUB: *P<0.001 compared to basal, +FSK and +Piretanide. ALI: †P<0.001 compared to basal and +FSK.

5.4 Cl^-/HCO_3^- exchange activity in Calu-3 cells

pH_i experiments performed on supports grown at ALI for 2 days (7 days post seeding-including initial 5 days submerged) showed a similar switch from basolateral AE under non-stimulated conditions, to apical AE activity following forskolin-stimulation. However, both basolateral and apical anion exchange activities produced relatively small increases in pH_i in response to the removal of Cl^- compared to Calu-3 cells that were grown fully submerged (**Figure 5.07**).

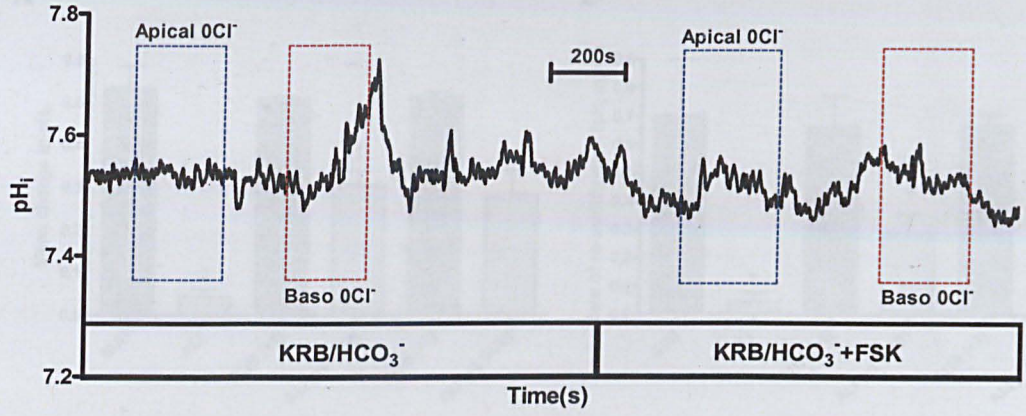

Figure 5.07 –AE activity in ALI grown Calu-3 cells. The effects of forskolin (5 μM) on changes in pH_i following the independent removal of apical and basolateral chloride in ALI grown Calu-3 cells.

Interestingly, both basolateral and apical AE could be significantly enhanced in ALI grown Calu-3 monolayers following re-submersion in apical media. The mean alkalinisation in pH_i produced by apical Cl^- removal in forskolin-stimulated ALI cells increased from 0.04 ± 0.02 to 0.53 ± 0.05 pH units after 24 hours re-submersion in apical media ($P<0.001$; n=4; **Figure 5.08**). However, neither the mean change in pH_i nor the rate of apical AE activity of ALI cells reached that of the apical AE present in Calu-3 cells maintained under submerged conditions, even 48 hours after re-submersion in media ($P<0.05$; n=4).

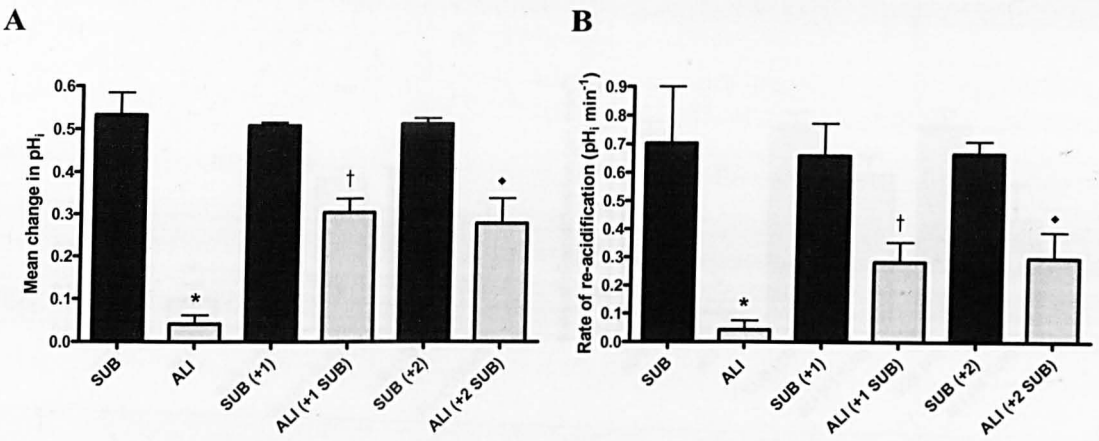

Figure 5.08 – Apical AE activity is partially restored in ALI grown Calu-3 cells following re-submersion. Comparison of the mean changes in pH_i following the removal of apical chloride (**A**) and the rate of re-acidification following chloride re-addition (**B**), in forskolin-stimulated submerged (SUB) and air-liquid interface (ALI) grown Calu-3 cells, and the effects of re-submersion on ALI grown Calu-3 cells. SUB= 7 days submerged post-seeding. ALI= 5 days submerged + 2 days ALI (7 days post-seeding). SUB +1/+2= 8/9 days submerged post-seeding. ALI +1/+2 SUB= ALI grown cells re-submerged for 1/2 days (8/9 days post-seeding). n=4. A: *P<0.001 compared to SUB. †P<0.01 compared to SUB+1. ♦P<0.05 compared to SUB+2. B: *P<0.01 compared to SUB. †P<0.05 compared to SUB+1. ♦P<0.05 compared to SUB+2.

Basolateral Cl^-/HCO_3^- exchange was fully restored and maintained at levels similar to submerged cells, following the re-addition of apical media for 24 hours to ALI grown Calu-3 cells (P>0.05; n=4; **Figure 5.09**).

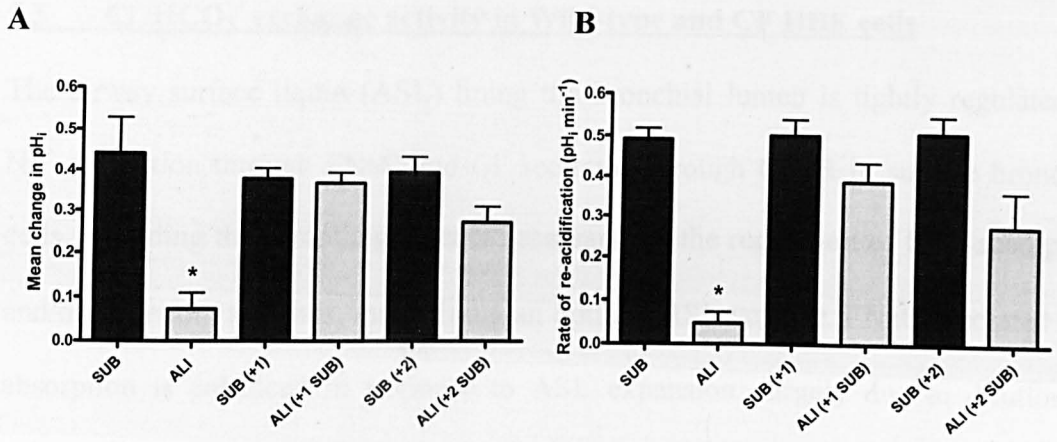

Figure 5.09 – Basolateral AE activity is fully restored in ALI grown Calu-3 cells following re-submersion. Comparison of the mean changes in pH_i following the removal of basolateral chloride (**A**) and the rate of re-acidification following chloride re-addition (**B**), in non-stimulated submerged (SUB) and air-liquid interface (ALI) grown Calu-3 cells, and the effects of re-submersion on ALI grown Calu-3 cells. n=4. See Figure 5.08 for further information. A: *P<0.001 compared to SUB. B: *P<0.001 compared to SUB.

Despite fluctuations in basolateral and apical AE activities in ALI Calu-3 cells, the intracellular acidification produced by forskolin addition remained similar to that of fully submerged cells (P>0.05; n=4; **Figure 5.10**).

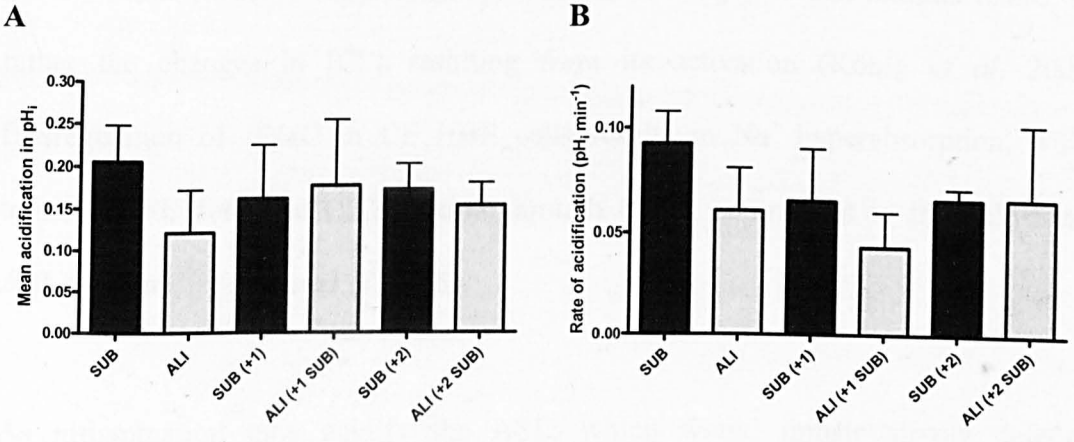

Figure 5.10 – Forskolin-induced acidification is present in both submerged and ALI grown Calu-3 cell monolayers. Comparison of the mean acidification (**A**) and rate of acidification (**B**) in pH_i produced by forskolin (5 μM) addition, in submerged (SUB) and air-liquid interface (ALI) grown Calu-3 cells, and the effects of re-submersion on ALI grown Calu-3 cells. n=4. See Figure 5.08 for further information.

5.5 Cl^-/HCO_3^- exchange activity in Wild-type and CF HBE cells

The airway surface liquid (ASL) lining the bronchial lumen is tightly regulated by Na^+ absorption through ENaC and Cl^- secretion through CFTR in surface bronchial cells, providing the osmotic gradients necessary for the regulation of fluid absorption and/or secretion, and thus, maintaining an optimal ASL volume. ENaC-mediated Na^+ absorption is enhanced in response to ASL expansion, largely due to dilution of soluble protease inhibitors enabling the stimulation of ENaC by membrane bound channel activating proteases (Myerburg *et al*, 2006; Tarran *et al*, 2006). Thus, HBE cells grown under submerged conditions (apical surface volume: 300 µl HCO_3^- buffered solution) display enhanced ENaC-mediated I_{SC} compared to cells grown under ALI (Myerburg *et al*, 2006; Myerburg et al, 2010). CFTR, in addition to mediating Cl^- secretion required for fluid secretion, is also known to inhibit Na^+ absorption through ENaC in response to an increase in cAMP-stimulation by decreasing the open channel probability of ENaC (Stutts *et al*, 1997; Konstas *et al*, 2003). However, ENaC could also be inhibited in *Xenopus* oocytes coexpressed with the Cl^- channel ClC-0, suggesting that it is not CFTR per se that inhibits ENaC, but rather the changes in $[Cl^-]_i$ resulting from its activation (König *et al*, 2001). Dysregulation of ENaC in CF HBE cells results in Na^+ hyperabsorption, which together with defective Cl^- secretion through CFTR contributes to the dehydrated ASL seen in CF (Tarran *et al*, 2005).

As inflammation may acidify the ASL, which would impair airway defence, homeostasis of ASL pH is likely to be another important role of the surface bronchial cells. Several acid and base transporters are known to be expressed throughout the human airway (small, medium and large bronchi, and trachea) including NHE1, AE2

and brain AE3 isoform mRNA (Dudeja *et al*, 1999). NBC3 and NBC4 isoform mRNA have also been detected in lung (Pushkin *et al*, 2000). pH_i experiments (performed under HEPES-buffered conditions) in the HBE cell line, 16HBE14o-, demonstrated that the apical ATP induced acidification in pH_i could be partially blocked by amiloride or apical Na^+ removal, suggesting the involvement of an apical NHE (Urbach *et al*, 2002). Similarly, pH_i experiments in human nasal epithelial (HNE) cells bathed in HEPES-buffered solution showed a Na^+-dependent (and Cl^--independent), amiloride-sensitive recovery from an NH_4^+ acid load, reportedly due to NHE, in both wild-type and CF HNE cells (Paradiso, 1992). Also, H^+-K^+-ATPase activity was present in HBE cells as assessed by ouabain-sensitive pH microelectrode measurements and like NHE activity, its activity was present in both WT and CF cell cultures (Coakley *et al*, 2003). Cl^- substitution (for gluconate) pH_i studies in rat alveolar type II epithelial cells, revealed the presence of a Na^+-independent, DIDS-sensitive (0.5 mM) basolateral Cl^-/HCO_3^- exchange activity under HCO_3^--buffered conditions, proposed to be mediated by AE2 (Lubman et al, 1995). Although the same study found that removal of apical Cl^- had no effect on pH_i. As the AE2 Cl^-/HCO_3^- exchanger and NBC are likely to be restricted to the basolateral membrane, as is the case in Calu-3 cells, they will only contribute indirectly to luminal secretion by regulating pH_i (Falkenberg & Jakobsson, 2010). While NHE and H^+-K^+-ATPase may contribute to secretion of H^+ across the apical membrane, secretion of HCO_3^- might be mediated by CFTR and/or an anion exchanger, which is of particular importance given the evidence that ASL [HCO_3^-] was shown to be greater in WT than CF HBE cell cultures (Coakley et al, 2003).

In pH_i experiments performed on tracheal epithelial cells exhibiting the physiological features of CF (with no functional CFTR; CFT-1 cells), Cl^- substitution studies under HCO_3^--buffered and HCO_3^--free conditions, showed the presence of a DIDS-sensitive apical Cl^-/HCO_3^- exchange activity, which could be enhanced by transfecting cells with WT CFTR (CFT-WT cells; Wheat *et al*, 2000). However, the activity of the apical AE could not be further increased by forskolin, suggesting it was already maximally active or not functionally linked to CFTR. Expression of the basolateral AE2 mRNA was unchanged in CFT-WT cells compared to CFT-1 cells, however SLC26A3 expression was upregulated in CFT-WT cells, suggesting that SLC26A3 mediated the constitutive Cl^-/HCO_3^- exchange activity seen in these cells. In contrast, pH_i experiments in HNE cells, found that apical Cl^- removal produced an alkalinisation in pH_i that was sensitive to the Cl^- channel inhibitor DPC, and could be enhanced by forskolin-stimulation (Paradiso *et al*, 2003). As this response to Cl^- removal was absent in CF HNE cells, the authors concluded that CFTR was responsible for mediating the changes in pH_i.

However, the high expression of SLC26A4 seen in these HBE cells (**Figures 5.03 & 5.04**) raises the possibility that an apical Cl^-/HCO_3^- exchanger mediates Cl^- absorption and HCO_3^- secretion in surface airway cells. In type B and non-A, non-B intercalated cells of the kidney, Pendrin is involved in NaCl absorption together with ENaC, the expression of which is reduced in Pendrin-null mice, suggesting a role for Pendrin in regulating the protein abundance and/or function of ENaC (Kim *et al*, 2007). SLC26A4 expression in HBE cells may also represent a role for Pendrin in secretion of SCN^-, a molecule with antimicrobial activity, due to a correlation between enhanced electroneutral Cl^-/SCN^- exchange and an up-regulation of SLC26A4

expression (as determined by global anion transporter gene expression microarrays and real-time RT-PCR) in IL-4 treated HBE cells (Pedemonte *et al*, 2007). Therefore the potential expression of an apical Cl^-/HCO_3^- exchanger, as well as the reported basolateral AE, was investigated in HBE cells.

HBE cells (passage 1) grown on transwells under submerged conditions for 7 days showed no pH_i response to either apical or basolateral Cl^- removal (n=2). After a further 14 days growth under air-liquid interface, HBE cells produced a mean alkalinisation of 0.19 ± 0.03 pH units, from a basal pH_i of 7.17 ± 0.10, following apical Cl^- removal (n=5; **Figures 5.11 & 5.12**). Upon the re-addition of apical Cl^-, HBE cells re-acidified at a rate of 0.11 ± 0.02 pH units min^{-1} (n=5). Forskolin addition produced no significant change in pH_i ($P>0.05$; n=5). The changes in pH_i seen upon removal and re-addition of apical Cl^- were unaffected by forskolin stimulation ($P>0.05$; n=5). Contrary to previous reports detailing AE2 expression in the tracheobrochial tree (Dudeja *et al*, 1999), HBE cells did not exhibit any significant change in pH_i in response to basolateral Cl^- removal under either non-stimulated or forskolin-stimulated conditions, suggesting basolateral Cl^-/HCO_3^- exchange was absent/not active under these conditions. Interestingly, mRNA expression studies in HNE cells, showed a progressive decrease in AE2 expression levels over time (AE2 mRNA expression decreased 4-fold from time of cell seeding to 28 days after confluence; Shin *et al*, 2007), consistent with the lack of basolateral AE activity seen in these HBE cells grown for 21 days post-seeding.

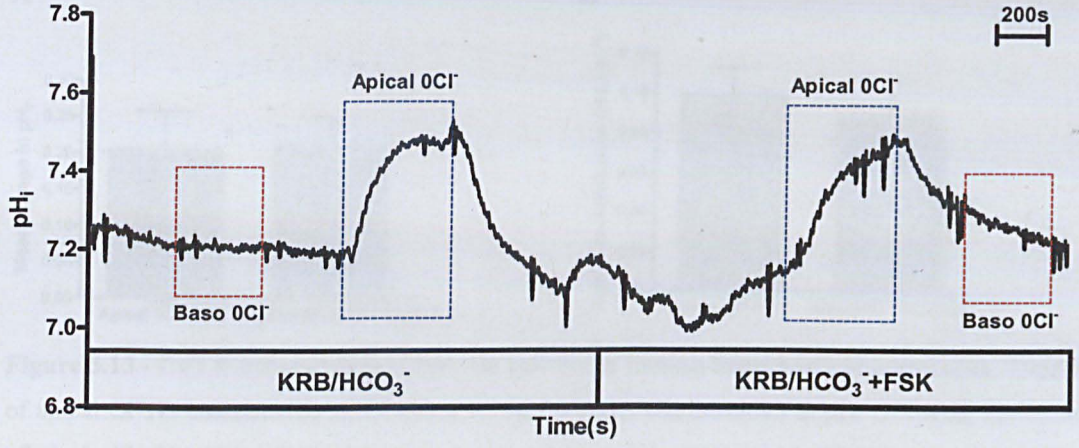

Figure 5.11 – pH_i experimental trace of constitutively active apical AE activity in HBE cells. The effects of forskolin (5 μM) on changes in pH_i following the independent removal of apical and basolateral chloride in ALI grown HBE cells.

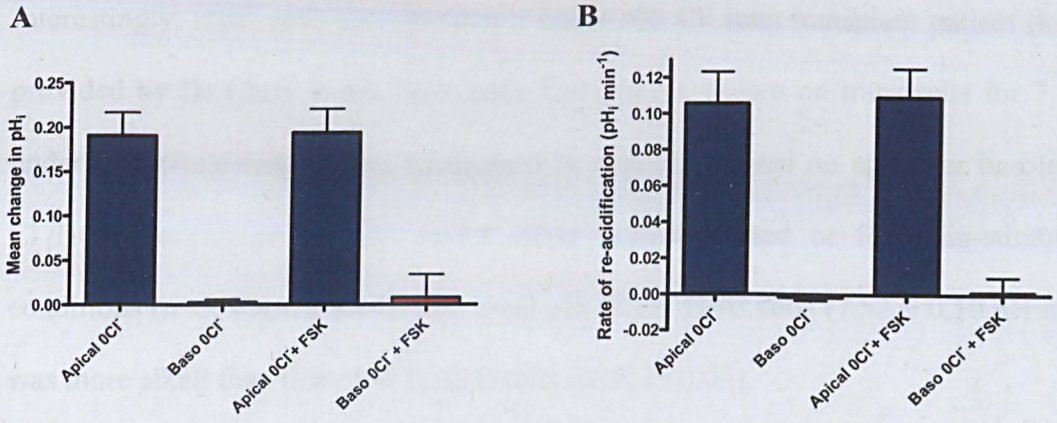

Figure 5.12 - Human bronchial epithelial cells displayed a constitutively active apical AE activity. Mean alkalinisation (pH_i) produced by chloride removal (**A**) and the rate of re-acidification upon chloride re-addition (**B**) in HBE cells, under non-stimulated and forskolin-stimulated (FSK; 5 μM) conditions. n=5.

The apical AE activity present in forskolin-stimulated HBE cells was insensitive to the CFTR pore blocker GlyH-101, consistent with changes in pH_i driven by a constitutively active apical Cl^-/HCO_3^- exchanger, rather than Cl^- dependent HCO_3^- flux through CFTR or the 'CFTR-like' channel SLC26A9 ($P>0.05$; n=3; **Figure 5.13**). GlyH-101 addition had no affect on HBE cell pH_i ($P>0.05$; n=3).

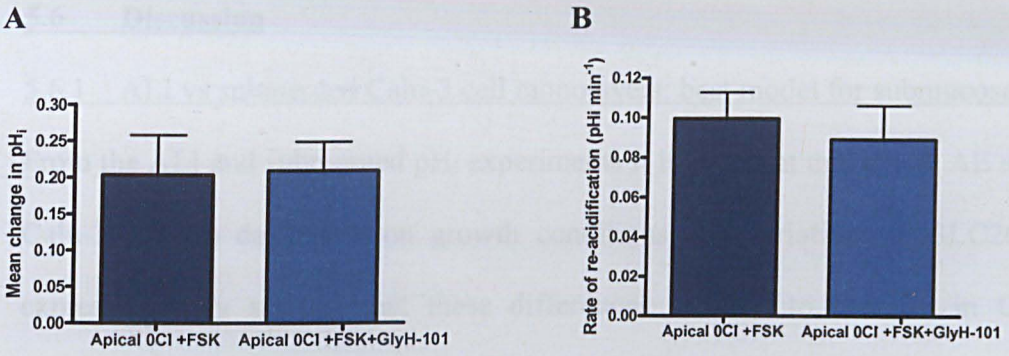

Figure 5.13 - CFTR-independent apical AE activity in human bronchial epithelial cells. The effect of apical CFTR inhibitor GlyH-101 (10 μM) on the mean alkalinisation in pH_i following the removal ofapical chloride (**A**) and the rate of re-acidification in pH_i upon apical chloride re-addition (**B**), in forskolin-stimulated (5 μM) HBE cells. n=3.

Interestingly, HBE cells derived from a deltaF508 CF lung transplant patient (kindly provided by Dr Chris Ward, Newcastle University), grown on transwells for 7 days under ALI (following 7 days submerged in media), showed no apical or basolateral Cl^-/HCO_3^- exchange activity, under either non-stimulated or forskolin-stimulated conditions (n=5; **Figure 5.14**). The basal pH_i of CF HBE cells (7.52 ± 0.10 pH units) was more alkali than that of WT HBE cells (n=5; $P<0.05$).

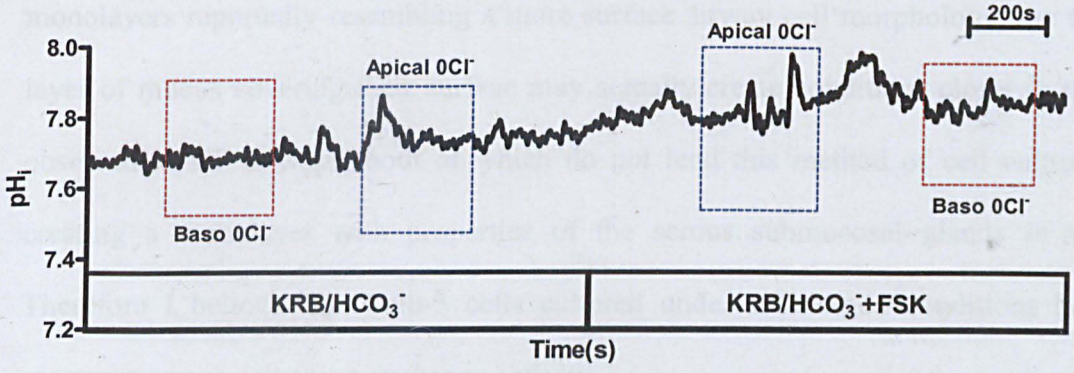

Figure 5.14 – Absence of AE activity in CF human bronchial epithelial cells. The effects of forskolin (5 μM) on changes in pH_i following the independent removal of apical and basolateral chloride in CF HBE cells.

5.6 Discussion

5.6.1 ALI vs submerged Calu-3 cell monolayers: best model for submucosal glands?

From the ALI and submerged pH_i experiments it is apparent that apical AE activity in Calu-3 cells is dependent on growth conditions and variations in SLC26 mRNA expression may suggest that these differences are due to changes in Cl^-/HCO_3^- exchanger expression. Since Calu-3 cell monolayers grown under ALI develop a thick layer of mucus across the apical surface, despite washing the monolayers prior to the start of experiments, it is possible that a remaining layer of mucus may impede access to the apical membrane and thus changes in the composition of the apical bathing solution (i.e. removal of Cl^-) may not reach the membrane and affect apical AE. However, as the basolateral AE was also nearly abolished under ALI conditions, it is unlikely that the differences in AE activity seen between submerged and ALI grown Calu-3 cultures are simply due to a mucus layer blocking access to the membrane. I would postulate that changes in expression of apical HCO_3^- transporters, such as elevated levels of CFTR (which I have previously shown to regulate the basolateral AE present in Calu-3 cells), may have an inhibitory effect on basolateral Cl^-/HCO_3^- exchange activity and/or expression in ALI grown Calu-3 cells. As well as ALI grown monolayers reportedly resembling a more surface airway cell morphology, the thick layer of mucus covering their surface may actually create conditions closer to those observed in CF airways, both of which do not lend this method of cell culture to creating a monolayer with properties of the serous submucosal glands *in vivo*. Therefore I believe that Calu-3 cells cultured under submerged conditions better represent serous cell anion exchange activity.

5.6.2 Apical AE activity in primary surface airway cells and regulation by CFTR

The changes in pH_i following apical Cl^- removal in ALI grown HBE cells, are consistent with the presence of a constitutively active apical Cl^-/HCO_3^- exchanger on the apical surface of the airway lumen, as was previously proposed in experiments using CFT-WT cells (Wheat *et al*, 2000). Wheat and colleagues concluded that SLC26A3 (DRA) was responsible for mediating the Cl^-/HCO_3^- exchange activity observed in CFT-WT cells. However, the mRNA expression studies (**Figures 5.02, 5.03 & 5.04**) showed that DRA was not expressed in HBE cells, suggesting another AE protein may mediate the Cl^--dependent changes in pH_i, such as the highly expressed Pendrin. As the CFT-WT cells were grown on coverslips and as such were not polarised, together with the fact that the CFT-1 cells were derived from a deltaF508 CF patient prior to transfection with WT CFTR, makes it difficult to directly compare the results of CFT-WT cell and polarised HBE cells, and may explain the differences in SLC26 transporter expression. This is the first time, to the best of my knowledge, that apical Cl^-/HCO_3^- exchange has been demonstrated in primary HBE cells.

Although inhibition of CFTR anion conductance in wild-type HBE cells did not result in a loss of apical Cl^-/HCO_3^- exchange activity, the absence of functional CFTR in CF HBE cells appeared to inhibit AE activity, either by dysregulation of a coupled exchanger present in the apical membrane (as is the case with ENaC) and/or by a reduction in exchanger expression. Therefore, like Calu-3 cells, CFTR appears to play an important role in regulating apical Cl^-/HCO_3^- exchange activity in HBE cells.

Regulation of apical Cl^-/HCO_3^- exchangers by CFTR has been extensively studied in the pancreas, which may offer insight into differences in apical AE activity in WT and CF HBE cells. Studies in CFPAC-1 cells, a human pancreatic ductal adenocarcinoma cell line that is homozygous for the deltaF508 CFTR mutation, found that introducing WT CFTR (using a recombinant Sendai virus vector) caused the upregulation of apical Cl^-/HCO_3^- exchange activity (Rakonczay *et al*, 2008). In uninfected CFPAC-1 cells, removal of apical Cl^- from the apical membrane had no affect on pH_i (as determined by BCECF microfluorimetry measurements). In contrast, apical Cl^- removal produced a marked alkalinisation in cells expressing WT CFTR, in the presence of cAMP. This response could be inhibited by 0.5 mM H_2-DIDS, but not by $CFTR_{inh}$-172, consistent with SLC26A6 Cl^-/HCO_3^- exchange activity. Interestingly, semi-quantative RT-PCR revealed that CFTR transduction did not increase SLC26A6 expression or induce SLC26A3 expression (A3 expression was not detected in either cell type), ruling out the possibility that changes in SLC26A6/A3 expression were responsible for the upregulation of AE activity in WT CFTR transfected cells (Rakonczay *et al*, 2008). Therefore it was postulated that CFTR expression, rather than Cl^- transport by CFTR, is required for apical Cl^-/HCO_3^- exchange in pancreatic duct cells (Rakonczay *et al*, 2008). These results correspond with the differences seen in WT and CF HBE cells and suggest that CFTR expression is crucial for apical AE activity in surface airway epithelial cells.

In CF, the potential hyperacidic pH of the dehydrated ASL (Coakley *et al*, 2003; Song *et al*, 2006) may involve a culmination of a reduction in HCO_3^- secretion through an apical Cl^-/HCO_3^- exchanger in the airway submucosal glands, together with a loss of ASL pH homeostasis in the airway lumen through an apical Cl^-/HCO_3^- exchanger in

surface bronchial cells, due to the downregulation of AE activity by reduced CFTR expression.

6. Fluid and Mucus secretion

6.1 Introduction

The osmotic gradient created by Cl^- and HCO_3^- secretion from serous submucosal gland (SMG) cells, provides the driving force for water secretion via aquaporin water channels. Aquaporin-5 (AQP5) is proposed to be the primary water channel involved in transmonolayer fluid transport, due to its localisation in serous gland cells, and the fact that fluid secretion from the SMG of the mouse nasopharynx was reduced two-fold in AQP5 null mice, as determined by dilution of a radioactive fluid volume marker (Song & Verkman, 2001).

Calu-3 cells have been previously shown to secrete fluid under open-circuit conditions, with confluent monolayers secreting the equivalent of 120% (under basal conditions; rate of fluid secretion = 2.7 ± 0.5 $\mu l/cm^2/h$) to 550% (in the presence of both forskolin and thapsigargin; rate of fluid secretion = 12.2 ± 1.0 $\mu l/cm^2/h$) of the estimated Calu-3 cell volume each hour (volume of Calu-3 cells on a 1.12 cm^2 transwell insert is ~2 µl), as measured using an oil-immersion optical technique (Irokawa *et al*, 2004). These experiments showed that basal Calu-3 cell fluid secretion could be abolished by a combination of bumetanide addition and replacement of HCO_3^- with a HEPES-buffered solution to bathe the cells, suggesting that basal fluid secretion was mediated by both Cl^- and HCO_3^- secretion. Forskolin addition (5 µM) increased both the rate (by 64%) and the $[HCO_3^-]$ (to 80 mM) of the Calu-3 cell fluid secretion, which could be prevented by replacement of HCO_3^- with HEPES, indicating that the increase in fluid secretion by forskolin was mediated by an increase in HCO_3^- secretion. Whereas, thapsigargin-stimulated fluid secretion (333 nM; 213% compared to basal secretion) could be completely inhibited by treating Calu-3 cells with

bumetanide, consistent with thapsigargin increasing Calu-3 fluid secretion by activating Cl^- secretion. Overall, the study showed a positive correlation between the rate and $[HCO_3^-]$ of Calu-3 cell fluid secretion. However, relatively few studies have been conducted on SMG secretions in intact airways due to difficulties in isolating SMG secretions from the total airway surface liquid. Earlier studies of single SMG secretion rates in sheep showed a similar decrease in mucus volume in the presence of bumetanide or in the absence of HCO_3^- from carbachol-stimulated glands (Joo *et al*, 2001b). HCO_3^- removal also reduced basal gland secretions by half. However, pH measurements taken at the mouth of carbachol, forskolin or VIP-stimulated porcine SMG duct, only showed a pH of 7.2, relative to a bath pH of 7.4 (Joo *et al*, 2002). In CF, SMG secretions in response to agonists that raise intracellular cAMP levels, such as VIP, are absent and overall mucus secretions mediated by acetylcholine-induced increases in $[Ca^{2+}]_i$ are thicker (Wine & Joo, 2004).

Mucins, the glycosylated proteins contained within mucus secretions of the SMG, are secreted by mucous cells, of which MUC5B was proposed to be predominant mucin type secreted (Sharma *et al*, 1998). Electron microscopic studies of Calu-3 cell monolayers revealed 1 μm diameter round granules in ~30-40% of cells, which closely resembled mucin granules of airway mucous goblet cells, that were found to contain the secretory mucin MUC5AC (Kreda *et al*, 2007). RT-PCR analysis of mucins commonly expressed in airway epithelia, showed that Calu-3 cells expressed both MUC5AC and MUC5B, which are known to be expressed in airway goblet cells (Kreda *et al*, 2005). Interestingly, inflammatory cytokine IL-13, has been shown to induce mucus production from primary human tracheal cells (Nakao *et al*, 2008). IL-13 was proposed to cause mucus overproduction via the up-regulation of Pendrin, as

detected by microarray analysis. Pendrin was found to induce MUC5AC expression, plus the enforced expression of Pendrin in mouse airway epithelial cells in vivo resulted in mucus overproduction. This effect of IL-13 on mucus production may be compounded by the finding that AQP5 expression is completely abolished by the cytokine in human airway epithelial cells (Skorwron-zwarg *et al*, 2007). Similarly IL-1β addition increased MUC5AC, but MUC5B, secretion from human tracheobronchial cell cultures in a dose- and time-dependent manner (Gray *et al*, 2004). Recent studies measuring mucus secretion in segments of the mouse intestine found that mucin release was dependent on the presence of HCO_3^- in the bathing medium, as detected by a periodic acid Schiff (PAS) assay (Garcia *et al*, 2009). In the absence of HCO_3^- mucin secretion was approximately halved and inhibition of CFTR (using the CFTR pore blocker GlyH-101) completely abolished stimulated mucin release. From these results it was hypothesised that CFTR-dependent HCO_3^- secretion is important for mucin release, as HCO_3^- may displace bound shielding Ca^{2+} ions from mucins following exocytosis, thus enabling normal mucin expansion and disaggregation to form mucus (De Lisle, 2009; Garcia *et al*, 2009).

Therefore fluid and mucin secretions from Calu-3 cell monolayers were investigated, in order to understand the physiological role of HCO_3^- transport by apical Cl^-/HCO_3^- exchange and CFTR in these cells.

6.2 cAMP and Ca^{2+}-mediated fluid secretion

Non-stimulated wild-type Calu-3 monolayers, submerged in HCO_3^--buffered Krebs solution, increased the apical fluid volume from 200 µl to 210 ± 1 µl/cm^2/24 h ($P<0.05$; n=6; **Figure 6.01**). Forskolin addition (5 µM) increased the rate of fluid

secretion approximately five-fold, to 54 ± 3 µl/cm^2/24 h ($P<0.001$; n=6). Cl^--free and HEPES-buffered Krebs solutions were used to investigate the Cl^-- and HCO_3^--dependence of the Calu-3 fluid secretions, respectively. Bilateral Cl^- removal abolished any fluid secretion produced under non-stimulated conditions and reduced forskolin-stimulated secretion by 88 ± 22% ($P<0.001$; n=6). No significant fluid secretion was observed from Calu-3 monolayers bathed in HEPES-buffered Krebs solutions under either non-stimulated or forskolin-stimulated conditions ($P>0.05$; n=6). These results would suggest that both basal and forskolin-stimulated Calu-3 fluid secretions are Cl^-- and HCO_3^--dependent.

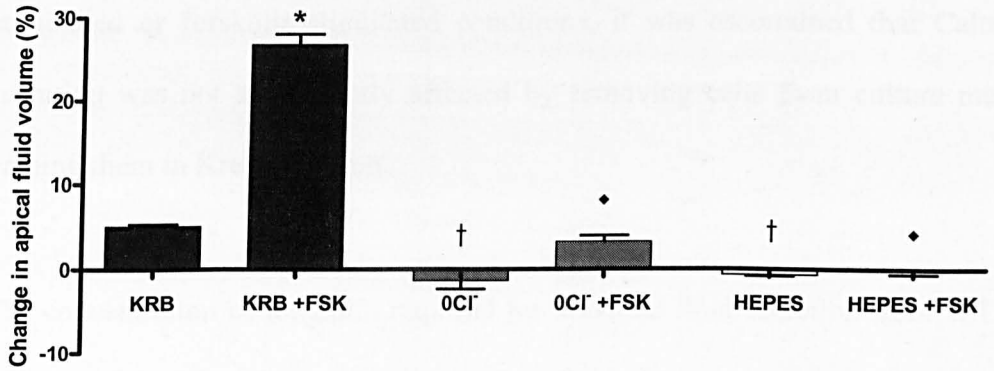

Figure 6.01 - Cl^- and HCO_3^- dependent Calu-3 cell fluid secretion is enhanced by forskolin stimulation. The effect of bilateral Cl^- and HCO_3^- removal, using Cl^--free HCO_3^--buffered ($0Cl^-$) and HEPES-buffered Krebs (HEPES) solutions, on WT Calu-3 apical fluid secretion under non-stimulated and forskolin-stimulated (+FSK) conditions over 24 hours, compared to secretions in standard HCO_3^--buffered Krebs solution (KRB). Forskolin (5 µM) was applied to both the apical and basolateral solutions. Changes in apical fluid volume are expressed as a percentage compared to the starting volume of 200 µl. n=6. *$P<0.001$ compared to KRB. †$P<0.01$ compared to KRB. ◆$P<0.001$ compared to KRB+FSK.

Krebs solutions were used instead of media for fluid secretion studies, as this allowed alterations to be made to the composition of the external fluid bathing the cells (such as Cl^- removal). To ensure the changes in apical fluid volume were not due to differences in the composition of the media and Krebs solutions, such as osmolarity,

fluid secretion measurements were also carried out on Calu-3 cells bathed in media (using the same protocol as Krebs bathed cells- 200 µl of media on the apical surface of the transwell and 1 ml of media in the basolateral compartment). Non-stimulated Calu-3 cells bathed in media, produced a similar change in apical fluid volume to those bathed in HCO_3^--buffered Krebs solution (9 ± 2 µl/cm^2/24 h; P>0.05; n=3). Forskolin addition (5 µM) increased the rate of fluid secretion from Calu-3 cells bathed in media to 46 ± 8 µl/cm^2/24 h (P>0.05 compared to forskolin-stimulated Calu-3 cell secretion in HCO_3^--buffered Krebs solution; n=3). As the mean changes in apical fluid volume was not significantly different between Calu-3 monolayers bathed media and monolayers bathed in HCO_3^--buffered Krebs solution, under either non-stimulated or forskolin-stimulated conditions, it was ascertained that Calu-3 fluid secretion was not significantly affected by removing cells from culture media and bathing them in Krebs solution.

The concentration of forskolin required for maximal fluid secretion from WT Calu-3 cells was determined by applying a range of forskolin concentrations between 0.1 µM and 10 µM (**Figure 6.02**). Application of 0.1 µM or 0.3 µM forskolin did not produce a significant change in fluid secretion compared to basal levels (P>0.05; n=3). Fluid secretion was enhanced at concentrations of forskolin of 0.7 µM (P<0.01 compared to 0 µM FSK control; n=3) and above (1 µM- 10 µM FSK; P<0.001 compared to 0 µM FSK; n=3). 3 µM was the lowest forskolin concentration to significantly increase fluid secretion above that produced by 0.1 µM and 0.3 µM forskolin (P<0.001 and P<0.01 respectively; n=3), to a level that could not be further enhanced by increasing the concentration (P>0.05; n=3). 5 µM forskolin was used in subsequent fluid secretion experiments to ensure maximal forskolin-stimulated fluid secretion and to enable

comparisons to be made between fluid secretion measurements and apical AE activity.

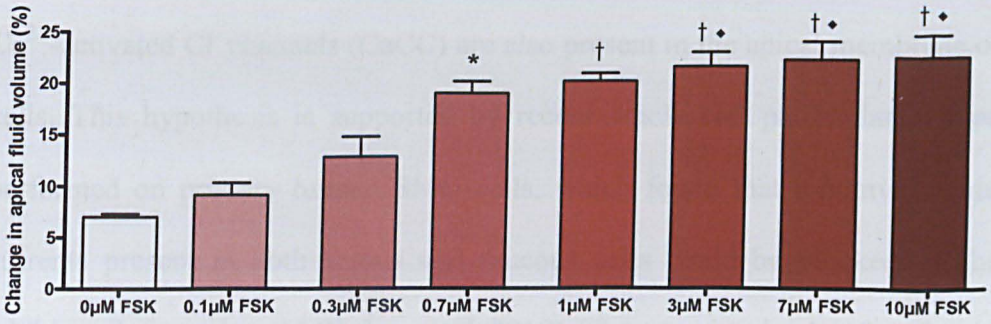

Figure 6.02 - Forskolin-stimulated fluid secretion dose-response in WT Calu-3 cells. The effect of increasing forskolin concentration (0.1, 0.3, 0.7, 1, 3, 7 and 10 μM) on WT Calu-3 apical fluid secretion (% change in volume), bathed in HCO_3^--buffered Krebs solution over 24 hours. n=3. *P<0.01 compared to 0 μM FSK and P<0.05 compared to 0.1 μM FSK. †P<0.001 compared to 0 μM FSK and 0.1 μM FSK.◆P<0.01 compared to 0.3 μM FSK.

Fluid secretion could also be enhanced by the Ca^{2+} agonist thapsigargin, to levels similar to those produced by forskolin (55 ± 1 μl/cm^2/24 h compared to 56 ± 1 μl/cm^2/24 h; P>0.05; n=3; **Figure 6.03**). In comparison, carbachol only stimulated a small increase in fluid secretion above basal levels (from 10 ± 1 μl/cm^2/24 h to 19 ± 2 μl/cm^2/24 h; P<0.001; n=3). This maybe due to this agonist only causing a transient increase in intracellular calcium. Like forskolin, both thapsigargin and carbachol stimulated fluid secretion could be completely abolished by HCO_3^- removal (P<0.001; n=3). As thapsigargin and carbachol are likely to mediate their effects via Ca^{2+}, rather than the cAMP-PKA pathway which is known to predominately regulate CFTR, it is uncertain whether CFTR is the principal apical transporter driving fluid secretion in Calu-3 cells. However, if CFTR is constitutively active in these cells, then anion efflux through CFTR could be predominately controlled by changes in cell membrane potential induced by alteration of basolateral Ca^{2+}-dependent K^+ conductances, which

has been previously proposed to explain anion secretion responses to the elevation of $[Ca^{2+}]_i$ in both Calu-3 cells (Moon *et al*, 1997) and primary human SMG cells (Yamaya *et al*, 1993). Alternatively, it is possible that alternative Cl^- channels, such as Ca^{2+}-activated Cl^- channels (CaCC) are also present in the apical membrane of Calu-3 cells. This hypothesis is supported by recent whole cell patch clamp experiments performed on primary human SMG cells, which found that ionomycin-induced Cl^- currents present in both serous and mucous cells could be blocked by the CaCC inhibitor flufenamic acid (Fisher *et al*, 2010). The same study also found evidence of the CaCC TMEM16A mRNA expression in both the mucous and serous cells of the human tracheal glands (Fisher *et al*, 2010).

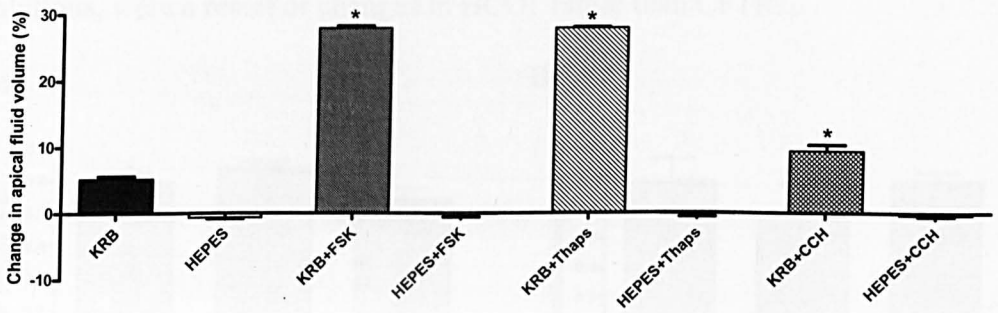

Figure 6.03 – cAMP and Ca^{2+} stimulated Calu-3 cell fluid secretion. The effects of forskolin (FSK; 5 μM), thapsigargin (Thaps; 200 nM) and carbachol (CCH; 10 μM) addition on apical fluid secretion (% change in volume) in WT Calu-3 cells in HCO_3^--buffered (KRB) and HCO_3^--free (HEPES) Krebs solutions over 24 hours. n=3. *P<0.001 compared to KRB.

In order to determine whether exposing Calu-3 cells to a HCO_3^--free, HEPES-buffered solution for 24 hours (used to investigate the HCO_3^- dependence of the Calu-3 fluid secretions) affected CFTR-dependent HCO_3^- transport, as CFTR expression has been shown to be drastically reduced under such conditions (Baudouin-Legros *et al*, 2008), cells were incubated with HEPES and HCO_3^--buffered solutions for 24 hours and then studied in pH_i experiments to look for differences in anion exchange

activity (**Figure 6.04**). As the changes in pH_i mediated by apical Cl^- removal and re-addition in forskolin-stimulated Calu-3 cells were CFTR-dependent, then a large reduction in CFTR expression (similar to CFTR KD cells) would be expected to result in a decrease in apical AE activity. However, no significant change in apical AE activity was observed in Calu-3 cells exposed to HCO_3^- or HEPES-buffered Krebs solutions for 24 hours, compared to control cells kept in media ($P>0.05$; $n=5$). Therefore CFTR activity does not appear to be significantly reduced in cells bathed in HEPES solution, or any change in CFTR expression/activity in HEPES bathed cells is not sufficient to significantly affect apical AE activity, suggesting the differences in the rate of Calu-3 fluid secretion, between HCO_3^- and HEPES-buffered Krebs solutions, were a result of changes in HCO_3^- rather than CFTR.

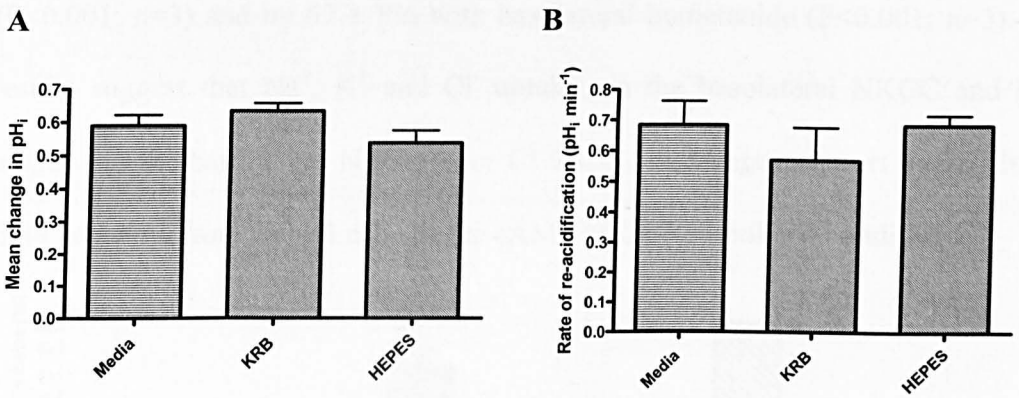

Figure 6.04 – Exposing Calu-3 cells to HCO_3^--free Krebs solution for 24 hours has no affect on apical AE activity. Comparison of mean changes in pH_i following the removal of apical chloride (**A**) and the rates of re-acidification upon apical chloride re-addition (**B**) under forskolin-stimulated conditions in Calu-3 cells grown in media (control) and cells bathed in HCO_3^- (KRB) or HEPES-buffered Krebs solution for 24 hours. n=5.

To investigate the basolateral transporters involved in Calu-3 cell fluid secretion, cells were exposed to the anion transport inhibitor H_2-DIDS and the NKCC inhibitor bumetanide (**Figure 6.05**). Neither basolateral H_2-DIDS nor bumetanide addition significantly altered the basal fluid secretion of Calu-3 cells over 24 hours ($P>0.05$;

n=3). As both HCO_3^- and Cl^- uptake through the basolateral NBC and NKCC are inhibited under these conditions, this result would suggest another mechanism must be driving basal Calu-3 fluid secretion, such as the intracellular generation of HCO_3^- by carbonic anhydrase, or that these inhibitors are not 100% effective over such a long time course (24 h). Although it should be noted that changes in the volume of fluid secreted under non-stimulated conditions were so small that this assay may not be able to detect partial inhibition at these levels. However, both inhibitors significantly decreased forskolin and thapsigargin stimulated fluid secretion. Basolateral H_2-DIDS and bumetanide decreased forskolin-stimulated secretion by 29 ± 3% ($P<0.05$; n=3) and 54 ± 2% ($P<0.001$; n=3) respectively. Thapsigargin-stimulated apical fluid secretions were decreased by 54 ± 15% in the presence of basolateral H_2-DIDS ($P<0.001$; n=3) and by 67 ± 8% with basolateral bumetanide ($P<0.001$; n=3). These results suggest that Na^+, K^+ and Cl^- uptake via the basolateral NKCC and HCO_3^- uptake via the basolateral NBC and/or Cl^-/HCO_3^- exchanger support overall luminal fluid secretion from Calu-3 cells under cAMP or Ca^{2+} stimulated conditions.

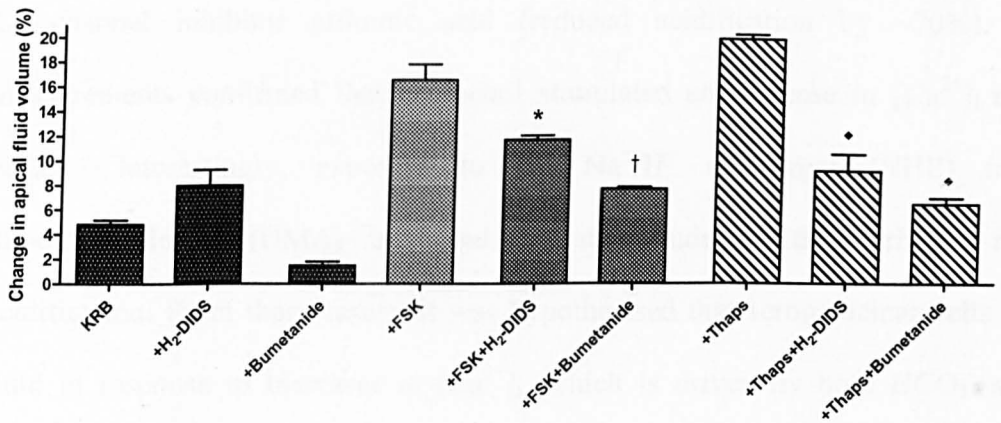

Figure 6.05 – Basolateral H_2-DIDS and bumetanide impair apical Calu-3 cell fluid secretion. The effects of basolateral inhibitors H_2-DIDS (500 μM) and bumetanide on basal, forskolin-stimulated and thapsigargin-stimulated on apical fluid secretion (% change in volume) in WT Calu-3 cells bathed in HCO_3^- -buffered Krebs solution (KRB) for 24 hours. n=3. *$P<0.05$ compared to +FSK. †$P<0.001$ compared to +FSK. ◆$P<0.001$ compared to +Thaps.

Thapsigargin-stimulated fluid secretion, could be driven by Ca^{2+}-activated Cl^- secretion, as bumetanide would lower $[Cl^-]_i$ by inhibiting the basolateral NKCC, and H_2-DIDS may also reduce $[Cl^-]_i$ by inhibiting Cl^- uptake via a basolateral Cl^-/HCO_3^- exchanger. However, since thapsigargin-mediated fluid secretion is abolished by external HCO_3^- removal (see **Figure 6.03**), this would suggest that thapsigargin enhances Calu-3 fluid secretion by stimulating both Cl^- and HCO_3^- secretion.

Similar results were obtained in pH_i experiments on murine submucosal gland serous acinar cells, which demonstrated that a transient, HCO_3^--dependent, acidification in pH_i was produced upon stimulation with carbachol, consistent with HCO_3^- secretion (Lee *et al*, 2008). Carbachol stimulated acinar cells produced an acidification in pH_i that was absent in HCO_3^--free media and could be strongly inhibited through either the elimination of the driving forces for HCO_3^- efflux by ion substitution (altering the extracellular Cl^- and K^+ concentrations to clamp cell membrane potential to the equilibrium potential for HCO_3^-; reduced acidification by ~80%) or the addition of the Cl^- channel inhibitor niflumic acid (reduced acidification by ~70%). $[Ca^{2+}]_i$ measurements confirmed that carbachol stimulated an increase in $[Ca^{2+}]_i$ in these cells. Interestingly, exposure to the Na^+/H^+ exchanger (NHE) inhibitor dimethylamiloride (DMA) increased the magnitude of the carbachol-induced acidification. From these results it was hypothesised that serous acinar cells secrete fluid in response to increases in $[Ca^{2+}]_i$, which is driven by both HCO_3^- and Cl^- secretion, with HCO_3^- secretion sustained in part by the activation of the basolateral NHE (by removal of H^+ to maintain an alkali pH_i).

As no apical Cl^-/HCO_3^- exchange activity is observed in thapsigagrin or carbachol stimulated Calu-3 cells (see section 3.3), would suggest that Ca^{2+}-stimulated HCO_3^- secretion is mediated through another apical exit pathway, or that the effects of apical AE activity on pH_i is masked by the effects of other acid/base transporters, such as the basolateral NHE, under these conditions.

6.3 Role of CFTR in fluid and mucus secretion from Calu-3 cells

To determine the role played by apical CFTR in Calu-3 cell fluid secretion, experiments were performed using the CFTR pore blocker GlyH-101 and studied on CFTR KD Calu-3 cells. In the presence of GlyH-101, non-stimulated Calu-3 cells absorbed rather than secreted fluid (-4 ± 1 $\mu l/cm^2/24$ h; $P<0.001$; n=3; **Figure 6.06A**), suggesting that basal Calu-3 fluid secretion involves CFTR. Forskolin-stimulated fluid secretion could be partially inhibited by GlyH-101 (60 ± 7% inhibition), but to levels significantly greater than control levels ($P<0.001$, n=3), suggesting the presence of CFTR-independent cAMP-stimulated fluid secretion or that the inhibitor was not 100% effective under these conditions. The pH of secreted fluid under non-stimulated conditions was not significantly different to that of the bathing Krebs solution at the start of the experiment (compared to pH 7.4; $P>0.05$; n=3), but pH did significantly increase to 7.8 ± 0.1 following forskolin-stimulation ($P<0.001$; n=3; **Figure 6.06B**). Interestingly, despite altering the volume of fluid secretion, GlyH-101 addition had no effect on the pH of secreted fluid under either non-stimulated or forskolin-stimulated conditions ($P>0.05$; n=3).

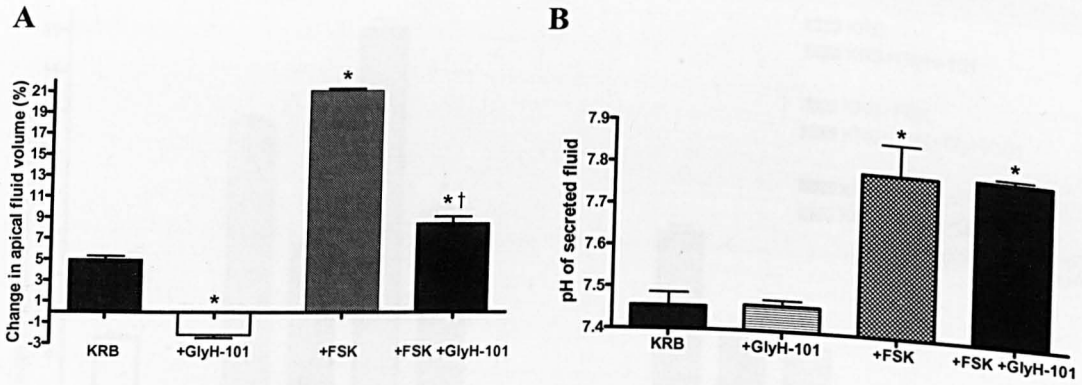

Figure 6.06 – Calu-3 cell fluid secretion volume, but not pH, is inhibited by CFTR pore blocker GlyH-101. The effect of CFTR inhibition by GlyH-101 (10 μM) on apical fluid secretion volume (% change in volume; **A**) and pH (**B**) in basal and forskolin-stimulated WT Calu-3 cells over 24 hours. n=3. Fluid volume and pH measurements represent paired observations from same transwells. A: *P<0.001 compared to KRB. †P<0.001 compared to +FSK. B: *P<0.001 compared to KRB and KRB+GlyH-101.

Under non-stimulated conditions, CFTR KD Calu-3 cells failed to increase the volume of apical fluid (200 μl) over 24 hours (P>0.05; n=4; **Figure 6.07**). However, like WT Calu-3 cells, CFTR KD cells absorbed fluid under basal conditions in the presence of GlyH-101 (-2 ± 0.5 μl/cm^2/24 h; P<0.05; n=4). CFTR KD Calu-3 cells secreted significantly less fluid compared to WT cells under forskolin and thapsigargin-stimulated conditions (34 ± 3% and 88 ± 12% compared to WT, respectively; P<0.001; n=4). Both forskolin and thapsigargin-stimulated fluid secretion from WT and CFTR KD Calu-3 cells were significantly inhibited by the addition of GlyH-101 (P<0.001; n=4). However, like GlyH-101 addition in WT cells, CFTR KD had no significant effect on the pH of apical fluid secretion under either non-stimulated or forskolin-stimulated conditions, compared to WT Calu-3 cells (P>0.05; n=3; **Figure 6.08**).

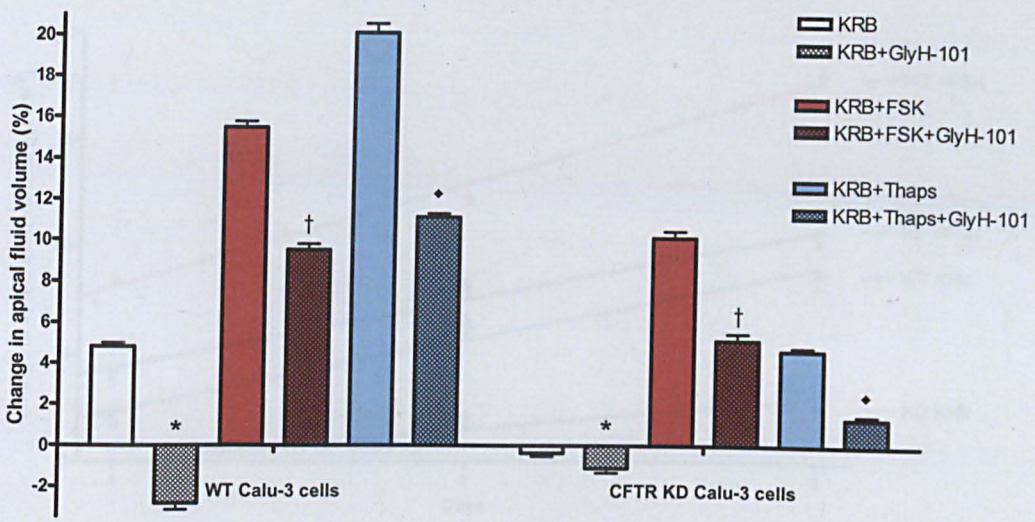

Figure 6.07 – CFTR-dependent fluid secretion from Calu-3 cells. Comparison of the effect of CFTR inhibitor GlyH-101 (10 μM) on basal, forskolin-stimulated (5 μM) and thapsigargin-stimulated (200 nM) apical fluid secretion (% change in volume) in WT and CFTR KD Calu-3 cells over 24 hours. n=3. WT vs CFTR KD Calu-3 cells: $P<0.001$ under all conditions tested. WT Calu-3 cells: *$P<0.001$ compared to KRB. †$P<0.001$ compared to KRB+FSK. ◆$P<0.001$ compared to KRB+Thaps. CFTR KD cells: *$P<0.05$ compared to KRB. †$P<0.001$ compared to KRB+FSK. ◆$P<0.001$ compared to KRB+Thaps.

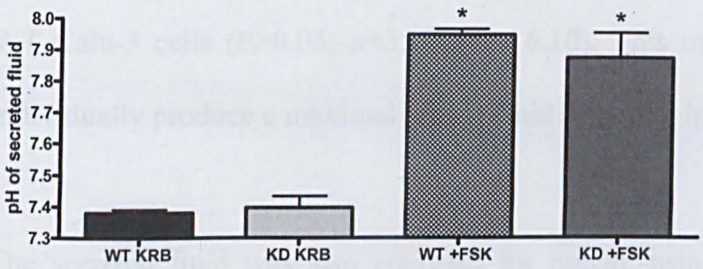

Figure 6.08 – Reduced CFTR expression has no affect on the pH of Calu-3 cell fluid secretion. Comparison of the pH of the apical fluid secreted by WT and CFTR knockdown (KD) Calu-3 cells, under non-stimulated (KRB) and forskolin-stimulated (+FSK; 5 μM), over 24 hours. n=3. *$P<0.001$ compared to WT KRB and KD KRB.

Both WT and CFTR KD Calu-3 cells continued to steadily increase the apical fluid volume over 72 hours (**Figure 6.09**). Interestingly, after 48 hours, there was a net gain in the apical fluid volume of non-stimulated CFTR KD cells (10 ± 1 μl cm^{-2} after 48 hours; n=3).

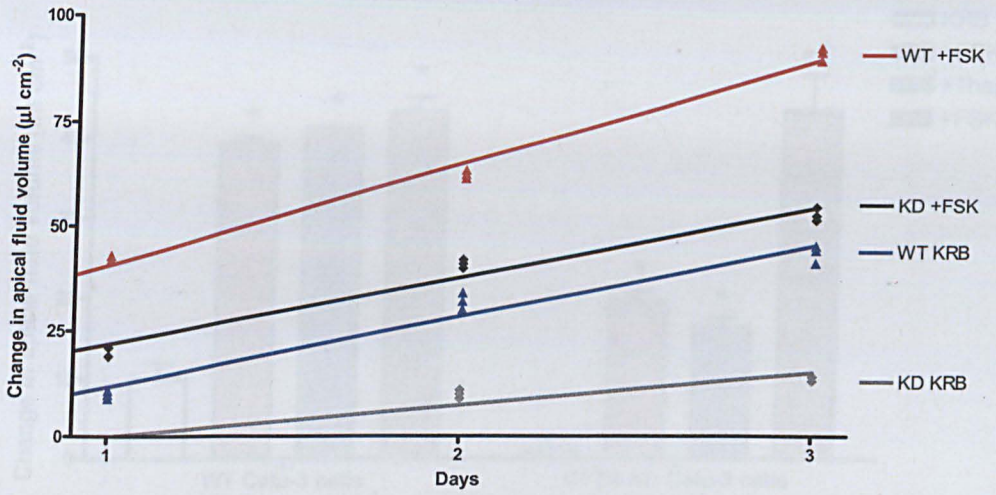

Figure 6.09 – Comparison of basal and forskolin-stimulated apical fluid secretion in WT and CFTR KD Calu-3 cells over 72 hours. Volume of apical fluid secreted above 200 µl at start of experiment in non-stimulated and forskolin-stimulated (5 µM), WT and CFTR knockdown (KD) Calu-3 cells after 24, 48 and 72 hours (µl cm^{-2}). n=3.

Interestingly, the addition of thapsigargin and forskolin together had a synergistic effect on the volume of apical fluid secreted by CFTR KD ($P<0.001$; n=3), but not WT Calu-3 cells ($P>0.05$; n=3; **Figure 6.10**). This may suggest that both agonists individually produce a maximal rate of fluid secretion in WT Calu-3 cells.

The secreted fluid was also analysed for mucin, using a PAS assay (see methods section 2.6.3), which showed that the glycoprotein (mainly mucin) content of CFTR KD Calu-3 cell secretions was significantly reduced compared to WT cells under all conditions ($P<0.001$; n=3; **Figure 6.11**). In WT Calu-3 cells, mucin secretion was unaffected by forskolin-stimulation, compared to basal secretions ($P>0.05$; n=3), but was enhanced by thapsigargin addition ($P<0.05$; n=3). By contrast, CFTR KD Calu-3 cells produced a similar level of mucin secretion under non-stimulated, forskolin-stimulated and thapsigargin-stimulated conditions ($P>0.05$; n=3).

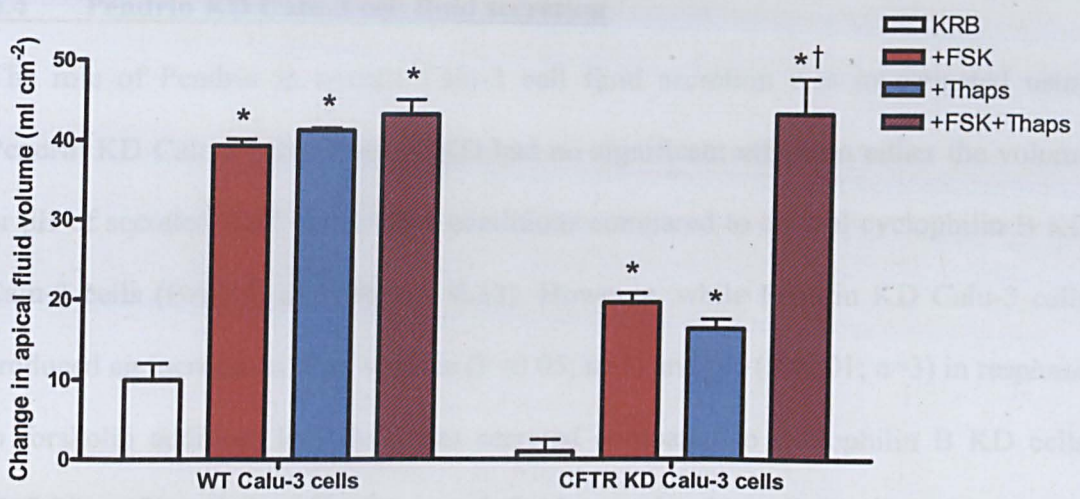

Figure 6.10 – Synergistic effect of forskolin and thapsigargin stimulation in CFTR KD Calu-3 cells. WT and CFTR KD Calu-3 cell fluid secretion (% change in volume) over 24 hours, under forskolin and thapsigargin-stimulated conditions. n=3. WT vs CFTR KD Calu-3 cells: $P<0.001$ under all conditions tested, except +FSK+Thaps $P>0.05$. WT Calu-3 cells: *$P<0.001$ compared to KRB. CFTR KD cells: *$P<0.001$ compared to KRB. †$P<0.001$ compared to +FSK and +Thaps.

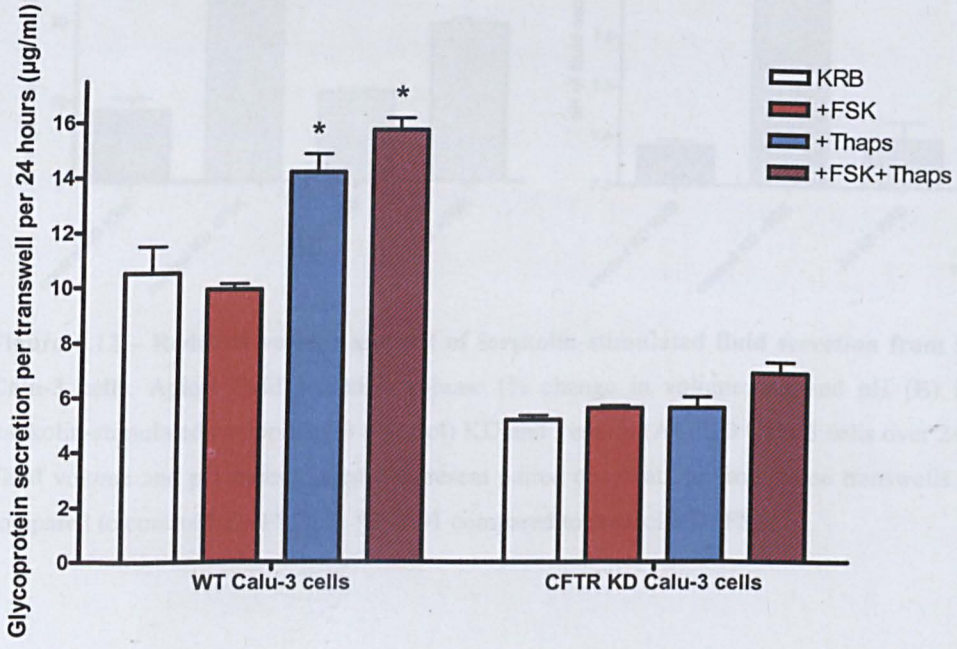

Figure 6.11 – Reduced mucin secretion from CFTR KD Calu-3 cells. WT and CFTR KD Calu-3 cell glycoprotein (mainly mucin) secretion over 24 hours, under forskolin and thapsigargin-stimulated conditions (µg/ml). n=3. Mucin secretion represents paired experiment with fluid secretion measurements in Figure 6.10. WT vs CFTR KD Calu-3 cells: $P<0.001$ under all conditions tested. WT Calu-3 cells: *$P<0.05$ compared to KRB and +FSK.

6.4 Pendrin KD Calu-3 cell fluid secretion

The role of Pendrin in overall Calu-3 cell fluid secretion was investigated using Pendrin KD Calu-3 cells. Pendrin KD had no significant effect on either the volume or pH of secreted fluid under basal conditions compared to control cyclophilin B KD Calu-3 cells ($P>0.05$; n=3; **Figure 6.12**). However, while Pendrin KD Calu-3 cells produced an increase in fluid volume ($P<0.05$; n=3) and pH ($P<0.01$; n=3) in response to forskolin addition, less fluid was secreted compared to cyclophilin B KD cells ($P<0.05$; n=3) and the pH of secreted fluid was also less alkali (pH 7.54 ± 0.01; $P<0.001$; n=3).

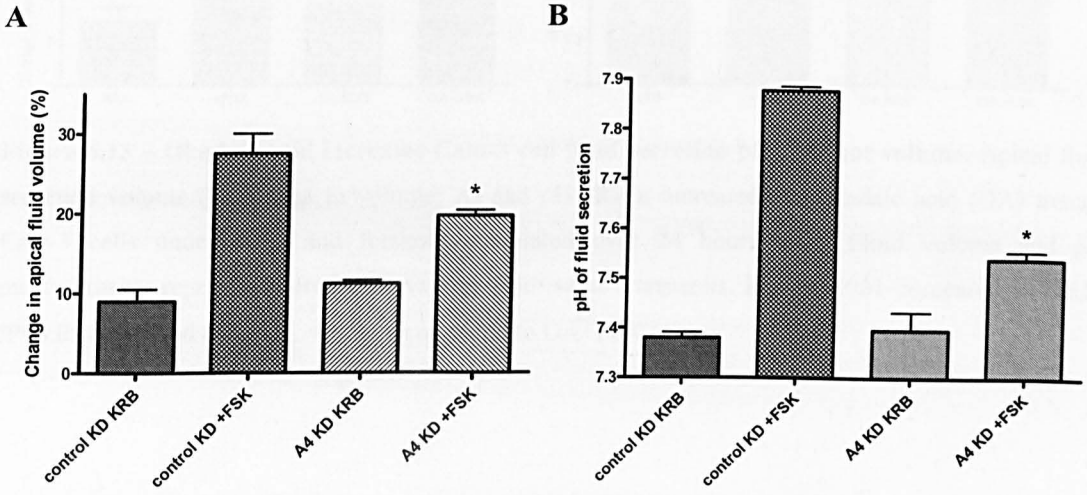

Figure 6.12 – Reduced volume and pH of forskolin-stimulated fluid secretion from Pendrin KD Calu-3 cells. Apical fluid secretion volume (% change in volume; **A**) and pH (**B**) in basal and forskolin-stimulated cyclophilin B (control) KD and Pendrin (A4) KD Calu-3 cells over 24 hours. n=3. Fluid volume and pH measurements represent paired observations from same transwells. A: *$P<0.05$ compared to control KD+FSK. B: *$P<0.01$ compared to control KD+FSK.

6.5 Fluid secretion from okadaic acid treated Calu-3 cells

As previously shown in chapter 3 (section 3.6), okadaic acid activates an apical Cl^-/HCO_3^- exchange activity under non-stimulated conditions. To investigate if this AE activity could contribute to basal Calu-3 cell HCO_3^- secretion, apical fluid secretion

from Calu-3 cells was studied in the presence of okadaic acid. Interestingly, okadaic acid treatment enhanced the pH of the apical fluid from 7.37 ± 0.02 to 7.77 ± 0.02 pH units ($P<0.001$; n=4; **Figure 6.13**), without producing a significant change in the overall volume of fluid secreted ($P>0.05$; n=4). Forskolin-stimulation increased both the volume and pH of apical fluid from okadaic acid treated Calu-3 cells to levels similar to untreated cells ($P>0.05$; n=4).

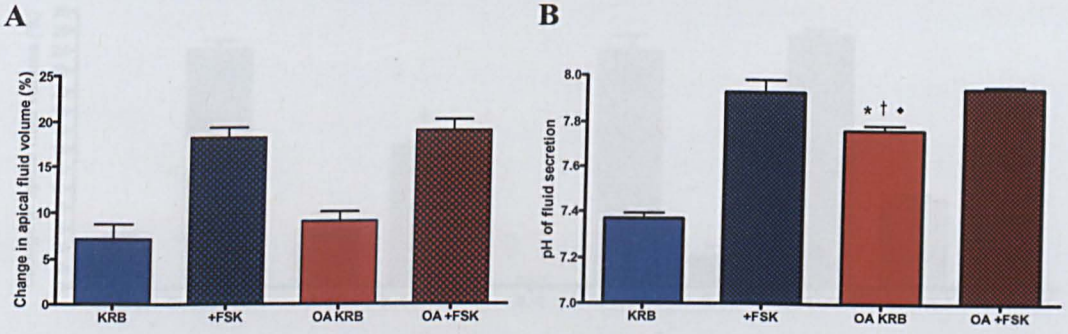

Figure 6.13 – Okadaic acid increases Calu-3 cell fluid secretion pH, but not volume. Apical fluid secretion volume (% change in volume; **A**) and pH (**B**) in untreated and okadaic acid (OA) treated Calu-3 cells under basal and forskolin-stimulated over 24 hours. n=4. Fluid volume and pH measurements represent paired observations from same transwells. B: *$P<0.001$ compared to KRB. †$P<0.05$ compared to +FSK. •$P<0.01$ compared to OA+FSK.

6.6 Cytokine treated Calu-3 cell fluid secretion

Since inflammatory cytokines have been previously shown to alter SMG fluid secretion, the effect of interleukin (IL)- 1β, 4, 13 and 17A treatment on fluid secretion from Calu-3 cells was examined. IL-1β treatment had no significant effect on basal Calu-3 fluid secretion, but decreased the volume of forskolin-stimulated secretion over 24 hours ($P<0.001$; n=3; **Figure 6.14**). No significant change in apical fluid volume was seen in non-stimulated IL-4 treated Calu-3 cells after 24 hours ($P>0.05$; n=3), which increased above untreated Calu-3 cells after 48 hours ($P<0.001$; n=3; **Figure 6.15**). Despite studies showing that AQP5 expression is lost in primary airway

epithelial cells exposed to IL-13 (Skorwron-zwarg *et al*, 2007), IL-13 treatment actually enhanced both basal and forskolin-stimulated fluid secretion from Calu-3 cells over 48 hours ($P<0.001$; n=3). IL-17A exposure had no effect on Calu-3 cell fluid secretion under basal or forskolin-stimulated conditions over 24 hours, but significantly reduced secretion under both conditions after 48 hours ($P<0.001$; n=3).

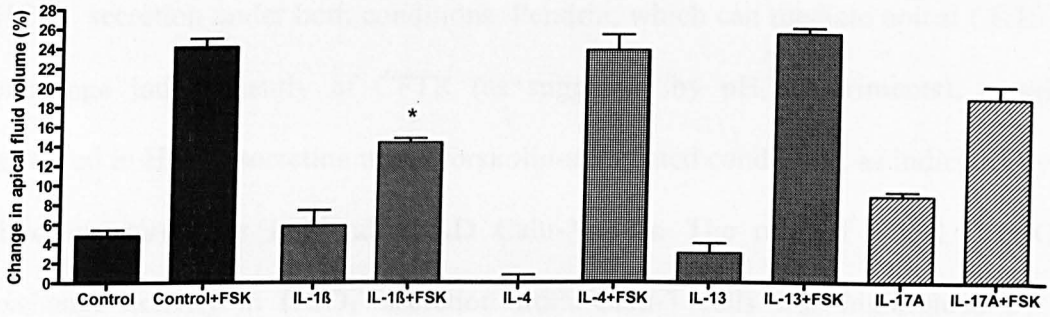

Figure 6.14 – The effects of interleukin 1β, 4, 13 & 17A on basal and forskolin-stimulated apical fluid secretion in WT Calu-3 cells over 24 hours. Changes in apical fluid volume (%) from Calu-3 cells pre-treated with cytokine IL-1β (20 ng/ml), IL-4 (10 ng/ml), IL-13 (10 ng/ml) and IL-17A (50 ng/ml), compared to untreated WT Calu-3 cells (Control), under non-stimulated and forskolin-stimulated conditions over 24 hours. n=3. *P<0.001 compared to Control+FSK.

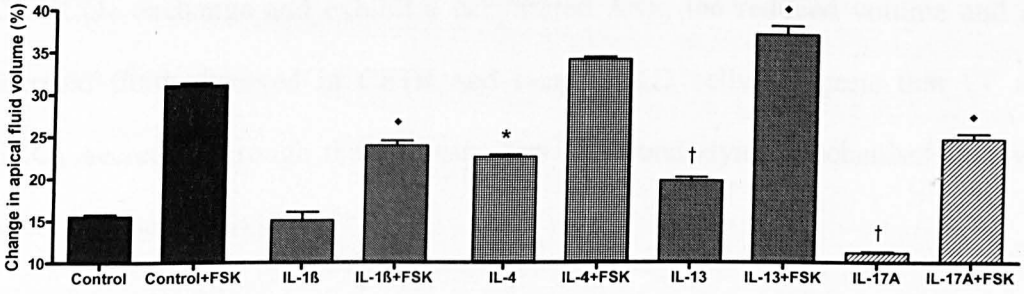

Figure 6.15 – The effects of interleukin 1β, 4, 13 & 17A on basal and forskolin-stimulated apical fluid secretion in WT Calu-3 cells over 48 hours. Changes in apical fluid volume (%) from Calu-3 cells pre-treated with cytokine IL-1β (20 ng/ml), IL-4 (10 ng/ml), IL-13 (10 ng/ml) and IL-17A (50 ng/ml), compared to untreated WT Calu-3 cells (Control), under non-stimulated and forskolin-stimulated conditions over 48 hours. n=3. *P<0.001 compared to Control. †P<0.01 compared to Control. ◆P<0.001 compared to Control+FSK.

6.7 Discussion

These results show that Calu-3 fluid secretion is dependent on both CFTR and Pendrin expression. CFTR inhibitor and knockdown studies suggest that CFTR is involved in net fluid secretion under both non-stimulated and forskolin-stimulated conditions. However, CFTR activity did not appear to alter or contribute to pH changes in the secreted fluid, consistent with the presence of CFTR-independent HCO_3^- secretion under both conditions. Pendrin, which can mediate apical Cl^-/HCO_3^- exchange independently of CFTR (as suggested by pH_i experiments), could be involved in HCO_3^- secretion under forskolin-stimulated conditions, as indicated by pH fluid measurements in Pendrin KD Calu-3 cells. The role of apical Cl^-/HCO_3^- exchange activity in HCO_3^- secretion from Calu-3 cells was highlighted by the increase in fluid pH in okadiac acid treated Calu-3 cells. However, since there was no change in the overall volume secreted by okadaic acid treated cells, compared to untreated Calu-3 cells, this result suggests that HCO_3^- and fluid secretion are not necessarily coupled. Since CF submucosal glands lack functional CFTR and/or apical Cl^-/HCO_3^- exchange and exhibit a dehydrated ASL, the reduced volume and pH of secreted fluid observed in CFTR and Pendrin KD cells, suggests that Cl^- and/or HCO_3^- secretion through these transporters is an underlying mechanism involved in SMG fluid secretion.

The differences seen in the mucin content of fluid secreted by WT and CFTR KD Calu-3 cells are not consistent with a reliance of mucin secretion on CFTR-dependent HCO_3^- secretion, as the pH of the secreted fluid was similar in the two cell types. The reduced volume of fluid secretion in CFTR KD cells may suggest a coupling of mucin and fluid secretion in Calu-3 cells, although the synergistic effect of thapsigargin and

forskolin on fluid but not mucin secretion in CFTR KD Calu-3 cells, would suggest otherwise.

A previous study by Babu and colleagues (Babu *et al*, 2004), measuring the rate of apical fluid secretion over 24 hours from ALI grown Calu-3 cells by micropipette, found much lower rates of secretion under both non-stimulated (~2 $\mu l/cm^2/24$ h compared to 10 ± 1 $\mu l/cm^2/24$ h in the present study) and forskolin-stimulated (5 μM) conditions (13 ± 2 $\mu l/cm^2/24$ h compared to 54 ± 3 $\mu l/cm^2/24$ h in the present study using 50 μM forskolin). As cells were grown on transwells under ALI for 11 days, the differences in Calu-3 fluid secretion compared to the present study could be due to differences in apical transporter expression and/or activity, as highlighted by the reduction in apical AE activity in ALI grown Calu-3 cells (see chapter 5). However, measurements of fluid secretion from ALI grown Calu-3 cells using the 'virtual gland' technique showed much greater rates of fluid secretion (Irokawa *et al*, 2004). Calu-3 cell fluid secretion from the 'virtual gland' were quantified by applying a thin film of apical fluid (10 μl) to cells on a snapwell filter, with a plastic barrier placed on top containing a 0.6 mm hole to serve as a virtual duct, conveying secreted fluid into an oil filled collection chamber. The diameter of the spherical bubble of fluid that forms was measured optically every 30 minutes and converted to volume. Under these conditions, non-stimulated Calu-3 cells secreted fluid at a consistent rate of 2.7 ± 0.5 $\mu l/cm^2/h$ over 6 hours (compared to ~0.4 $\mu l/cm^2/h$ in the present study). The rate of secretion increased to 4.0 ± 0.4 $\mu l/cm^2/h$ following the addition of 5 μM forskolin (compared to ~2.3 $\mu l/cm^2/h$ in the present study) and to 6.4 ± 0.9 $\mu l/cm^2/h$ upon thapsigargin (333 nM) stimulation (compared to ~2.3 $\mu l/cm^2/h$ in the present study). As the current study did not quantify fluid secretion volumes over a shorter time-

course, it is difficult to ascertain whether fluid secretion was constant over 24 hours. However, measuring apical fluid secretion using a 1 µl Gilson pipette would not be accurate enough to measure the small volumes of fluid secreted over an hour. As the apical fluid volume (200 µl) used in the present study is large in comparison to previous studies (0-10 µl), the hydrostatic pressure placed upon the cell monolayer may affect secretion rates. However, removing all apical fluid, while reducing the potential hydrostatic pressure, would render the apical membrane inaccessible for the addition of inhibitors such as GlyH-101. Another limitation of this method is that it is difficult to measure the pH of the apical fluid, as the HCO_3^--buffered solution gradually alkalinises when removed from the CO_2 gassed incubator. This could be overcome by using micro chambers, such as those used by Irokawa and colleagues, which contain a miniature pH electrode (Irokawa *et al*, 2004).

7. Concluding Discussion

7.1 Summary of findings

The aim of this thesis was to investigate the potential role of SLC26 Cl^-/HCO_3^- exchange in airway epithelia. Fluorescence microscopy measurements showed Cl^--dependent changes in pH_i, consistent with Cl^-/HCO_3^- exchange activity, observed on the apical membrane of the serous submucosal gland cell line, Calu-3. Using pharmacological inhibitors and assessing the anion selectivity of this apical anion exchange activity, revealed a CFTR-independent Cl^-/HCO_3^- exchanger with a profile similar to SLC26A4 (Pendrin). These data were supported by immunocytochemical analysis, which demonstrated Pendrin expression localised to the apical membrane of Calu-3 cells. Changes in pH_i consistent with the activity of a CFTR-independent apical Cl^-/HCO_3^- exchanger were also identified in primary human bronchial epithelial cells. Quantative real time-PCR analysis of the SLC26 gene family, revealed the expression of several SLC26 members, including SLC26A4, in both Calu-3 and human bronchial epithelial cells, suggesting that SLC26 anion exchangers maybe present in both the glandular and surface epithelia of the airways. Okadaic acid treatment activated CFTR-independent apical Cl^-/HCO_3^- exchange in non-stimulated Calu-3 cells, under which conditions Calu-3 cells alkalinised the pH of the fluid bathing the apical membrane (which was not apparent in non-treated cells), without stimulating fluid secretion above basal levels. These results are consistent with Pendrin mediating electroneutral apical Cl^-/HCO_3^- exchange, which contributes to the HCO_3^- content of Calu-3 cell fluid secretions.

7.2 Apical Cl^-/HCO_3^- exchanger in Calu-3 cells

The results of the current study have demonstrated for the first time, the presence of an apical Cl^-/HCO_3^- exchange activity in forskolin-stimulated Calu-3 cells, with an anion selectivity and pharmacological profile consistent with SLC26A4 (Pendrin). As this apical AE is active under forskolin-stimulated conditions, in the presence of both basolateral H_2-DIDS and CFTR inhibitor GlyH-101 (**Figures 3.37 & 3.38**) suggests that apical HCO_3^- transport can be mediated independently of CFTR, contrary to previous Calu-3/SMG studies (Illek *et al*, 1997; Krouse *et* al, 2004; Thiagarajah *et al*, 2004). The difference between these results and previous hypotheses of SMG serous cell secretion, could perhaps be due to the regulation of basolateral Cl^-/HCO_3^- exchange activity by CFTR, since in the absence of an apical CFTR conductance (by GlyH-101 inhibition), an active basolateral AE will 'short-circuit' the supply of HCO_3^- for secretion across the apical membrane and thus mask the effects of the apical Cl^-/HCO_3^- exchanger. As the changes in pH_i in the presence of both of these inhibitors is likely to reflect Cl^--dependent HCO_3^- transport mediated by apical Cl^-/HCO_3^- exchange activity alone, further pharmacological studies of this response under these conditions will be necessary for a more complete profile of this apical AE to be established. Another important difference is that many studies of polarised Calu-3 cells were made with cells grown at air-liquid interface (ALI), under which conditions apical AE activity is diminished (see chapter 5).

7.3 cAMP- and CFTR-dependent regulation of Cl^-/HCO_3^- exchange activity in Calu-3 cells

The hypothesis proposed by many investigators, that Calu-3 cell HCO_3^- transport requires CFTR, rather than implicating CFTR as the sole source of apical HCO_3^-

secretion, may instead reflect its regulatory role within these cells. Like other epithelia expressing both SLC26 Cl^-/HCO_3^- exchangers and CFTR, such as the pancreas, apical Cl^-/HCO_3^- exchange in Calu-3 cells appears to be regulated by CFTR, as indicated by the reduced rate of apical AE activity seen in CFTR knockdown Calu-3 cells (**Figure 3.42**). However, CFTR also seems to have a role in the regulation of basolateral Cl^-/HCO_3^- exchange activity, as indicated by the partial inhibition of basolateral AE under forskolin-stimulated conditions in WT Calu-3 cell treated with GlyH-101 or in CFTR KD Calu-3 cells (see section 4.5). These results suggest that CFTR plays a central role in mediating the switch in Calu-3 cells from pH_i regulatory to HCO_3^- secretory modes, following an elevation in cAMP. Co-immunoprecipitation of CFTR and Pendrin would be useful to determine whether a direct structural interaction exists between the proteins in Calu-3 cells.

The mechanisms by which increased cAMP levels mediate this 'switch' in AE activity (inhibition of basolateral AE and stimulation of apical AE activity) was assessed using a range of protein kinase and protein phosphatase inhibitors. The 65% inhibition of apical Cl^-/HCO_3^- exchange activity in the presence of PKA inhibitor H-89 (**Figure 3.08**), in forskolin-stimulated Calu-3 cells, is consistent with CFTR regulation of the exchanger, as CFTR activity requires PKA phosphorylation. However, if CFTR/PKA activity was the sole stimulant of apical Cl^-/HCO_3^- exchange, then one may have expected complete inhibition of apical AE activity by H-89. Therefore, either PKA is not fully inhibited under these conditions by H-89 or the general protein kinase inhibitor staurosporine (**Figure 3.09**), or another pathway is involved in the regulation of the apical AE. As protein phosphatase 1 (PP1) inhibition by okadaic acid activates an apical AE under non-stimulated conditions, with

properties similar to the apical AE seen in the presence of forskolin, I would propose that it is regulated by another, PKA/CFTR-independent, mechanism (see section 3.6). Although (the identity of) this mechanism may not simply be cAMP inhibition of PP1-dependent dephosphorylation, as inhibition of protein phosphatase activity by okadaic acid could also produce a corresponding decrease in protein kinase activity.

The presence of basolateral Cl^-/HCO_3^- exchange activity in forskolin-stimulated Calu-3 cells, when CFTR is inhibited by GlyH-101, highlights the potential dominant effect of CFTR, under cAMP-elevated conditions. Since Calu-3 cells exhibit only basolateral AE activity under non-stimulated conditions, and under forskolin-stimulated conditions, when CFTR is active, only CFTR-dependent apical AE activity is seen, it could be argued that the high expression of CFTR in these cells dominates the effects of Cl^- removal on pH_i and thus masks the effects of both the basolateral and apical Cl^-/HCO_3^- exchangers. However, the results from these pH_i measurements in Calu-3 cells are not consistent with a dominant effect of highly expressed CFTR, rather than a regulatory process, as basolateral AE activity is still present in forskolin-stimulated SLC26A4/A9 knockdown Calu-3 cells, despite stimulation of CFTR-dependent apical AE activity. Also in WT Calu-3 cells stimulated with apical adenosine, basolateral AE is still fully active (see **Figure 4.09**). Therefore I believe my results are consistent with CFTR-dependent regulation and/or changes in anion gradients (i.e. Cl^- or HCO_3^-), which inhibits basolateral Cl^-/HCO_3^- exchange activity under forskolin-stimulated conditions, rather than a dominant effect of active transporters.

The regulation of the basolateral Cl^-/HCO_3^- exchanger by CFTR under $[cAMP]_i$ elevated conditions, fits with the role of the basolateral AE in maintaining pH_i. Under forskolin-stimulated conditions, it would be necessary to inhibit the basolateral AE to avoid 'short-circuiting' HCO_3^- secretion across the apical membrane via CFTR and apical Cl^-/HCO_3^- exchange, and therefore acidifying pH_i even further. Whereas, upon the inhibition of CFTR (by GlyH-101), basolateral AE is active, potentially in order to prevent an alkali load within the cell, due to HCO_3^- accumulation from HCO_3^- uptake through the basolateral NBC.

The exact mechanisms involved in the cAMP/CFTR-dependent inhibition of the basolateral AE are not clear, although one potential mechanism is the efflux of HCO_3^- across the apical membrane upon forskolin stimulation, producing an intracellular acidification, which could inhibit the basolateral Cl^-/HCO_3^- exchanger. Further experiments, such as the addition of a weak acid to Calu-3 cells, are required to establish the pH-dependence of the basolateral AE. Regulation via protein kinase phosphorylation is not apparent, as neither PKA inhibitor H-89 nor the general protein kinase inhibitor staurosporine had any effect on the basolateral AE activity (**Figure 4.11**). However, as PP1 inhibition by okadaic acid abolished basolateral Cl^-/HCO_3^- exchange under non-stimulated conditions, regulation of the basolateral AE may involve protein phosphatase dephosphorylation (**Figure 4.20**).

Based on the results of this thesis, the mechanisms regulating the cAMP-dependent 'switch' from basolateral to apical Cl^-/HCO_3^- exchange activity is summarised in **Figure 7.01**.

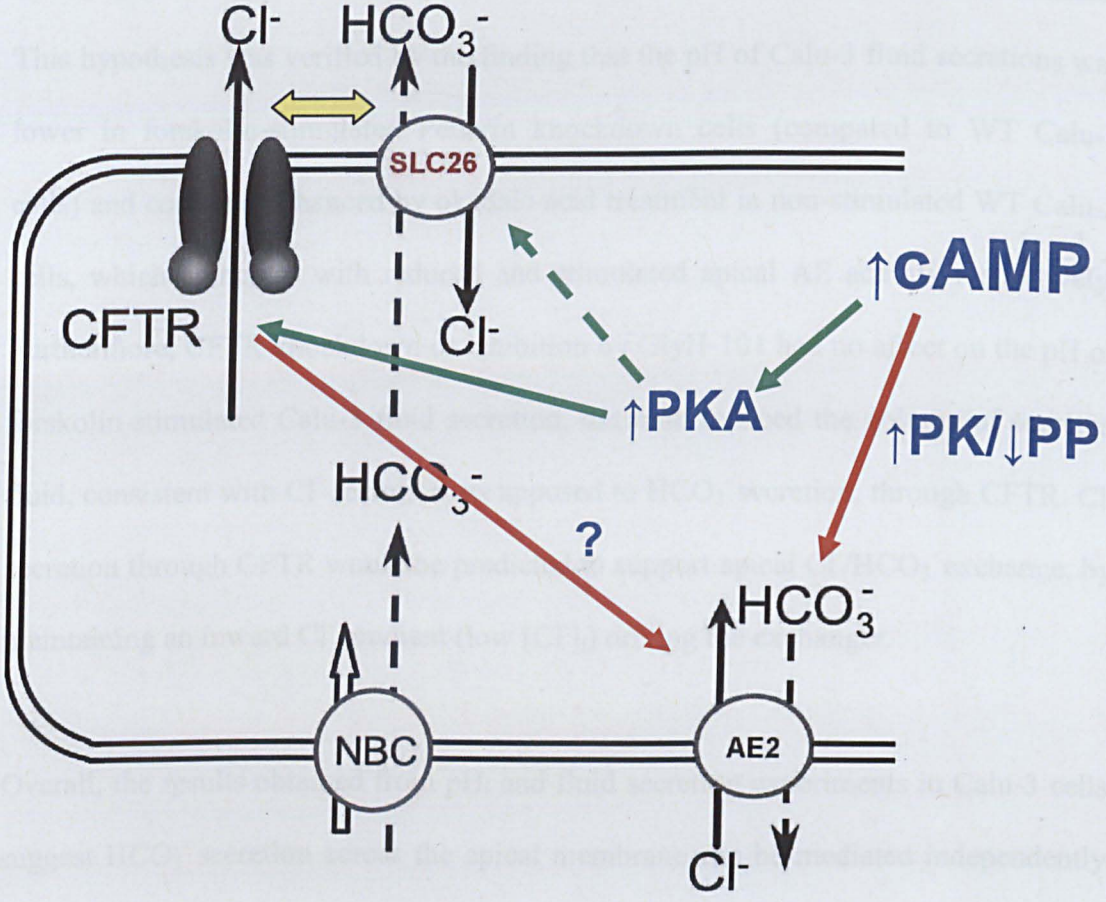

Figure 7.01 – Co-ordinated CFTR-dependent regulation of apical and basolateral Cl^-/HCO_3^- exchangers in cAMP-stimulated Calu-3 cells. Summary of the potential mechanisms regulating the cAMP-dependent 'switch' in AE activity in Calu-3 cells, as determined by protein kinase (PK) and protein phosphatase (PP) inhibitor studies on the apical and basolateral Cl^--dependent changes in pH_i. Green lines indicate stimulatory regulation- cAMP elevation activates PKA, which in turn stimulates CFTR and may also stimulate apical SLC26 Cl^-/HCO_3^- exchange. Yellow arrow indicates the potential reciprocal regulation of CFTR and the apical Cl^-/HCO_3^- exchanger. Red lines indicate inhibitory regulation- cAMP elevation inhibits a basolateral Cl^-/HCO_3^- exchanger, believed to be AE2, indirectly through stimulation of CFTR, or directly by a PKA/PKC-independent mechanism, such as inhibition of PP1.

7.4 Role of apical Cl^-/HCO_3^- exchange in the airways

An insight into the potential role of the apical Cl^-/HCO_3^- exchanger present in Calu-3 cells was determined by looking at the apical fluid secretion from these cells (see chapter 6). From the pH_i experiments, the exchanger would be predicted to facilitate

HCO_3^- secretion across the apical membrane under forskolin-stimulated conditions. This hypothesis was verified by the finding that the pH of Calu-3 fluid secretions was lower in forskolin-stimulated Pendrin knockdown cells (compared to WT Calu-3 cells) and could be enhanced by okadaic acid treatment in non-stimulated WT Calu-3 cells, which coincides with reduced and stimulated apical AE activity respectively. Furthermore, CFTR knockdown or inhibition by GlyH-101 had no affect on the pH of forskolin-stimulated Calu-3 fluid secretion, but both reduced the volume of secreted fluid, consistent with Cl^- secretion, as apposed to HCO_3^- secretion, through CFTR. Cl^- secretion through CFTR would be predicted to support apical Cl^-/HCO_3^- exchange, by maintaining an inward Cl^- gradient (low $[Cl^-]_i$) driving the exchanger.

Overall, the results obtained from pH_i and fluid secretion experiments in Calu-3 cells suggest HCO_3^- secretion across the apical membrane can be mediated independently of CFTR, through an apical SLC26 Cl^-/HCO_3^- exchanger under cAMP-stimulated conditions, with a profile consistent with Pendrin. Although the electrogenicity of the apical AE is uncertain, the high Cl^- concentration (~90 mM; Jayaraman *et al*, 2001a) present in SMG secretions *in vivo*, would be adequate to drive HCO_3^- secretion through either a 1:1 or 2:1 Cl^-/HCO_3^- exchanger to generate a $[HCO_3^-]$ similar to those seen in native tissue (~20 mM; Jayaraman *et al*, 2001a).

Similarly in human (surface) bronchial epithelial cells, apical Cl^-/HCO_3^- exchange activity was observed, which was not affected by CFTR inhibitor GlyH-101, highlighting that Cl^-/HCO_3^- exchange maybe present in other regions of the airways, outside the SMG (see section 5.5). The fact that apical AE activity is absent in CF HBE cells, may indicate that dysregulation of airway Cl^-/HCO_3^- exchange contributes

to the apparent acidic ASL observed in CF airways, due to a lack of HCO_3^- secretion from serous SMG cells and surface airway cells.

7.5 Future experiments

The presence of an apical Cl^-/HCO_3^- exchanger in airway epithelia could have important implications for CF, since it may provide a CFTR-independent source of HCO_3^- in the airways. In addition to the potential future experiments described above, it would be beneficial to study the role of Pendrin in native serous submucosal gland tissue, using a methodology similar to those outlined in this thesis. For instance, intracellular and extracellular pH measurements, in the presence of CFTR inhibitors and basolateral H_2-DIDS, in order to isolate the effects of the exchanger on pH.

The physiological role of the apical Cl^-/HCO_3^- exchanger in the airway submucosal glands could also be investigated in Pendrin knockout mice, in which to date many studies have focussed on Pendrin's role in the inner ear. However, as Pendrin knockout mice do not develop hypothyroidism, as seen in Pendred syndrome, another knockout animal may need to be developed to provide a model which better represents Pendrin's role in humans. As Pendrin has also been shown to be expressed in primary bronchial epithelial cells and my data is consistent with an apical Cl^-/HCO_3^- exchange activity in these cells, then studying bronchial epithelial cells obtained from lung brushings in patients with Pendred syndrome would provide the most ideal way of studying the role of Pendrin in surface cells of the airways.

In order to better understand the regulation of the apical Cl^-/HCO_3^- exchanger present in Calu-3 cells by CFTR, it would be useful to determine whether a structural

interaction exists between Pendrin and CFTR. This could be achieved by co-immunoprecipitation of the two proteins or, as Pendrin and CFTR may interact via a STAS-R domain interaction, by studying apical Cl^-/HCO_3^- exchange activity in Calu-3 cells in which the R-domain of CFTR has been deleted.

The most important of all potential future experiments, would be to assess apical Cl^-/HCO_3^- exchange in CF serous SMG cells (such as the deltaF508 CF tracheobronchial cell lines CFSMEo- and 6CFSMEo-; da Paula *et al*, 2005), since a novel agonist of Pendrin could stimulate HCO_3^- secretion through the exchanger and alleviate some of the HCO_3^--dependent pathological changes observed in CF airways, such as the impaired function of mucins in dehydrated mucus secretions.

References

Ahdieh, M., Vandenboos, T. and Youakim, A. (2001) 'Lung epithelial barrier function and wound healing are decreased by IL-4 and IL-13 and enhanced by IFN-γ', *Am J Physiol Cell Physiol*, 281, (6), pp. C2029-2038.

Akiyama, T., Ishida, J., Nakagawa, S., Ogawara, H., Watanabe, S., Itoh, N., Shibuya, M. and Fukami, Y. (1987) 'Genistein, a specific inhibitor of tyrosine-specific protein kinases', *J Biol Chem*, 262, (12), pp. 5592-5595.

Al-Bazzaz, F. J., Hafez, N., Tyagi, S., Gailey, C. A., Toofanfard, M., Alrefai, W. A., Nazir, T. M., Ramaswany, K. and Dudeja, P. K. (2001) 'Detection of Cl^--HCO_3^- and Na^+-H^+ exchangers in human airways epithelium', *J Pancreas*, 2, (4), pp. 285-290.

Alper, S. L. (2006) 'Molecular physiology of SLC4 anion exchangers', *Exp Physiol*, 91, (1), pp. 153-161.

Alper, S. L. (2009) 'Molecular physiology and genetics of Na^+-independent SLC4 anion exchangers', *J Exp Biol*, 212, (11), pp. 1672-1683.

Alper, S. L., Stuart-Tilley, A. K., Biemesderfer, D., Shmukler, B. E. and Brown, D. (1997) 'Immunolocalization of AE2 anion exchanger in rat kidney', *Am J Physiol Renal Physiol*, 273, (4), pp. F601-614.

Amlal, H., Petrovic, S., Xu, J., Wang, Z., Sun, X., Barone, S. and Soleimani, M. (2010) 'Deletion of the anion exchanger Slc26a4 (pendrin) decreases apical Cl^-/HCO_3^- exchanger activity and impairs bicarbonate secretion in kidney collecting duct', *Am J Physiol Cell Physiol*, 299, (1), pp. C33-41.

Anderson, M. P., Berger, H. A., Rich, D. P., Gregory, R. J., Smith, A. E. and Welsh, M. J. (1991a) 'Nucleoside triphosphates are required to open the CFTR chloride channel', *Cell,* 67, (4), pp. 775-784.

Anderson, M. P., Gregory, R. J., Thompson, S., Souza, D. W., Paul, S., Mulligan, R. C., Smith, A. E. and Welsh, M. J. (1991b) 'Demonstration that CFTR is a chloride channel by alteration of its anion selectivity', *Science,* 253, (5016), pp. 202-205.

Aravind, L. and Koonin, E. V. (2000) 'The STAS domain - a link between anion transporters and antisigma-factor antagonists', *Curr Biol,* 10, (2), pp. R53-R55.

Avella, M., Loriol, C., Boulukos, K., Borgese, F. and Ehrenfeld, J. (2010) 'SLC26A9 stimulates CFTR expression and function in human bronchial cell lines', *J Cell Physiol.* (published online prior to journal publication).

Babu, P. B. R., Chidekel, A., Utidjian, L. and Shaffer, T. H. (2004) 'Regulation of apical surface fluid and protein secretion in human airway epithelial cell line Calu-3', *Biochem Biophys Res Comms,* 319, (4), pp. 1132-1137.

Ballard, S. T. and Inglis, S. K. (2004) 'Liquid secretion properties of airway submucosal glands', *J Physiol,* 556, (1), pp. 1-10.

Ballard, S. T., Trout, L., Bebok, Z., Sorscher, E. J. and Crews, A. (1999) 'CFTR involvement in chloride, bicarbonate, and liquid secretion by airway submucosal glands', *Am J Physiol Lung Cell Mol Physiol,* 277, (4), pp. L694-699.

Basbaum, C. B., Jany, B. and Finkbeiner, W. E. (1990) 'The Serous Cell', *An Rev Physiol,* 52, (1), pp. 97-113.

Baudouin-Legros, M., Hamdaoui, N., Borot, F., Fritsch, J., Ollero, M., Planelles, G. and Edelman, A. (2008) 'Control of basal CFTR gene expression by bicarbonate-sensitive adenylyl cyclase in human pulmonary cells', *Cell Physiol Biochem,* 21, (1-3), pp. 075-086.

Bear, C. E., Duguay, F., Naismith, A. L., Kartner, N., Hanrahan, J. W. and Riordan, J. R. (1991) 'Cl^- channel activity in Xenopus oocytes expressing the cystic fibrosis gene', *J Biol Chem,* 266, (29), pp. 19142-19145.

Bebök, Z., Tousson, A., Schwiebert, L. M. and Venglarik, C. J. (2001). 'Improved oxygenation promotes CFTR maturation and trafficking in MDCK monolayers', *Am J Physiol Cell Physiol,* 280, pp. C135-145.

Becq, F., Jensen, J., Chang, X. B., Savoia, A., Rommens, J. M., Tsui, L. C., Buchwald, M., Riordan, J. R. and Hanrahan, J. W. (1994) 'Phosphatase inhibitors activate normal and defective CFTR chloride channels, *Proc Natl Acad Sci U.S.A.*, 91, (19), pp. 9160-9164.

Berger, H. A., Travis, S. M. and Welsh, M. J. (1993) 'Regulation of the cystic fibrosis transmembrane conductance regulator Cl^- channel by specific protein kinases and protein phosphatases', *J Biol Chem,* 268, (3), pp. 2037-2047.

Bertrand, C. A., Zhang, R., Pilewski, J. M. and Frizzell, R. A. (2009) 'SLC26A9 is a constitutively active, CFTR-regulated anion conductance in human bronchial epithelia', *J Gen Physiol,* 133, (4), pp. 421-438.

Bhaskar, K. R., Gong, D. H., Bansil, R., Pajevic, S., Hamilton, J. A., Turner, B. S. and LaMont, J. T. (1991) 'Profound increase in viscosity and aggregation of pig gastric mucin at low pH', *Am J Physiol Gastrointest Liver Physiol,* 261, (5), pp. G827-832.

Bissig, M., Hagenbuch, B., Stieger, B., Koller, T. and Meier, P. J. (1994) 'Functional expression cloning of the canalicular sulfate transport system of rat hepatocytes', *J Biol Chem,* 269, (4), pp. 3017-3021.

Boucher, R. C., Stutts, M. J., Knowles, M. R., Cantley, L. and Gatzy, J. T. (1986) 'Na^+ transport in cystic fibrosis respiratory epithelia. Abnormal basal rate and response to adenylate cyclase activation', *J Clin Invest,* 78, (5), pp. 1245-1252.

Brouillard, F., Bouthier, M., Leclerc, T., Clement, A., Baudouin-Legros, M. and Edelman, A. (2001) 'NF-kappa B mediates up-regulation of CFTR gene expression in Calu-3 cells by interleukin-1beta', *J Biol Chem*, 276, (12), pp. 9486-9491.

Brown, A. M., Riddoch, F. C., Robson, A., Redfern, C. P. F. and Cheek, T. R. (2005) 'Mechanistic and functional changes in Ca^{2+} entry after retinoic acid-induced differentiation of neuroblastoma cells', *Biochem J*, 388, pp.941-948.

Caohuy, H., Jozwik, C. and Pollard, H. B. (2009) 'Rescue of deltaF508-CFTR by the SGK1/Nedd4-2 signaling pathway', *J Biol Chem,* 284, (37), pp. 25241-25253.

Chang, M.-H., DiPiero, J., Sonnichsen, F. D. and Romero, M. F. (2008) 'Entry to "formula tunnel" revealed by SLC4A4 human mutation and structural model', *J Biol Chem,* 283, (26), pp. 18402-18410.

Chappe, F., Loewen, M. E., Hanrahan, J. W. and Chappe, V. (2008) 'Vasoactive intestinal peptide Increases cystic fibrosis transmembrane conductance regulator levels in the apical membrane of calu-3 cells through a protein kinase C-dependent mechanism', *J Pharmacol Exp Ther,* 327, (1), pp. 226-238.

Chappe, V., Hinkson, D. A., Zhu, T., Chang, X. B., Riordan, J. R. and Hanrahan, J. W. (2003) 'Phosphorylation of protein kinase C sites in NBD1 and the R domain control CFTR channel activation by PKA', *J Physiol,* 548, (1), pp. 39-52.

Cheng, S. H., Gregory, R. J., Marshall, J., Paul, S., Souza, D. W., White, G. A., O'Riordan, C. R. and Smith, A. E. (1990) 'Defective intracellular transport and processing of CFTR is the molecular basis of most cystic fibrosis', *Cell,* 63, (4), pp. 827-834.

Chernova, M. N., Jiang, L., Friedman, D. J., Darman, R. B., Lohi, H., Kere, J., Vandorpe, D. H. and Alper, S. L. (2005) 'Functional comparison of mouse SLC26A6 anion exchanger with human SLC26A6 polypeptide variants', *J Biol Chem,* 280, (9), pp. 8564-8580.

Chijiwa, T., Mishima, A., Hagiwara, M., Sano, M., Hayashi, K., Inoue, T., Naito, K., Toshioka, T. and Hidaka, H. (1990) 'Inhibition of forskolin-induced neurite outgrowth and protein phosphorylation by a newly synthesized selective inhibitor of cyclic AMP-dependent protein kinase, N-[2-(p-bromocinnamylamino)ethyl]-5-isoquinolinesulfonamide (H-89), of PC12D pheochromocytoma cells', *J Biol Chem,* 265, (9), pp. 5267-5272.

Clancy, J. P., Ruiz, F. E. and Sorscher, E. J. (1999) 'Adenosine and its nucleotides activate wild-type and R117H CFTR through an A_{2B} receptor-coupled pathway', *Am J Physiol Cell Physiol*, 276, pp. 361-369.

Clary-Meinesz, C., Mouroux, J., Cosson, J., Huitorel, P. and Blaive, B. (1998) 'Influence of external pH on ciliary beat frequency in human bronchi and bronchioles', *Eur Respir J,* 11, (2), pp. 330-333.

Coakley, R. D., Grubb, B. R., Paradiso, A. M., Gatzy, J. T., Johnson, L. G., Kreda, S. M., O'Neal, W. K. and Boucher, R. C. (2003) 'Abnormal surface liquid pH regulation by cultured cystic fibrosis bronchial epithelium', *Proc Natl Acad Sci U.S.A.,* 100, (26), pp. 16083-16088.

Communi, D., Paindavoine, P., Place, G. A., Parmentier, M., Boeynaems, J. M. (1999) 'Expression of P2Y receptors in cell lines derived form human lung', *Br J Pharmacol*, 127, (2), pp. 562-568.

Courtney, J. M., Ennis, M. and Elborn, J. S. (2004) 'Cytokines and inflammatory mediators in cystic fibrosis', *J Cyst Fibros*, 3, (4), pp. 223-231.

Cuthbert, A. W. and MacVinish, L. J. (2003) 'Mechanisms of anion secretion in Calu-3 human airway epithelial cells by 7,8-benzoquinoline', *Br J Pharmacol*, 140, (1), pp. 81-90.

da Paula, A. C., Ramalho, A. S., Farinha, C. M., Cheung, J., Maurisse, R., Gruenert, D. C., Ousingsawat, J., Kunzelmann, K. and Amaral, M. D. (2005) 'Characterization of novel airway submucosal gland cell models for cystic fibrosis', *Cell Physiol Biochem,* 15, (6), pp. 251-262.

Davis, P. B. (2006) 'Cystic fibrosis since 1938', *Am J Respir Crit Care Med,* 173, (5), pp. 475-482.

de Lisle, R. C. (2009) 'Pass the bicarb: the importance of HCO_3^- for mucin release', *J Clin Invest,* 119, (9), pp. 2535-2537.

de Rooij, J., Zwartkrius, J. T., Verheijen, M. H. G., Cool, R. H., Nijman, S. M. B., Wittinghofer, A. and Bos, J. L. (1998) 'Epac is a Rap1 guanine-nucleotide-exchange factor directly activated by cyclic AMP', *Nature*, 396, pp. 474-477.

Derand, R., Montoni, A., Bulteau-Pignoux, L., Janet, T., Moreau, B., Muller, J. M. and Becq, F. (2004). 'Activation of $VPAC_1$ receptors by VIP and PACAP-27 in human bronchial epithelial cells induces CFTR-dependent chloride secretion', *Br J Pharmacol*, 141, 4, pp. 698- 708.

Devor, D. C., Singh, A. K., Lambert, L. C., DeLuca, A., Frizzell, R. A. and Bridges, R. J. (1999) 'Bicarbonate and chloride secretion in Calu-3 human airway epithelial cells', *J Gen Physiol,* 113, (5), pp. 743-760.

Di Virgilio, F., Fasolato, C. and Steinberg, T. H. (1988) 'Inhibitors of membrane transport system for organic anions block fura-2 excretion from PC12 and N2A cells', *Biochem J,* 256, (3), pp. 959-963.

Divangahi, M., Balghi, H., Danialou, G., Comtois, A. S., Demoule, A., Ernest, S., Haston, C., Robert, R., Hanrahan, J. W., Radzioch, D. and Petrof, B. J. (2009) 'Lack of CFTR in skeletal muscle predisposes to muscle wasting and diaphragm muscle pump failure in cystic fibrosis mice', *PLoS Genet,* 5, (7), pp. e1000586.

Dorwart, M. R., Shcheynikov, N., Wang, Y., Stippec, S. and Muallem, S. (2007) 'SLC26A9 is a Cl^- channel regulated by the WNK kinases', *J Physiol,* 584, (1), pp. 333-345.

Dorwart, M. R., Shcheynikov, N., Yang, D. and Muallem, S. (2008) 'The solute carrier 26 family of proteins in epithelial ion transport', *Physiol,* 23, (2), pp. 104-114.

Dossena, S., Maccagni, A., Vezzoli, V., Bazzini, C., Garavaglia, M. L., Meyer, G., Furst, J., Ritter, M., Fugazzola, L., Persani, L., Zorowka, P., Storelli, C., Beck-Peccoz, P., Botta, G. and Paulmichl, M. (2005) 'The expression of wild-type pendrin (SLC26A4) in human embryonic kidney (HEK 293 Phoenix) cells leads to the activation of cationic currents', *Eur J Endocrinol,* 153, (5), pp. 693-699.

Dossena, S., Vezzoli, V., Cerutti, N., Bazzini, C., Tosco, M., Sironi, C., Rodighiero, S., Meyer, G., Fascio, U., Fürst, J., Ritter, M., Fugazzola, L., Persani, L., Zorowka, P., Storelli, C., Peccoz, P., BottÃ , G. and Paulmichl, M. (2006) 'Functional characterization of wild-type and a mutated form of SLC26A4 identified in a patient with pendred syndrome', *Cell Physiol Biochem,* 17, (5-6), pp. 245-256.

Dubin, R. F., Robinson, S. K. and Widdicombe, J. H. (2004) 'Secretion of lactoferrin and lysozyme by cultures of human airway epithelium', *Am J Physiol Lung Cell Mol Physiol,* 286, (4), pp. L750-755.

Dudeja, P. K., Hafez, N., Tyagi, S., Gailey, C. A., Toofanfard, M., Alrefai, W. A., Nazir, T. M., Ramaswamy, K. and Al-Bazzaz, F. J. (1999) 'Expression of the Na^+/H^+ and Cl^-/HCO_3^- exchanger isoforms in proximal and distal human airways', *Am J Physiol Lung Cell Mol Physiol,* 276, (6), pp. L971-978.

Duta, V., Szkotak, A. J., Nahirney, D. and Duszyk, M. (2004) 'The role of bestrophin in airway epithelial ion transport', *FEBS Lett,* 577, (3), pp. 551-554.

Egan, M., Flotte, T., Afione, S., Solow, R., Zeitlin, P. L., Carter, B. J. and Guggino, W. B. (1992) 'Defective regulation of outwardly rectifying Cl^- channels by protein kinase A corrected by insertion of CFTR', *Nature,* 358, (6387), pp. 581-584.

Engelhardt, J. F., Yankaskas, J. R., Ernst, S. A., Yang, Y., Marino, C. R., Boucher, R. C., Cohn, J. A. and Wilson, J. M. (1992) 'Submucosal glands are the predominant site of CFTR expression in the human bronchus', *Nat Genet,* 2, (3), pp. 240-248.

Everett, L. A., Glaser, B., Beck, J. C., Idol, J. R., Buchs, A., Heyman, M. a., Adawi, F., Hazani, E., Nassir, E., Baxevanis, A. D., Sheffield, V. C. and Green, E. D. (1997) 'Pendred syndrome is caused by mutations in a putative sulphate transporter gene (PDS)', *Nat Genet,* 17, (4), pp. 411-422.

Falkenberg, C. V. and Jakobsson, E. (2010) 'A biophysical model for integration of electrical, osmotic, and pH regulation in the human bronchial epithelium', *Biophys J,* 98, (8), pp. 1476-1485.

Fanning, A. S. and Anderson, J. M. (1999) 'PDZ domains: fundamental building blocks in the organization of protein complexes at the plasma membrane', *J Clin Invest,* 103, (6), pp. 767-772.

Feranchak, A. P., Roman, R. M., Doctor, R. B., Salter, K. D., Toker, A. and Fitz, J. G. (1999) 'The lipid products of phosphoinositide 3-kinase contribute to regulation of cholangiocyte ATP and chloride transport', *J Biol Chem*, 274, (43), pp. 30979-30986.

Feschenko, M. S., Stevenson, E., Nairn, A. C. and Sweadner, K. J. (2002) 'A novel cAMP-stimulated pathway in protein phosphatase 2A activation', *J Pharm Exp Therap,* 302, (1), pp. 111-118.

Fiegel, J., Ehrhardt, C., Schaefer, U. F., Lehr, C.-M. and Hanes, J. (2003) 'Large porous particle impingement on lung epithelial cell monolayers- toward improved particle characterization in the lung', *Pharm Res,* 20, (5), pp. 788-796.

Fischer, H., Illek, B., Sachs, L., Finkbeiner, W. E. and Widdicombe, J. H. (2010) 'CFTR and Ca-activated Cl channels in primary cultures of human airway gland cells of serous or mucous phenotype', *Am J Physiol Lung Cell Mol Physiol*, pp. ajplung.00421.2009.

Flemstrom, G. and Isenberg, J. I. (2001) 'Gastroduodenal mucosal alkaline secretion and mucosal protection', *News Physiol Sci,* 16, (1), pp. 23-28.

Florea, B. I., Cassara, M. L., Junginger, H. E. and Borchard, G. (2003) 'Drug transport and metabolism characteristics of the human airway epithelial cell line Calu-3', *J Control Release,* 87, (1-3), pp. 131-138.

Forbes, B. and Ehrhardt, C. (2005) 'Human respiratory epithelial cell culture for drug delivery applications', *Euro J Pharm Biopharm,* 60, (2), pp. 193-205.

Foster, K. A., Avery, M. L., Yazdanian, M. and Audus, K. L. (2000) 'Characterization of the Calu-3 cell line as a tool to screen pulmonary drug delivery', *Int J Pharm,* 208, (1-2), pp. 1-11.

French, P. J., Bijman, J., Bot, A. G., Boomaars, W. E., Scholte, B. J. and de Jonge, H. R. (1997) 'Genistein activates CFTR Cl^- channels via a tyrosine kinase- and protein phosphatase-independent mechanism', *Am J Physiol Cell Physiol,* 273, (2), C747-753.

Gabriel, S. E., Clarke, L. L., Boucher, R. C. and Stutts, M. J. (1993) 'CFTR and outwardly rectifying chloride channels are distinct proteins with a regulatory relationship', *Nature*, 363, pp. 263-266.

Gadsby, D. C. and Nairn, A. C. (1999) 'Control of CFTR channel gating by phosphorylation and nucleotide hydrolysis', *Physiol Rev,* 79, (1), pp. 77-107.

Garcia, M. A. S., Yang, N. and Quinton, P. M. (2009) 'Normal mouse intestinal mucus release requires cystic fibrosis transmembrane regulator-dependent bicarbonate secretion', *J Clin Invest,* 119, (9), pp. 2613-2622.

Gawenis, L. R., Bradford, E. M., Alper, S. L., Prasad, V. and Shull, G. E. (2010) 'AE2 Cl^-/HCO_3^- exchanger is required for normal cAMP-stimulated anion secretion in murine proximal colon', *Am J Physiol Gastrointest Liver Physiol,* 298, (4), pp. G493-503.

Gelman, M. S., Kannegaard, E. S. and Kopito, R. R. (2002) 'A principal role for the proteasome in endoplasmic reticulum-associated degradation of misfolded intracellular cystic fibrosis transmembrane conductance regulator', *J Biol Chem,* 277, (14), pp. 11709-11714.

Grainger, C., Greenwell, L., Lockley, D., Martin, G. and Forbes, B. (2006) 'Culture of calu-3 cells at the air interface provides a representative model of the airway epithelial barrier', *Pharm Res,* 23, (7), pp. 1482-1490.

Gray, M. A. (2004) 'Bicarbonate secretion: it takes two to tango', *Nat Cell Biol,* 6, pp. 292-294.

Gray, M. A., Greenwell, J. R. and Argent, B. E. (1988) 'Secretin-regulated chloride channel on the apical plasma membrane of pancreatic duct cells', *J Memb Biol,* 105, (2), pp. 131-142.

Gray, M. A., Plant, S. and Argent, B. E. (1993) 'cAMP-regulated whole cell chloride currents in pancreatic duct cells', *Am J Physiol Cell Physiol,* 264, (3), pp. C591-602.

Gray, M. A., Pollard, C. E., Harris, A., Coleman, L., Greenwell, J. R. and Argent, B. E. (1990) 'Anion selectivity and block of the small-conductance chloride channel on pancreatic duct cells', *Am J Physiol Cell Physiol,* 259, (5), pp. C752-761.

Gray, T., Coakley, R., Hirsh, A., Thornton, D., Kirkham, S., Koo, J.-S., Burch, L., Boucher, R. and Nettesheim, P. (2004) 'Regulation of MUC5AC mucin secretion and airway surface liquid metabolism by IL-1β in human bronchial epithelia', *Am J Physiol Lung Cell Mol Physiol,* 286, (2), pp. L320-330.

Greeley, T., Shumaker, H., Wang, Z., Schweinfest, C. W. and Soleimani, M. (2001) 'Downregulated in adenoma and putative anion transporter are regulated by CFTR in cultured pancreatic duct cells', *Am J Physiol Gastrointest Liver Physiol,* 281, (5), pp. G1301-1308.

Green, J., Yamaguchi, D. T., Kleeman, C. R. and Muallem, S. (1990) 'Cytosolic pH regulation in osteoblasts. Regulation of anion exchange by intracellular pH and Ca^{2+} ions', *J Gen Physiol*, 95, (1), pp. 121-145.

Grichtchenko, I. I., Choi, I., Zhong, X., Bray-Ward, P., Russell, J. M. and Boron, W. F. (2001) 'Cloning, characterization, and chromosomal mapping of a human electroneutral Na^+-driven Cl-HCO_3 exchanger', *J Biol Chem,* 276, (11), pp. 8358-8363.

Groneberg, D. A., Hartmann, P., Dinh, Q. T. and Fischer, A. (2001) 'Expression and distribution of vasoactive intestinal polypeptide receptor VPAC2 mRNA in human airways', *Lab Invest,* 81, (5), pp. 749-755.

Groneberg, D. A., Rabe, K. F. and Fischer, A. (2006) 'Novel concepts of neuropeptide-based drug therapy: vasoactive intestinal polypeptide and its receptors', *Euro J Pharm,* 533, (1-3), pp. 182-194.

Grynkiewicz, G., Poenie, M. and Tsien, R. Y. (1985) 'A new generation of Ca^{2+} indicators with greatly improved fluorescence properties', *J Biol Chem,* 260, (6), pp. 3440-3450.

Guimbellot, J. S., Fortenberry, J. A., Siegal, G. P., Moore, B., Wen, H., Venglarik, C., Chen, Y.-F., Oparil, S., Sorscher, E. J. and Hong, J. S. (2008) 'Role of oxygen availability in CFTR expression and function', *Am J Respir Cell Mol Biol,* 39, (5), pp. 514-521.

Haas, M. (1994) 'The Na-K-Cl cotransporters', *Am J Physiol Cell Physiol,* 267, (4), pp. C869-885.

Haghi, M., Young, P. M., Traini, D., Jaiswal, R., Gong, J. and Bebawy, M. (2010) 'Time- and passage-dependent characteristics of a Calu-3 respiratory epithelial cell model', *Drug Dev Ind Pharm,* 36, (10), pp. 1207-1214.

Hasegawa, I., Niisato, N., Iwasaki, Y. and Marunaka, Y. (2006) 'Ambroxol-induced modification of ion transport in human airway Calu-3 epithelia', *Biochem Biophys Res Comms,* 343, (2), pp. 475-482.

Hassan, H. A., Mentone, S., Karniski, L. P., Rajendran, V. M. and Aronson, P. S. (2007) 'Regulation of anion exchanger SLC26A6 by protein kinase C', *Am J Physiol Cell Physiol,* 292, (4), pp. C1485-1492.

Hastbacka, J., de la Chapelle, A., Kaitila, I., Sistonen, P., Weaver, A. and Lander, E. (1992) 'Linkage disequilibrium mapping in isolated founder populations: diastrophic dysplasia in Finland', *Nat Genet,* 2, (3), pp. 204-211.

Haws, C., Finkbeiner, W. E., Widdicombe, J. H. and Wine, J. J. (1994) 'CFTR in Calu-3 human airway cells: channel properties and role in cAMP-activated Cl^- conductance', *Am J Physiol Lung Cell Mol Physiol,* 266, (5), pp. L502-512.

Haws, C., Krouse, M. E., Xia, Y., Gruenert, D. C. and Wine, J. J. (1992) 'CFTR channels in immortalized human airway cells', *Am J Physiol Lung Cell Mol Physiol,* 263, (6), pp. L692-707.

Hegyi, P., Gray, M. A. and Argent, B. E. (2003) 'Substance P inhibits bicarbonate secretion from guinea pig pancreatic ducts by modulating an anion exchanger', *Am J Physiol Cell Physiol,* 285, (2), pp. C268-276.

Hegyi, P., Rakonczay, Z. J., Gray, M. A. and Argent, B. E. (2004) 'Measurement of intracellular pH in pancreatic duct cells: a new method for calibrating the fluorescence data', *Pancreas,* 28, pp. 427-434.

Hoglund, P., Haila, S., Scherer, S. W., Tsui, L. C., Green, E. D., Weissenbach, J., Holmberg, C., de la Chapelle, A. and Kere, J. (1996) 'Positional candidate genes for congenital chloride diarrhea suggested by high-resolution physical mapping in chromosome region 7q31', *Genome Res,* 6, (3), pp. 202-210.

Holma, B. and Hegg, P. O. (1989) 'pH- and protein-dependent buffer capacity and viscosity of respiratory mucus. Their interrelationships and influence of health', *Sci Tot Enviro,* 84, pp. 71-82.

Hoque, K. M., Woodward, O. M., van Rossum, D. B., Zachos, N. C., Chen, L., Leung, G. P. H., Guggino, W. B., Guggino, S. E. and Tse, C. M. (2010) 'Epac1 mediates protein kinase A-independent mechanism of forskolin-activated intestinal chloride secretion', *J Gen Physiol,* 135, (1), pp. 43-58.

Huang, P., Lazarowski, E. R., Tarran, R., Milgram, S. L., Boucher, R. C. and Stutts, M. J. (2001) 'Compartmentalized autocrine signaling to cystic fibrosis transmembrane conductance regulator at the apical membrane of airway epithelial cells', *Proc Natl Acad Sci U.S.A.,* 98, (24), pp. 14120-14125.

Humphreys, B. D., Jiang, L., Chernova, M. N. and Alper, S. L. (1994) 'Functional characterization and regulation by pH of murine AE2 anion exchanger expressed in Xenopus oocytes', *Am J Physiol Cell Physiol,* 267, (5), pp. C1295-1307.

Hunter, M. J. (1977) 'Human erythrocyte anion permeabilities measured under conditions of net charge transfer', *J Physiol,* 268, (1), pp. 35-49.

Hwang, T. C. and Sheppard, D. N. (1999) 'Molecular pharmacology of the CFTR Cl^- channel', *Trends Pharm Sci,* 20, (11), pp. 448-453.

Hwang, T. C. and Sheppard, D. N. (2009) 'Gating of the CFTR Cl^- channel by ATP-driven nucleotide-binding domain dimerisation', *J Physiol,* 587, (10), pp. 2151-2161.

Hwang, T., C., Wang, F., Yang, I. C. and Reenstra, W. W. (1997) 'Genistein potentiates wild-type and delta F508-CFTR channel activity', *Am J Physiol Cell Physiol*, 273, (3), pp. C988-998.

Illek, B., Fischer, H. and Machen, T. E. (1996) 'Alternate stimulation of apical CFTR by genistein in epithelia', *Am J Physiol Cell Physiol,* 270, (1), pp. C265-275.

Illek, B., Yankaskas, J. R. and Machen, T. E. (1997) 'cAMP and genistein stimulate HCO_3^- conductance through CFTR in human airway epithelia', *Am J Physiol Lung Cell Mol Physiol,* 272, (4), pp. L752-761.

Inglis, S. K., Finlay, L., Ramminger, S. J., Richard, K., Ward, M. R., Wilson, S. M. and Olver, R. E. (2002) 'Regulation of intracellular pH in Calu-3 human airway cells', *J Physiol,* 538, (2), pp. 527-539.

Inglis, S. K., Wilson, S. M. and Olver, R. E. (2003) 'Secretion of acid and base equivalents by intact distal airways', *Am J Physiol Lung Cell Mol Physiol,* 284, (5), pp. L855-862.

Irokawa, T., Krouse, M. E., Joo, N. S., Wu, J. V. and Wine, J. J. (2004) 'A "virtual gland" method for quantifying epithelial fluid secretion', *Am J Physiol Lung Cell Mol Physiol,* 287, (4), pp. L784-793.

Ishiguro, H., Namkung, W., Yamamoto, A., Wang, Z., Worrell, R. T., Xu, J., Lee, M. G. and Soleimani, M. (2007) 'Effect of SLC26A6 deletion on apical Cl^- /HCO_3^- exchanger activity and cAMP-stimulated bicarbonate secretion in pancreatic duct', *Am J Physiol Gastrointest Liver Physiol,* 292, (1), pp. G447-455.

Ishiguro, H., Naruse, S., Kitagawa, M., Mabuchi, T., Kondo, T., Hayakawa, T., Case, R. M. and Steward, M. C. (2002) 'Chloride transport in microperfused interlobular ducts isolated from guinea-pig pancreas', *J Physiol,* 539, (1), pp. 175-189.

Ishihara, H., Shimura, S., Satoh, M., Masuda, T., Nonaka, H., Kase, H., Sasaki, T., Sasaki, H., Takishima, T. and Tamura, K. (1992) 'Muscarinic receptor subtypes in feline tracheal submucosal gland secretion', *Am J Physiol Lung Cell Mol Physiol,* 262, (2), pp. L223-228.

Ito, Y., Mizuno, Y., Aoyama, M., Kume, H. and Yamaki, K. (2000) 'CFTR-mediated anion conductance regulates Na^+-K^+-pump activity in Calu-3 human airway cells', *Biochem Biophys Res Comms,* 274, (1), pp. 230-235.

Jayaraman, S., Joo, N. S., Reitz, B., Wine, J. J. and Verkman, A. S. (2001a) 'Submucosal gland secretions in airways from cystic fibrosis patients have normal [Na+] and pH but elevated viscosity', *Proc Natl Acad Sci U.S.A.*, 98, (41), pp. 8119-8123.

Jayaraman, S., Song, Y. and Verkman, A. S. (2001b) 'Airway surface liquid pH in well-differentiated airway epithelial cell cultures and mouse trachea', *Am J Physiol Cell Physiol,* 281, (5), pp. C1504-1511.

Jayaraman, S., Song, Y., Vetrivel, L., Shankar, L. and Verkman, A. S. (2001c) 'Noninvasive in vivo fluorescence measurement of airway-surface liquid depth, salt concentration, and pH', *J Clin Invest,* 107, (3), pp. 317-324.

Jiang, Z., Asplin, J. R., Evan, A. P., Rajendran, V. M., Velazquez, H., Nottoli, T. P., Binder, H. J. and Aronson, P. S. (2006) 'Calcium oxalate urolithiasis in mice lacking anion transporter SLC26A6', *Nat Genet,* 38, (4), pp. 474-478.

Joo, N. S., Irokawa, T., Wu, J. V., Robbins, R. C., Whyte, R. I. and Wine, J. J. (2002a) 'Absent secretion to vasoactive intestinal peptide in cystic fibrosis airway glands', *J Biol Chem,* 277, (52), pp. 50710-50715.

Joo, N. S., Saenz, Y., Krouse, M. E. and Wine, J. J. (2002b) 'Mucus secretion from single submucosal glands of pig', *J Biol Chem,* 277, (31), pp. 28167-28175.

Joo, N. S., Wu, J. V., Krouse, M. E., Saenz, Y. and Wine, J. J. (2001) 'Optical method for quantifying rates of mucus secretion from single submucosal glands', *Am J Physiol Lung Cell Mol Physiol,* 281, (2), pp. L458-468.

Kagawa, T., Varticovski, L., Sai, Y. and Arias, I. M. (2002) 'Mechanism by which cAMP activates PI-3 kinase and increases bile acid secretion in WIF-B9 cells', *Am J Physiol Cell Physiol,* 283, pp. C1655-1666.

Kang, G., Joseph, J. W., Chepurny, O. G., Monaco, M., Wheeler, M. B., Bos, J. L., Schwede, F., Genieser, H. G. & Holz, G. G. (2003) 'Epac-selective cAMP analog 8-pCPT-2'-*O*-Me-cAMP as a stimulus for Ca^{2+}-induced Ca^{2+} release and exocytosis in pancreatic β-cells', *J Biol Chem,* 278, pp. 8279-8285.

Kerem, E., Bistritzer, T., Hanukoglu, A., Hofmann, T., Zhou, Z., Bennett, W., MacLaughlin, E., Barker, P., Nash, M., Quittell, L., Boucher, R., Knowles, M. R., Homolya, V. and Keenan, B. (1999) 'Pulmonary epithelial sodium-channel dysfunction and excess airway liquid in pseudohypoaldosteronism', *N Engl J Med,* 341, (3), pp. 156-162.

Khan, T. Z., Wagener, J. S., Bost, T., Martinez, J., Accurso, F. J. and Riches, D. W. (1995) 'Early pulmonary inflammation in infants with cystic fibrosis', *Am J Repir Crit Care Med*, 151, (4), pp. 1075-1082.

Kim, K. H., Shcheynikov, N., Wang, Y. and Muallem, S. (2005) 'SLC26A7 is a Cl^- channel regulated by intracellular pH', *J Biol Chem,* 280, (8), pp. 6463-6470.

Kim, Y. H., Pech, V., Spencer, K. B., Beierwaltes, W. H., Everett, L. A., Green, E. D., Shin, W., Verlander, J. W., Sutliff, R. L. and Wall, S. M. (2007) 'Reduced ENaC protein abundance contributes to the lower blood pressure observed in pendrin-null mice', *Am J Physiol Renal Physiol,* 293, (4), pp. F1314-1324.

Ko, S. B. H., Shcheynikov, N., Choi, J. Y., Luo, X., Ishibashi, K., Thomas, P. J., Kim, J. Y., Kim, K. H., Lee, M. G., Naruse, S. and Muallem, S. (2002) 'A molecular mechanism for aberrant CFTR-dependent HCO_3^- transport in cystic fibrosis', *EMBO J,* 21, (21), pp. 5662-5672.

Ko, S. B. H., Zeng, W., Dorwart, M. R., Luo, X., Kim, K. H., Millen, L., Goto, H., Naruse, S., Soyombo, A., Thomas, P. J. and Muallem, S. (2004) 'Gating of CFTR by the STAS domain of SLC26 transporters', *Nat Cell Biol,* 6, pp. 343-350.

König, J., Schreiber, R., Voelcker, T., Mall, M. and Kunzelmann, K. (2001) 'The cystic fibrosis transmembrane conductance regulator (CFTR) inhibits ENaC through an increase in the intracellular Cl^- concentration ', *EMBO Rep,* 2, (11), pp. 1047-1051.

Konstas, A.-A., Koch, J.-P. and Korbmacher, C. (2003) 'cAMP-dependent activation of CFTR inhibits the epithelial sodium channel (ENaC) without affecting its surface expression', *Pflügers Arch,* 445, (4), pp. 513-521.

Kopito, R. R., Lee, B. S., Simmons, D. M., Lindsey, A. E., Morgans, C. W. and Schneider, K. (1989) 'Regulation of intracellular pH by a neuronal homolog of the erythrocyte anion exchanger', *Cell,* 59, (5), pp. 927-937.

Kreda, S. M., Mall, M., Mengos, A., Rochelle, L., Yankaskas, J., Riordan, J. R. and Boucher, R. C. (2005) 'Characterization of wild-type and deltaF508 cystic fibrosis transmembrane regulator in human respiratory epithelia', *Mol Biol Cell,* 16, (5), pp. 2154-2167.

Kreda, S. M., Okada, S. F., van Heusden, C. A., O'Neal, W., Gabriel, S., Abdullah, L., Davis, C. W., Boucher, R. C. and Lazarowski, E. R. (2007) 'Coordinated release of nucleotides and mucin from human airway epithelial Calu-3 cells', *J Physiol,* 584, (1), pp. 245-259.

Kreindler, J. L., Bertrand, C. A., Lee, R. J., Karasic, T., Aujla, S., Pilewski, J. M., Frizzel, R. A. and Kolls, J. K. (2009) 'Interleukin-17A bicarbonate secretion in normal human bronchial epithelial cells', *Am J Physiol Lung Cell Mol Physiol*, 296, pp. L257-266.

Kreindler, J. L., Peters, K. W., Frizzell, R. A. and Bridges, R. J. (2006) 'Identification and membrane localization of electrogenic sodium bicarbonate cotransporters in Calu-3 cells', *Biochim Biophys Acta,* 1762, (7), pp. 704-710.

Krouse, M. E., Talbott, J. F., Lee, M. M., Joo, N. S. and Wine, J. J. (2004) 'Acid and base secretion in the Calu-3 model of human serous cells', *Am J Physiol Lung Cell Mol Physiol,* 287, (6), pp. L1274-1283.

Lamprecht, G., Baisch, S., Schoenleber, E. and Gregor, M. (2005) 'Transport properties of the human intestinal anion exchanger DRA (down-regulated in adenoma) in transfected HEK293 cells', *Pflügers Arch,* 449, (5), pp. 479-490.

Lansdell, K. A., Cai, Z., Kidd, J. F. and Sheppard, D. N. (2000) 'Two mechanisms of genistein inhibition of cystic fibrosis transmembrane conductance regulator Cl^- channels expressed in murine cell line', *J Physiol,* 524, (2), pp. 317-330.

Lee, M. C., Penland, C. M., Widdicombe, J. H. and Wine, J. J. (1998) 'Evidence that Calu-3 human airway cells secrete bicarbonate', *Am J Physiol Lung Cell Mol Physiol,* 274, (3), pp. L450-453.

Lee, M. G., Choi, J. Y., Luo, X., Strickland, E., Thomas, P. J. and Muallem, S. (1999) 'Cystic fibrosis transmembrane conductance regulator regulates luminal Cl^-/HCO_3^- exchange in mouse submandibular and pancreatic ducts', *J Biol Chem,* 274, (21), pp. 14670-14677.

Lee, R. J., Harlow, J. M., Limberis, M. P., Wilson, J. M. and Foskett, J. K. (2008) 'HCO_3^- secretion by murine nasal submucosal gland serous acinar cells during Ca^{2+}-stimulated fluid secretion', *J Gen Physiol,* 132, (1), pp. 161-183.

Li, H. and Sheppard, D. N. (2009) 'Therapeutic potential of cystic fibrosis transmembrane conductance regulator (CFTR) inhibitors in polycystic kidney disease', *BioDrugs,* 23, (4), pp. 203-216.

Li, M., McCann, J. D., Liedtket, C. M., Nairn, A. C., Greengard, P. and Welsh, M. J. (1988) 'Cyclic AMP-dependent protein kinase opens chloride channels in normal but not cystic fibrosis airway epithelium', *Nature,* 331, (6154), pp. 358-360.

Liedtke, C. M., Wang, X. and Smallwood, N. D. (2005) 'Role for PP2A in the regulation of Calu-3 epithelial NKCC1 function', *J Biol Chem*, 280, (27), pp. 25491-25498.

Linsdell, P. and Hanrahan, J. W. (1996) 'Disulphonic stilbene block of cystic fibrosis transmembrane conductance regulator Cl^- channels expressed in a mammalian cell line and its regulation by a critical pore residue', *J Physiol,* 496, (Pt 3), pp. 687-693.

Linsdell, P., Tabcharani, J. A., Rommens, J. M., Hou, Y.-X., Chang, X.-B., Tsui, L.-C., Riordan, J. R. and Hanrahan, J. W. (1997) 'Permeability of wild-type and mutant cystic fibrosis transmembrane conductance regulator chloride channels to polyatomic anions', *J Gen Physiol,* 110, (4), pp. 355-364.

Loffing, J., Moyer, B. D., Reynolds, D., Shmukler, B. E., Alper, S. L. and Stanton, B. A. (2000) 'Functional and molecular characterization of an anion exchanger in airway serous epithelial cells', *Am J Physiol Cell Physiol,* 279, (4), pp. C1016-1023.

Lohi, H., Kujala, M., Makela, S., Lehtonen, E., Kestila, M., Saarialho-Kere, U., Markovich, D. and Kere, J. (2002) 'Functional characterization of three novel tissue-specific anion exchangers SLC26A7, -A8, and -A9', *J Biol Chem,* 277, (16), pp. 14246-14254.

Lohi, H., Lamprecht, G., Markovich, D., Heil, A., Kujala, M., Seidler, U. and Kere, J. (2003) 'Isoforms of SLC26A6 mediate anion transport and have functional PDZ interaction domains', *Am J Physiol Cell Physiol,* 284, (3), pp. C769-779.

Loriol C, D. S., Avella M, Gabillat N, Boulukos K, Borgese F, Ehrenfeld J. (2008) 'Characterization of SLC26A9, facilitation of Cl^- transport by bicarbonate', *Cell Physiol Biochem,* 1-4, (22), pp. 15-30.

Lubman, R. L., Danto, S. I., Chao, D. C., Fricks, C. E. and Crandall, E. D. (1995) 'Cl^--HCO_3^- exchanger isoform AE2 is restricted to the basolateral surface of alveolar epithelial cell monolayers', *Am J Respir Cell Mol Biol,* 12, (2), pp. 211-219.

Luo, J., Pato, M. D., Riordan, J. R. and Hanrahan, J. W. (1998) 'Differential regulation of single CFTR channels by PP2C, PP2A, and other phosphatases', *Am J Physiol Cell Physiol*, 274, (5), pp. C1397-1410.

Ma, T., Thiagarajah, J. R., Yang, H., Sonawane, N. D., Folli, C., Galietta, L. J. V. and Verkman, A. S. (2002) 'Thiazolidinone CFTR inhibitor identified by high-throughput screening blocks cholera toxin-induced intestinal fluid secretion', *J Clin Invest,* 110, (11), pp. 1651-1658.

Maas, A. H. J. (1970) 'A titrimetric method for the determination of actual bicarbonate in cerebrospinal fluid and plasma or serum', *Clinica Chimica Acta,* 29, (3), pp. 567-574.

MacVinish, L. J., Cope, G., Ropenga, A. and Cuthbert, A. W. (2007) 'Chloride transporting capability of Calu-3 epithelia following persistent knockdown of the cystic fibrosis transmembrane conductance regulator, CFTR', *Br J Pharmacol,* 150, (8), pp. 1055-1065.

Mantle, M. and Allen, A. (1978) 'A colourimetric assay for glycoprotein based on the periodic acid/Schiff stain.' *Biochem Soc Trans,* 6, pp. 601-609.

Marilyn, R. J.-K. (1992) 'Quick and accurate method to convert BCECF fluorescence to pH_i: Calibration in three different types of cell preparations', *J Cell Physiol,* 151, (3), pp. 596-603.

Mathia, N. R., Timoszyk, J., Stetsko, P. I., Megill, J. R., Smith, R. L. and Wall, D. A. (2002) 'Permeability characteristics of Calu-3 human bronchial epithelial cells: in vitro - in vivo correlation to predict lung absorption in rats', *J Drug Target,* 10, (1), pp. 31-40.

Matsui, H., Grubb, B. R., Tarran, R., Randell, S. H., Gatzy, J. T., Davis, C. W. and Boucher, R. C. (1998) 'Evidence for periciliary liquid layer depletion, not abnormal ion composition, in the pathogenesis of cystic fibrosis airways disease', *Cell,* 95, (7), pp. 1005-1015.

Melvin, J. E., Park, K., Richardson, L., Schultheis, P. J. and Shull, G. E. (1999) 'Mouse down-regulated in adenoma (DRA) is an intestinal Cl^-/HCO_3^- exchanger and is up-regulated in colon of mice lacking the NHE3 Na^+/H^+ exchanger', *J Biol Chem,* 274, (32), pp. 22855-22861.

Meyrick, B. and Reid, L. (1970) 'Ultrastructure of cells in human bronchial submucosal glands.' *J Anat,* 107, pp. 281-299.

Moon, S., Singh, M., Krouse, M. E. and Wine, J. J. (1997) 'Calcium-stimulated Cl^- secretion in Calu-3 human airway cells requires CFTR', *Am J Physiol Lung Cell Mol Physiol,* 273, (6), pp. L1208-1219.

Mount, D. and Romero, M. (2004) 'The SLC26 gene family of multifunctional anion exchangers', *Pflügers Arch,* 447, (5), pp. 710-721.

Muanprasat, C., Sonawane, N. D., Salinas, D., Taddei, A., Galietta, L. J. V. and Verkman, A. S. (2004) 'Discovery of glycine hydrazide pore-occluding CFTR inhibitors', *J Gen Physiol,* 124, (2), pp. 125-137.

Myerburg, M. M., Butterworth, M. B., McKenna, E. E., Peters, K. W., Frizzell, R. A., Kleyman, T. R. and Pilewski, J. M. (2006) 'Airway surface liquid volume regulates ENaC by altering the serine protease-protease inhibitor balance: a mechanism for sodium hyperabsorption in cystic fibrosis. ' *J Biol Chem,* 281, (38), pp. 27942-27949.

Myerburg, M. M., Harvey, P. R., Heidrich, E. M., Pilewski, J. M. and Butterworth, M. (2010) 'Acute regulation of ENaC in airway epithelia by proteases and trafficking', *Am J Respir Cell Mol Biol,* pp. 2009-0348OC.

Nagaki, M., Ishihara, H., Shimura, S., Sasaki, T., Takishima, T. and Shirato, K. (1994) 'Tachykinins induce a $[Ca^{2+}]_i$ rise in the acinar cells of feline tracheal submucosal gland', *Respir Physiol,* 98, (1), pp. 111-120.

Nagel, G., Hwang, T.-C., Nastiuk, K. L., Nairn, A. C. and Gadsbyt, D. C. (1992) 'The protein kinase A-regulated cardiac Cl^- channel resembles the cystic fibrosis transmembrane conductance regulator', *Nature,* 360, (6399), pp. 81-84.

Nakao, I., Kanaji, S., Ohta, S., Matsushita, H., Arima, K., Yuyama, N., Yamaya, M., Nakayama, K., Kubo, H., Watanabe, M., Sagara, H., Sugiyama, K., Tanaka, H., Toda, S., Hayashi, H., Inoue, H., Hoshino, T., Shiraki, A., Inoue, M., Suzuki, K., Aizawa, H., Okinami, S., Nagai, H., Hasegawa, M., Fukuda, T., Green, E. D. and Izuhara, K. (2008) 'Identification of pendrin as a common mediator for mucus production in bronchial asthma and chronic obstructive pulmonary disease', *J Immunol,* 180, (9), pp. 6262-6269.

Namkung, W., Lee, J. A., Ahn, W., Han, W., Kwon, S. W., Ahn, D. S., Kim, K. H. and Lee, M. G. (2003) 'Ca^{2+} activates cystic fibrosis transmembrane conductance regulator- and Cl^--dependent HCO_3^- transport in pancreatic duct cells', *J Biol Chem*, 278, (1), pp. 200-207.

Novak, I. and Greger, R. (1988) 'Properties of the luminal membrane of isolated perfused rat pancreatic ducts', *Pflügers Arch,* 411, (5), pp. 546-553.

Ohana, E., Yang, D., Shcheynikov, N. and Muallem, S. (2009) 'Diverse transport modes by the solute carrier 26 family of anion transporters', *J Physiol,* 587, (10), pp. 2179-2185.

Ostedgaard, L. S., Baldursson, O. and Welsh, M. J. (2001) 'Regulation of the cystic fibrosis transmembrane conductance regulator Cl^- channel by its R domain', *J Biol Chem,* 276, (11), pp. 7689-7692.

Paradiso, A. M. (1992) 'Identification of Na^+-H^+ exchange in human normal and cystic fibrotic ciliated airway epithelium', *Am J Physiol Lung Cell Mol Physiol,* 262, (6), pp. L757-764.

Paradiso, A. M., Coakley, R. D. and Boucher, R. C. (2003) 'Polarized distribution of HCO_3^- transport in human normal and cystic fibrosis nasal epithelia', *J Physiol,* 548, (1), pp. 203-218.

Parker, M. D., Ourmozdi, E. P. and Tanner, M. J. (2001) 'Human BTR1, a new bicarbonate transporter superfamily member and human AE4 from kidney', *Biochem Biophys Res Comms*, 282, (5), pp. 1103-1109.

Patel, J., Pal, D., Vangala, V., Gandhi, M. and Mitra, A. K. (2002) 'Transport of HIV-protease inhibitors across 1 alpha,25di-hydroxy vitamin D3-treated Calu-3 cell monolayers: modulation of P-glycoprotein activity', *Pharm Res,* 19, (11), pp. 1696-1703.

Pedemonte, N., Caci, E., Sondo, E., Caputo, A., Rhoden, K., Pfeffer, U., Di Candia, M., Bandettini, R., Ravazzolo, R., Zegarra-Moran, O. and Galietta, L. J. V. (2007) 'Thiocyanate transport in resting and IL-4 stimulated human bronchial epithelial cells: role of pendrin and anion channels', *J Immunol,* 178, (8), pp. 5144-5153.

Pedemonte, N., Tomati, V., Sondo, E. and Galietta, L. J. V. (2010) 'Influence of cell background on pharmacological rescue of mutant CFTR', *Am J Physiol Cell Physiol,* 298, (4), pp. C866-874.

Petrovic, S., Barone, S., Xu, J., Conforti, L., Ma, L., Kujala, M., Kere, J. and Soleimani, M. (2004) 'SLC26A7: a basolateral Cl^-/HCO_3^- exchanger specific to intercalated cells of the outer medullary collecting duct', *Am J Physiol Renal Physiol,* 286, (1), pp. F161-169.

Petrovic, S., Ju, X., Barone, S., Seidler, U., Alper, S. L., Lohi, H., Kere, J. and Soleimani, M. (2003) 'Identification of a basolateral Cl^-/HCO_3^- exchanger specific to gastric parietal cells', *Am J Physiol Gastrointest Liver Physiol,* 284, (6), pp. G1093-1103.

Phillips, J. E., Hey, J. A. and Corboz, M. R. (2003) 'Tachykinin NK3 and NK1 receptor activation elicits secretion from porcine airway submucosal glands', *Br J Pharmacol,* 138, (1), pp. 254-260.

Pushkin, A., Abuladze, N., Newman, D., Lee, I., Xu, G. and Kurtz, I. (2000) 'Cloning, characterization and chromosomal assignment of NBC4, a new member of the sodium bicarbonate cotransporter family', *Biochimica Biophysica Acta,* 1493, (1-2), pp. 215-218.

Pushkin, A. and Krutz, I. (2006) 'SLC4 base (HCO_3^-, CO_3^{2-}) transporters: classification, function, structure, genetic diseases, and knockout models', *Am J Physiol Renal Physiol*, 290, (3), pp. F580-599.

Quinton, P. M. (1979) 'Composition and control of secretions from tracheal bronchial submucosal glands', *Nature,* 279, (5713), pp. 551-552.

Quinton, P. M. (1983) 'Chloride impermeability in cystic fibrosis', *Nature,* 301, (5899), pp. 421-422.

Quinton, P. M. (1990) 'Cystic fibrosis: a disease in electrolyte transport', *FASEB J,* 4, (10), pp. 2709-2717.

Quinton, P. M. (2001) 'The neglected ion: HCO_3^-', *Nat Med,* 7, (3), pp. 292-293.

Rakonczay, Z., Hegyi, P., Hasegawa, M., Inoue, M., You, J., Iida, A., Ignáth, I., Alton, E. W., Griesenbach, U., Óvári, G., Vág, J., Da Paula, A. C., Crawford, R. M., Varga, G., Amaral, M. D., Mehta, A., Lonovics, J., Argent, B. E. and Gray, M. A. (2008) 'CFTR gene transfer to human cystic fibrosis pancreatic duct cells using a Sendai virus vector', *J Cell Physiol,* 214, (2), pp. 442-455.

Reddy, M. M. and Quinton, P. M. (1999) 'Bumetanide blocks CFTR G_{Cl} in the native sweat duct', *Am J Physiol Cell Physiol,* 276, (1), pp. C231-237.

Reenstra, W. W., Yurko-Mauro, K., Dam, A., Raman, S. and Shorten, S. (1996) 'CFTR chloride channel activation by genistein: the role of serine/threonine protein phosphatases', *Am J Physiol Cell Physiol,* 271, (2), pp. C650-657.

Reid, L. (1960) 'Measurement of the bronchial mucous gland layer: a diagnostic yardstick in chronic bronchitis.' *Thorax,* 15, pp. 132-141.

Rich, D. P., Gregory, R. J., Anderson, M. P., Manavalan, P., Smith, A. E. and Welsh, M. J. (1991) 'Effect of deleting the R domain on CFTR-generated chloride channels', *Science,* 253, (5016), pp. 205-207.

Riordan, J. R., Rommens, J. M., Kerem, B., Alon, N., Rozmahel, R., Grzelczak, Z., Zielenski, J., Lok, S., Plavsic, N., Chou, J. L., Drumm, M. L., Iannuzzi, M. C., Collins, F. S. and Tsui, L. C. (1989) 'Identification of the cystic fibrosis gene: cloning and characterization of complementary DNA', *Science,* 245, (4922), pp. 1066-1073.

Robert, R., Norez, C. and Becq, F. (2005) 'Disruption of CFTR chloride channel alters mechanical properties and cAMP-dependent Cl^- transport of mouse aortic smooth muscle cells', *J Physiol,* 568, (2), pp. 483-495.

Romero, M. F., Henry, D., Nelson, S., Harte, P. J., Dillon, A. K. and Sciortino, C. M. (2000) 'Cloning and characterization of a Na^+-driven anion exchanger (NDAE1)', *J Biol Chem,* 275, (32), pp. 24552-24559.

Romero, M. F. (2005). 'Molecular pathophysiology of SLC4 bicarbonate transporters', *Curr Opin Nephrol Hypertens*, 14, (5), pp. 495-501.

Roos, A. and Boron, W. F. (1981) 'Intracellular pH', *Physiol Rev*, 61, pp. 296-434.

Royaux, I. E., Wall, S. M., Karniski, L. P., Everett, L. A., Suzuki, K., Knepper, M. A. and Green, E. D. (2001) 'Pendrin, encoded by the Pendred syndrome gene, resides in the apical region of renal intercalated cells and mediates bicarbonate secretion', *Proc Natl Acad Sci U.S.A.,* 98, (7), pp. 4221-4226.

Salinas, D., Haggie, P. M., Thiagarajah, J. R., Song, Y., Rosbe, K., Finkbeiner, W. E., Nielson, D. W. and Verkman, A. S. (2005) 'Submucosal gland dysfunction as a primary defect in cystic fibrosis', *FASEB J.,* 19, (3), pp. 431-433.

Schmidt, A., Hughes, L. K., Cai, Z., Mendes, F., Li, H., Sheppard, D. N. and Amaral, M. D. (2008) 'Prolonged treatment of cells with genistein modulates the expression and function of the cystic fibrosis transmembrane conductance regulator', *Br J Pharmacol,* 153(6), pp. 1311–1323.

Schoumacher, R. A., Shoemaker, R. L., Halm, D. R., Tallant, E. A., Wallace, R. W. and Frizzell, R. A. (1987) 'Phosphorylation fails to activate chloride channels from cystic fibrosis airway cells', *Nature,* 330, (6150), pp. 752-754.

Schwiebert, E. M., Egan, M. E., Hwang, T. H., Fulmer, S. B., Allen, S. S., Cutting, G. R. and Guggino, W. B. (1995) 'CFTR regulates outwardly rectifying chloride channels through an autocrine mechanism involving ATP', *Cell,* 81, (7), pp. 1063-1073.

Scott, D. A. and Karniski, L. P. (2000) 'Human pendrin expressed in Xenopus laevis oocytes mediates chloride/formate exchange', *Am J Physiol Cell Physiol,* 278, (1), pp. C207-211.

Scott, D. A., Wang, R., Kreman, T. M., Sheffield, V. C. and Karniski, L. P. (1999) 'The Pendred syndrome gene encodes a chloride-iodide transport protein', *Nat Genet,* 21, (4), pp. 440-443.

Sharma, P., Dudus, L., Nielsen, P. A., Clausen, H., Yankaskas, J. R., Hollingsworth, M. A. and Engelhardt, J. F. (1998) 'MUC5B and MUC7 are differentially expressed in mucous and serous cells of submucosal glands in human bronchial airways', *Am. J Respir Cell Mol Biol,* 19, (1), pp. 30-37.

Shcheynikov, N., Wang, Y., Park, M., Ko, S. B. H., Dorwart, M., Naruse, S., Thomas, P. J. and Muallem, S. (2006) 'Coupling modes and stoichiometry of Cl^-/HCO_3^- exchange by SLC26A3 and SLC26A6', *J Gen Physiol,* 127, (5), pp. 511-524.

Shcheynikov, N., Yang, D., Wang, Y., Zeng, W., Karniski, L. P., So, I., Wall, S. M. and Muallem, S. (2008) 'The SLC26A4 transporter functions as an electroneutral $Cl^-/I^-/HCO_3^-$ exchanger: role of SLC26A4 and SLC26A6 in I^- and HCO_3^- secretion and in regulation of CFTR in the parotid duct', *J Physiol,* 586, (16), pp. 3813-3824.

Shen, B. Q., Finkbeiner, W. E., Wine, J. J., Mrsny, R. J. and Widdicombe, J. H. (1994) 'Calu-3: a human airway epithelial cell line that shows cAMP-dependent Cl^- secretion', *Am J Physiol Lung Cell Mol Physiol,* 266, (5), pp. L493-501.

Sheppard, D. N. and Welsh, M. J. (1999) 'Structure and function of the CFTR chloride channel', *Physiol Rev,* 79, (1), pp. 23-45.

Shin, J. H., Son, E. J., Lee, H. S., Kim, S. J., Kim, K., Choi, J. Y., Lee, M. G. and Yoon, J. H. (2007) 'Molecular and functional expression of anion exchangers in cultured normal human nasal epithelial cells', *Acta Physiologica,* 191, (2), pp. 99-110.

Shumaker, H., Amlal, H., Frizzell, R., Ulrich II, C. D. and Solemani, M. (1999) 'CFTR drives Na^+-*n*HCO_3^- cotransport in pancreatic duct cells: a basis for defective HCO_3^- secretion in CF', *Am J Physiol Cell Physiol,* 276, (1), pp. C16-25.

Simpson, J. E., Gawenis, L. R., Walker, N. M., Boyle, K. T. and Clarke, L. L. (2005) 'Chloride conductance of CFTR facilitates basal Cl^-/HCO_3^- exchange in the villous epithelium of intact murine duodenum', *Am J Physiol Gastrointest Liver Physiol,* 288, (6), pp. G1241-1251.

Singh, M., Krouse, M., Moon, S. and Wine, J. J. (1997) 'Most basal I(SC) in Calu-3 human airway cells is bicarbonate-dependent Cl^- secretion', *Am J Physiol Lung Cell Mol Physiol,* 272, (4), pp. L690-698.

Skowron-zwarg, M., Boland, S., Caruso, N., Coraux, C., Marano, F. and Tournier, F. (2007) 'Interleukin-13 interferes with CFTR and AQP5 expression and localization during human airway epithelial cell differentiation', *Exp Cell Res,* 313, (12), pp. 2695-2702.

Smith, J. J., Travis, S. M., Greenberg, E. P. and Welsh, M. J. (1996) 'Cystic fibrosis airway epithelia fail to kill bacteria because of abnormal airway surface fluid', *Cell,* 85, (2), pp. 229-236.

Smith, J. J. and Welsh, M. J. (1992) 'cAMP stimulates bicarbonate secretion across normal, but not cystic fibrosis airway epithelia', *J Clin Invest,* 89, (4), pp. 1148-1153.

Soleimani, M. (2006) 'Expression, regulation and the role of SLC26 Cl^-/HCO_3^- exchangers in kidney and gastrointestinal tract', in *Epithelial Anion Transport in Health and Disease: The Role of the SLC26 Transporters Family.* Vol. 273 Novartis Foundation Symposium, pp. 91-106.

Soleimani, M., Greeley, T., Petrovic, S., Wang, Z., Amlal, H., Kopp, P. and Burnham, C. E. (2001) 'Pendrin: an apical $Cl^-/OH^-/HCO_3^-$ exchanger in the kidney cortex', *Am J Physiol Renal Physiol,* 280, (2), pp. F356-364.

Song, Y., Ishiguro, H., Yamamoto, A., Xiang Jin, C. and Kondo, T. (2009) 'Effects of SLC26A6 deletion and CFTR inhibition on HCO_3^- secretion by mouse pancreatic duct', *J Med Invest,* 56, (Supplement), pp. 332-335.

Song, Y., Salinas, D., Nielson, D. W. and Verkman, A. S. (2006) 'Hyperacidity of secreted fluid from submucosal glands in early cystic fibrosis', *Am J Physiol Cell Physiol,* 290, (3), pp. C741-749.

Song, Y. and Verkman, A. S. (2001) 'Aquaporin-5 dependent fluid secretion in airway submucosal glands', *J Biol Chem,* 276, (44), pp. 41288-41292.

Songyang, Z., Fanning, A. S., Fu, C., Xu, J., Marfatia, S. M., Chishti, A. H., Crompton, A., Chan, A. C., Anderson, J. M. and Cantley, L. C. (1997) 'Recognition of unique carboxyl-terminal motifs by distinct PDZ domains', *Science,* 275, (5296), pp. 73-77.

Sprague, R. S., Ellsworth, M. L., Stephenson, A. H., Kleinhenz, M. E. and Lonigro, A. J. (1998) 'Deformation-induced ATP release from red blood cells requires CFTR activity', *Am J Physiol Heart Circ Physiol,* 275, (5), pp. H1726-1732.

Stewart, A. K., Chernova, M. N., Kunes, Y. Z. and Alper, S. L. (2001) 'Regulation of AE2 anion exchanger by intracellular pH: critical regions of the NH_2-terminal cytoplasmic domain', *Am J Physiol Cell Physiol,* 281, (4), pp. C1344-1354.

Stewart, A. K., Kurschat, C. E., Burns, D., Banger, N., Vaughan-Jones, R. D. and Alper, S. L. (2007) 'Transmembrane domain histidines contribute to regulation of AE2-mediated anion exchange by pH', *Am J Physiol Cell Physiol,* 292, (2), pp. C909-918.

Stewart, A. K., Yamamoto, A., Nakakuki, M., Kondo, T., Alper, S. L. and Ishiguro, H. (2009) 'Functional coupling of apical Cl^-/HCO_3^- exchange with CFTR in stimulated HCO_3^- secretion by guinea pig interlobular pancreatic duct', *Am J Physiol Gastrointest Liver Physiol,* 296, (6), pp. G1307-1317.

Stuart-Tilley, A., Sardet, C., Pouyssegur, J., Schwartz, M. A., Brown, D. and Alper, S. L. (1994) 'Immunolocalization of anion exchanger AE2 and cation exchanger NHE-1 in distinct adjacent cells of gastric mucosa', *Am J Physiol Cell Physiol,* 266, (2), pp. C559-568.

Stutts, M. J., Canessa, C. M., Olsen, J. C., Hamrick, M., Cohn, J. A., Rossier, B. C. and Boucher, R. C. (1995) 'CFTR as a cAMP-dependent regulator of sodium channels', *Science,* 269, (5225), pp. 847-850.

Stutts, M. J., Rossier, B. C. and Boucher, R. C. (1997) 'Cystic fibrosis transmembrane conductance regulator inverts protein kinase A-mediated regulation of epithelial sodium channel single channel kinetics', *J Biol Chem*, 272, (22), pp. 14037-14040.

Sun, F., Hug, M. J., Lewarchik, C. M., Yun, C. H. C., Bradbury, N. A. and Frizzell, R. A. (2000) 'E3KARP mediates the association of ezrin and protein kinase A with the cystic fibrosis transmembrane conductance regulator in airway cells', *J Biol Chem,* 275, (38), pp. 29539-29546.

Szalmay, G., Varga, G., Kajiyama, F., Yang, X. S., Lang, T. F., Case, R. M. and Steward, M. C. (2001) 'Bicarbonate and fluid secretion evoked by cholecystokinin, bombesin and acetylcholine inisolated guinea-pig pancreatic ducts', *J Physiol*, 535, (3), pp. 795-807.

Szkotak, A. J., Man, S. F. P. and Duszyk, M. (2003) 'The role of the basolateral outwardly rectifying chloride channel in human airway epithelial anion secretion', *Am J Respir Cell Mol Biol,* 29, (6), pp. 710-720.

Tabcharani, J. A., Chang, X. B., Riordan, J. R. and Hanrahan, J. W. (1992) 'The cystic fibrosis transmembrane conductance regulator chloride channel. Iodide block and permeation', *Biophys J*, 62, (1), pp. 1-4.

Tamada, T., Hug, M. J., Frizzell, R. A. and Bridges, R. J. (2001) 'Microelectrode and impedance analysis of anion secretion in Calu-3 cells', *J Pancreas*, 2, (4), pp. 219-228.

Tamaoki, T. and Nakano, H. (1990) 'Potent and specific inhibitors of protein kinase C of microbial origin', *Nat Biotech,* 8, (8), pp. 732-735.

Tarran, R. (2004) 'Regulation of airway surface liquid volume and mucus transport by active ion transport', *Proc Am Thorac Soc,* 1, (1), pp. 42-46.

Tarran, R., Button, B., Picher, M., Paradiso, A. M., Ribeiro, C. M., Lazarowski, E. R., Zhang, L., Collins, P. L., Pickles, R. J., Fredberg, J. J. and Boucher, R. C. (2005) 'Normal and cystic fibrosis airway surface liquid homeostasis: the effects of phasic shear stress and viral infections', *J Biol Chem,* 280, (42), pp. 35751-35759.

Tarran, R., Trout, L., Donaldson, S. H. and Boucher, R. C. (2006) 'Soluble mediators, not cilia, determine airway surface liquid volume in normal and cystic fibrosis superficial airway epithelia', *J Gen Physiol,* 127, (5), pp. 591-604.

Taylor, C. J. and Aswani, N. (2002) 'The pancreas in cystic fibrosis', *Paediatr Respir Rev,* 3, (1), pp. 77-81.

Thastrup, O., Cullen, P. J., Drabak, B. K., Hanley, M. R. and Dawson, A. P. (1990) 'Thapsigargin, a tumor promoter, discharges intracellular Ca^{2+} stores by specific inhibition of the endoplasmic reticulum Ca^{2+}-ATPase', *Proc Nat Acad Sci U.S.A.,* 87, (7), pp. 2466-2470.

Thelin, W. R., Kesimer, M., Tarran, R., Kreda, S. M., Grubb, B. R., Sheehan, J .K., Stutts, M. J. and Milgram, S. L. (2005) 'The cystic fibrosis transmembrane conductance regulator is regulated by a direct interaction with the protein phosphatase 2A', *J Biol Chem*, 280, (50), pp. 41512-41520.

Thiagarajah, J. R., Song, Y., Haggie, P. M. and Verkman, A. S. (2004) 'A small molecule CFTR inhibitor produces cystic fibrosis-like submucosal gland fluid secretions in normal airways', *FASEB J.*, 18, (7), pp. 875-7.

Tousson, A., Van Tine, B. A., Naren, A. P., Shaw, G. M. and Schwiebert, L. M. (1998) 'Characterization of CFTR expression and chloride channel activity in human endothelia', *Am J Physiol Cell Physiol,* 275, (6), pp. C1555-1564.

Travis, S. M., Berger, H. A. and Welsh, M. J. (1997) 'Protein phosphatase 2C dephosphorylates and inactivates cystic fibrosis transmembrane conductance regulator', *Proc Nat Acad Sci U.S.A.,* 94, (20), pp. 11055-11060.

Travis, S. M., Singh, P. K. and Welsh, M. J. (2001) 'Antimicrobial peptides and proteins in the innate defense of the airway surface', *Curr Opin Immunol,* 13, (1), pp. 89-95.

Trout, L., Corboz, M. R. and Ballard, S. T. (2001) 'Mechanism of substance P-induced liquid secretion across bronchial epithelium', *Am J Physiol Lung Cell Mol Physiol,* 281, (3), pp. L639-645.

Trout, L., Gatzy, J. T. and Ballard, S. T. (1998) 'Acetylcholine-induced liquid secretion by bronchial epithelium: role of Cl^- and HCO_3^- transport', *Am J Physiol Lung Cell Mol Physiol,* 275, (6), pp. L1095-1099.

Ueki, I., German, V. and Nadel, J. (1980) 'Micropipette measurement of airway submucosal gland secretion. Autonomic effects.' *Am Rev Respir Dis* , 121, (2), pp. 351-357.

Urbach, V., Helix, N., Renaudon, B. and Harvey, B. J. (2002) 'Cellular mechanisms for apical ATP effects on intracellular pH in human bronchial epithelium', *J Physiol*, 543, (1), pp. 13-21.

Verlander, J. W., Madsen, K. M., Low, P. S., Allen, D. P. and Tisher, C. C. (1988) 'Immunocytochemical localization of band 3 protein in the rat collecting duct', *Am J Physiol Renal Physiol,* 255, (1), pp. F115-125.

Vince, J. W. and Reithmeier, R. A. F. (2000) 'Identification of the carbonic anhydrase II binding site in the Cl^-/HCO_3^- anion exchanger AE1', *Biochemistry,* 39, (18), pp. 5527-5533.

Wan, H., Winton, H. L., Soeller, C., Stewart, G. A., Thompson, P. J., Gruenert, D. C., Cannell, M. B., Garrod, D. R. and Robinson, C. (2000) 'Tight junction properties of the immortalized human bronchial epithelial cell lines Calu-3 and 16HBE14o', *Eur Respir J,* 15, (6), pp. 1058-1068.

Wang, Y., Soyombo, A. A., Shcheynikov, N., Zeng, W., Dorwart, M., Marino, C. R., Thomas, P. J. and Muallem, S. (2006) 'SLC26A6 regulates CFTR activity in vivo to determine pancreatic duct HCO_3^- secretion: relevance to cystic fibrosis', *EMBO J,* 25, pp. 5049-5057.

Wang, Z., Wang, T., Petrovic, S., Tuo, B., Riederer, B., Barone, S., Lorenz, J. N., Seidler, U., Aronson, P. S. and Soleimani, M. (2005) 'Renal and intestinal transport defects in SLC26A6-null mice', *Am J Physiol Cell Physiol*, 288, pp. C957-965.

Welsh, M. J. (1990) 'Abnormal regulation of ion channels in cystic fibrosis epithelia', *FASEB J.*, 4, (10), pp. 2718-2725.

Wheat, V. J., Shumaker, H., Burnham, C., Shull, G. E., Yankaskas, J. R. and Soleimani, M. (2000) 'CFTR induces the expression of DRA along with Cl^- /HCO_3^- exchange activity in tracheal epithelial cells', *Am J Physiol Cell Physiol,* 279, (1), pp. C62-71.

Wine, J. J. and Joo, N. S. (2004) 'Submucosal glands and airway defense', *Proc Am Thorac Soc,* 1, (1), pp. 47-53.

Wine, J. J. (2007) 'Parasympathetic control of airway submucosal glands: central relexes and the airway intrinsic nervous system', *Auton Neurisci*, 133, (1), pp. 35-54.

Winter, M. C. and Welsh, M. J. (1997) 'Stimulation of CFTR activity by its phosphorylated R domain', *Nature,* 389, (6648), pp. 294-296.

Wu, J. V., Krouse, M. E., Rustagi, A., Joo, N. S. and Wine, J. J. (2004) 'An inwardly rectifying potassium channel in apical membrane of Calu-3 cells', *J Biol Chem,* 279, (45), pp. 46558-46565.

Xia, Y., Haws, C. M. and Wine, J. J. (1997). 'Disruption of monolayer integrity enables activation of a cystic fibrosis "bypass" channel in human airway epithelia', *Nat Med*, 3, pp. 263-268.

Xie, Q., Welch, R., Mercado, A., Romero, M. F. and Mount, D. B. (2002) 'Molecular characterization of the murine SLC26A6 anion exchanger: functional comparison with SLC26A1', *Am J Physiol Renal Physiol,* 283, (4), pp. F826-838.

Xu, J., Henriksnas, J., Barone, S., Witte, D., Shull, G. E., Forte, J. G., Holm, L. and Soleimani, M. (2005) 'SLC26A9 is expressed in gastric surface epithelial cells, mediates Cl^-/HCO_3^- exchange, and is inhibited by NH_4^+', *Am J Physiol Cell Physiol,* 289, (2), pp. C493-505.

Xu, J., Song, P., Nakamura, S., Miller, M., Barone, S., Alper, S. L., Riederer, B., Bonhagen, J., Arend, L. J., Amlal, H., Seidler, U. and Soleimani, M. (2009) 'Deletion of the chloride transporter SLC26A7 causes distal renal tubular acidosis and impairs gastric acid secretion', *J Biol Chem,* 284, (43), pp. 29470-29479.

Yamaya, M., Finkbeiner, W. E., Chun, S. Y. and Widdicombe, J. H. (1992) 'Differentiated structure and function of cultures from human tracheal epithelium', *Am J Physiol Lung Cell Mol Physiol,* 262, (6), pp. L713-724.

Yamaya, M., Ohrui, T., Finkbeiner, W. E. and Widdicombe, J. H. (1993) 'Calcium-dependent chloride secretion across cultures of human tracheal surface epithelium and glands', *Am J Physiol Lung Cell Mol Physiol,* 265, (2), pp. L170-177.

Zhang, Y., Chernova, M. N., Stuart-Tilley, A. K., Jiang, L. and Alper, S. L. (1996) 'The cytoplasmic and transmembrane domains of AE2 both contribute to regulation of anion exchange by pH. *J Biol Chem*, 271, pp. 5741-5749.

Zhao, H., Star, R. A. and Muallem, S. (1994) 'Membrane localization of H^+ and HCO_3^- transporters in the rat pancreatic duct', *J Gen Physiol,* 104, (1), pp. 57-85.

Zünd, G., Madara, J. L., Dzus, A. L., Awtrey, C. S. and Colgan, S. P. (1996) 'Interleukin-4 and interleukin-13 differentially regulate epithelial chloride secretion', *J Biol Chem*, 271, pp. 7460-7464.